UNIVERSITÄT
BERN

Graduate School for Cellular and Biomedical Sciences

University of Bern

Msp1 in *Trypanosoma brucei* mitochondrial quality control

PhD Thesis submitted by

Markus Daniel Gerber

for the degree of

PhD in Biochemistry and Molecular Biology

Supervisor
Prof. Dr. André Schneider
Department of Chemistry, Biochemistry and Pharmaceutical Sciences
Faculty of Science of the University of Bern

Co-advisor
Prof. Dr. Torsten Ochsenreiter
Institute of Cell Biology
Faculty of Science of the University of Bern

Accepted by the Faculty of Medicine, the Faculty of Science and the Vetsuisse Faculty of the University of Bern at the request of the Graduate School for Cellular and Biomedical Sciences

Bern, Dean of the Faculty of Medicine

Bern, Dean of the Faculty of Science

Bern, Dean of the Vetsuisse Faculty Bern

Content

Abstract

Mitochondria are vital organelles, prominently known for their role in ATP production. Even though mitochondria contain their own DNA, almost all mitochondrial proteins are encoded in the nucleus. These nuclear encoded mitochondrial proteins are translated in the cytosol and subsequently imported into the organelle. Disturbance of mitochondrial proteostasis by mislocalized or destabilized proteins, whose accumulation can lead to mitochondrial dysfunction, is an issue that demands immediate resolution. Therefore, eukaryotes contain a wide range of pathways to prevent and restore dysfunctional mitochondria. The ATPase-associated with diverse cellular activities (AAA) Msp1 contributes to mitochondrial proteostasis by extracting mislocalised tail-anchored proteins from the mitochondrial outer membrane (OM). Yeast Msp1 can extract substrate proteins from a lipid bilayer independently from associated proteins and substrate modifications. However, little is known about Msp1 orthologs outside the eukaryotic supergroup of the Opisthokonts, which includes animals and fungi. Trypanosoma brucei is a well-established eukaryotic model organism which belongs to the Discoba group and thus is essentially unrelated to Opisthokonts. The trypanosome-specific pATOM36 mediates complex assembly of α-helically anchored mitochondrial outer membrane proteins, such as proteins of the atypical protein translocase of the outer mitochondrial membrane (ATOM), into their respective complexes. Inhibition of ATOM complex assembly via RNAi knockdown of pATOM36 triggers a pathway that results in the degradation of unassembled ATOM subunits by the cytosolic proteasome.

Here we have investigated this novel trypanosomal mitochondria-associated degradation pathway. We show that the trypanosomal Msp1 homolog (TbMsp1) and the trypanosomal homolog of the AAA-ATPase VCP (TbVCP) are involved in this quality control pathway. The RNAi knockdown of pATOM36 in combination with either TbMsp1 RNAi or TbVCP RNAi does not affect the pathway as pATOM36 substrates are still being degraded by the cytosolic proteasome. However, the simultaneous knockdown of TbMsp1 and TbVCP in the pATOM36 RNAi background prevents the removal of pATOM36 substrates from the OM despite the ablation of pATOM36. This suggests that there is some redundancy between TbMsp1 and TbVCP in this pathway. Furthermore, we show by in situ tagging, coimmunoprecipitation and mass spectrometry that TbMsp1 localises to both, glycosomes and the OM. Additionally, we demonstrate by reciprocal coimmunoprecipitations that TbMsp1 forms a stable complex with the four OM proteins POMP19, POMP31, TbJ31 and TbTsc13. Interestingly, upon pATOM36 and TbVCP ablation, POMP31, TbJ31 and TbTsc13 are required for efficient proteasomal degradation of pATOM36 substrates, suggesting these three TbMsp1-interacting proteins assist TbMsp1 in extracting the destabilized OM proteins. pATOM36 is a functional analogue of the yeast OM MIM complex and likely of the animal-specific OM protein MTCH2, suggesting that similar mitochondrial quality control pathways linked to Msp1 might also exist in yeast and

humans. The molecular details underlaying the interactions within the TbMsp1-containing complex, and the role of the individual TbMsp1-associated proteins in the extraction of pATOM36 substrates have yet to be elucidated. Additionally, it is unclear whether these interaction partners are required for the extraction of all TbMsp1 substrates. It is possible that their activity might be limited to a specific subset of TbMsp1 substrates which includes the pATOM36 substrates. Other TbMsp1 substrates than those extracted upon pATOM36 and TbVCP ablation could not yet be identified. Furthermore, it also remains unclear whether TbMsp1 functions independently of ubiquitin, as has been suggested for yeast Msp1.

1. Introduction

1.1 Mitochondria, the powerhouse of the cell

Mitochondria are cellular organelles best known for their role in producing adenosine 5'-triphosphate (ATP), the cells 'energy currency'. ATP is used for various processes including ion transport, muscle contraction, nerve impulse propagation, substrate phosphorylation, and chemical synthesis. Furthermore, mitochondria are also involved in several other pathways ranging from fatty acid metabolism to iron/sulphur cluster synthesis. As a result of their involvement in vital pathways, mitochondria are essential for all eukaryotes with only few exceptions (Henze and Martin, 2003; Karnkowska et al., 2016; Simpson et al., 2002; Tovar et al., 2003; Yahalomi et al., 2020).

1.1.1 Basic architecture

Depending on the organism and cell type, mitochondria are present in various shapes and numbers (Ahmad et al., 2013; Neves et al., 2010; Shaw and Nunnari, 2002). However, all mitochondria can be separated into four compartments: Outer membrane (OM), intermembrane space (IMS), inner membrane (IM) and matrix (Figure 1).

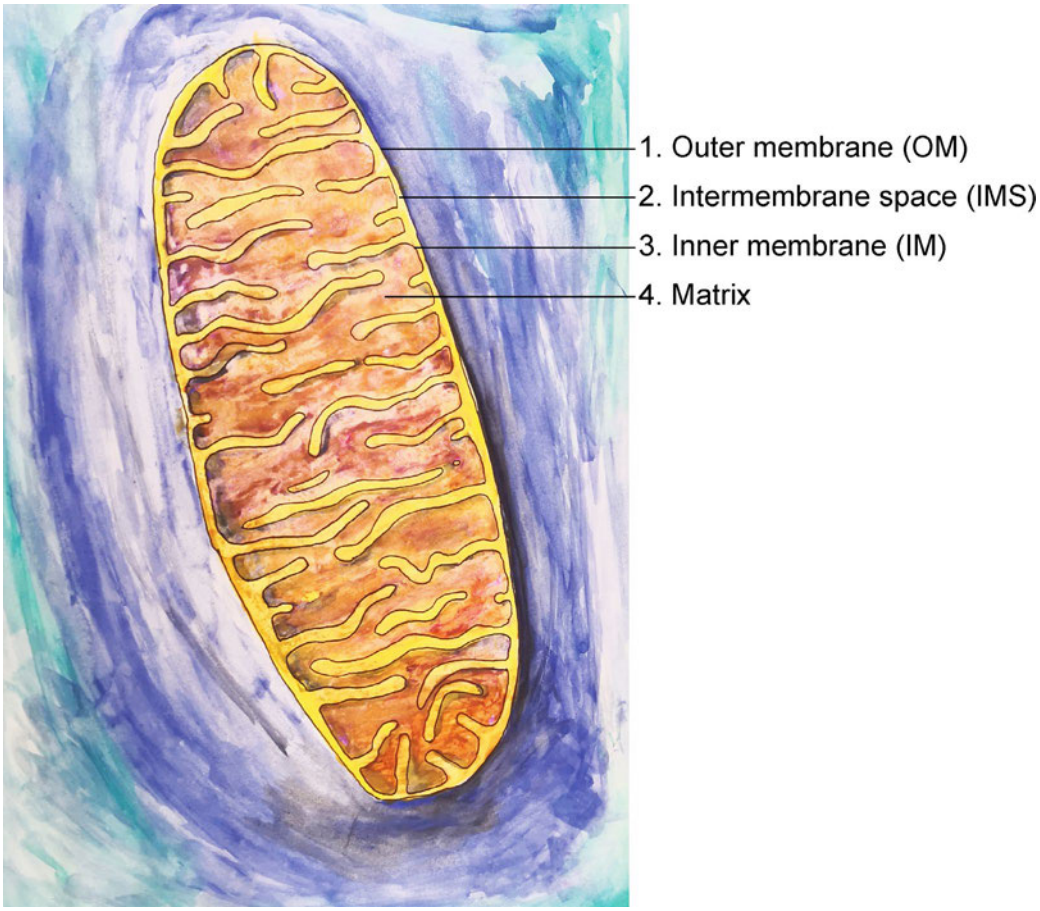

Figure 1: Schematic depiction of mitochondrial structure. Mitochondria can be separated in four compartments. The outer membrane (OM), the intermembrane space (IMS), the inner membrane (IM), and the matrix.

The outer membrane (OM) surrounds the mitochondrion and separates it from the cytosol. It also serves as a communication platform between mitochondria and other cellular organelles (Audano et al., 2020; Y. Liao et al., 2020). The OM contains a variety of membrane proteins. Based on proteomic studies performed with fungi, trypanosomes and human cell culture the OM is suggested to contain 80 to 140 integral membrane proteins (Hung et al., 2017; Morgenstern et al., 2017; Niemann et al., 2013; Schmitt et al., 2006; Zahedi et al., 2006). The most abundant protein in the OM is the voltage-dependent anion channel (VDAC) which allows ions and small molecules to pass freely through the membrane via its beta barrel pore (Hoogenboom et al., 2007). Proteins that are imported into mitochondria cross the OM through a protein complex called translocase of the outer membrane (TOM) (Model et al., 2002). Unlike canonical mitochondrial proteins, OM proteins do not contain cleavable N-terminal mitochondrial targeting sequences (MTS). Instead, they contain mitochondrial targeting signals at either end or in the middle of the protein (Jores et al., 2016; Rapaport, 2003).

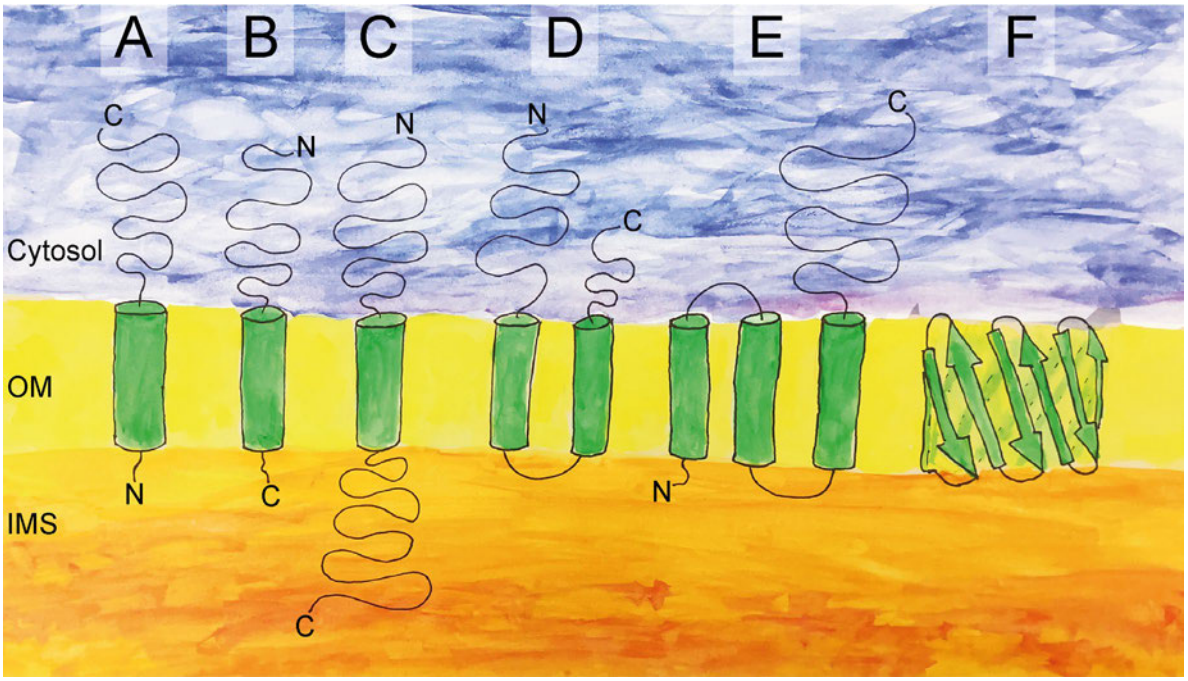

Figure 2: Topology of integral outer mitochondrial membrane (OM) proteins. Mitochondrial OM proteins can be classified according to their topology. There are signal- and tail- anchored proteins (A, B respectively), proteins that are internally α-helically anchored (C), proteins with two or more α-helical transmembrane domains (D, E) and beta barrel proteins (F). (Walther and Rapaport, 2009; Zheng et al., 2019)

Integral OM proteins can be classified based on their topology as shown in Figure 2. N- or C-terminally anchored proteins (Figure 2 A, B) make up a big part of integral OM proteins. They are also referred to as signal- or tail- anchored proteins, respectively. In both cases, only a

small portion of the protein is facing the IMS, while the large majority is facing the cytosol. In yeast, there are two known proteins Mim1 and Tom22, in which the transmembrane domain is found in the middle of the protein, with the N terminus facing the cytosol and the C terminus facing the IMS (Figure 2 C) (Walther and Rapaport, 2009). Interestingly, the biogenesis of these single α-helically anchored proteins is mediated by non-orthologous proteins in different eukaryotic clades. Of these analogous insertases, the mitochondrial import complex (MIM) was discovered first. MIM is fungi-specific and is composed off the proteins Mim1 and Mim2 (Becker et al., 2011; Dimmer et al., 2012; Doan et al., 2020; Papić et al., 2011). The second insertase, peripheral atypical protein translocase of the OM of 36kDa (pATOM36), was discovered in *Trypanosoma brucei* and is restricted to kinetoplastids (Bruggisser et al., 2017; Käser et al., 2016). MIM and pATOM36 have been shown to reciprocally complement the biogenesis defect which occur upon the ablation of the other in yeast and trypanosomes, respectively (Vitali et al., 2018). Thirdly, α-helically anchored proteins are inserted by the mitochondrial animal-specific carrier homolog 2 (MTCH2) that was discovered in human cells (Guna et al., 2022). However, there is evidence that not all α-helically anchored proteins are dependent on an insertase for OM insertion. Some proteins seem to be able to spontaneously insert into the OM (Kemper et al., 2008; Vögtle et al., 2015).

Furthermore, a couple of multipass membrane proteins containing two or more transmembrane helices can be found in the OM (Figure 2 D, E) (Coonrod et al., 2007; Fritz et al., 2001; Rojo et al., 2002). There is some indication of a multipass membrane protein insertion pathway that is dependent on the TOM receptor Tom70, but not on other TOM components (Otera et al., 2007). Other studies found that Mim1 and VDAC are assisting the integration of a multipass OM protein, though none of the proteins were absolutely required for insertion (Becker et al., 2011; Zhou et al., 2022). This suggests that depending on the substrate, multiple proteins contribute to the insertion-efficiency of multipass OM proteins (Zhou et al., 2022). Lastly, there are β-barrel proteins, which span the membrane via multiple anti-parallel amphipathic β-sheets arranged to form a tunnel (Figure 2 F) (Diederichs et al., 2020). They are typically inserted by the sorting and assembly of machinery (SAM) complex (Kozjak-Pavlovic et al., 2007). Examples for β-barrel proteins in the OM are Tom40, the pore of the TOM complex, or VDAC (Ahting et al., 2001; Hill et al., 1998; Mannella et al., 1996). All known OM proteins are encoded in the nucleus, which means they are synthesized in the cytosol and inserted through either TOM, SAM, MIM, or their respective analogues.

The IMS is the space between the OM and the IM. As small solutes such as ions and sugars can freely cross the OM through pores such as VDAC, the concentration of these molecules is the same as in the cytosol (Shoshan-Barmatz et al., 2010). Proteins localized in the IMS often contain disulfide bridges whose oxidative folding is assisted by the protein Mia40 (Figure 3) (Boos et al., 2020; Mesecke et al., 2005). Proteomic studies in fungi and mammals have

identified approximately 50 soluble IMS proteins (Edwards et al., 2021; Hung et al., 2014; Morgenstern et al., 2017; Vögtle et al., 2017, 2012).

The IM separates the IMS from the matrix. It contains several invaginations called cristae, increasing the surface of the membrane. The IM is very densely populated with proteins, which are estimated to make up half of its hydrophobic volume (Schlame, 2021). Among other proteins, the complexes of the respiratory chain can be found in the IM. In contrast to the OM, the IM is not permeable for ions, which is a key requisite for keeping the electrochemical gradient that is required for ATP production and protein import (Mannella, 2006). In trypanosomes and yeast, between 240 and 290 different IM proteins were detected (Da Cruz and Martinou, 2008; Morgenstern et al., 2017; Niemann et al., 2013; Vögtle et al., 2017). However, the number of IM proteins is likely higher; estimates are as high as 840 proteins (Bohovych et al., 2015). In yeast, nuclear encoded IM proteins are mostly inserted into the IM via the presequence pathway by the translocase of the inner mitochondrial membrane 22 (TIM22), while most mtDNA encoded IM proteins are inserted by the oxidase assembly (OXA) complex (Schmidt et al., 2010; Stiller et al., 2016; Stuart, 2002). Matrix proteins can cross the inner membrane through TIM23 (Sim et al., 2021; Sirrenberg et al., 1996).

The matrix is the viscous lumen encapsulated by the IM. It contains various enzymes, metabolites and the mtDNA (Bogenhagen, 2012; Mazunin et al., 2015). The matrix proteome contains around 500 different proteins, including several IM proteins with residues in the matrix (Rhee et al., 2013). Many of these proteins contain an N-terminal mitochondrial targeting sequence (MTS) and are imported via the presequence pathway (Figure 3).

1.1.2 Evolutionary origin

Mitochondria have an interesting evolutionary origin. They emerged from an endosymbiotic event estimated to have occurred ~2 billion years ago, when an alphaproteobacterium was taken up by an archaea (Dolezal et al., 2006; Gabaldón, 2021; Gargaud et al., 2011; Hedges et al., 2004; Wang and Luo, 2021). Over a long time span mitochondria evolved from free-living bacteria to the cellular organelles eukaryotes share today (Burki et al., 2020; Gabaldón, 2021; Gargaud et al., 2011). The remaining mitochondrial DNA (mtDNA) is a direct consequence of their bacterial origin (Mishra, 2017; Nass and Nass, 1963). However, almost all mitochondrial genes have been transferred to the nucleus (Calvo and Mootha, 2010; Friedman and Nunnari, 2014; Nunnari and Suomalainen, 2012). Human mtDNA encodes for only 13 out of ~1’500 known mitochondrial proteins (Calvo et al., 2016; Cotter et al., 2004; Friedman and Nunnari, 2014; Pagliarini et al., 2008; Schmidt et al., 2010; Taylor et al., 2003). The exact numbers differ between species, but in all eukaryotes only a small number of proteins are encoded on the mtDNA. This means over 95% of all mitochondrial proteins are encoded in the nucleus (Dolezal et al., 2006; Schmidt et al., 2010). These nuclear encoded

mitochondrial proteins are synthesized in the cytosol and subsequently imported into the organelle, explaining why mitochondrial protein import is a crucial process for survival.

1.1.3 Mitochondrial proteostasis

Most studies on mitochondrial protein import have been conducted in yeast. Most mitochondrial proteins are imported by TOM and subsequently either TIM22 or TIM23. Even though the TOM complex was thought to be highly conserved, recent work has shown that there are quite some variations in different eukaryotes such as kinetoplastids or plants (Ghifari et al., 2018; Hoogenraad et al., 2002; Mani et al., 2015; Schneider, 2022). Thus, protein import receptors evolved independently in different eukaryotic supergroups (Fukasawa et al., 2017; Ghifari et al., 2018; Mani et al., 2015; Rout et al., 2021; Schneider, 2022; Vitali et al., 2018).

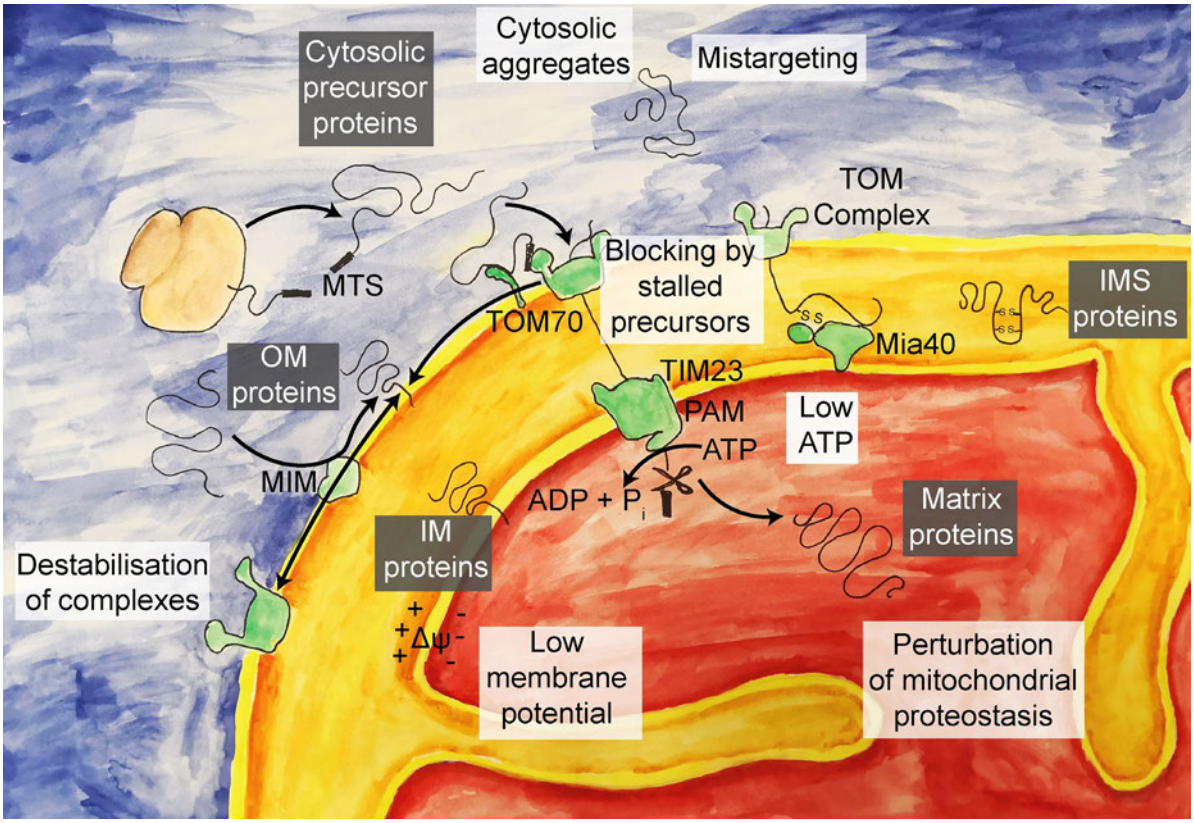

Figure 3: Dangers to mitochondrial proteostasis in yeast. Almost all mitochondrial proteins are translated in the cytosol and subsequently imported into mitochondria. Proteins destined for the matrix, or the IM often contain an N-terminal mitochondrial targeting sequence (MTS) that is recognized by receptors on the OM surface, such as Tom70. These receptors direct the protein through the mitochondrial protein import complexes TOM and TIM. Translocation through the OM and IM is coupled and is driven by the membrane potential across the IM (Δψ) and the ATP-driven presequence translocase-associated motor (PAM). IMS and OM proteins mostly do not contain a mitochondrial targeting sequence (MTS) and therefore use different import routes. The import IMS of proteins is often associated with oxidative protein folding catalysed by Mia40. The import of OM and IMS proteins usually depends on neither ATP nor the membrane potential across the IM. These mitochondrial biogenesis pathways can be disturbed by various problems in the cytosol or inside

mitochondria. A selection of challenges to mitochondrial proteostasis is indicated in light boxes in this figure (Boos et al., 2020).

As illustrated in Figure 3, several problems can occur during mitochondrial biogenesis that affect mitochondrial proteostasis. A potential problem is that protein import does not function properly. This can then lead to cytosolic aggregation of precursor proteins, mistargeting or blocking of the import channel. Matrix proteins need to cross the OM and the IM and are dependent on ATP and the IM potential for import. If there is too little ATP or the membrane potential is lost, matrix proteins cannot be imported correctly. However, not all problems in mitochondrial proteostasis are directly related to protein import. Misfolding, destabilisation or aggregation of proteins can also occur independently from import. Normally, the levels of mitochondrial proteins are regulated by synthesis and degradation. If this protein turnover is disturbed, mitochondrial proteostasis is disrupted (Kowalski et al., 2018). To prevent damage and to secure mitochondrial function, the cell has a network of different mitochondrial quality control (MQC) pathways regulating proteostasis (Baker and Haynes, 2011; Fischer et al., 2012; Quiles and Gustafsson, 2020). These pathways are often accompanied by nuclear responses, upregulating a variety of factors involved in MQC (Callegari and Dennerlein, 2018). It is important to mention that many of the quality control pathways introduced below are interconnected (Fischer et al., 2012).

1.2 The cytosolic proteasome in MQC

Proteasomes are large, multisubunit structures that are the main eukaryotic protein turnover machineries. Besides in eukaryotes, they are also found in Archaea and in some Bacteria (Becker and Darwin, 2016; Maupin-Furlow et al., 2006; Peters et al., 1994). The 26S proteasome degrades proteins into 3 to15 amino acid long oligopeptides that are then further degraded into individual amino acids by downstream proteases (Tanaka, 2009). Ubiquitin (Ub) is used as a marker for proteins that are to be targeted for proteasomal degradation (Hershko and Ciechanover, 1998). Ub is a 76 amino acid long protein that can be covalently bound to other proteins or to itself. There are three proteins, which are involved in the ubiquitination pathway: Ub-activating enzyme (E1), Ub-conjugating-enzyme (E2) and Ub-protein ligase (E3) (Callis, 2014; Guo et al., 2023).

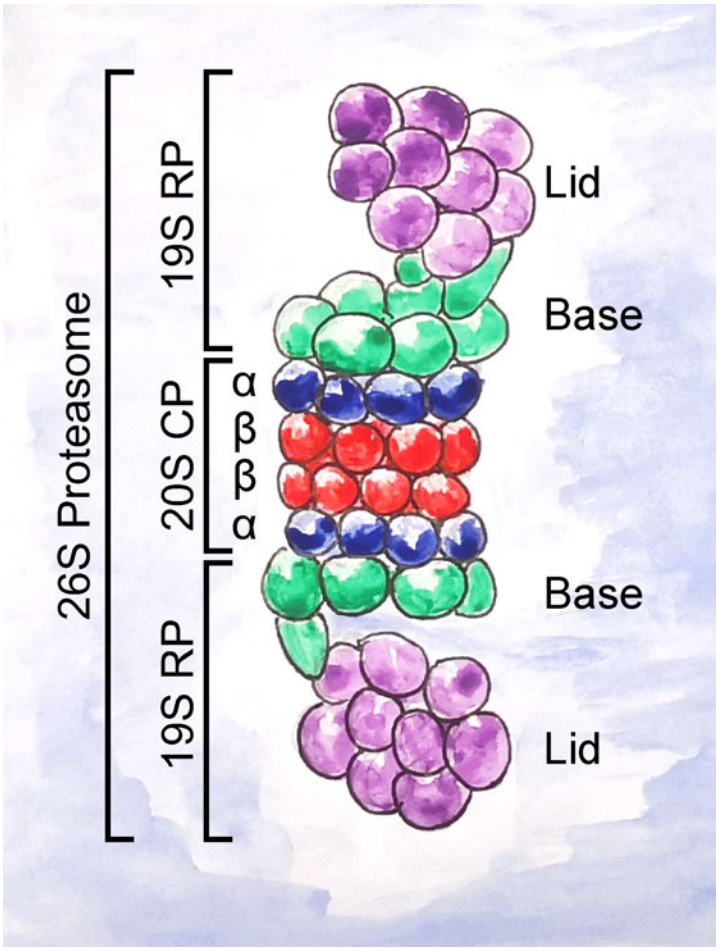

Figure 4: Schematic depiction of the 26S proteasome. Classic proteasomes have a symmetrical structure consisting of a cylindrical 20S central particle (CP) with regulatory proteins (RP) assembled into base and lid subcomplexes attached at both ends (Tanaka, 2009).

The symmetrical 2.5 mega Dalton proteasome complex consists of a central 20S central particle (CP) that is capped by 19S regulatory proteins (RP), which are organized in a base and a lid subcomplex on each side (Figure 4). The cylindrical 20S CP is made up of two inner *β*-rings and two outer *α*-rings each of which contains seven *α*- or *β*-subunits (Figure 4). The proteolytically active site is situated in the inner *β*-rings, while the *α*-rings are a physical barrier, blocking access of proteins to the proteolytically active site (Bochtler et al., 1999; Tanaka,

2009). The main function of the lid subcomplex is to deubiquitinate the captured proteins, which enables the recycling of Ub (Tanaka, 2009). RPs in the base subcomplex recognize and capture polyubiquitinated proteins, unfold them and open the *α*-gate so that substrates can be digested in the proteolytic centre (Tanaka, 2009). Generally, substrates subjected for proteasomal degradation are ubiquitinated (Ciechanover and Schwartz, 1998; Guo et al., 2023; Hershko and Ciechanover, 1998). However, it has been demonstrated that ubiquitination is not an absolute prerequisite for proteasomal degradation (Baugh et al., 2009; Murakami et al., 1992).

Due to its ability to degrade proteins quickly and specifically it is no surprise that the cytosolic proteasome plays an important role in various MQC pathways, which will be discussed in the following chapters.

1.2.1 UPR^{am}

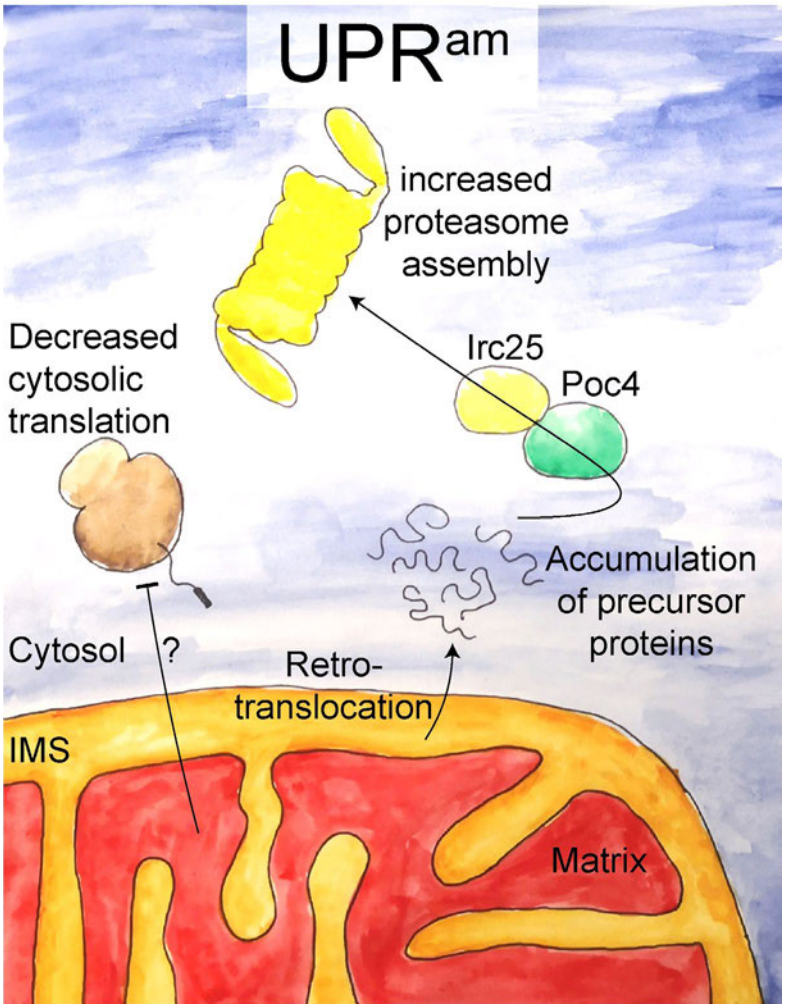

Figure 5: Schematic overview of the unfolded protein response activated by mistargeting of proteins (UPR^{am}). Upon accumulation of precursor proteins in the cytosol, UPR^{am} is triggered. This leads to increased activity of Irc25 and Poc4, which are chaperones involved in proteasome assembly leading to higher proteasome abundance. This speeds up the degradation of the accumulated proteins. It has been demonstrated that increased proteasome activity in mammals is coupled to downregulation of translation in the cytosol. The molecular mechanisms behind this connection have yet to be elucidated (Callegari and Dennerlein, 2018).

The unfolded protein response activated by mistargeting of proteins (UPR^{am}) is a pathway triggered upon the accumulation of cytosolic mitochondrial precursor proteins. It does not appear to be substrate-specific. Rather it is a universal response to mitochondrial stress that manifests in the accumulation of proteins in the cytosol. It has been demonstrated that UPR^{am} can also be triggered by proteins and peptides that migrated from the IMS back to the cytosol (Bragoszewski et al., 2015; Wasilewski et al., 2017). UPR^{am} upregulates proteasome activity by promoting proteasome assembly (Callegari and Dennerlein, 2018; Wasilewski et al., 2017; Wrobel et al., 2015). This is achieved through increased activity of proteasome assembly factors Irc25 and Poc4. These two proteins form a chaperone complex that is involved in the assembly of *α*-subunits into the proteasome (Callegari and Dennerlein, 2018; Wrobel et al., 2015). While most studies investigating UPR^{am} were performed in yeast, increased proteasome activity can also be detected in mammalian cells upon stress conditions in proteostasis (Papa and Germain, 2014). In addition, there appears to be a pathway coupled to mitochondrial stress conditions that decreases cytosolic translation (Topf et al., 2016; Wang and Chen, 2015; Wrobel et al., 2015). The link between these two responses to mitochondrial protein stress is not yet fully understood. However, it has been suggested that the downregulation of translation in the cytosol is achieved by reducing the nuclear export of the ribosomal 60S subunit (Wasilewski et al., 2017).

In summary, while the broad principles of UPR^{am} and its role in reduction of stress is known, there are still molecular mechanisms and interactions connecting this pathway to the network of MQC that have yet to be elucidated.

1.2.2 VCP mediated MQC pathways

The cytosolic proteasome degrades proteins only when they are free in the cytosol. Nonetheless, mitochondrial proteins can also be subjected to proteasomal degradation. However, to become accessible for degradation, OM proteins need to be extracted from the membrane. Membrane-extraction requires energy in the form of ATP and ATPases that catalyse the process. There are two types of ATPases known to contribute to MQC by making OM proteins accessible for proteasomal degradation: The valosin-containing protein (VCP, homologs are also known as p97, Cdc48, TER94 or VAT) and mitochondrial sorting of proteins 1 (Msp1, homologous to ATAD1 in mammals) (Koller and Brownstein, 1987; Pamnani et al., 1997; van den Boom and Meyer, 2018; Wohlever et al., 2017; Ye et al., 2017). VCP and Msp1 both belong to the group of ATPases associated with diverse cellular activities (AAA) (Hanson and Whiteheart, 2005; Yedidi et al., 2017). While Msp1 is a membrane protein, VCP is a soluble protein that resides in the cytosol. However, it has been shown that VCP in addition to the cytosol localizes to the nucleus as well as to the cytosolic side of various organelles such

as the endoplasmic reticulum (ER), Golgi, mitochondria, and endosomes (Acharya et al., 1995; Latterich et al., 1995; Madeo et al., 1998; Rabouille et al., 1995; Ramanathan and Ye, 2012; Xu et al., 2011). This demonstrates that VCP is involved in a variety of pathways associated with different organelles. The molecular mechanisms underlying the interactions of VCP with different organelles are not well understood but likely are mediated by specific adaptor proteins on the organellar surface (Christianson and Ye, 2014; Ye et al., 2017).

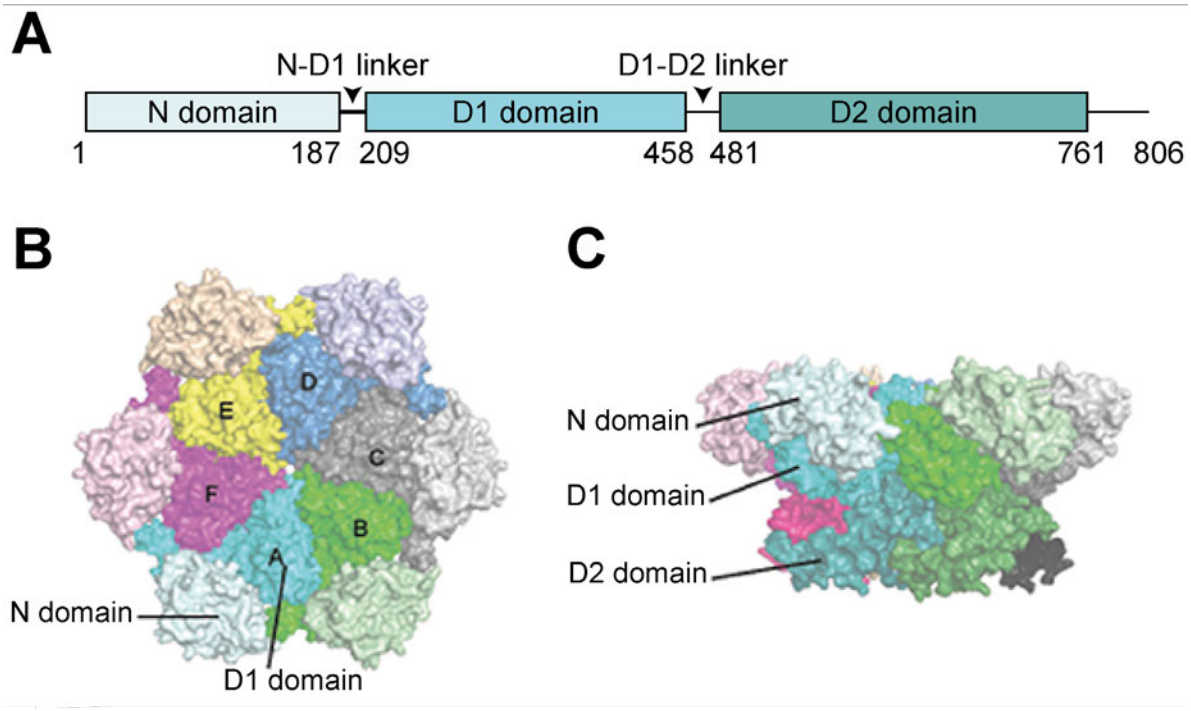

Figure 6: The structure of VCP. A) Schematic depiction of domains within VCP. D1 and D2 are both ATPase domains. B and C) Top and side view of the hexameric VCP complex in the ADP-bound form. The six subunits labelled A-F, are also indicated in colours. The colour code of the scheme in A) was applied to subunit A. (Ye et al., 2017)

Generally, VCP substrates are ubiquitinated and subjected to degradation by the cytosolic proteasome. The interaction between VCP and ubiquitinated proteins is likely also mediated by adapter proteins (Ye, 2006; Ye et al., 2017). However, a few substrates that are not subjected to proteasomal degradation were found in the controversially discussed nuclear function of VCP (Chang et al., 2021; Ndoja et al., 2014; Ramadan et al., 2007; Wilcox and Laney, 2009; Ye et al., 2017). VCP has been shown to interact with several nuclear proteins. Correct chromosomal segregation is promoted by VCP extracting the kinase Aurora B from chromatin (Dobrynin et al., 2011; He et al., 2015; Ramadan et al., 2007). Mediator of DNA damage checkpoint protein 1 (MDC1) is another VCP substrate (Chang et al., 2021). Accumulation of MDC1 was observed in cells lacking a functional VCP, leading to expansion of the nucleus (Chang et al., 2021). But VCP is not only involved in DNA maintenance and segregation but also in transcription. It remodels repressor-promotor DNA complexes and

strips transcription factors from the DNA (Ndoja et al., 2014; Wilcox and Laney, 2009). All these pathways are located inside the nucleus and the proteins interacting with VCP are therefore not available for proteasomal degradation. Their fate after their delocalisation by VCP is not known.

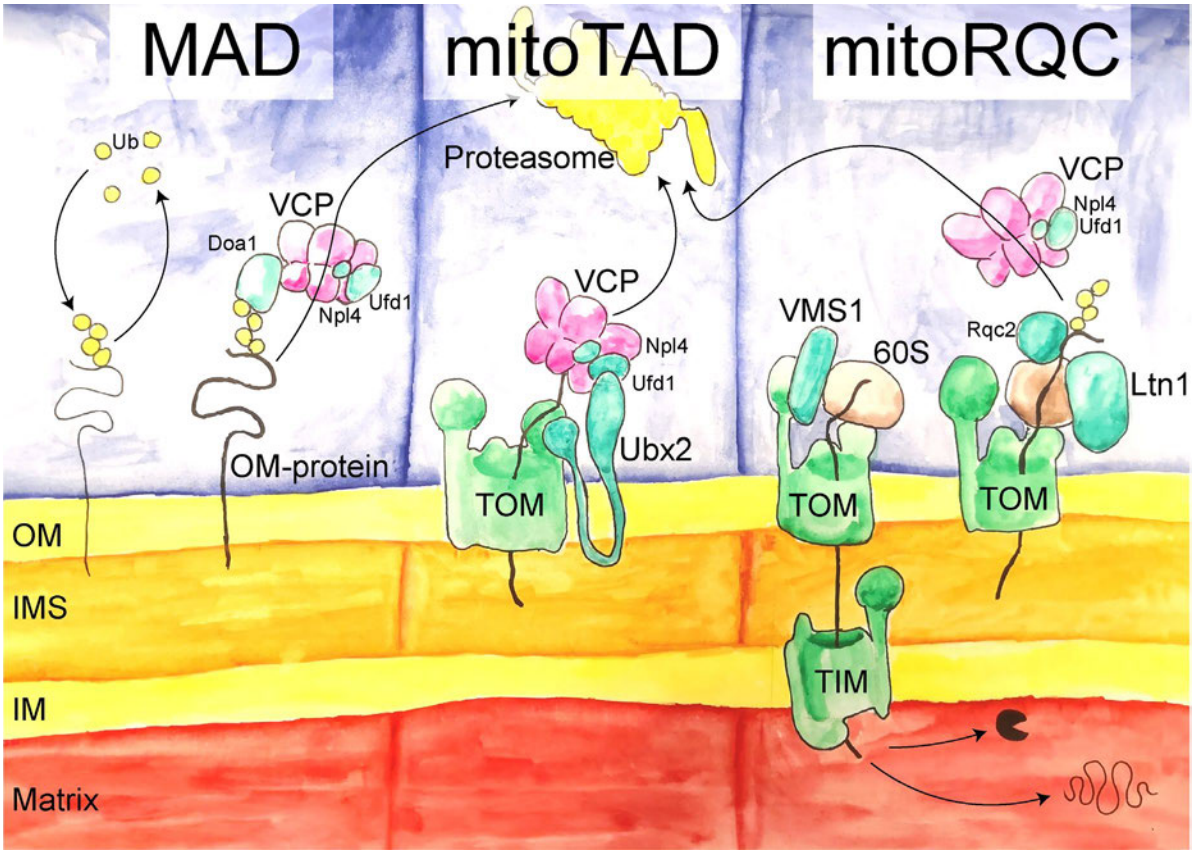

Figure 7: Schematic overview of VCP involvement in MQC pathways. Left) Mitochondria-associated degradation (MAD): Ubiquitin (Ub) is continuously covalently bound and detached from integral outer mitochondrial membrane (OM) proteins. VCP is recruited to ubiquitinated proteins by Doa1. The ubiquitinated proteins are extracted by VCP and degraded by the cytosolic proteasome (Krämer et al., 2021). Middle) Mitochondrial protein translocation-associated degradation (mitoTAD): Blockage of the translocase of the outer mitochondrial membrane (TOM) leads to the recruitment of VCP by Ubx2. VCP removes the stalled protein and delivers it to the proteasome. Right) The ribosome quality control pathway for mitochondrial polypeptides (mitoRQC) contains two alternative routes. Vms1 (left) suppresses CAT-tailing by Rqc2. This supports the import and subsequent degradation of the protein in the mitochondrial matrix. Ltn1 (right) allows ubiquitination of the CAT tailed protein, which leads to its removal by VCP followed by proteasomal degradation. (P.-C. Liao et al., 2020)

As schematically illustrated in Figure 6A, VCP contains an N-terminal N domain, and the two ATPase domains D1 and D2 that are connected by short linkers. VCP is present in a hexameric complex (Figure 6 B, C). D1 and D2 are structurally similar but contribute to different functions of VCP. While D1 is required for assembly into the hexameric complex and contributes to heat-induced activity, D2 shows ATPase activity at physiological temperatures (Song et al., 2003;

Wang et al., 2003). The N-domain is suggested to be present in two conformations, one of which allows ATP hydrolysis while the other renders the complex inactive (Niwa et al., 2012). Additionally, the N-domain has also been shown to be sensitive to pathogenic mutations (Wang et al., 2016). The C-terminus of the protein is required for the stability of the hexameric complex (Niwa et al., 2012).

There are three well described MQC pathways in which VCP extracts mitochondrial proteins and feeds them to the cytosolic proteasome: Mitochondria-associated degradation (MAD), mitochondrial protein translocation-associated degradation (mitoTAD) and the ribosome quality control pathway for mitochondrial polypeptides (mitoRQC) (Figure 7).

1.2.2.1 MAD

MAD is often described as a MQC pathway subjecting defective or mislocalized OM proteins for proteasomal degradation (Fang et al., 2015; Krämer et al., 2021). However, MAD is not very precisely defined. Therefore, the pathways summarized as “MAD” vary between authors (Krämer et al., 2021; P.-C. Liao et al., 2020; Wang and Walter, 2020). Mostly, MAD is defined as a pathway with VCP functioning in a complex alongside Npl4 and Ufd1 to remove ubiquitinated proteins from mitochondria, similar to their function in the ER-associated degradation (ERAD) pathway (Nowis et al., 2006). MAD has mainly been studied in yeast but homologous processes occur in mammals (Krämer et al., 2021; Tanaka et al., 2010). Experiments in yeast found that the VCP-Ufd1-Npl4 complex is recruited to mitochondria by Doa1 to remove various ubiquitinated OM proteins (Goodrum et al., 2019; Neutzner and Youle, 2005; Saladi et al., 2020; Wu et al., 2016) (Figure 7). OM proteins can be ubiquitinated by the E3 Ub ligases Mdm30 and Rsp5 (Fritz et al., 2003; Goodrum et al., 2019; Nahar et al., 2020). This Ub tail can be removed from proteins by the two deubiquitinating enzymes (DUBs) Ubp2 and Ubp12 (Nahar et al., 2020). The continuous cycle of ubiquitination and deubiquitination controls the abundance, and hence, the activity of various OM proteins (Fritz et al., 2003; Goodrum et al., 2019; Nahar et al., 2020).

Recent research demonstrated that IMS and matrix proteins can also be subject to VCP assisted proteasomal degradation (P.-C. Liao et al., 2020). For this process to work, retro-translocation from the matrix or the IMS, to the cytosol has to be postulated.

1.2.2.2 MitoTAD

Obstruction of the TOM complex is very harmful and demands immediate resolution. Two pathways were described that unclog the TOM translocation pore. They work with the help of either Msp1, which will be discussed later, or by VCP. The removal of stalled protein via VCP is referred to as mitoTAD (Mårtensson et al., 2019). Ubx2 bound to the TOM complex plays a pivotal role in this pathway because its exposed UBX domain functions as a binding site for VCP (Mårtensson et al., 2019). Interestingly, Ubx2 can also be found on the ER, where it is a

part of the ERAD pathway (Schuberth and Buchberger, 2005). VCP extracts and unfolds the clogged proteins, rendering the TOM complex functional again. The extracted proteins are subjected to degradation by the proteasome (Mårtensson et al., 2019). Experiments in mammalian cells have determined that the ubiquitination of precursor proteins at the TOM complex is regulated by the E3 Ub ligase March5 and the deubiquitinating enzyme USP30 (Ordureau et al., 2020; Phu et al., 2020). While ubiquitination of precursor proteins targets them for degradation, deubiquitination promotes their import (Ordureau et al., 2020; Phu et al., 2020). However, it has not yet been shown whether Mdm30, Ubp2 and Ubp12 perform a similar function in yeast (den Brave et al., 2021). Vice versa, it is yet to be determined if VCP is also involved in unclogging of mammalian TOM (den Brave et al., 2021).

1.2.2.3 MitoRQC

MitoRQC has been characterized in yeast and describes the rescue of polypeptides stalled in the cytosolic ribosome at mitochondria (Izawa et al., 2017). There are two mitoRQC pathways, dependent on the presence or absence of Vms1. Several mitochondrial proteins are imported co-translationally. Such co-translational import is facilitated by Vms1, Ltn1 and Rqc2 bound to the 60S ribosome at the OM (Izawa et al., 2017). Mistakes in this process lead to the formation of ribosome-stalled polypeptide aggregates at the OM (Shen et al., 2015). Under such conditions Rqc2 adds C-terminal alanyl/threonine residues (CAT-tails) to the stuck proteins (Shen et al., 2015). Vms1 prevents CAT-tailing by separating Rqc2 from the 60S ribosome. This promotes the import of proteins into mitochondria, where they can either be folded or are subjected to downstream intramitochondrial MQC pathways (Ng et al., 2021). In the absence of Vms1, CAT-tails can be attached to the stalled polypeptide by Rqc2. CAT-tails do not contain lysins themselves, nonetheless, they promote ubiquitination of C-terminal lysine residues of the stuck protein by the E3 ligase Ltn1 (Izawa et al., 2017; Sitron and Brandman, 2019). The ubiquitinated protein is extracted by VCP and subjected to degradation by the cytosolic proteasome (Izawa et al., 2017). Despite mitoRQC not being described in mammals yet, there are several indications that the Vms1 homolog ankyrin repeat and zinc-finger-domain-containing 1 (ANKZF1) might be involved in a similar mitochondria-associated RQC in mammals (Haaften-Visser et al., 2017; Kuroha et al., 2018; Verma et al., 2018; Yip et al., 2019).

1.2.3 Msp1 mediated MQC pathways

Similar to VCP, Msp1 is an ATPase that facilitates the degradation of nonfunctional OM proteins via the cytosolic proteasome (Wohlever et al., 2017). However, unlike soluble VCP, Msp1 is anchored in the OM by a single α-helical TMD (Wohlever et al., 2017). It can be found in the OM and on peroxisomes (Y.-C. Chen et al., 2014; Okreglak and Walter, 2014). It has

been shown that peroxisomal proteins, that are mislocalized to mitochondria, are targeted for degradation by Msp1, whereas if the same proteins are correctly localized to peroxisomes, they are not. A great variety of proteins need to be targeted for degradation by both mitochondrial and peroxisomal Msp1. It is therefore interesting to investigate how Msp1 substrates are recognized. It has been proposed that Msp1 contacts substrate proteins directly by hydrophobic amino acids in its N-domain and that Msp1 substrates contain a extraction signal that Msp1 directly recognizes if the protein is orphaned, and thus not integrated in a complex (Figure 8) (Dederer et al., 2019; Li et al., 2019; Okreglak and Walter, 2014; Weir et al., 2017). This implies that when the substrate is in a complex, the extraction signal is shielded by interacting proteins. The extraction signal is likely a hydrophobic region in proximity to the transmembrane domain (TMD) of substrate proteins (Li et al., 2019). However, among all identified Msp1 substrates, Pex15 is the only protein that contains a clear extraction signal of this type, it is therefore clear that other recognition mechanisms exist (Wang and Walter, 2020). Msp1 might not always require specific extraction signals, the mere presence as an orphaned protein in the organellar membrane might be sufficient to trigger Msp1-assissted degradation of the protein (Dederer et al., 2019; Wang and Walter, 2020).

The mechanisms of AAA ATPases such as Msp1 have been studied intensively (Augustin et al., 2009; Hanson and Whiteheart, 2005). AAA ATPases classically contain an N-domain followed by one or two AAA domains. While the ATPase AAA domains are highly conserved and convert ATP hydrolysis to a mechanical force, the N-domains responsible for substrate recognition are much less conserved (Puchades et al., 2020).

The N-domain of Msp1 consists of a TMD and a linker domain (LD) (Figure 8 A). It allows recognition and extraction of a diverse set of substrates (L. Wang et al., 2020; Wang and Walter, 2020). The LD domain consists of two α-helices (α0 and α1) and two loops (L1 and L2). α0 and L1 form a fishhook-shaped structure, similar to the one in katanin, another AAA protein (Figure 8 A) (Wang and Walter, 2020; Zehr et al., 2017). It has been suggested that the melting and refolding of α0 allows Msp1 to dynamically adapt during translocation of substrates (Wang and Walter, 2020). Like other AAA ATPases, Msp1 functions in a hexameric complex. Whether Msp1 in the OM assembles into a complex only upon the binding of a substrate or whether the substrate is recruited to preassembled Msp1 hexamers is presently unknown (Wang and Walter, 2020; Wohlever et al., 2017).

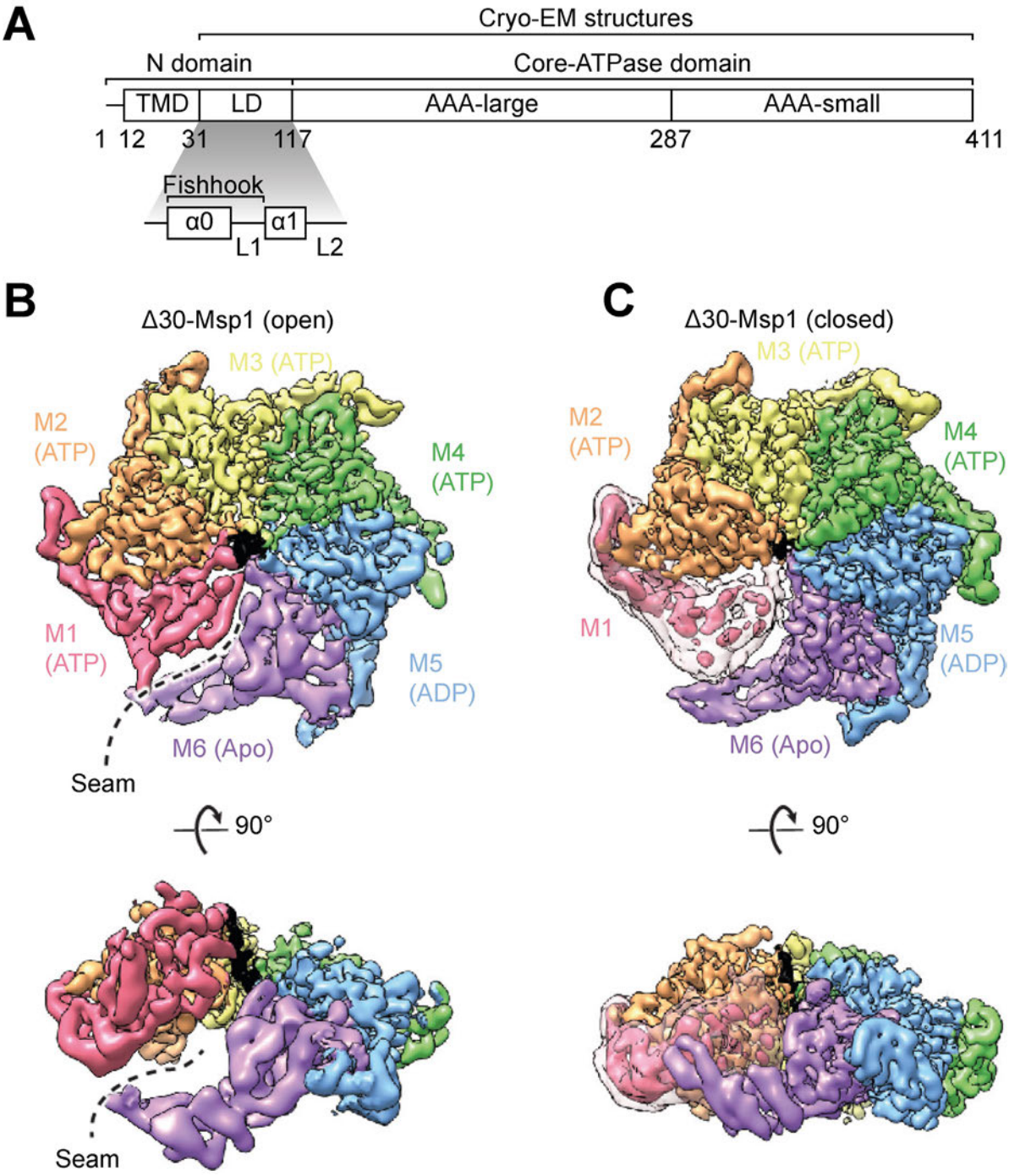

Figure 8: Structure of the Msp1 hexamer. (A) Schematic representation of domains and structural elements within *Chaetomium thermophilum* Msp1. (B, C) Cryo-electron microscopy, top and side view of the *C. thermophilum* Msp1 hexameric complex in open and closed conformation, respectively. Both structures lack 30 amino acids on the N terminus consisting of the TMD. Msp1 subunits (M1 – M6) are shown in different colours, while the substrate is depicted in black. ATP, ADP, and Apo in brackets indicate the nucleotide bound to the subunit. Apo means that there is no nucleotide bound. The dashed line indicates the spiral seam of the open conformation. In B, subunit M1 is depicted with two colours indicating two different thresholds: solid pink indicates σ = 5.3 which is also how the other subunits are displayed, translucent pink indicates σ = 2.5. This suggests that M1 does not dissociate from the complex completely but is rather flexible (L. Wang et al., 2020; Wang and Walter, 2020).

Using cryo-electron microscopy (EM) the structure of a N-terminally truncated *Chaetomium thermophilum* Msp1 (Δ30-Msp1) hexameric complex with a peptide substrate was resolved (L. Wang et al., 2020). An open and a closed complex conformation was observed (Figure 8 B, C) (L. Wang et al., 2020). The open conformation is characterized by an open seam between the M1 and M6 subunits forming a right-handed open spiral (Figure 8 B). If the Δ30-Msp1 complex is in its closed conformation, the seam of the spiral is closed by subunit M1 (Figure 8 C). In the closed state, the M1 subunit has a low cryo-EM density, which suggests that M1 is flexible and present in a variety of states (Wang and Walter, 2020). The investigated Δ30-Msp1 hexamer contained a 10 amino acid peptide in the central cavity (Figure 8 B, C, indicated in black). This short peptide probably originated from *Escherichia coli* and copurified with Δ30-Msp1 (L. Wang et al., 2020).

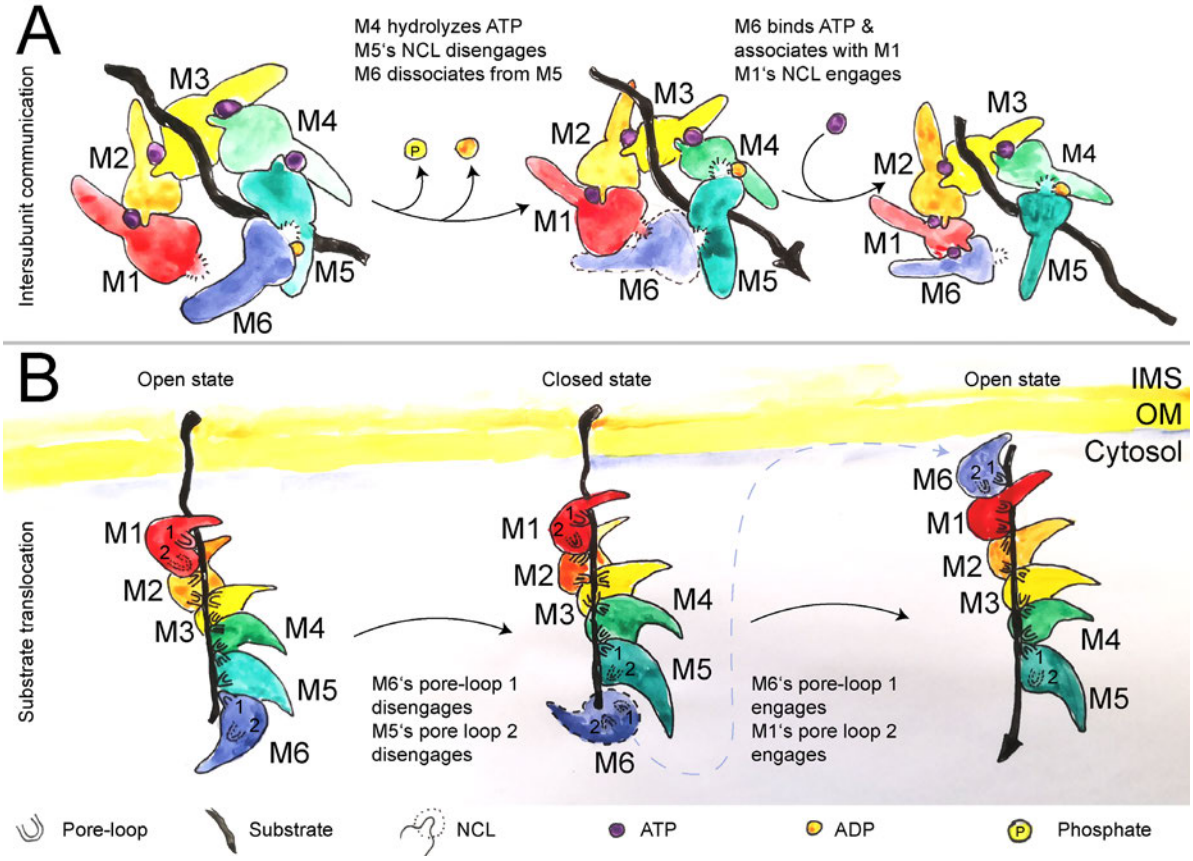

Figure 9: Schematic depiction of Msp1 extracting a peptide. The mechanistic model for Msp1 extraction contains three major steps as illustrated. This model was developed based on the EM data shown in Figure 8, therefore the transmembrane domains (TMDs) of Msp1 are not shown. A) Schematic depiction of nucleotide communication loop (NCL) that mediates communication between the six Msp1 subunits. Dislodged NCLs are outlined with dashed lines. The disordered subunit in the closed state is also outlined with dashed lines. B) Schematic depiction of substrate translocation during Msp1 extraction from the OM. Illustrated are the disengagement of M6's pore-loops 1 and two and the subsequent engagement of them at the M1 position. The disordered subunit as well as the disordered pore-loops are outlined in dashed lines. (L. Wang et al., 2020)

The detection of two different conformations of the Δ30-Msp1 complex raises the question of the function of these two distinct states. A possible explanation is that in the open conformation, Msp1 is ready to integrate substrates into the middle of the hexamer through the open seam (Wang and Walter, 2020). This would favour the model of a preassembled Msp1 complex. Furthermore, it has been suggested that Msp1 alternates between open and closed conformation during the extraction of substrate proteins (Figure 9) (L. Wang et al., 2020).

Msp1 is a key player in two further MQC pathways: The Msp1-linked MAD pathway and the mitochondrial compromised import response (mitoCPR).

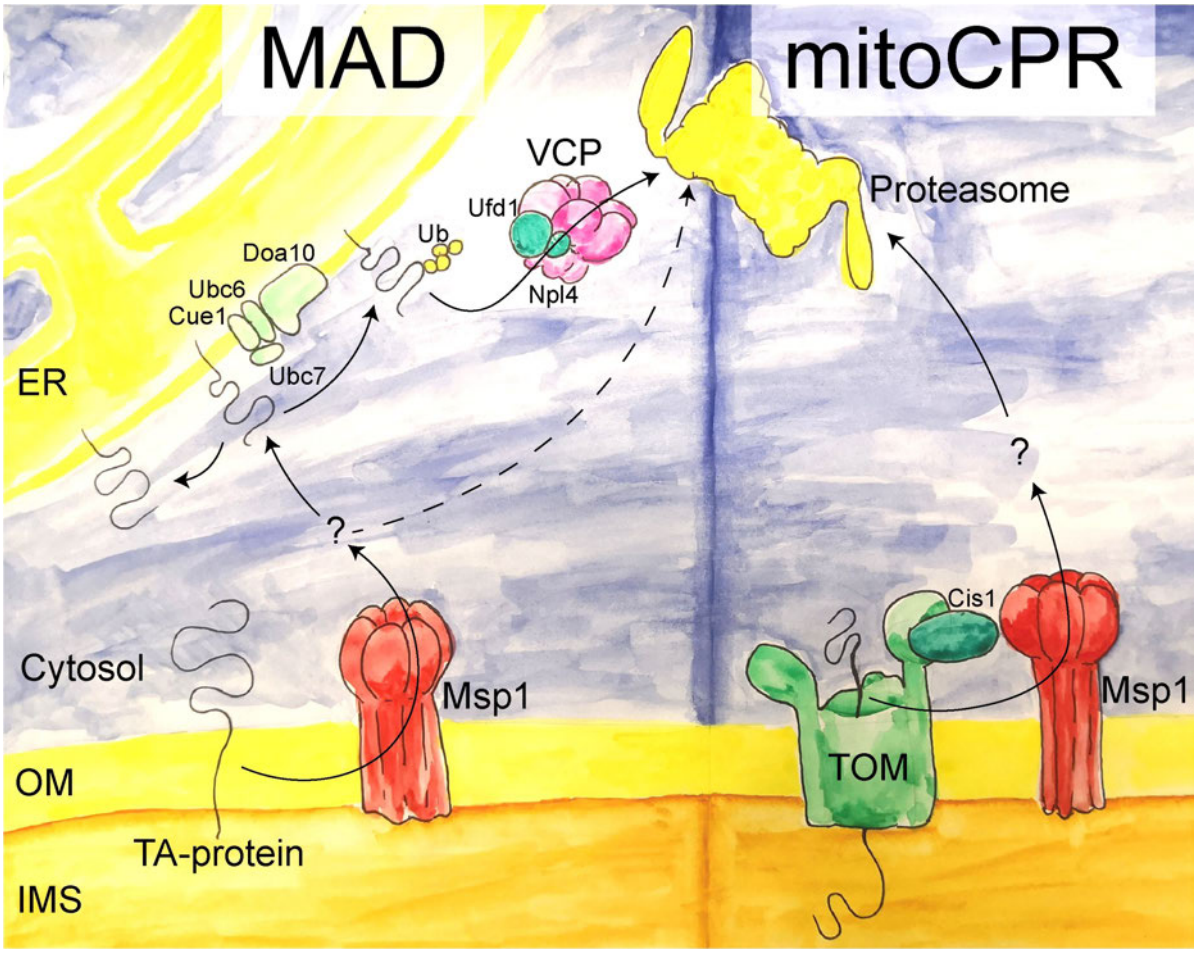

Figure 10: Schematic overview of Msp1 involvement in MQC pathways. Left) Schematic depiction of the Msp1-dependent mitochondria-associated degradation (MAD) pathway. Msp1 extracts tail-anchored (TA) proteins from the OM. They are transferred to the endoplasmic reticulum (ER) where they either travel to their correct target organelle or targeted for degradation via the ERAD machineries. Right) Schematic depiction of the mitochondrial compromised protein import response mitoCPR. Upon stalling of the TOM complex, Msp1 is recruited via Cis1. Msp1 is capabale of extracting stalled precurser proteins from the TOM complex and forwarding them to the proteasome for degradation. The molecular mechanisms of how proteins are targeted to the proteasome have yet to be determined.

1.2.3.1 MAD

Msp1 removes mislocalised tail anchored (TA) proteins from the OM in a pathway that is also referred to as MAD (Y.-C. Chen et al., 2014; Okreglak and Walter, 2014). It is an alternative pathway to the previously discussed VCP-linked MAD pathway. The Msp1-linked MAD pathway has been suggested to remove mislocalized TA proteins from the OM, before they are reintroduced into the ER membrane from where they are either targeted towards their correct organellar localisation or subjected for degradation using the ERAD system. One example for re-localisation is the Golgi protein Gos1. Mitochondrial mis-localisation of Gos1 results in its removal from the OM by Msp1. Gos1 is then directed to the ER but escapes degradation. Instead, it is re-localised to the Golgi apparatus, which is where it normally localizes (Y.-C. Chen et al., 2014). In the case Msp1 substrates get degraded after ER targeting, they are ubiquitinated by a complex containing Ubc7, Cue1, Ubc6 and Doa10. The ubiquitinated proteins are then removed by the VCP-Ufd1-Npl4 complex and degraded by the cytosolic proteasome (Dederer et al., 2019; Matsumoto et al., 2019) (Figure 10 A). However, while this pathway was convincingly demonstrated for the Msp1 substrate Pex15Δ30, it is unclear whether all Msp1 substrates are following this route for degradation (Matsumoto et al., 2019). It seems energetically inefficient to extract the same substrate from two different membranes instead of only one. However, the possibility to correct the localisation of proteins such as Gos1 may be a big advantage for the cell (Wang and Walter, 2020). There is another challenge; it is unlikely for membrane proteins to shuttle through the cytosol without chaperones. It was therefore suggested that the OM extraction of proteins by Msp1 is connected to a membrane protein shuttling system, such as the GET pathway. However, how exactly proteins move from the OM to the ER has yet to be elucidated (Wang and Walter, 2020).

1.2.3.2 MitoCPR

As previously mentioned, mitoTAD is not the only pathway that can clear the TOM complex from stalled precursor proteins. The other pathway that clears the TOM via Msp1 is called the mitochondrial compromised protein import response (mitoCPR) and has been discovered in yeast. In this pathway the accumulation of unimported mitochondrial proteins in the cytosol triggers the expression of Cis1 (Boos et al., 2019; Weidberg and Amon, 2018). Cis1 is a soluble cytosolic protein, that interacts with Tom70 and Msp1and recruits Msp1 to stalled import complexes. Subsequently Msp1 extracts the stalled precursor protein from the import machinery allowing its proteasomal degradation (Figure 10) (Basch et al., 2020). It is not yet well understood how Msp1 gains access to the stalled intermediate. The involvement of as yet undiscovered factors seems likely (Wang and Walter, 2020). It has been shown that upon the overexpression of Cis1, Msp1 is hindered in its function of extracting mislocalized proteins (Weidberg and Amon, 2018). This indicates that Cis1 forces Msp1 to exclusively localize at the

TOM complex, preventing function outside the mitoCPR pathway (Weidberg and Amon, 2018). How extracted precursors reach the proteasome is not completely understood. Msp1 has been shown to directly interact with proteasomal subunit Rpn10 (Basch et al., 2020). This suggests that Msp1 might directly pass substrate proteins to the proteasome (Basch et al., 2020). It is worth mentioning that it is not yet known how conserved mitoCPR is, as there are no obvious Cis1 orthologs in mammals. However, it is possible that another adaptor protein might be used to connect TOM and Msp1, or that Msp1 is able to interact with TOM independent of adaptors (Wang and Walter, 2020).

Both described Msp1 pathways, MAD and mitoCPR have been characterized in yeast under stress conditions. Thus, little is known about the activity of Msp1 in the cell under physiological conditions in the absence of stress (Wang and Walter, 2020).

1.3 Mitochondrial proteases in MQC

Defective mitochondrial proteins are not exclusively degraded by the cytosolic proteasome; mitochondria harbour various proteases themselves. These mitochondrial proteases are involved in different pathways regulating mitochondrial proteostasis. However, their role is not limited to MQC. They also have a variety of crucial regulatory functions in mitochondria (Deshwal et al., 2020). However, this differentiation is difficult to make, as these functions and pathways are all interconnected. In the context of this thesis, the focus will lay solely on the MQC functions of mitochondrial proteases. Figure 11 provides an overview of different mitochondrial proteases involved in MQC. ATP-dependent proteases in mitochondria assemble into mono- or multimeric cylindrical complexes. Two of these complexes, the IMS facing-AAA (i-AAA) and the matrix facing AAA (m-AAA), are localized in the IM, while Lon protease 1 (LONP1) and CLPXP reside in the matrix (Levytskyy et al., 2017). The proteases HtrA serine peptidase 2 (HTRA2) and ATP23 metallopeptidase and ATP synthase assembly factor homolog (ATP23) reside in the IMS (Figure 11).

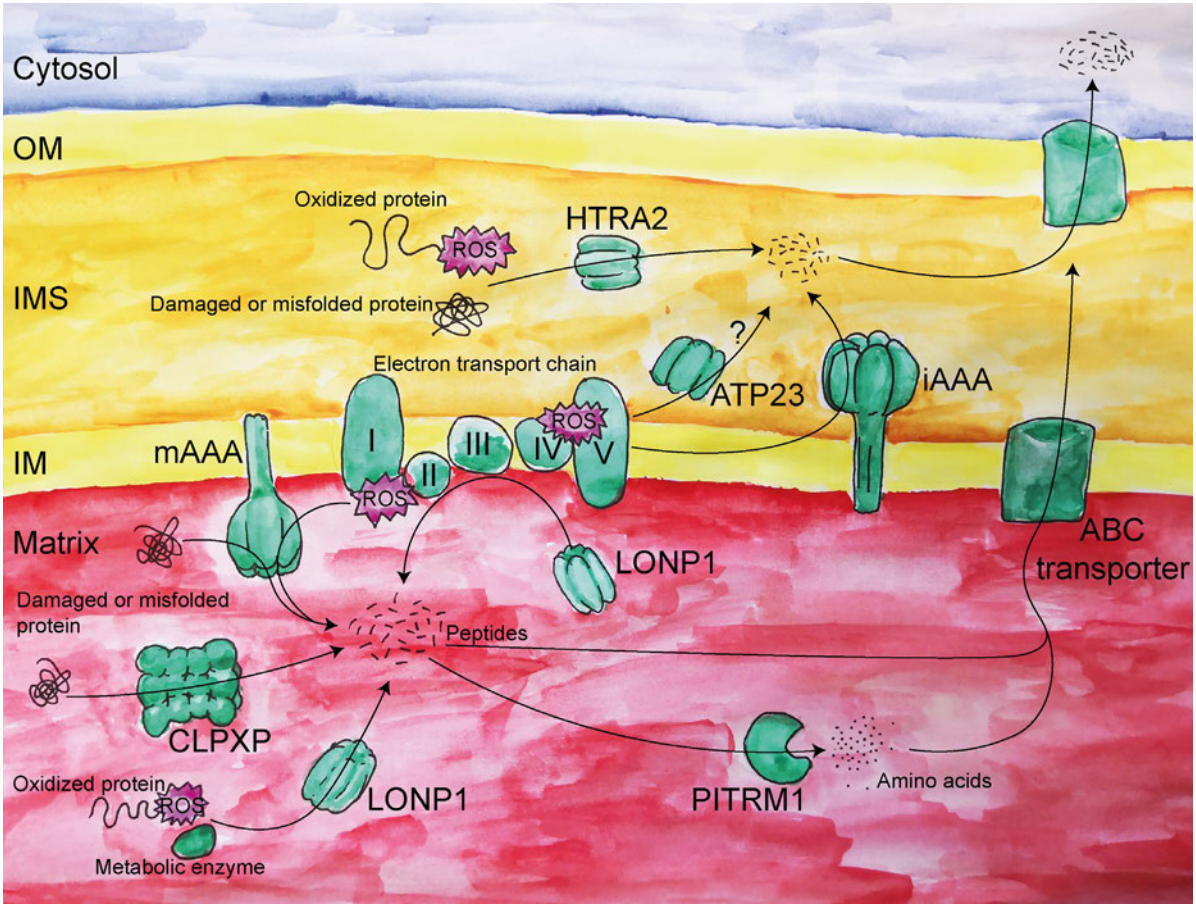

Figure 11: Mitochondrial proteases in MQC. Mitochondrial proteases degrade damaged or misfolded proteins in the IMS and the matrix. In the matrix, the m-AAA, CLPXP and LONP1 complexes monitor mitochondrial proteostasis by degrading damaged proteins and turning over metabolic enzymes. CLPXP consists of the Ser protease ATP-dependent Clp protease proteolytic subunit (ClPP) and the chaperone ATP-dependent Clp protease ATP-binding subunit ClpX-like (CLPX). The

different complexes of the electron transport chain in the IM are partially maintained by LONP1 and m-AAA. Peptides residing in the matrix that result from protein digestion, can either be exported and further be processed in the cytosol or degraded into single amino acids by the oligopeptidase presequence protease (PITRM1). In the IMS, damaged proteins can be degraded by HTRA2. The electron transport chain is maintained on the IMS side by ATP23 and i-AAA. The role of ATP23 is yet to be elucidated. Digested IMS proteins are exported as peptides to the cytosol for further digestion. (Quirós et al., 2015)

1.3.1 Quality control in the IMS

The i-AAA complex in the IM is facing the IMS and consists of six YME1L (yeast mtDNA escape 1-like) subunits (Puchades et al., 2017). The main substrates of i-AAA are membrane-embedded proteins (Stiburek et al., 2012). The high temperature requirement mitochondrial serine protease A2 (HTRA2) and ATP23 are other mitoproteases located in the IMS. The C-terminus of HTRA2 harbours a PDZ interaction motif. PDZ domains generally interact with a short region of the C-terminus of other specific proteins. Upon release into the cytosol, HTRA2 contributes to apoptosis (Hartkamp et al., 2010; Vande Walle et al., 2008). ATP23 has been primarily studied in yeast and is involved in various processes including precursor protein processing, chaperone activity and protein turnover control (Mossmann et al., 2012). Furthermore, it is a crucial element in the process of ATP synthase assembly (Osman et al., 2007; Zeng et al., 2007). Additionally, ATP23 is involved in the degradation of the IMS protein Ups1 (Potting et al., 2010). While ATP23 has been well characterized in yeast, its function in mammals remains largely elusive to date. However, the role of ATP23 is likely not conserved, as alignment of the yeast ATP23 protein sequence with fungal, animal and plant homologues revealed high amino acid variation at the N terminus of the protein (Zeng et al., 2007). Furthermore, *Arabidopsis thaliana* ATP23 cannot complement lack of yeast ATP23 in yeast (Migdal et al., 2017). The further quality control functions of ATP23 remain elusive.

1.3.2 Quality control in the matrix

The integral IM protease m-AAA is degrading proteins in the matrix. The primary substrates of m-AAA are IM proteins with a matrix exposed domain. Whether a protein is a substrate for i-AAA or m-AAA depends on whether the recognition site for the protease is on the IMS or the matrix side of the IM. In contrast to i-AAA, m-AAA subunits contain not only one but two TMDs (Leonhard et al., 2000). The IM harbours two different m-AAA isoforms containing distinct subunits. One isoform is a homo-oligomer consisting of AFG3-like subunit 2 (AFG3L2), and the other is hetero-oligomeric, composed of AFG3L2 and Paraplegin subunits (Koppen et al., 2007). The abundance of these two isoforms is cell type dependent and heteromeric complexes are more abundant in neuron cells (Koppen et al., 2007).

The soluble matrix ATPase LONP1 forms homohexameric complexes (Vieux et al., 2013). It contains three highly conserved domains: the N-terminal domain, the Walker-type AAA+ domain and the P-domain (M. Shin et al., 2021). The function of the three domains is similar to other AAA ATPases: The N-domain is used to recognize substrates, the AAA+ domain binds and hydrolyses ATP and the P domain harbours the proteolytically active site. LONP1 participates in maintaining mitochondrial proteostasis by digesting a subset of proteins (Zurita Rendón and Shoubridge, 2018). Furthermore, it is involved in the maintenance of several mitochondrial respiratory chain complexes (Besse et al., 2020; Bezawork-Geleta et al., 2014; Pryde et al., 2016). Interestingly, independent of the protease activity, LONP1 is suggested to have a chaperone-like activity in the assembly of oxidative phosphorylation (OXPHOS) complexes (Kao et al., 2015; C.-S. Shin et al., 2021; Sung et al., 2018).

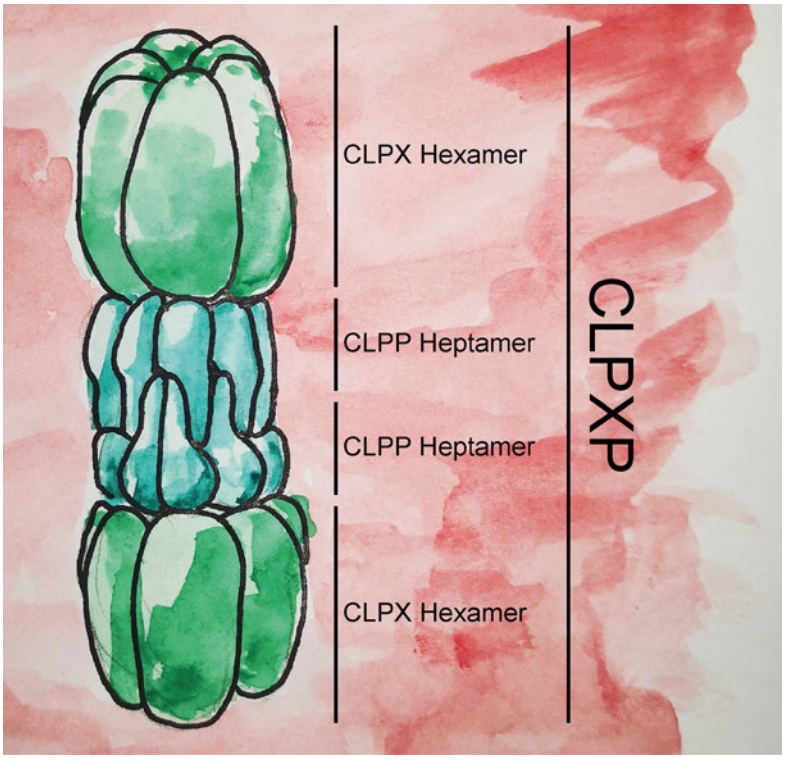

Figure 12: Schematic depiction of the CLPXP complex. The CLPP heptamers form a central barrel containing the proteolytic ceter. Each site of the CLPP barrel harbours a CLPX hexamer for the recognition and unfolding of substrates. (Lakemeyer et al., 2019)

The CLPXP complex consists of two heptamers containing proteolytic caseinolytic peptidase subunit P (CLPP) and two hexamers of caseinoltic peptidase subunit X (CLPX) (Figure 12) (Kang et al., 2005; Tremblay et al., 2020). Both CLPP and CLPX are nuclear encoded and contain an N-terminal MTS (Fischer et al., 2013). The C-terminus of CLPP is suggested to promote heptameric assembly and the interaction with CLPX (Fischer et al., 2015). CLPP can form stable homo-heptamers. However, these complexes do not possess ATPase activity and therefore cannot hydrolyse peptides longer than six amino acids (Gispert et al., 2013). CLPX can form a hexamer independently from CLPP that is stabilized by binding ATP (Stahl and Sieber, 2017). It is also known to have chaperone activity and stabilizes a number of proteins

(Kasashima et al., 2012; Nouri et al., 2020; Rondelli et al., 2021). When assembled into CLPXP, two CLPP heptamers form a central barrel with a CLPX hexamer on each end (Amor et al., 2019). While CLPX identifies and unfolds substrates, the proteolytic cavity within the centre of the CLPP barrel degrades the substrate into short polypeptides (Figure 12) (Amor et al., 2019; Sha et al., 2020). CLPXP participates in MQC by degrading misfolded or damaged proteins, and also regulates the levels of a variety of proteins in different mitochondrial pathways, including the tricarboxylic acid cycle, the respiratory chain, protein import and other metabolic processes (Al-Furoukh et al., 2014; Fischer et al., 2015; Seo et al., 2016; Stahl et al., 2018; van Ginkel et al., 2018). Interestingly, the expression of CLPXP is increased upon mitochondrial stress (Cormio et al., 2017; Wong and Houry, 2019). Furthermore, CLPXP is also linked to supporting UPR (Al-Furoukh et al., 2015; Deepa et al., 2016).

1.4 Nuclear responses to mitochondrial stress

Mitochondrial stress is resolved by a combination of pathways described previously. In order to assist the restoration of proteostasis, the cell upregulates the transcription of various proteins, which are involved in MQC. The connection between mitochondrial stress and the increased transcription of MQC components is best understood in a pathway called the mitochondrial unfolded protein response (UPR^{mt}). This pathway is triggered by mitochondrial dysfunction and leads to increased transcription of UPR^{mt} genes coding for mitochondrial chaperones, mitochondrial proteases, reactive oxygen species (ROS) detoxifying enzymes and compartments of the mitochondrial import machinery (Melber and Haynes, 2018). After translation, these proteins enter the damaged mitochondria to restore their functionality. UPR^{mt} was first discovered in mammalian cells, which upon depletion of mtDNA increased the expression of mitochondrial chaperones and proteases (Martinus et al., 1996). A similar response could be detected in cells expressing dysfunctional matrix proteins (Zhao et al., 2002). It has been suggested that the dysfunctional proteins overload the capacity of mitochondrial chaperones (Melber and Haynes, 2018; Yoneda et al., 2004). In summary, these results suggested a link between mitochondrial function and the expression of UPR^{mt} genes (Melber and Haynes, 2018). UPR^{mt} was further characterized in *Caenorhabditis elegans* as well as in mammalian cells. A variety of chemical, genetic as well as proteotoxic stress factors were demonstrated to induce the transcription of UPR^{mt} genes (Desjardins et al., 1985; Martinus et al., 1996; Yoneda et al., 2004). Additionally, compromising the function of various mitochondrial proteins involved in mitochondrial protein import, oxidative phosphorylation, coenzyme Q biosynthesis or lipid biogenesis also triggers UPR^{mt} (Baker et al., 2012; Durieux et al., 2011; Kim et al., 2016; Nargund et al., 2012; Yoneda et al., 2004).The same is also true for disruption of the electron transport chain as well as inhibition of mitochondrial ribosomes (Moullan et al., 2015; Nargund et al., 2012).

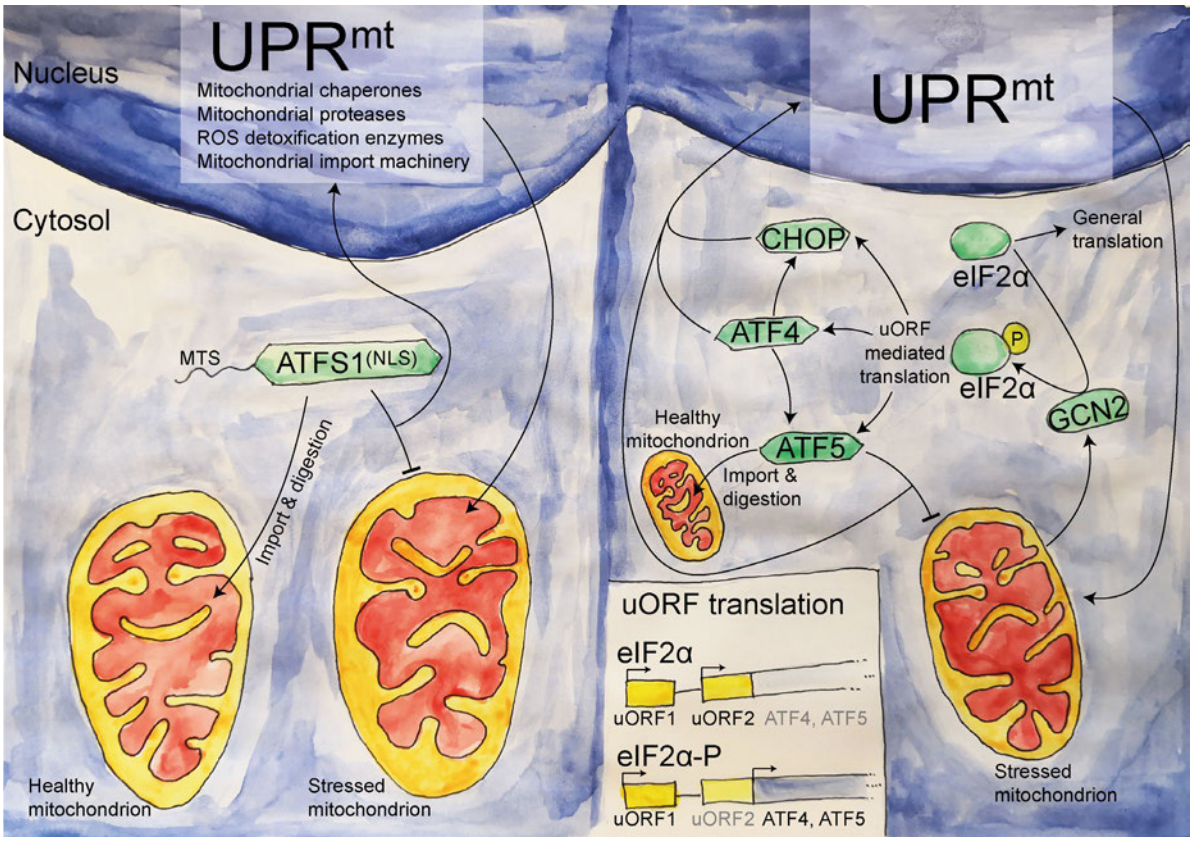

Figure 13: The mitochondrial unfolded protein response (UPR^{mt}) in *Caenorhabditis elegans* (left) and in mammals (right). Left panel: In *C. elegans* UPR^{mt} gene expression is mediated by the transcription factor ATFS1. ATFS1 harbours a mitochondrial targeting sequence (MTS) in addition to a nuclear localisation sequence (NLS). ATFS1 is imported into healthy mitochondria, where it is subsequently degraded by the LON protease in the matrix. However, if the import efficiency of mitochondria is reduced and ATFS1 fails reach mitochondria, ATFS1 is imported into the nucleus. Nuclear ATFS1 induces the transcription of UPR^{mt} genes, which include mitochondrial chaperones, mitochondrial proteases, ROS detoxification enzymes and components of the mitochondrial import machinery. The import of these factors into stressed mitochondria promote their recovery and stabilization. Right panel: In mammals the expression of UPR^{mt} genes is entangled with the integrated stress response (ISR). Mitochondrial dysfunction leads to the phosphorylation of the translation initiation factor eIF2α via GCN2, or one of the other eIF2α-specific kinases (PERK, PKR, or HRI). Phosphorylation of eIF2α activates ISR and reduces overall translation but increases the translation of mRNAs containing small upstream open reading frames (uORFs) in the 5' untranslated region (UTR). The mRNAs of the transcription factors CHOP, ATF4 and ATF5 all contain multiple such uORFs and therefore their translation is increased upon mitochondrial stress (inset). All three of these transcription factors are necessary to activate UPR^{mt} gene transcription. CHOP and ATF4 promote the transcription of ATF5. ATF5 contains an MTS as well as an NLS, similar to ATFS1 in *C. elegans*, and is therefore also monitoring mitochondrial import efficiency. The exact relationship between CHOP, ATF4 and ATF5, and the molecular principles underlaying their activity during mitochondrial stress, has yet to be elucidated. (Melber and Haynes, 2018)

1.4.1 UPR^{mt} in *C. elegans*

A multitude of factors directly control UPR^{mt}, one of which is the basic leucine zipper (bZIP) transcription factor ATFS-1 (Figure 13, left). Upon nuclear import of ATFS-1, it promotes the transcription of UPR^{mt} genes (Nargund et al., 2015). However, in addition to a nuclear localization sequence, ATFS-1 also contains a MTS (Haynes et al., 2010). Under non-stress conditions, ATFS-1 is effectively imported into the mitochondrial matrix, where it is degraded by the LON protease. Multiple forms of mitochondrial dysfunction lead to impaired mitochondrial protein import, which results in ATFS-1 not being efficiently imported into mitochondria (Narendra et al., 2010; Nargund et al., 2012; Wright et al., 2001; Wrobel et al., 2015). This leads to the nuclear localization of ATFS-1, where it activates the expression of UPR^{mt} genes (Figure 13, left). Therefore, mitochondrial import efficiency is used by the cell as a measure of mitochondrial fitness. In that sense, ATFS-1 is serving as a sensor as well as a communicator between mitochondria and the nucleus (Melber and Haynes, 2018).

However, this model raises a question: If AFTS-1 promotes the expression of UPR^{mt} genes, upon mitochondrial import deficiency, how do these proteins get inside mitochondria? There are two answers to this question. First, some of the genes that are upregulated by AFTS-1, code for components of the mitochondrial import machinery (Nargund et al., 2012). Therefore, activation of UPR^{mt} rapidly enhances the mitochondrial import capacity. Second, MTS used by mitochondrial chaperones and proteases are predicted to be more efficient than the one of ATFS-1 (Dinur-Mills et al., 2008; Fukasawa et al., 2015).

In the last decade, it has become apparent that mitochondrial stress-induced chromatin remodelling is required for UPR^{mt} activation (Lorch and Kornberg, 2015; Merkwirth et al., 2016; Tian et al., 2016). UPR^{mt} gene expression is dependent on the histone methyltransferase, MET-2, the nuclear co-factor LIN-65 and two jumonji domain histone demethylases, JMJD-3.1 and JMJD1-.2 (Merkwirth et al., 2016; Tian et al., 2016). Mitochondrial stress activates MET-2 as well as the histone demethylases (Melber and Haynes, 2018). LIN-65 and MET-2 stimulate chromatin condensation. The homeobox protein DVE-1 and the Ub-like protein UBL-5 stabilize this chromatin state and both of these proteins are also required for the activation of UPR^{mt} (Benedetti et al., 2006; Haynes et al., 2007; Tian et al., 2016). The promotors of UPR^{mt} genes are kept in a transcriptionally competent state by JMJD-3.1 and JMJD1-.2. Strikingly, these two histone demethylases are capable of inducing UPR^{mt} independent of ATFS-1 (Merkwirth et al., 2016).

Furthermore, using endocrine signalling, the activation of UPR^{mt} can also be communicated between cells and tissues. This has been studied using a variety of neuronal-specific mitochondrial stressors, which leads to intestinal UPR^{mt} (Durieux et al., 2011; Shao et al., 2016). Additionally, upon the expression of mutant huntingtin protein in neurons, serotonin

dependent UPR^{mt} was observed at other sites of *C. elegans* (Berendzen et al., 2016). These results suggest that the induction of UPR^{mt} via endocrines or mitokines could be used to coordinate the stress response between tissues. Therefore, it could also serve as an early warning system (Melber and Haynes, 2018).

1.4.2 UPR^{mt} in mammals

In mammals the bZIP transcription factor ATF5 functions analogous to *C. elegans* ATFS-1 (Figure 13, right) (Fiorese et al., 2016). In ATFS-1-less *C. elegans*, the expression of ATF5 restores the activation of UPR^{mt} (Fiorese et al., 2016). ATF4 and CHOP, which both are bZIP transcription factors as well, also contribute to the activation of UPR^{mt} (Martínez-Reyes et al., 2012; Michel et al., 2015; Quirós et al., 2017; Silva et al., 2009; Tyynismaa et al., 2010). Activity of the integrated stress response (ISR) is required for UPR^{mt} in mammals because the expression of ATF5, ATF4 and CHOP depends on it (Teske et al., 2013; Zhou et al., 2008). Phosphorylation of eIF2α by one of four kinases activates ISR (Pakos-Zebrucka et al., 2016). Each of these ISR kinases reacts to specific stressors. Triggers for ISR include unfolded proteins, double stranded RNA, heme depletion, mitochondrial stress, amino acid depletion, ROS, and ribosome stalling (Baker et al., 2012; Barbosa et al., 2013; Pakos-Zebrucka et al., 2016). While IRS supresses protein synthesis in general, it stimulates the translation of mRNAs containing small upstream open reading frames (uORFs) in the 5' untranslated region (UTR) (Figure 13, inset) (Melber and Haynes, 2018; Pakos-Zebrucka et al., 2016). Because the 5' UTR of their mRNAs contains such uORFs, ATF4, ATF5 and CHOP require eIF2α phosphorylation for their translation. Interestingly, in nematodes, UPR^{mt} functions independently of eIF2α phosphorylation (Baker et al., 2012). The exact molecular mechanisms underlaying the relationships between ATF4, ATF5 and CHOP are yet to be elucidated. In conditions unrelated to mitochondrial stress, ATF5 expression is regulated by ATF4 and CHOP (Teske et al., 2013; Zhou et al., 2008). Upon expression and nuclear localization, ATF5 can activate UPR^{mt}. Nonetheless, ATF4 and CHOP are also hypothesized to directly participate in adapting transcription to mitochondrial stress (Melber and Haynes, 2018). Interestingly, mechanistic target of rapamycin complex 1 (mTORC1) has also been suggested to participate in UPR^{mt} regulation through uORF-mediated regulation of translation. Activity of mTORC1 promotes translation, while inhibition of mTORC1 activity leads to reduced protein synthesis (Magnuson et al., 2012; Thoreen et al., 2012; Zhao et al., 2015). Increased mTORC1 activation increases ATF5 and ATF4 activity (Khan et al., 2017). The mechanisms underlaying mTORC1 stimulation during mitochondrial stress and how or whether mTORC1 is connected to the ISR to regulate UPR^{mt} are yet to be elucidated.

1.5 Mitochondrial-derived vesicles

Another control system to combat proteotoxicity is to selectively bud off damaged proteins via mitochondrial-derived vesicles (MDVs). This defence mechanism seems to be derived from the bacterial ancestors of mitochondria (Sugiura et al., 2014). MDVs are usually 50-200 nm in diameter and transport mitochondrial cargo to lysosomes and peroxisomes (Popov, 2022; Soubannier et al., 2012a). They also have crucial roles in many diseases such as myocardial ischemia, neurodegenerative diseases or cancer, to name just a few (König et al., 2021; Li et al., 2020; Matheoud et al., 2019, 2016; Poillet-Perez and White, 2021; Popov, 2022; Sugiura et al., 2014; Towers et al., 2021). MDVs can bud off as single- or double-membrane-bound vesicles upon mild oxidative stress and transport oxidized proteins to lysosomes for degradation (Figure 14) (Picca et al., 2019; Ramirez et al., 2022; Soubannier et al., 2012b). Most studies investigating MDVs have been conducted in mammals (Collier et al., 2023).

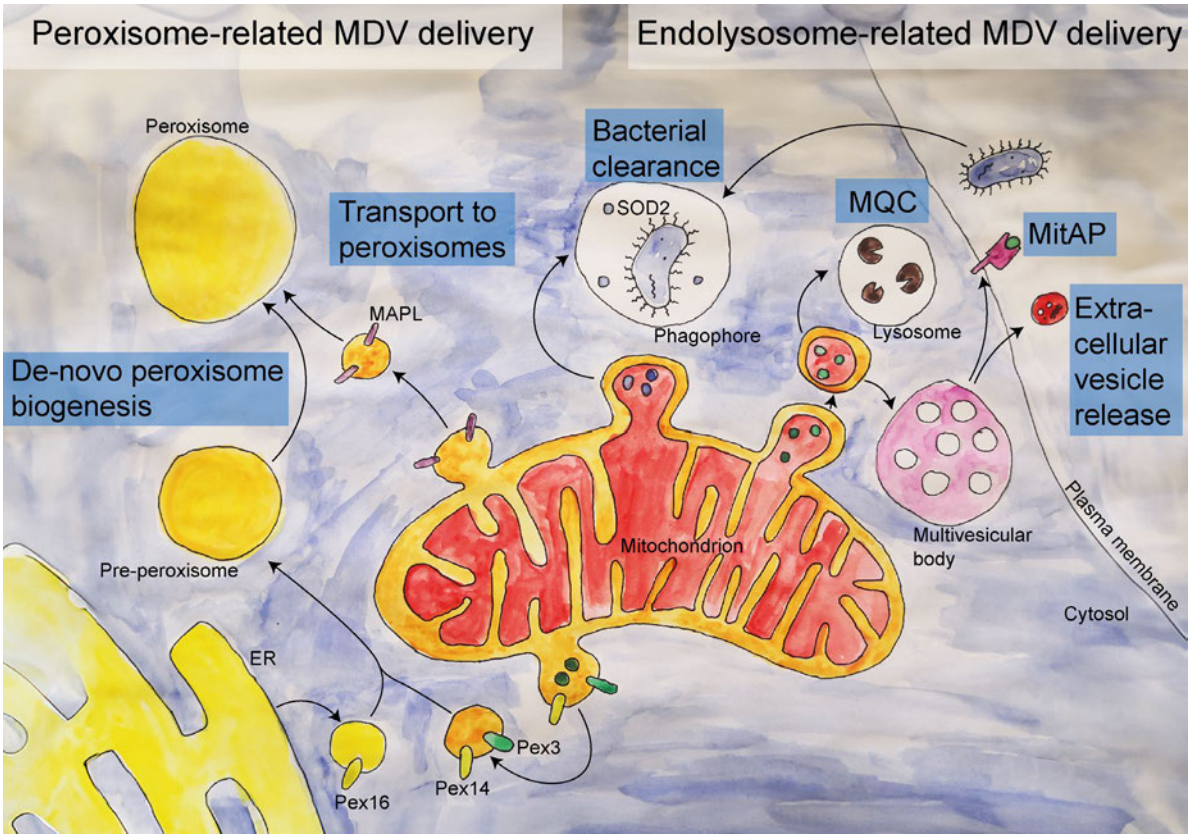

Figure 14: Schematic depiction of pathways involving mitochondrial-derived vesicles (MDVs). MDVs are used for signalling as well as for quality control and immune responses. They transport mitochondrial proteins and lipids to peroxisomes, lysosomes or multivesicular bodies. The different pathways which are utilizing MDVs are indicated in blue boxes. Abbreviations: ER (endoplasmic reticulum), MAPL (mitochondria-associated protein ligase), Pex (peroxisome biogenesis factors), SOD2 (superoxide dismutase 2), MQC (mitochondrial quality control), MitAP (mitochondrial antigen presentation). (Collier et al., 2023)

MDVs containing TOM20 are generated by tubulation of the mitochondrial membranes via mitochondrial Rho GTPases (MIRO) 1 and 2 and subsequent scission mediated by dynamin-related protein 1 (DRP1) (König et al., 2021). Alternatively, MDVs can form upon mitochondrial reconstitution of clathrin (Küey et al., 2022). Clathrin is a protein that plays a pivotal role in the formation of various vesicles by inducing budding via coating of a bulge in the membrane (Pearse, 1976; Royle et al., 2005). The pathway transporting cargo from mitochondria to peroxisomes has been demonstrated to depend on retromers (Neuspiel et al., 2008; Soubannier et al., 2012a). Retromers are large protein complexes that are also involved in shuttling membrane proteins between the Golgi and endosomes (Burd and Cullen, 2014). Additionally, there is a pathway of peroxisome-bound MDVs that generates new peroxisomes (Sugiura et al., 2017). Peroxins Pex3 and Pex14 are localized to mitochondria in the absence of peroxisomes (Sugiura et al., 2017). MDVs containing Pex3 and Pex14 fuse with ER-derived vesicles containing Pex16. Interestingly, the presence of these three proteins, which are then capable of importing other peroxisomal proteins, is sufficient to generate a new peroxisome (Figure 14) (Sugiura et al., 2017).

The ability of MDVs to selectively load and transport cargo proteins to specific compartments implies they can also function in signalling. MDVs take part in the adaptive immune response via mitochondrial antigen presentation (MitAP). They transport antigens to endolysosomes, where they are processed to be presented on the cellular surface via major histocompatibility complex (MHC) class I (Matheoud et al., 2019; Towers et al., 2021). MDVs also contribute to the innate immune system by transporting mitochondrial superoxide dismutase 2 (SOD2) to phagosomes, which helps to combat invading bacteria, and also by delivering proinflammatory mitochondrial components to lysosomes (Figure 14) (Abuaita et al., 2018; Todkar et al., 2021). Interestingly, different pathways mediate the generation of lysosome-bound MDVs under varying circumstances (Collier et al., 2023). Phosphatase and tensin homolog-induced kinase 1 (PINK1) and Parkin mediate MDVs to fuse with phagosomes or lysosomes (Abuaita et al., 2018; Ryan et al., 2020). Other mechanisms target them towards multivesicular bodies, which leads to inflammation by releasing mitochondrial damage-associated molecular patterns (DAMPs) via extracellular vesicles (Todkar et al., 2021). Thus, there is a tight connection of MDVs with the immune response (Collier et al., 2023).

1.6 Mitophagy

Defective mitochondria that despite the various MQC pathways cannot be rescued by the repair pathways mentioned above pose a threat to the cell and are targeted for mitochondrial autophagy (mitophagy) (Onishi et al., 2021). The degradation of deficient mitochondria needs to take place in a protected area of the cell because some mitochondrial components are toxic if they are released into the cytoplasm. Moreover, mitochondria are essential for the cell and missing mitochondria therefore need to be replaced. This is achieved by coupling mitophagy to mitochondrial biogenesis. The process of mitophagy can be divided into four steps (Figure 15):

1. Defective mitochondria depolarize and lose the membrane potential across the IM. This loss of the membrane potential is essential for the initiation of mitophagy.
2. Double membrane-bound autophagosomes form and finally envelope the targeted mitochondria.
3. Mitochondrial autophagosomes fuse with lysosomes.
4. Mitochondria are degraded and recycled.

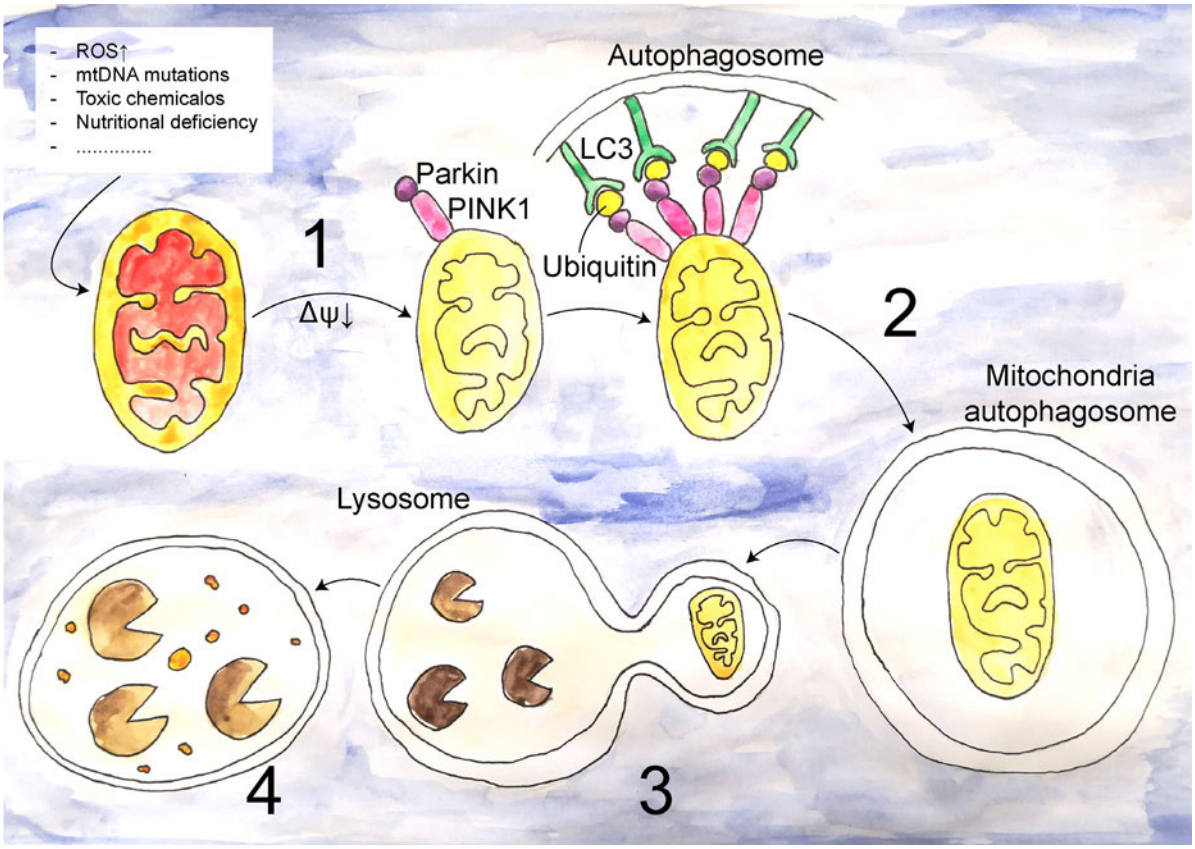

Figure 15: Schematic depiction of the major steps of the mitophagy process. (1) In order to be subjected to mitophagy, damaged mitochondria need to lose their membrane potential. (2) After induction of autophagy, the autophagosome wraps around the targeted mitochondrion. (3) Lysosomes fuse with the mitochondria autophagosome. (4) Mitochondria are degraded and recycled in this double membrane enclosed protected area.

There are a variety of pathways that can induce mitophagy. They are separated into Ub-dependent and Ub-independent pathways. The main Ub-dependent pathway used by the cell is the PINK1/Parkin pathway. Additionally, there are a couple of OM proteins that do not require Ub to interact with the microtubule-associated protein 1A/1B-light chain 3 (LC3) to form a mitochondrial autophagosome.

1.6.1 Ub-dependent mitophagy

Ub-dependent mitophagy pathways depend on the ubiquitination of proteins on the mitochondrial surface. The PINK1/Parkin pathway in mammals is the best studied such pathway (Ashrafi and Schwarz, 2013). PINK1 is highly conserved. It participates in the regulation of a variety of processes, mainly concerning mitochondrial function (N. Wang et al., 2020). In healthy mitochondria, PINK1 is imported and inserted into the IM and subsequently cleaved by the PINK1/PGAM5-associated rhomboid-like protease (PARL) (Deas et al., 2011). Upon a loss of the membrane potential, insertion of PINK1 into the IM is inhibited, leading to PINK1 accumulation in the OM. Therefore, OM accumulation of PINK1 serves as a signal for mitochondrial disfunction (Matsuda et al., 2010). This results in the activation and recruitment of the cytosolic E3 Ub ligase to mitochondria (Lazarou et al., 2015; Matsuda et al., 2010; Riley et al., 2013). PINK1 activates Parkin by phosphorylation of Parkin as well as of its substrate Ub at Ser65 (pSer65-Ub) (Kazlauskaite et al., 2015; Lazarou et al., 2015). PINK1 and Parkin cooperate in modifying mitochondria with Ub-chains. The accumulation of pSer65-Ub on the OM leads to recruitment of the autophagy receptors nuclear dot protein 52 (NDP52) and optineurin (OPTN) to the defective organelles. These receptors recruit autophagy initiation factors such as Unc-51-like kinase 1 (ULK1), Double FYVE-containing protein 1 (DFCP1) and WD repeat domain, phosphoinositide interacting 1 (WIPI1) (Lamb et al., 2013; Vargas et al., 2019). Ub-labelled mitochondria can be anchored inside the nascent autophagosome by OPTN and NDP52 which directly interact with LC3 (Padman et al., 2019; Qiu et al., 2022). Another option is to recruit autophagy receptors via Parkin assembled Ub chains and TANK-binding kinase 1 (TBK1) (Heo et al., 2018). This leads to the phosphorylation of all known autophagy receptors creating a positive feedback loop (Onishi et al., 2021).

Alternatively, PINK1 is able to directly recruit autophagy receptors OPTN and NDP52 via Ub phosphorylation independently of Parkin (Lazarou et al., 2015; Richter et al., 2016). Nonetheless, Parkin amplifies the PINK1 induced signal pathway and thus enhances mitophagy. In addition to Parkin, a number of other E3 Ub ligases, which are capable of ubiquitinating proteins at the OM, exist. These include the smad ubiquitination regulatory factor-1 (SMURF1), mitochondrial E3 Ub protein ligase 1 (MUL1) and Gp78 (Mukherjee and

Chakrabarti, 2016; Orvedahl et al., 2011). SMURF1 mediates mitophagy by facilitating the transport of autophagy factors to the nascent autophagosome (Orvedahl et al., 2011). MUL1 promotes mitophagy by mediating PINK1 stability in the OM (Igarashi et al., 2020). Gp78 is capable of inducing mitophagy independent of Parkin by mitochondrial disruption as well as by ubiquitination (Fu et al., 2013).

1.6.2 Ub independent mitophagy

The OM harbours a number of proteins containing LC3 interacting regions (LIR), which allow them to bind LC3 independent of Ub. The main receptors in mammals are the Nip3-like protein X (NIX), B-cell lymphoma 2-interacting protein 3 (BNIP3) and FUN14 domain containing 1 (FUNDC1) (Lu et al., 2023). NIX is able to induce mitophagy through binding to LC3 via its B-cell lymphoma 2 homology (BH3) domain (Novak et al., 2010; Sandoval et al., 2008). BNIP3 also contains a BH3 domain allowing it to bind to LC3 (Schweers et al., 2007). Interestingly, it was shown in murine neurons that loss of BNIP3 leads to an increase of NIX and reduced mitophagy (Shi et al., 2014). By inhibiting mitophagy, lack off BNIP3 also leads to increased apoptosis and kidney injury (Lin et al., 2021). Induced by hypoxia, FUNDC1 is also capable of inducing parkin-independent mitophagy (Liu et al., 2012). However, another E3 Ub ligase, membrane-associated ring finger (C3HC4) 5 (MARCH5) is regulating FUNDC1 via Ub-dependent degradation (Chen et al., 2017). Additionally, receptor-interacting serine/threonine-protein kinase 3 (RIPK3) can inhibit FUNDC1 induced mitophagy and thus promote apoptosis (Zhou et al., 2017).

1.7 *Trypanosoma brucei*

The unicellular parasite *Trypanosoma brucei* was discovered 1894 while studying cattle suffering from “Nagana”, in southern Africa (Joubert et al., 1993). Shortly after its discovery, the parasite was also identified as the causative agent of African sleeping sickness in humans, also called human African trypanosomiasis. *T. brucei* is transmitted via bites of the bloodsucking Tsetse fly (genus *Glossina*) (Figure 16) (Balfour, 1912; Stitt and Strong, 1944). The first stage of African sleeping sickness leads to fever, headache, itchiness, and joint pain, and is followed by a second stage in which trypanosomes cross the blood brain barrier and induce neurological symptoms such as confusion, poor coordination, numbness, and disturbance of the sleep cycle (Brun et al., 2010; Büscher et al., 2017; Kennedy, 2013). Since their discovery, trypanosomes have been intensively studied because the diseases they cause in humans and livestock are invariably fatal, if left untreated (Batista et al., 2011; Kennedy, 2013). Thus, there are great medical as well as economical interest to study these parasites in order to find new drugs, develop vaccines or establish vector control measurements (Saini et al., 2017).

T. brucei contains three morphologically identical subspecies:

1. *T. brucei gambiense* which is the main causative agent of human African trypanosomiasis, accounting for over 92% of cases (Barrett et al., 2003). Infection with this subspecies leads to a slow and chronic from of trypanosomiasis in humans. While *T. b. gambiense* mainly infects humans, it has been reported to also infect wildlife and livestock (Büscher et al., 2017; Molyneux, 1973).
2. *T. brucei rhodesiense* which infects vertebrates including humans, leading to a fast acute form of human trypanosomiasis. This subspecies is highly zoonotic, with animals harbouring the main reservoir (Barrett et al., 2003; Franco et al., 2014).
3. *T. brucei brucei*, which in contrast to the other two subspecies is unable to infect humans (Rifkin, 1984; Stephens et al., 2012).

During the last decades, *T. brucei* has been established as an important and experimentally accessible eukaryotic model system. The replicative procyclic and bloodstream form stages of the parasite can be easily cultured and genetically modified (Figure 16). Therefore, in addition to their clinical importance, they are used as a model organism for eukaryotic cell biology. As a parasite with two different hosts, trypanosomes have to adapt to different conditions during their life cycle (Figure 16). In the Tsetse fly there is a temperature of approximately 27°C and the parasite cells are producing their energy mainly via oxidative phosphorylation. In the mammalian host the temperature is approximately 37°C and the cells are producing energy mainly by glycolysis (Nare et al., 2023; Smith et al., 2017). This explains the larger volume of

the single mitochondrion in procyclic and epimastigote forms compared to the bloodstream forms (Figure 16).

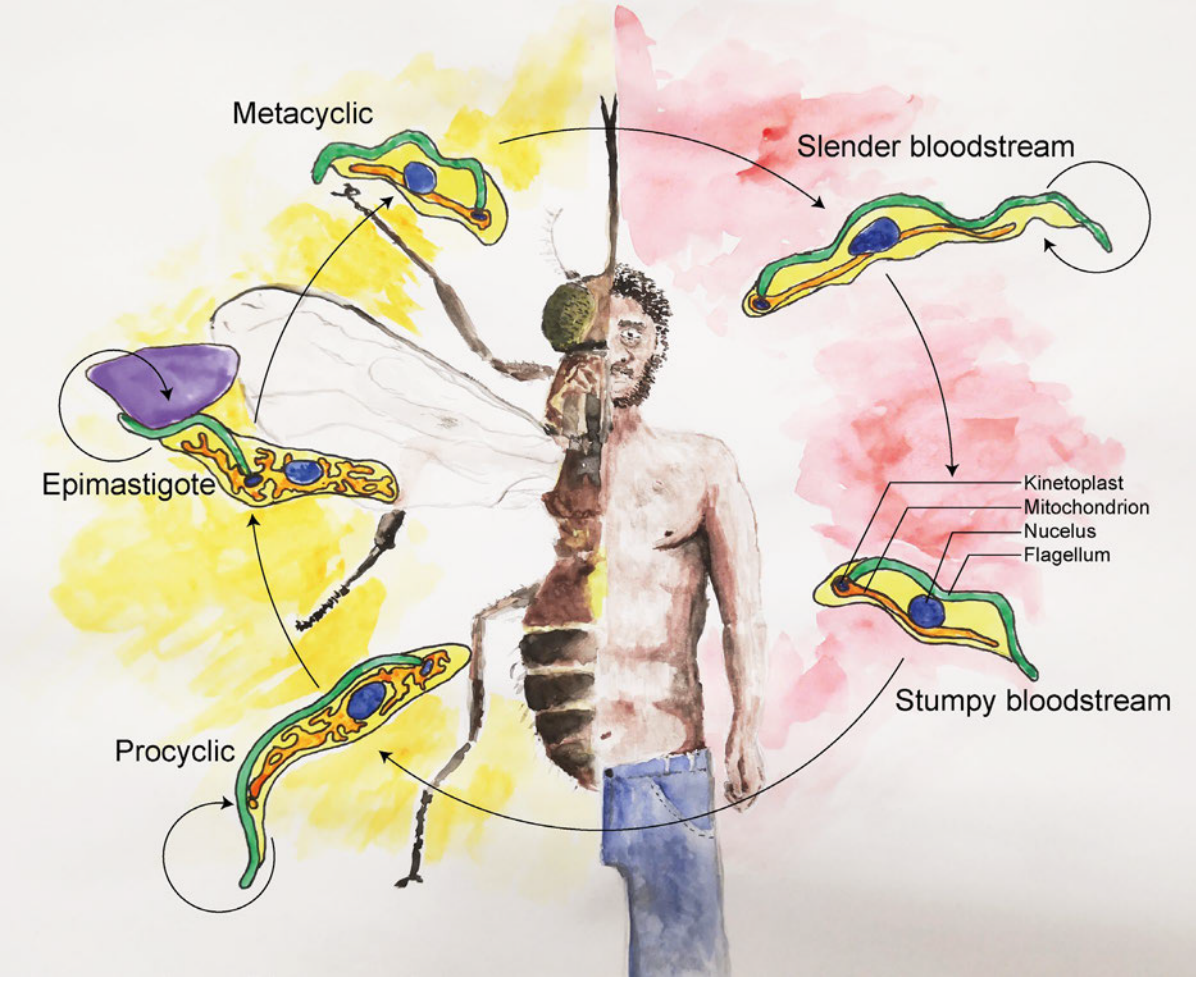

Figure 16: Life cycle of *Trypanosoma brucei* broken down to the main five stages. During its life cycle, *T. brucei* alternates between the Tsetse fly vector (left) and a mammalian host (right). Indicated by circling arrows are proliferative stages of the parasite; Procyclic and epimastigote in the fly and the slender bloodstream form in the vertebrate host. Epimastigote form trypanosomes use their flagellum to bind epithelial cells (depicted in purple) in the salivary gland of the fly. Morphological changes of the cells concerning their shape, kinetoplast position and size are indicated. Epimastigotes utilize their flagellum to adhere to epithelial cells of the salivary glands of the fly. (Wheeler et al., 2019)

Trypanosomes belong to the family of the Kinetoplastida of the Discoba clade (Figure 17) (Burki et al., 2020). This position in the eukaryotic evolutionary tree makes them an interesting organism for cell biological studies. Most other classical eukaryotic model organisms, such as mammals, zebrafish, *C. elegans*, *Drosophila melanogaster* and also yeast belong to the clade of the Opisthokonta (Figure 17) (Burki et al., 2020). This means they provide only a very narrow view of the variety of eukaryotic cell biological processes. By studying trypanosomes and comparing them to Opisthokonts, we can get a much wider view of the evolution and diversity of eukaryotic biology. All kinetoplastids have a single mitochondrion which harbours a single

mtDNA unit called kinetoplast (Jakob et al., 2016; Shapiro and Englund, 1995). The kinetoplast is attached to the flagellum via the tripartite attachment complex (TAC) (Figure 16) (Aeschlimann et al., 2023; Zhao et al., 2008).

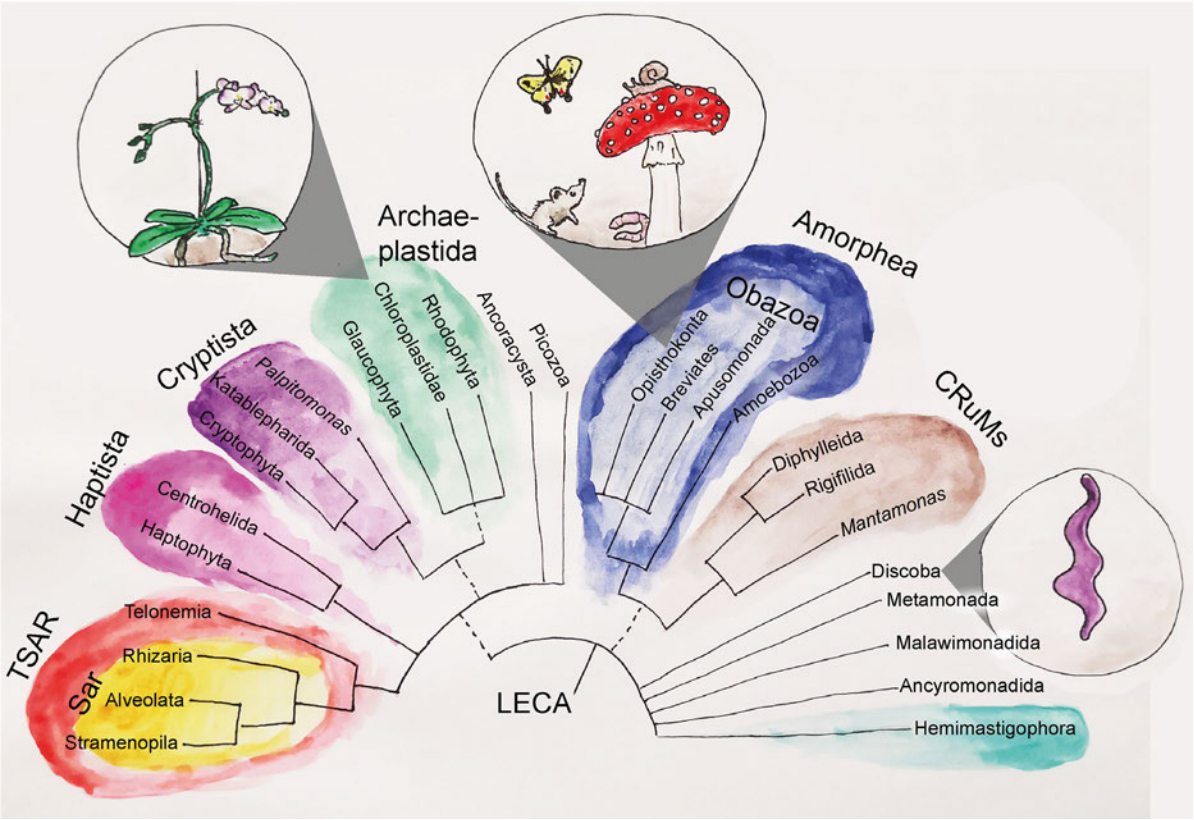

Figure 17: The evolutionary tree of eukaryotes. All eukaryotes are descendants of the last eukaryotic common ancestor (LECA). The coloured groupings indicate the current 'supergroups' according to Burki et al., 2020. Multifurcations indicate that the branching order in this lineage has yet to be resolved. Dashed lines indicate lesser uncertainties about whether these groups actually are monophyletic. Insets show a small selection of organisms belonging to Chloroplastidae, Opisthokonta, or Discoba. (Burki et al., 2020; Gargaud et al., 2011)

1.7.1 MQC in *T. brucei*

Even though MQC is not well studied in trypanosomes, it is likely that such mechanisms also exist. In contrast to other well studied model organisms, such as human cells or yeast, trypanosomes do not have the option to perform mitophagy because they only contain a single mitochondrion. However, trypanosomes most likely harbour a set of MQC pathways that are quite different from the known MQC mechanisms in Opisthokonts. One reason for this is the fact that transcription in the nucleus of trypanosomes is exclusively polycistronic (Clayton, 2019). This means that trypanosomes cannot transcriptionally regulate single genes. Trypanosomes are compensating this by controlling processing, translation, and degradation of mRNAs. Therefore, MQC pathways that regulate transcription in other eukaryotes need to function differently in trypanosomes. As all eukaryotes, *T. brucei* has an ubiquitin proteasome

system (Hua et al., 1996; Huang et al., 1999; Lowrie et al., 1993; Wong et al., 1992). Furthermore, orthologs of VCP as well as Msp1 were found in *T. brucei*. However, orthologs of other proteins that are involved in MQC pathways in other eukaryotes such as Npl4, Ubx2, Cue1 or Doa10 appear to be absent. Generally, orthologs of most of the other commonly identified MQC factors could not be identified in trypanosomes (Dewar et al., 2022a). While the core subunits of the mitochondrial protein import system are conserved, this is not true for many other subunits, such as the import receptors, and the architecture of the protein import translocases. Furthermore, MIM in yeast, MTCH2 mammals and pATOM36 in trypanosomes are three convergent insertases for alpha helically anchored OM proteins. Thus, many features of the protein import systems evolved independently in the different eukaryotic group. This is surprising since the function of the import system is conserved in all eukaryotes (Schneider, 2022). Therefore, it is assumed that pathways dealing with obstruction of these import pathways are examples for convergent evolution as well.

In 2022, Dewar et al. published a MQC pathway in *T. brucei* in which the ubiquitin-like protein TbUbL1 plays a pivotal role. Upon inducing an import defect by ablating the ATOM complex import receptor ATOM69, a protein of unknown function, an E3 ligase and TbUbL1 are all recruited to the mitochondrion. Interestingly, TbUbL1 normally localizes to the nucleus, but is released into the cytosol upon ATOM69 depletion. It is suggested that TbUbL1 binds non-imported mitochondrial precursor proteins and feeds them to the proteasome to counteract their aggregation in the cytoplasm (Dewar et al., 2022a). The function of this pathway under physiological conditions, as well as the exact mechanism that triggers it, have yet to be elucidated.

The *T. brucei* ortholog of Yme1 (TbYme1) harbours a duplicated TMD (Kovalinka et al., 2020). Surprisingly, this double TMD is only found in *T. brucei*, but not in other kinetoplastids such as *Trypanosoma cruzi*, *Leishmania major* or *Bodo saltans*. This additional TMD leads to the complex facing the matrix instead of the IMS. TbYme1 forms a complex with the inner mitochondrial membrane protein stomatin-like protein 2 (TbSlp2) (Serricchio and Bütikofer, 2021). This IM protein complex is suggested to have a dual role in stabilisation and degradation of mitochondrial proteins (Serricchio and Bütikofer, 2021). However, the molecular mechanisms underlaying these observations are unknown (Serricchio and Bütikofer, 2021).

The existence of an another MQC pathway in trypanosomes that clears the OM from destabilized proteins has been implied (Käser et al., 2016). It has been demonstrated that pATOM36 is required for the assembly of the ATOM complex. Upon pATOM36 ablation, the unassembled ATOM subunits ATOM46, ATOM12, ATOM14 and ATOM19 are cleared from the membrane and subsequently degraded by the cytosolic proteasome (Käser et al., 2016). This MQC pathway was characterized in detail in the present PhD thesis (Chapter 3.1). We

found, that TbMsp1 and TbVCP, the *T. brucei* orthologs of AAA ATPases involved in MQC in yeast and mammals, are both implicated in the clearance of pATOM36 substrates (Gerber et al., 2023). We focused on the role of TbMsp1 in this pathway. We showed that TbMsp1 stably interacts with four integral OM proteins, and that three of them are required for efficient TbMsp1-mediated extraction and degradation of pATOM36 substrates (Gerber et al., 2023). These findings contrast with previous studies of yeast Msp1 which functions independent of other proteins in MAD-linked pathways (Wohlever et al., 2017).

2. Aim and Hypothesis

The unicellular parasite *Trypanosoma brucei* is an interesting model organism to study mitochondrial quality control (MQC). MQC has already been intensively studied in Opisthokonts, such as yeast and mammals (den Brave et al., 2021; Ng et al., 2021). However, in trypanosomes, which belong to the Discoba and are essentially unrelated to Opisthokonts, MQC pathways are not very well studied to date. Unique features in its biology indicate that in trypanosomes MQC of the mitochondrial proteome must in some respects differ from the MQC pathways that have been described in other organisms.

Firstly, individual dysfunctional mitochondria cannot be disposed via mitophagy because there is only a single mitochondrion per trypanosome cell. Furthermore, transcription in the nucleus of trypanosomes is exclusively polycistronic, indicating that individual mRNAs cannot be transcriptionally regulated (Clayton, 2019). Therefore, pathways such as the mitochondrial untranslated protein response (UPR^{mt}), that functions via transcriptional control by the activation of specific transcription factors, cannot be operational in trypanosomes (Melber and Haynes, 2018). Moreover, even though the core components of the mitochondrial protein import systems are conserved across all eukaryotes, several components such as the import receptors or the import machinery for alpha helically anchored OM proteins, evolved convergently in trypanosomes (Bruggisser et al., 2017; Doan et al., 2020; Guna et al., 2022; Schneider, 2022). It is therefore likely that the responses to the obstruction of the trypanosomal import pathways also evolved independently. Additionally, orthologs of many MQC proteins conserved in other eukaryotes seem to be absent in trypanosomes (Dewar et al., 2022a).

Previous results in our lab have shown that a trypanosomal MQC pathway is triggered by ablation of pATOM36 (Käser et al., 2016). pATOM36 mediates biogenesis of a subset of OM proteins. It is a trypanosome-specific protein that is a functional analogue of the yeast MIM complex, which functions as an insertase for α-helically anchored OM proteins. Upon ablation of pATOM36, several ATOM complex subunits such as ATOM46, ATOM14 or ATOM19 are destabilized and degraded by the cytosolic proteasome (Käser et al., 2016).

The aim of this thesis was to analyse and characterize this novel MQC pathway that is triggered by pATOM36 ablation. Intriguingly, we could show that the pathway is mediated by the conserved trypanosomal orthologs of VCP and Msp1. Moreover, three TbMsp1-associated proteins also contribute to the activity (Gerber et al., 2023).

3. Results

3.1 A Msp1-containing complex removes orphaned proteins in the mitochondrial outer membrane of *T. brucei*

Markus Gerber[1, 2], Ida Suppanz[3], Silke Oeljeklaus[3], Moritz Niemann[1], Sandro Käser[1], Bettina Warscheid[3, 4], André Schneider[1, 5], Caroline E Dewar[1]

[1] Department of Chemistry, Biochemistry and Pharmaceutical Sciences, University of Bern, Bern, Switzerland

[2] Graduate School for Cellular and Biomedical Sciences, University of Bern, Switzerland

[3] Signalling Research Centres BIOSS and CIBSS, University of Freiburg, Freiburg, Germany

[4] Faculty of Chemistry and Pharmacy, Biochemistry II, Theodor Boveri-Institute, University of Würzburg, Würzburg, Germany

[5] Institute for Advanced Study (Wissenschaftskolleg) Berlin, Berlin, Germany

Published manuscript in Life Science Alliance, first authorship. This work is a collaborative effort of the group of Prof. Dr. André Schneider and the group of Prof. Dr. Bettina Warscheid. The group of Prof. Dr. Bettina Warscheid performed all mass spectrometry analysis. Dr. Caroline E. Dewar supervised this project.

My contributions:

- Generated data for: Figure 1 A, Figure 2, Figure 3, Figure 5, Figure S1, Figure S2, Figure S3, Figure S5, Figure S6, Figure S7, Figure S8

- Visualisation of Mass Spectrometry Data in Figure 1B, Figure 4, Figure S9 with R

- Creating all the figures in Adobe Illustrator, except Figure 6

- Conceptualization, Investigation, Methodology, Writing—original draft, Writing—review and editing

Published Online: 16 August, 2023 | Supp Info: http://doi.org/10.26508/lsa.202302004
Downloaded from life-science-alliance.org on 23 August, 2023

Research Article

TRANSPARENT PROCESS SOURCE DATA OPEN ACCESS
Life Science Alliance

Check for updates

A Msp1-containing complex removes orphaned proteins in the mitochondrial outer membrane of *T. brucei*

Markus Gerber[1], Ida Suppanz[2], Silke Oeljeklaus[3], Moritz Niemann[1], Sandro Käser[1], Bettina Warscheid[2,3], André Schneider[1,4], Caroline E Dewar[1]

The AAA-ATPase Msp1 extracts mislocalised outer membrane proteins and thus contributes to mitochondrial proteostasis. Using pulldown experiments, we show that trypanosomal Msp1 localises to both glycosomes and the mitochondrial outer membrane, where it forms a complex with four outer membrane proteins. The trypanosome-specific pATOM36 mediates complex assembly of α-helically anchored mitochondrial outer membrane proteins such as protein translocase subunits. Inhibition of their assembly triggers a pathway that results in the proteasomal digestion of unassembled substrates. Using inducible single, double, and triple RNAi cell lines combined with proteomic analyses, we demonstrate that not only Msp1 but also the trypanosomal homolog of the AAA-ATPase VCP are implicated in this quality control pathway. Moreover, in the absence of VCP three out of the four Msp1-interacting mitochondrial proteins are required for efficient proteasomal digestion of pATOM36 substrates, suggesting they act in concert with Msp1. pATOM36 is a functional analog of the yeast mitochondrial import complex complex and possibly of human mitochondrial animal-specific carrier homolog 2, suggesting that similar mitochondrial quality control pathways linked to Msp1 might also exist in yeast and humans.

DOI 10.26508/lsa.202302004 | Received 22 February 2023 | Revised 27 July 2023 | Accepted 31 July 2023 | Published online 16 August 2023

Introduction

The mitochondrial outer membrane (OM) forms the interface between mitochondria and the cytosol, and many of its proteins have important functions in cytoplasmic-mitochondrial communication. Integral OM proteins are often α-helically anchored, and many have just a single transmembrane domain (TMD). Intriguingly, there are at least three unrelated protein factors mediating the biogenesis of α-helically anchored OM proteins in different eukaryotic clades. The mitochondrial import complex (MIM) was discovered in *Saccharomyces cerevisiae* and consists of two small proteins, Mim1 and Mim2, that are restricted to fungi (Becker et al, 2011; Papić et al, 2011; Dimmer et al, 2012; Doan et al, 2020). In the parasitic protozoan *Trypanosoma brucei*, the kinetoplastid-specific peripheral atypical protein translocase of the outer membrane 36 (pATOM36) has the same function (Käser et al, 2016; Bruggisser et al, 2017). Expression of pATOM36 in yeast lacking the MIM complex restores growth under non-permissive conditions, and vice versa, expression of the MIM complex complements the OM protein biogenesis defect in pATOM36-ablated trypanosomes (Vitali et al, 2018). In human cells, the mitochondrial animal-specific carrier homolog 2 (MTCH2) is necessary and sufficient to insert α-helically anchored membrane proteins into the OM (Guna et al, 2022). However, at least in yeast, spontaneous insertion into the OM also seems possible for some proteins (Kemper et al, 2008; Vögtle et al, 2015).

Safeguarding mitochondrial functions requires mitochondria-associated degradation (MAD) pathways that survey the OM and guarantee that its proteins are correctly targeted and assembled (Mohanraj et al, 2020; den Brave et al, 2021; Krämer et al, 2021). The highly conserved Msp1, an ATPase associated with diverse cellular activities (AAA), plays a key role in this process. It consists of an N-terminal TMD and a C-terminal AAA domain, which faces the cytosol (Nakai et al, 1993), and localises to both the OM and the peroxisomal membrane. Msp1 extracts mislocalised and/or misassembled proteins from the OM and feeds them to the cytosolic proteasome (Chen et al, 2014; Okreglak & Walter, 2014; Weir et al, 2017; Wohlever et al, 2017; Weidberg & Amon, 2018). Non-mitochondrial tail-anchored (TA) proteins, which have a single TMD at their C-terminus, can be prone to OM mistargeting under both normal and stress conditions (Kalbfleisch et al, 2007; Chen et al, 2014; Okreglak & Walter, 2014; Rao et al, 2016; Costello et al, 2017; Weir et al, 2017; Wohlever et al, 2017). The latter includes a deficient guided-entry of TA protein pathway in the ER or an impaired peroxisomal targeting machinery (Schuldiner et al, 2008; Jonikas et al, 2009; Chen et al, 2014; Okreglak & Walter, 2014). There is no

[1]Department of Chemistry, Biochemistry and Pharmaceutical Sciences, University of Bern, Bern, Switzerland [2]Signalling Research Centres BIOSS and CIBSS, University of Freiburg, Freiburg, Germany [3]Faculty of Chemistry and Pharmacy, Biochemistry II, Theodor Boveri-Institute, University of Würzburg, Würzburg, Germany [4]Institute for Advanced Study (Wissenschaftskolleg) Berlin, Berlin, Germany

Correspondence: andre.schneider@unibe.ch; bettina.warscheid@uni-wuerzburg.de; c.dewar1@lancaster.ac.uk
Ida Suppanz's present address is Max-Planck-Institute of Immunobiology and Epigenetics, Freiburg, Germany
Moritz Niemann's present address is Mattei team, EMBL Imaging Centre, Heidelberg, Germany
Sandro Käser's present address is Institute of Cell Biology, University of Bern, Bern, Switzerland

clear sequence consensus between Msp1 substrates (Chen et al, 2014; Okreglak & Walter, 2014; Weir et al, 2017; Wohlever et al, 2017; Dederer et al, 2019; Li et al, 2019). However, Msp1 recognises and extracts orphan TA proteins that are normally found in a complex, which suggests that their oligomeric state is an important determinant (Weir et al, 2017; Dederer et al, 2019). Intriguingly, mitochondrial Msp1 is not known to form stable complexes with other proteins and appears to extract its substrates from the OM without help from other proteins (Wohlever et al, 2017; Dederer et al, 2019). However, adaptor proteins may still be required for substrate selectivity or regulation of activity. For example, Msp1 is able to clear stuck precursor proteins from the TOM complex via a transient interaction with the inducible peripheral OM protein Cis1 and the TOM receptor Tom70 in response to mitochondrial protein import stress (Weidberg & Amon, 2018).

Msp1 deletion in yeast causes a mild growth phenotype only, which suggests some redundancy in OM quality control (Chen et al, 2014; Okreglak & Walter, 2014). In line with this, it was shown that under stress conditions, the AAA-ATPase VCP, a soluble cytoplasmic component of the ER-associated protein degradation system, can also extract mistargeted proteins from the OM (Heo et al, 2010). For degradation by the proteasome, proteins generally require ubiquitination. It has been shown that mislocalised proteins can be extracted from the OM by Msp1 and transferred to the ER, where they are ubiquitinated by the ER-resident E3 ligase Doa10. This allows for their extraction from the membrane by VCP and subsequent degradation by the proteasome (Dederer et al, 2019; Matsumoto et al, 2019). However, as E3 ligases normally have specific sets of substrates, this pathway might not be required for all Msp1 substrates, and some may be degraded by the proteasome without prior ubiquitination (Matsumoto et al, 2019).

Studies of mitochondrial processes, including MAD pathways, have mainly focused on yeast and mammals, which belong to the same eukaryotic supergroup of the Opisthokonts. However, a better understanding of their basic features and evolutionary history requires that these processes be studied across divergent eukaryotes. Arguably the best-studied mitochondrion outside of yeast and mammals is that of *T. brucei*. It belongs to the Discoba supergroup, which is essentially unrelated to the Opisthokonts (Verner et al, 2015; Harsman & Schneider, 2017; Schneider, 2020).

It has previously been shown that ablation of pATOM36 triggers a MAD pathway, resulting in the proteasomal digestion of destabilised pATOM36 substrates from the OM. Results of the present study, using cells depleted for Msp1 and/or TbVCP, are consistent with the notion that TbVCP and TbMsp1 contribute to this pathway. In addition, we found four integral OM proteins that interact with TbMsp1 and showed that ablation of three of them interferes with the MAD pathway in cells where TbMsp1 levels are not affected.

Results

TbMsp1 interacts with proteins of the mitochondrial OM and the glycosomes

Msp1 is highly conserved within eukaryotes, with TbMsp1 showing 34.5 and 33.5% identity to that of yeast and human Msp1, respectively. This conservation is in contrast to many other trypanosomal OM proteins, most of which are specific to kinetoplastids (Niemann et al, 2013). TbMsp1 has the expected conserved sequence motifs including the AAA domain and the Walker A and Walker B motifs required for ATP binding and hydrolysis (Figs 1A and S1). To identify TbMsp1 interaction partners and determine its intracellular localisation, we produced a cell line expressing a C-terminally in situ HA-tagged TbMsp1 variant. Digitonin-extracted crude mitochondrial fractions of this cell line were subjected to a stable isotope labelling by amino acids in cell culture (SILAC) immunoprecipitation experiment using anti-HA antibodies. TbMsp1-HA precipitated 10 proteins with enrichment factors of more than threefold (Fig 1B). From previous proteomic analyses, three were identified as OM proteins, five are glycosomal proteins, TbTsc13 showed both localisations, and Tb927.3.4500 is the cytosolic fumarate hydratase, which was hypothesised to interact with the cytosolic side of the glycosomal membrane (Colasante et al, 2006; Coustou et al, 2006; Niemann et al, 2013; Güther et al, 2014). Of the glycosomal proteins, the peroxisome biogenesis protein Pex11 (Tb927.11.11520), tyrosine phosphatase (Tb927.10.10610), glycosomal metabolite transporters GAT1 (Tb927.4.4050), and GAT2 (Tb927.11.3130) all contain TMDs (Lorenz et al, 1998; Yernaux et al, 2006; Igoillo-Esteve et al, 2011),

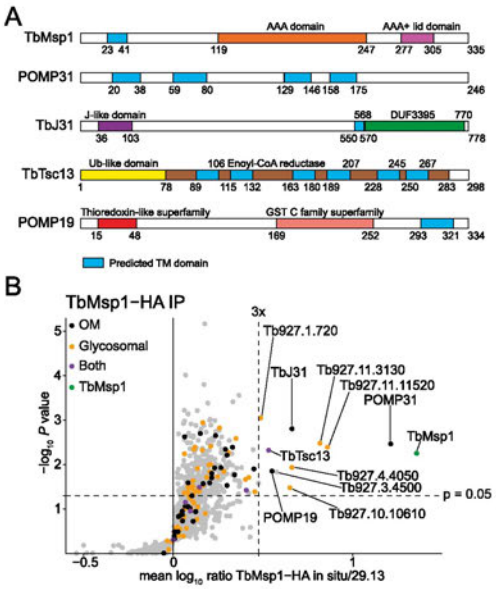

Figure 1. TbMsp1 forms complexes in the OM and glycosomes.
(A) Schematic depiction of predicted domain structures of TbMsp1 and four interacting OM proteins. The indicated domains were predicted as described in the Material and Methods section. **(B)** TbMsp1 complexes were immunoprecipitated from crude mitochondrial fractions of differentially stable isotope labelling by amino acids in cell-labelled 29.13 parent cells and cells expressing in situ tagged TbMsp1-HA analysed by quantitative mass spectrometry (n = 3). Proteins found to be significantly enriched more than threefold in TbMsp1 complexes are labelled with either their name or their accession number.

whereas phosphoglycerate kinase A (Tb927.1.720) is localised in the glycosomal lumen (Alexander & Parsons, 1993; Peterson et al, 1997).

In the present study, we focused on the four most enriched OM proteins (Fig 1). The first is the protein of the mitochondrial OM proteome 31 (POMP31), which is a kinetoplastid-specific protein of unknown function with four predicted TMDs. The second one is TbJ31, a J-like protein which has a single predicted TMD (Bentley et al, 2019). It is the homolog of mammalian DNAJC11, with which it also shares the domain of unknown function 3,395 (Muñoz-Gómez et al, 2015). The third is POMP19, a kinetoplastid-specific protein with a single TMD that contains a predicted thioredoxin-like and a predicted glutathione S-transferase domain, and the fourth is TbTsc13, which was previously detected in a proteomic study of glycosomes (Güther et al, 2014). It shows homology to the mammalian enoyl-CoA reductase of the ER elongase complex and has six predicted TMDs (Cinti et al, 1992). TbTsc13 contains a predicted ubiquitin-like domain at the N-terminus.

Cell fractionation using low concentration of digitonin results in a soluble fraction, containing the cytosol, and a crude mitochondrial fraction which also contains most of the ER marker binding protein (BiP), the glycosomal marker aldolase (ALD), and other particulate cell components (Fig S2A and B). TbMsp1-HA and its four epitope-tagged OM interactors co-fractionated with the voltage-dependent anion channel (VDAC), as would be expected for mitochondrial proteins (Fig S2A). A proteinase K protection assay furthermore showed that the mitochondria were still intact in the digitonin pellet because the intermembrane space-localised Tim9 and the matrix marker mitochondrial heat shock protein 70 (mHsp70) were protected from the added proteinase K and were only digested after the addition of Triton X-100 (Fig S2C). TbMsp1 and three interactors, on the other hand, were as proteinase K-sensitive as the atypical protein translocase of the OM 69 (ATOM69), the OM protein that serves as a control (Fig S2C). Finally, TbMsp1 and its interactors were predominantly recovered in the pellet when subjected to alkaline carbonate extraction at high pH, indicating that, in line with their predicted TMDs, they are all integral membrane proteins (Fig S2A, lower panels).

Immunofluorescence of cells expressing either TbMsp1-myc or an epitope-tagged interactor revealed a close degree of co-localisation of POMP31, TbJ31, and POMP19 with the mitochondrial marker ATOM40 (Fig S3A). As expected from the SILAC-pulldown experiment (Fig 1B) and previous analyses (Cinti et al, 1992; Güther et al, 2014), TbMsp1-myc and TbTsc13-HA are not exclusively mitochondrially localised. TbMsp1-myc, in addition to mitochondrial staining, partially co-localised with the glycosomal marker ALD (Fig S3B). The localisation of TbTsc13-HA, in line with its predicted function as an enoyl-CoA reductase, partially overlapped with the ER luminal BiP (Fig S3C).

In addition, normalised abundance profiles of untagged native TbMsp1 and its four interactors from a previous proteomic analysis with six subcellular fractions, including crude and pure OM, confirm the OM localisation of all four proteins (Fig S4) (Niemann et al, 2013).

Finally, we validated the interactions of the four proteins with TbMsp1 and between each other by immunoprecipitations using cell lines in which both Msp1 and one candidate interactor were epitope-tagged. It is important to note that expression of the tagged TbMsp1 only marginally affects growth (Fig S5). Interactions could

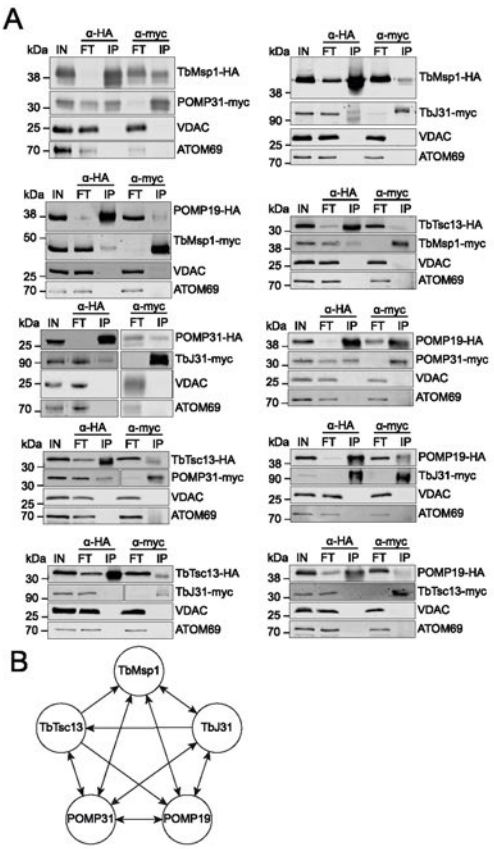

Figure 2. Reciprocal IPs reveal a TbMsp1-centric interaction network in the OM.
(A) Crude mitochondrial fractions from cells overexpressing the indicated C-terminally myc- and HA-tagged proteins were analysed by immunoprecipitation. Crude mitochondrial fractions (IN), unbound proteins (FT), and final eluates (IP) were separated by SDS–PAGE. Resulting immunoblots were probed with anti-tag antibodies and antisera against voltage-dependent anion channel and ATOM69. **(B)** Summary of the confirmed interactions detected by coimmunoprecipitation. Two-sided arrows indicate reciprocal interactions.

be confirmed between TbMsp1 and each of POMP31, TbJ31, POMP19, and TbTsc13 (Fig 2A), whereas interactions were not detected between these proteins and the most abundant OM protein, VDAC, or the α-helically anchored protein import receptor ATOM69. Using the same method, we could also detect mostly reciprocal interactions between POMP31, TbJ31, POMP19, and TbTsc13. As a further control, we subjected cell lines individually expressing tagged TbMsp1 and each of its four tagged interactors to pulldown with anti-HA and myc beads, respectively. As expected, the tagged proteins were only recovered in the pellet when using resin with matching anti-HA or myc beads; no unspecific interaction of the tagged proteins with the

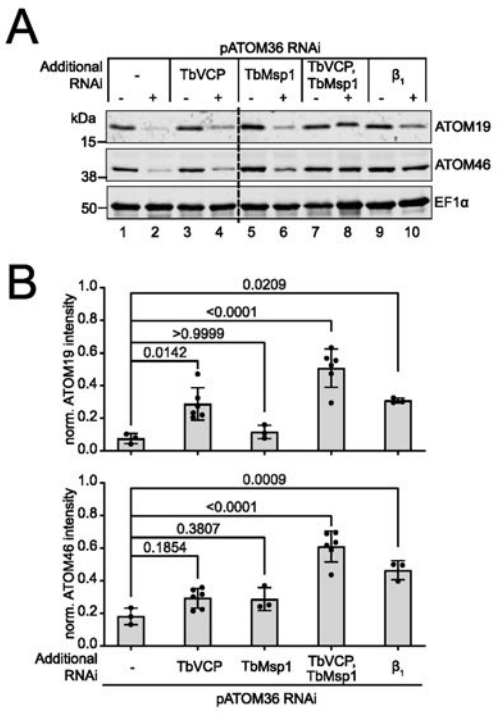

Figure 3. TbVCP and TbMsp1 are synergistically involved in the degradation of ATOM19 and ATOM46 by the cytosolic proteasome.
(A) Western blot analysis of total cellular extract (3×10^6 cells each) of the indicated uninduced and induced single, double, and triple RNAi cell lines (−/+ Tet), probed with ATOM19 and ATOM46 antisera. EF1α serves as loading control. **(B)** Quantifications of ATOM46 and ATOM19 levels in the RNAi cell lines from immunoblots shown in (A). The signal for each sample was normalised to its respective EF1α signal and then to the respective signal in uninduced cells. Data are presented as mean values with error bars corresponding to the SD (n = 3–6). The *P*-values indicated in the graph were calculated using a one-way ANOVA followed by a Bonferroni post hoc test to allow for multiple comparisons.

resin was observed (Fig S6). In summary, these results suggest that at least a fraction of all five proteins are present in the same protein complex (Fig 2B).

Finally, to investigate the importance of TbMsp1 and the four TbMsp1-interacting proteins for cell viability, we produced inducible RNAi cell lines targeting the ORFs of these proteins. However, despite the fact that the RNAi efficiently depleted the corresponding target mRNAs (Fig S7), only the RNAi cell line targeting TbTsc13 showed a clear inhibition of growth (Fig S7, bottom panel). This was expected as TbTsc13 is likely to play an essential role in fatty acid elongation, as in yeast (Kohlwein et al, 2001). Thus, within the limit of the RNAi analysis, which does not completely deplete gene products, TbMsp1, POMP19, POMP31, and TbJ31 are not essential for normal cell growth in the procyclic form of trypanosomes.

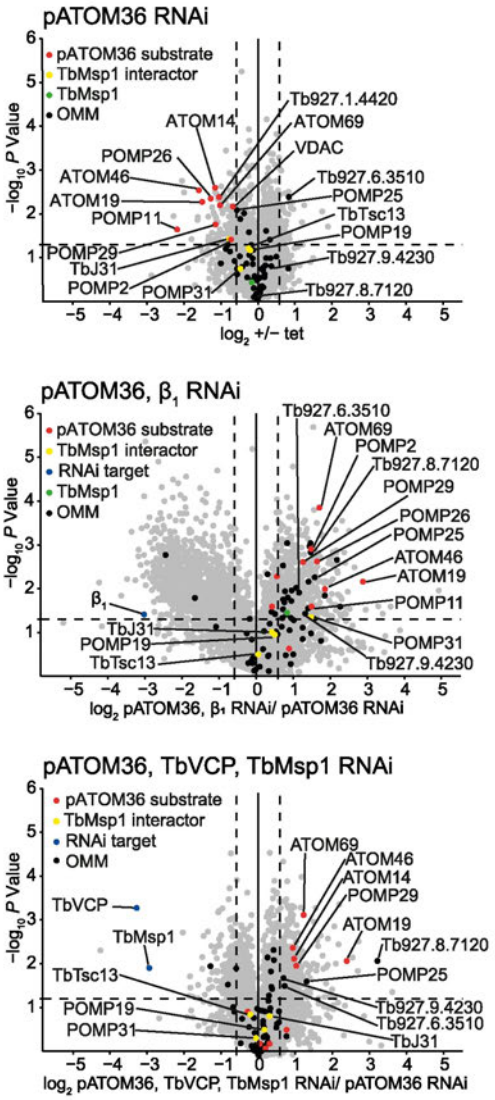

Figure 4. Proteomic analysis shows that TbVCP and TbMsp1 are involved in the proteasomal degradation of pATOM36 substrates.
Volcano plots visualising quantitative MS data of whole cell extracts from the indicated RNAi cell lines (n = 3) used in Fig 3. Relative protein quantification was based on peptide stable isotope dimethyl labelling. Shown are comparisons of uninduced and induced pATOM36 RNAi cells (top), induced pATOM36 RNAi cells and induced pATOM36/proteasome subunit β1 double RNAi cells (middle), and induced pATOM36 RNAi cells and induced pATOM36/TbVCP/TbMsp1 triple RNAi cells (bottom).

pATOM36 RNAi results in proteasomal depletion of its substrates

The biogenesis of many α-helically membrane-anchored mitochondrial OM proteins is mediated by distinct protein factors in yeast (MIM complex), humans (MTCH2), and trypanosomes (pATOM36) (Becker et al, 2011; Papić et al, 2011; Dimmer et al, 2012; Käser et al, 2016; Bruggisser et al, 2017; Doan et al, 2020; Guna et al, 2022). Moreover, for the MIM complex and pATOM36, reciprocal complementation experiments demonstrate that they are functionally interchangeable (Vitali et al, 2018). In the present study, we focussed on the proteomic consequences of pATOM36 depletion in trypanosomes. The total cellular levels of the ATOM complex subunits ATOM19 and ATOM46 were massively reduced after induction of pATOM36 RNAi (Fig 3A, lanes 1 and 2; Fig 3B), in agreement with a previous proteomic analysis of crude mitochondrial fractions of pATOM36-depleted cells (Käser et al, 2016). This was confirmed when whole cell samples of the same uninduced and induced pATOM36 RNAi cell line were compared using a proteomic analysis (Fig 4, top panel). The experiment also showed that the levels of 11 OM proteins, including ATOM19 and ATOM46, were significantly reduced by more than 1.5-fold in the induced RNAi cells (Fig 4, top panel, pATOM36 substrates). This group of proteins consists of ATOM subunits, OM membrane proteins of unknown function termed POMPs (Niemann et al, 2013), TbJ31, VDAC, and the putative ABC transporter Tb927.1.4420. Eight of them have been identified as pATOM36 substrates in a previous study (Käser et al, 2016). Moreover, Tb927.1.4420 and POMP33 were found to be depleted ~1.4-fold in the previous study which is only marginally below the threshold of 1.5-fold. Approximately two-thirds of the other proteins found to be more than 1.5-fold depleted (Fig 4, top panel) belong to the mitochondrial importome, and thus their depletion is likely an indirect consequence of reduced import because of the diminished levels of the ATOM subunits. However, whereas the level of the Msp1 interactor TbJ31 was significantly decreased by 1.7-fold, the same was not the case for TbMsp1 itself or for any of the three remaining interactors. The fact that many more non-OM proteins were detected in the present experiment compared with the previous study (Käser et al, 2016) can be explained because induction of pATOM36 RNAi was 1 d longer and because, instead of crude mitochondrial fractions, whole cellular extracts were analysed.

To test whether destabilised pATOM36 substrates are digested by the cytosolic proteasome, we produced a cell line able to knockdown both pATOM36 and the proteasomal subunit β1 (for a characterisation of all double and triple RNAi cell lines used in this study; see Fig S8). A comparison of this pATOM36/subunit β_1 double RNAi cell line with the single pATOM36 RNAi cell line by immunoblot analysis indicated that the levels of ATOM46 and ATOM19 were significantly stabilised (Fig 3A, compare lanes 2 and 10). Three-to-fivefold more ATOM19 and ATOM46 were found in cells depleted for pATOM36 and proteasomal subunit β_1 in comparison with cells only depleted for pATOM36. This was in line with data from a quantitative proteomics analysis of induced samples of the same two cell lines (Fig 4, middle panel), which showed a significant more than 1.5-fold enrichment of seven pATOM36 substrates, including ATOM19 and ATOM46, indicating that their levels were stabilised. Moreover, a number of other OM proteins not previously shown to be substrates of pATOM36 were also stabilised. We conclude from this experiment that pATOM36 depletion triggers a pathway which feeds destabilised pATOM36 substrates to the cytosolic proteasome.

TbMsp1 and TbVCP are implicated in proteasomal degradation of pATOM36 substrates

How can the cytosolic proteasome access membrane-integral pATOM36 substrates? In Opisthokonts, the AAA-ATPase Msp1 is able to extract TA proteins from the OM (Zheng et al, 2019). Thus, we decided to test whether TbMsp1 could be involved in the degradation of the integral OM proteins ATOM19 and ATOM46 in pATOM36-depleted cells using the same approach that was used to show the involvement of the proteasome. However, in contrast to the pATOM36/subunit β_1 double RNAi cell line (Fig 3A, compare lanes 9 and 10), combining TbMsp1 RNAi with pATOM36 RNAi (Fig 3A, compare lanes 5 and 6) did not significantly prevent the degradation of ATOM19 and ATOM46.

In Opisthokonts, the AAA-ATPase VCP is involved in various pathways that remove OM proteins from their membrane to allow for their degradation (Zheng et al, 2019). To find out whether TbVCP, the trypanosomal VCP homolog (Roggy & Bangs, 1999; Lamb et al, 2001), plays a similar role in the pATOM36-triggered pathway, we produced a double RNAi cell line allowing simultaneous depletion of pATOM36 and TbVCP (Fig S8). Immunoblot analyses of this cell line showed that, whereas the level of ATOM19 was slightly yet significantly stabilised upon pATOM36 and TbVCP depletion in comparison with the level found in pATOM36-depleted cells, the same was not the case for ATOM46 (Fig 3A and B). Thus, simultaneous ablation of pATOM36 and TbVCP gave essentially the same results that were observed in the pATOM36/TbMsp1 double RNAi cell line.

These results can best be explained if the depletion of one AAA-ATPase protein, TbMsp1 or TbVCP, allowed its activity to be at least partially compensated by the other. To directly test this hypothesis, we generated a triple RNAi cell line, targeting pATOM36, TbMsp1, and TbVCP simultaneously (Fig S8). With this cell line, we could show that depletion of all three proteins significantly restored the levels of ATOM19 and ATOM46 to approximately three-to-sixfold of their levels in pATOM36-depleted cells (Fig 3A, compare lanes 7 and 8). These results were independently confirmed and extended by a complementary proteomic analysis which compared the induced pATOM36 cell line (corresponding to lane 2 in Fig 3A) with the induced triple RNAi cell line depleting pATOM36, TbMsp1, and TbVCP1 simultaneously (corresponding to lane 8 in Fig 3A). In this experiment, five pATOM36 substrates and a few other OM proteins were significantly enriched more than 1.5-fold, indicating that their levels were stabilised (Fig 4, bottom panel). The simplest explanation for these results is that TbMsp1 and TbVCP have redundant, at least partially synergistic functions in the MAD pathway that lead to the degradation of pATOM36-dependent substrates.

TbMsp1 interactors contribute to the function of the MAD pathway

Using the same approach, it was possible to test whether the four mitochondrial OM proteins that we identified to be in the same protein complex as TbMsp1 played a functional role in the MAD

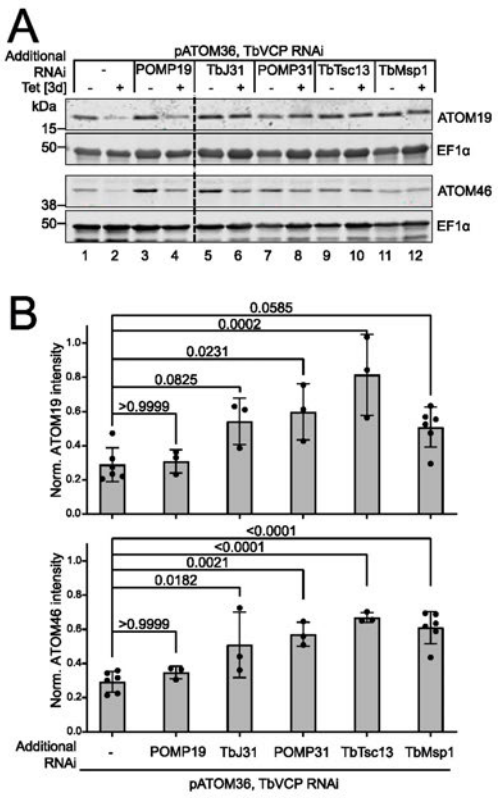

Figure 5. TbJ31, POMP31, and TbTsc13 are required for the mitochondria-associated degradation pathway triggered by the absence of pATOM36.
(A) Western blot analysis of total cellular extracts (3×10^6 cells each) of the indicated uninduced and induced double and triple RNAi cell lines (-/+ Tet), probed with ATOM19 and ATOM46 antisera. EF1α was used as a loading control. **(B)** Quantifications of ATOM46 and ATOM19 levels in the RNAi cell lines from immunoblots shown in Fig 3A. The signal for each sample was normalised to its respective EF1α signal and then to the respective level in uninduced cells. Data are presented as mean values with error bars corresponding to the SD (n = 3–6). The *P*-values indicated in the graph were calculated using a one-way ANOVA followed by a Bonferroni post hoc test to allow for multiple comparisons. Source data are available for this figure.

pathway investigated in this study. We constructed a series of triple RNAi cell lines, depleting either POMP31, POMP19, TbJ31, or TbTsc13 together with pATOM36 and TbVCP, to trigger the MAD pathway and to prevent pATOM36 substrates being degraded via the TbVCP-mediated arm of the pathway (Fig S8). Upon induction of RNAi, a significant restoration in the levels of ATOM19 and ATOM46 was detectable by immunoblot in triple RNAi cell lines where either TbJ31, POMP31, and TbTsc13 were depleted along with pATOM36 and TbVCP, in comparison with cells in which only pATOM36 and TbVCP were depleted (Fig 5A, compare lanes 2 with lanes 6, 8, 10, Fig 5B). In the case of TbJ31, only the level of ATOM46 restoration was significant. This observed restoration in the levels of ATOM19 and ATOM46 upon pATOM36, TbVCP, and either TbJ31, POMP31, or TbTsc13 depletion phenocopies the effects observed in the triple RNAi cell line targeting pATOM36, TbVCP1, and TbMsp1. This strongly suggests that TbJ31, POMP31, and TbTsc13 do not only form a complex with mitochondrial TbMsp1, but that each of the three proteins also contributes to the function in the MAD pathway triggered by pATOM36 depletion. The triple RNAi cell line depleted for POMP19 did not significantly restore the levels of ATOM46 or ATOM19, suggesting that it does not affect mitochondrial TbMsp1 activity.

Under WT conditions, Msp1 forms a complex with four interacting OM proteins (Fig 1B), three of which contribute to the activity of the MAD pathway (Fig 5). We wondered if this complex formed as a response to MAD pathway activation. We performed a SILAC-pulldown experiment of the in situ HA-tagged TbMsp1 expressed in induced pATOM36-ablated RNAi cell lines. The bait Msp1 and all four Msp1-interacting OM proteins were found to be enriched to very similar extents as in WT conditions (Fig S9). Moreover, essentially the same is the case for the glycosomal proteins. Thus, the TbMsp1-containing OM protein complex described in our study is present in both the presence and absence of pATOM36.

Discussion

We have discovered a pathway in *T. brucei* that removes destabilised α-helically anchored proteins from the mitochondrial OM. This pathway is triggered upon depletion of the OM protein biogenesis factor pATOM36 (Fig 6). Previous studies suggest that pATOM36 has two distinct functions. It mediates the integration of ATOM46 and ATOM19 into the heterooligomeric ATOM complex after the proteins have been inserted into the OM (Käser et al, 2016). However, it can also facilitate insertion of certain proteins into the OM, as was shown for POMP10 (Bruggisser et al, 2017). Removal of pATOM36 prevents integration of several ATOM subunits into the ATOM complex, leading to their degradation by the cytosolic proteasome (Fig 6). This degradation will require the selective extraction of these membrane proteins from the OM. TbMsp1 and TbVCP, the trypanosomal homologs of the Opisthokont mitochondrial quality control components Msp1 and VCP, are AAA-ATPases and therefore perfect candidates for such a job. Our results show that there is some redundancy in the system as knocking down only one of the two AAA-ATPases hardly affects the MAD pathway. Thus, this newly discovered TbMsp1 and TbVCP-linked MAD pathway likely function in safeguarding OM functions in trypanosomes, maintaining this essential interface for mitochondrial-intracellular communications.

Maintenance of protein homeostasis is essential to maintain cellular functions under both unstressed and stress conditions. Many membrane proteins in eukaryotes require selective trafficking to specific subcellular compartments and assembly into defined stoichiometric complexes before functioning. This assembly process is not 100% efficient and thus degradation of unassembled, potentially harmful complex subunits is required. Msp1 is known to extract these orphaned proteins from both the mitochondrial OM and the peroxisomal membrane, allowing their degradation by the

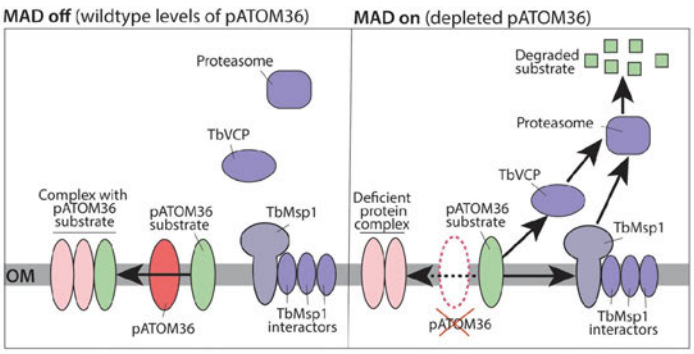

Figure 6. Schematic model of the trypanosomal mitochondria-associated degradation (MAD) pathways triggered by the absence of pATOM36.
Left panel, pATOM36 mediates the assembly of a subset of mitochondrial OM proteins (pATOM36 substrates) into their respective protein complexes. The mitochondrial fraction of TbMsp1 is constitutively associated with OM proteins (TbMsp1 interactors). Under these conditions, the described MAD pathways are not operational (MAD off). Right panel, RNAi-mediated ablation of pATOM36 triggers the MAD pathways (MAD on) that ultimately result in the proteasomal degradation of orphan pATOM36 substrates. This likely happens by parallel pathways linked to two different AAA-ATPases, the soluble TbVCP or the OM-integral TbMsp1. The TbMsp1-linked MAD pathway depends on three TbMsp1-interacting proteins for full activity.

proteasome (Chen et al, 2014; Hegde, 2014; Weir et al, 2017). In yeast, Msp1 has been shown to be sufficient for membrane protein extraction (Wohlever et al, 2017) or, in case of particular substrates, to function together with an interacting protein that is induced by a specific trigger, for example, in MitoCPR (Weidberg & Amon, 2018).

Trypanosomal TbMsp1 surprisingly forms a complex with at least four other integral mitochondrial OM proteins. Three of these interactors, POMP31, TbJ31, and TbTsc13, contribute to the activity of the MAD pathway that is triggered upon pATOM36 depletion.

Whereas POMP31 is only found in kinetoplastids, TbJ31 is an orthologue of the mammalian mitochondrial OM J-protein, DNAJC11, although it lacks a complete HPD motif and thus is a J-like protein (Muñoz-Gómez et al, 2015). TbJ31 and DNAJC11 both have a C-terminal DUF3395 domain suggested to mediate protein-protein interactions (Violitzi et al, 2019). It has also been reported that mammalian DNAJC11 may transiently interact with the mitochondrial contact site and cristae organizing system complex (Xie et al, 2007; Violitzi et al, 2019). TbTsc13 shows similarity to the enoyl-CoA reductase of the ER elongase complex (Miinalainen et al, 2003; Sickmann et al, 2003; Reinders et al, 2006; Parl et al, 2013). Interestingly, it has an N-terminal ubiquitin-like domain that is exposed to the cytosol (Uchida et al, 2021). As yet, we do not understand the specific role these TbMsp1-interacting proteins may play in the described MAD pathway. However, the notion that TbMsp1 may act in concert with a J-like protein that could directly or indirectly regulate chaperones seems plausible in this context. The same is the case for the ubiquitin-like domain of TbTsc13, which potentially could facilitate proteasome binding and activation (Collins & Goldberg, 2020).

How pATOM36 substrates are recognised by the MAD pathway is not yet understood; in particular, we do not know how these proteins can be recognised efficiently by both TbMsp1 and TbVCP. Msp1 substrate specificity is known to be multifaceted (Fresenius & Wohlever, 2019); however, as the pATOM36 substrates we focused on in this work, ATOM46 and ATOM19, are integral parts of the ATOM complex, we could hypothesise that these proteins become orphaned upon pATOM36 depletion, allowing them to become substrates of TbMsp1. Nevertheless, not all pATOM36 substrates are known to be components of multiprotein complexes. Cytosolic VCP is involved in diverse cellular processes, and its substrate specificity in other organisms is governed by its numerous cofactors, many of which interact with ubiquitin conjugated to its substrates (Buchberger et al, 2015; Escobar-Henriques & Anton, 2020). The potential requirement for selective ubiquitination cascades adds another layer of yet undefined diversity to the regulation of this process.

Understanding variations in mitochondrial biogenesis across eukaryotes can provide insight into their evolution as well as into the process of how the endosymbiotic bacterial ancestor of the mitochondrion converted into an organelle. VCP and Msp1 are conserved throughout eukaryotes and, thus, were present in the last eukaryotic common ancestor (LECA). However, the convergent evolution of known divergent OM protein biogenesis factors (pATOM36, MTCH2, and MIM) for α-helically anchored OM proteins between, and even within, distinct eukaryotic supergroups suggests that LECA did not contain a protein with this function (Vitali et al, 2018).

This is in agreement with the notion that LECA contained a much simpler β-barrel-based OM protein import system (Dolezal et al, 2006; Mani et al, 2016), whereas most additional α-helical subunits of the TOM complex, for example, the receptors, were added later after a first divergence of eukaryotes to confer specificity and efficiency of the import process (Perry et al, 2006; Mani et al, 2015, 2016; Rout et al, 2021). Thus, the role of Msp1 in removing orphan α-helical OM proteins is likely not its ancestral one. Instead, the requirement of Msp1 to clear precursor blockages in the OM protein import machinery may have evolved first (Weidberg & Amon, 2018). Whether TbMsp1 has retained this activity remains to be investigated.

Thus, the TbMsp1 function linked to surveillance of OM protein biogenesis likely arose after pATOM36 evolution, and the same is the case for the mitochondrial OM protein complex formed by Msp1 and its interactors, three of which contribute to its activity. The MAD pathway triggered by the depletion of pATOM36 is, to our knowledge, the first one to be characterised in any eukaryote that is specifically linked to defects in OM protein biogenesis.

If the emergence of pATOM36 drove the evolution of a Msp1/VCP-linked pathway to survey and maintain the integrity of its activity, did the same happen in Opisthokonts? Intriguingly, there are hints that depletion of yeast MIM or mammalian MTCH2 may drive MAD pathways. Loss of these proteins does result in depletion in the level of at least some of their substrates (Vitali et al, 2018; Guna et al, 2022),

reminiscent of the proteasomal degradation of pATOM36 substrates by the MAD pathway described here. Accumulation of orphan OM proteins is likely harmful for all mitochondria, suggesting that a pathway to deal with such proteins might be required in all eukaryotes.

We therefore expect that the independent establishment of specific OM protein biogenesis pathways in different phylogenetic groups resulted in the parallel evolution of the corresponding MAD pathways in the same groups. It is likely that these systems are also connected to the widely conserved AAA-ATPases Msp1 and VCP. Should this be the case, it will be interesting to find out whether they, as with TbMsp1, also require additional factors for full activity and, if yes, what their identity might be.

There has been much progress in defining mitochondrial quality control pathways in Opisthokonts such as yeast and metazoans. However, only very recently have studies on mitochondrial quality control expanded beyond this narrow range of eukaryotic diversity. A MAD pathway has been found in trypanosomes, a member of the Discoba supergroup, that facilitates the removal of mistargeted aggregation-prone mitochondrial proteins from the cytosol (Dewar et al, 2022a). The results suggested that the depletion of cytosolic chaperones may be a general trigger of MAD throughout eukaryotes. The present Msp1 and VCP-linked pathway is the second MAD pathway discovered in trypanosomes. Further studies in other non-classical model systems are expected to improve our understanding of the fundamental features of such pathways, which are similar not because of common descent but because all eukaryotes have to cope with the shared constraints imposed by hosting mitochondria.

Materials and Methods

Reagents and tools table.

Reagent type (species) or resource	Designation	Source or reference	Identifiers	Additional information
Cell line (*T.brucei*)	29.13, procyclic	Wirtz et al (1999)		WT
Antibody	Anti-HA (mouse, monoclonal)	BioLegend	901503 (MMS-101R)	WB (1:5,000), IFA (1:1,000)
Antibody	Anti-myc (mouse, monoclonal)	Invitrogen	132500	WB (1:2,000), IFA (1:50)
Antibody	Anti-ATOM19	Eurogentec	Polyclonal antibody against purified protein	WB (1:500)
Antibody	Anti-ATOM46	Mani et al (2015)		WB (1:500)
Antibody	Anti-pATOM36	Vitali et al (2018)		WB (1:250)
Antibody	Anti-TbVCP	Gift from Prof. James Bangs, SUNY Buffalo, US		WB (1:50)
Antibody	Anti-ALD	Gift from Paul Michels, University of Edinburgh, Scotland		IFA (1:1,500) WB (1:10,000)
Antibody	Anti-BiP	Gift from Prof. James Bangs, SUNY Buffalo, US		IFA (1:2,500) WB (1:50,000)
Antibody	Anti-TbMsp1	Eurogentec	Peptide antibody against C + DEALKRVRPSMASSV	WB (1:1,000)
Antibody	Anti-ATOM40 (rabbit, polyclonal)	Niemann et al (2013)		Bleed 1, IFA (1:1,000)
Antibody	Anti-VDAC (rabbit, polyclonal)	Niemann et al (2013)		WB (1:1,000)
Antibody	Anti-EF1α (mouse, monoclonal)	Merk Millipore	05-235	WB (1:10,000)
Antibody	Anti-cytochrome *c* (rabbit, polyclonal)	Crausaz Esseiva et al (2004)		WB (1:100)
Antibody	Anti-mitochondrial Hsp70	Niemann et al (2013)		WB (1:2000)
Antibody	Anti-ATOM69	Mani et al (2015)		WB (1:500)
Antibody	Anti-Tim9	Niemann et al (2013)		WB (1:100)
Antibody	Anti-mouse IRDye 680LT conjugated (goat)	LI-COR Biosciences	PN 926-68020	WB (1:20,000)

(Continued on following page)

Continued

Reagent type (species) or resource	Designation	Source or reference	Identifiers	Additional information
Antibody	Anti-rabbit IRDye 800CW conjugated (goat)	LI-COR Biosciences	PN 926-32211	WB (1:20,000)
Antibody	Goat Anti-mouse Alexa Fluor 596	Thermo Fisher Scientific	# A-11032	IFA (1:1,000)
Antibody	Goat Anti-rabbit Alexa Fluor 488	Thermo Fisher Scientific	# A-11008	IFA (1:1,000)
Commercial assay or kit	Prime-a-Gene labelling kit	Promega	U1100	Radioactive labelling of Northern probes
Commercial assay or kit	EZView Red Anti-c-myc affinity gel	Sigma-Aldrich	E6654	CoIP
Commercial assay or kit	Anti-HA affinity matrix	Roche	11815016001	CoIP
Commercial assay or kit	Proteinase K, recombinant, PCR Grade	Roche	3115879001	
Chemical compound, drug	Tetracycline Hydrochloride	Sigma-Aldrich	T7660	Tet
Chemical compound, drug	Digitonin	Biosynth	103203	Generation of crude mitochondrial fractions
Chemical compound, drug	PFA	Fluka	UN2213	
Chemical compound, drug	Albumin (BSA) Fraktion V (pH 7,0)	Applichem	A1391	
Chemical compound, drug	Triton X-100	Merck Millipore	108603	
Chemical compound, drug	Tween 20	AppliChem	A4974	
Chemical compound, drug	Lysine-L U-13C, U-15N (Lys8)	Euroisotop	CNLM-291-H	SILAC labelling
Chemical compound, drug	Arginine-L U-13C6, U-15N4 (Arg10)	Euroisotop	CNLM-539-H	SILAC labelling
Chemical compound, drug	Lysine-L, 4.4.5.5-D4 (Lys4)	Euroisotop	DLM-2640	SILAC labelling
Chemical compound, drug	Arginine-L 13C6 (Arg6)	Euroisotop	CLM-2265-H	SILAC labelling
Chemical compound, drug	Formaldeyde, light (CH_2O)	Sigma-Aldrich	252549	Peptide stable isotope dimehtyl labelling
Chemical compound, drug	Formaldeyde, heavy ($^{13}CD_2O$)	Sigma-Aldrich	492620	Peptide stable isotope dimehtyl labelling
Chemical compound, drug	Sodium cyano-borohydride ($NaBH_3CN$)	Sigma-Aldrich	156159	Peptide stable isotope dimehtyl labelling
Enzyme	Trypsin, MS approved	SERVA	37286	
Software, algorithm	GraphPad Prism, version 6.0 f	Graphpad software	www.graphpad.com	Depiction of growth curves and analysis of Western blot quantification
Software, algorithm	Fiji	ImageJ	Schindelin et al (2012)	Processing of images
Software, algorithm	FigureJ	ImageJ Plugin	Mutterer and Zinck (2013)	Assembly of microscopy figures
Software, algorithm	Image Studio Lite v. 5.2.5.	LI-COR Biosciences		Quantification of Western blots
Software, algorithm	Adobe Illustrator	Adobe	www.adobe.com	Figure assembly
Software, algorithm	RStudio	RStudio	www.rstudio.com	Mass spectrometry analysis, volcano plotting

Methods and protocols

Transgenic cell lines

Transgenic *T. brucei* cell lines were generated using the procyclic strain 29.13 (Wirtz et al, 1999). Cells were cultivated at 27°C in SDM-79 (Brun & Schonenberger, 1979) supplemented with 10% (vol/vol) FCS2, containing G418 (15 μg/ml; Gibco), hygromycin (25 μg/ml; InvivoGen), puromycin (2 μg/ml; InvivoGen), blasticidin (10 μg/ml; InvivoGen), and phleomycin (2.5 μg/ml; LifeSpan BioSciences) as required. RNAi or protein overexpression was induced by adding 1 μg/ml tetracycline to the medium.

To produce plasmids for ectopic expression of C-terminal triple c-myc- or HA-tagged TbMsp1 (Tb927.5.960), POMP31 (Tb927.6.3680), TbJ31 (Tb927.7.990), POMP19 (Tb927.10.510), and TbTsc13 (Tb927.3.1840), the complete ORFs of the respective gene were amplified by PCR and inserted in a modified pLew100 vector (Wirtz et al, 1999; Bochud-Allemann & Schneider, 2002) containing either a C-terminal triple c-myc- or HA-tag (Oberholzer et al, 2006). One TbMsp1 allele was tagged in situ at the C-terminus with a triple HA-tag via a PCR approach, using a pMOTag vector containing a phleomycin resistance cassette as described in Oberholzer et al (2006).

RNAi cell lines were prepared using a pLew100-derived vector with a 500 bp target gene fragment and its reverse complement present with a 460 bp stuffer in-between, generating a stem-loop construct. The RNAis targeted the indicated nucleotides (nt) of the ORF of proteasome subunit β_1 (nt 266–759), TbVCP (nt 423–896), TbTsc13 (nt 379–891), TbJ31 (nt 831–1,255), POMP31 (nt 170–568), POMP19 (nt 182–610), TbMsp1 (nt 530–940). The pATOM36 RNAi construct was previously published (Pusnik et al, 2012).

Digitonin extraction

Cell lines were induced for 16 h before the experiment to express the epitope-tagged proteins. Crude mitochondria-enriched fractions were obtained by incubating 1×10^8 cells on ice in 0.6 M sorbitol, 20 mM Tris–HCl (pH 7.5), and 2 mM EDTA (pH 8) containing 0.015% (wt/vol) digitonin for the selective solubilization of plasma membranes. Centrifugation (5 min, 6,800 *g*, 4°C) yielded a cytosolic supernatant and a mitochondria-enriched pellet. Equivalents of 1.3×10^6 cells of each fraction were analysed by SDS–PAGE and subsequent Western blotting to demonstrate organellar enrichment for proteins of interest.

Alkaline carbonate extraction

To separate soluble or peripherally membrane-associated proteins from integral membrane proteins, a mitochondria-enriched pellet was generated as described above by digitonin extraction and resuspended in 100 mM Na_2CO_3 (pH 11.5). Centrifugation (10 min, 100,000*g*, 4°C) yielded a supernatant containing soluble proteins and a pellet containing membrane fragments. Equivalents of 7.5×10^6 cells of each fraction were subjected to SDS–PAGE and immunoblotting.

Proteinase K protection assay

A mitochondria-enriched digitonin pellet from 5×10^7 cells overexpressing C-terminally tagged Msp1, POMP31, TbJ31, or TbTsc13 was generated as described above. The pellet was resuspended in 250 mM sucrose, 80 mM KCl, 5 mM MgAc, 2 mM KH2PO4, and 50 mM Hepes, and distributed in five equal samples. Triton X-100 was added to indicated samples to 0.5% (vol/vol). Proteinase K was added to the samples in concentrations as indicated. After 15 min incubation on ice, the reactions were stopped by adding PMSF to 5 mM. Samples without Triton X-100 were centrifuged (3 min, 6,800 *g*, 4°C) and all samples were resuspended in SDS loading buffer. In each sample, 1×10^6 cell equivalents were subjected to SDS–PAGE and Western blotting.

Immunoprecipitation

Digitonin-extracted mitochondria-enriched fractions of 1×10^8 induced cells were solubilized on ice in 20 mM Tris–HCl (pH 7.4), 0.1 mM EDTA, 100 mM NaCl, 25 mM KCl, 1x protease inhibitor mix (EDTA-free; Roche), and 1% (wt/vol) digitonin. After centrifugation (15 min, 20817g, 4°C), the lysate (IN, input) was transferred to either 50 μl of HA bead slurry (anti-HA affinity matrix; Roche) or 50 μl c-myc bead slurry (EZview red anti-c-myc affinity gel; Sigma-Aldrich), both of which had been equilibrated in wash buffer (20 mM Tris–HCl [pH 7.4], 0.1 mM EDTA, 100 mM NaCl, 10% glycerol, 0.2% [wt/vol] digitonin). After incubating at 4°C for 2 h on a rotating wheel, the supernatant containing the unbound proteins (FT, flow through) was removed. The bead slurry was washed three times with wash buffer. Bound proteins were eluted by boiling the resin in 60 mM Tris–HCl (pH 6.8) containing 2% SDS (IP). 2.5% of crude mitochondrial fractions (Input, IN), unbound proteins in the flow through (FT), and 50% of the final eluates (IP) were separated by SDS–PAGE and analysed by Western blot.

SILAC immunoprecipitations

Cells were grown for 5 d in SILAC medium (SDM80 containing 5.55 mM glucose, supplemented with 10% dialyzed, heat-inactivated FCS, 7.5 mg/l hemin) containing isotopically distinct variants of arginine ($^{12}C_6^{14}N_4$/Arg0, $^{13}C_6^{14}N_4$/Arg6, or $^{13}C_6^{15}N_4$/Arg10; 226 mg/l each) and lysine ($^{12}C_6^{14}N_2$/Lys0, $^{12}C_6^{14}N_2^2H_4$/Lys4, or $^{13}C_6^{15}N_4$/Lys8; 73 mg/l each) (Eurisotope). 2×10^8 WT cells and cells expressing in situ tagged Msp1-HA (in the presence or absence of pATOM36) were mixed and washed with 1x PBS. Crude mitochondria-enriched fractions were obtained by digitonin extraction as described above. The pellet of the digitonin extraction was subjected to immunoprecipitation as described above. Proteins were precipitated after the methanol-chloroform protocol (Wessel & Flügge, 1984) and further processed for liquid chromatography-mass spectrometry (LC-MS) analysis including reduction in cysteine residues, alkylation of thiol groups, and tryptic digestion as described before (Dewar et al, 2022b). The experiment was performed in three biological replicates with different labelling schemes.

RNA extraction and Northern blotting

Acid guanidinium thiocyanate-phenol-chloroform extraction according to Chomczynski and Sacchi (1987) was used for isolation of total RNA from uninduced and induced RNAi cells. Total cellular RNA was separated on a 1% agarose gel in 20 mM MOPS buffer supplemented with 0.5% formaldehyde. Northern probes were generated from gel-purified PCR products corresponding to the RNAi inserts and radioactively labelled using the Prime-a-Gene labelling system (Promega).

Immunofluorescence microscopy

Induced $\times 10^6$ cells overexpressing the indicated tagged proteins were harvested by centrifugation (5 min, 1,800*g*) and washed with 1x PBS. After resuspension in 1x PBS, the cells were left adhering on a glass slide in a wet chamber. The cells were fixed with 4% PFA, permeabilised with 0.2% Triton X-100, and blocked with 2% BSA in 1x PBS. Antibodies were incubated on the slides in 1% BSA and 1x PBS. The dried slides were mounted with Vectashield containing 4 DAPI (Vector Laboratories, P/N H-1200). Images were acquired with a DFC360 FX monochrome camera (Leica Microsystems) mounted on a DMI6000B microscope (Leica Microsystems). Image analysis and deconvolution were performed using LASX software (version 3.6.20104.0; Leica Microsystems). The acquired images were processed using Fiji (ImageJ version 2.10./1.53; Java 1.8.0_172 [64 bit]). The Pearson product-moment correlation coefficient (Pearson's *r*) was calculated for a region of interest defined as one representative cell that is shown in the Figure using Fiji's Coloc 2 analysis. Microscopy figures were composed using FigureJ (Mutterer & Zinck, 2013).

Peptide stable isotope dimethyl labelling and high-pH reversed-phase fractionation

RNAi cell lines were grown in triplicate in SDM-79 for 3 d, in the presence or absence of tetracycline. 1×10^8 cells were centrifuged (8 min, 1,258*g*, RT) and washed with 1x PBS. The pellets were flash frozen in liquid nitrogen and subsequently processed for tryptic in-solution digestion as described before (Peikert et al, 2017). Dried peptides were reconstituted in 100 mM tetraethylammonium bicarbonate, followed by differential labelling with "light" or "heavy" formaldehyde (CH_2O/$^{13}CD_2O$; Sigma-Aldrich) and sodium cyanoborohydride ($NaBH_3CN$; Sigma-Aldrich) (Morgenstern et al, 2021). Labelling efficiencies (>99% for all individual experiments) were determined by LC-MS analysis. Equal amounts of differentially "light" and "heavy" labelled peptides derived from the respective control and induced RNAi cells were mixed, purified, and fractionated by high pH reversed-phase chromatography using StageTips essentially as described previously (von Känel et al, 2020). In brief, peptides, reconstituted in 10 mM NH_4OH, were loaded onto StageTips and eluted stepwise with 0%, 2.7%, 5.4%, 9.0%, 11.7%, 14.4%, 36%, and 65% (vol/vol each) acetonitrile (ACN)/10 mM NH_4OH. Fractions 1 and 7 (0% and 36% ACN eluates) and fractions 2 and 8 (2.7% and 65% ACN eluates) were combined for LC-MS analysis.

Quantitative LC-MS analysis

Before LC-MS analysis, peptides were desalted using StateTips, vacuum-dried, and reconstituted in 0.1% (vol/vol) trifluoroacetic acid. LC-MS analyses were performed using either a Q Exactive Plus (Msp1-HA SILAC IPs) or an Orbitrap Elite (RNAi experiments) mass spectrometer connected to an UltiMate 3,000 RSLCnano HPLC system (all instruments from Thermo Fisher Scientific). Peptides were loaded and concentrated on PepMap C18 precolumns (length, 5 mm; inner diameter, 0.3 mm; Thermo Fisher Scientific) at a flow rate of 30 μl/min and separated using Acclaim PepMap C18 reversed-phase nano-LC columns (length, 500 mm; inner diameter, 75 μm; particle size, 2 μm; pore size, 100 Å; Thermo Fisher Scientific) at a flow rate of 0.25 μl/min. The solvent system used for the elution of peptides from Msp1-HA SILAC IP experiments consisted of 0.1% (vol/vol) formic acid (FA; solvent A1) and 86% (vol/vol) ACN/0.1% (vol/vol) FA (solvent B1). The following gradient was applied: 4–39% solvent B1 in 195 min followed by 39–54% B1 in 15 min, 54–95% B1 in 3 min, and 5 min at 95% B1. For the elution of peptides from RNAi experiments, 4% (vol/vol) dimethyl sulfoxide (DMSO)/0.1% (vol/vol) FA (solvent A2) and 48% (vol/vol) methanol/30% (vol/vol) ACN/4% (vol/vol) DMSO/0.1% (vol/vol) FA (solvent B2) were used. A gradient ranging from 3–65% solvent B2 in 65 min, 65–80% B2 in 5 min, and 5 min at 80% B2 was applied.

Mass spectrometric data were acquired in a data-dependent mode. The Q Exactive Plus was operated with the following settings: mass range, m/z 375 to 1,700; resolution, 70,000 (at m/z 200); target value, 3×10^6; and maximum injection time (max. IT), 60 ms for MS survey scans. Fragmentation of up to 12 of the most intense multiply charged precursor ions by higher energy collisional dissociation was performed with a normalised collision energy (NCE) of 28%, a target value of 10^5, a max. IT of 120 ms, and a dynamic exclusion (DE) time of 45 s. The parameters for MS analyses at the Orbitrap Elite were as follows: mass range, m/z 370 to 1,700; resolution, 120,000 (at m/z 400); target value, 10^6; and max. IT, 200 ms for survey scans. A TOP15 (pATOM36/subunit β_1 double and pATOM36/TbVCP/TbMsp1 triple RNAi experiments) or TOP25 (pATOM36 RNAi experiments) method was applied for fragmentation of multiply charged precursor ions by low energy collision-induced dissociation in the linear ion trap (NCE, 35%; activation q, 0.25; activation time, 10 ms; target value, 5,000; max. IT, 150 ms; DE, 45 s).

Proteins were identified and quantified using MaxQuant/Andromeda (Cox & Mann, 2008; Cox et al, 2011) (version 1.5.5.1 for Msp1-HA SILAC IP and 1.6.0.1 for RNAi data). Mass spectrometric raw data were searched against a TriTryp database specific for *T. brucei* TREU927 (release version 8.1 for Msp1-HA SILAC IP and 36 for RNAi data; downloaded from https://tritrypdb.org). For protein identification, MaxQuant default settings were applied, with the exception that only one unique peptide was required. For relative quantification, the appropriate settings for SILAC labelling (light labels, Lys0/Arg0; medium-heavy, Arg6/Lys4; heavy, Lys8/Arg10) or stable isotope dimethyl labelling (light, dimethylLys0/dimethylNterLys0; heavy, dimethylLys6/dimethylNterLys6) were chosen. Quantification was based on at least one ratio count. The options "match between runs" and "requantify" were enabled. Only proteins quantified in at least two independent replicates per dataset were considered for further analysis. The mean $\log_{10}$ (SILAC IP data) or mean $\log_2$ (RNAi data) of protein abundance ratios was determined, and a one-sided (SILAC IP data) or two-sided (RNAi data) *t* test was performed. For information about the proteins identified and quantified, see Table S1 (TbMsp1-HA SILAC IPs) and Table S2 (RNAi experiments) in the PRIDE database.

Computational analysis of proteins

Conserved structural elements of Msp1 (Ogura et al, 2004; Martin et al, 2008; Wang et al, 2020) are highlighted in Fig 1A. TMDs were predicted using Phobius (Madeira et al, 2022) (TbMsp1, POMP31, TbJ31, POMP19) or HMMTOP (Tusnády & Simon, 1998) (TbTsc13), and conserved domains were either predicted with ncbi.nlm.nih.gov/Structure (POMP19, TbTsc13) or annotated Pfam domains on HMMER (Potter et al, 2018) (TbMsp1, TbJ31). The ubiquitin-like domain of TbTsc13 was predicted by HHpred (Zimmermann et al, 2018). The multiple amino acid sequence alignment of TbMsp1, ATAD1 from

H. sapiens (HsATAD1), and Msp1 from *S. cerevisiae* (ScMsp1) shown in Fig S1 was performed with Clustal Omega (Sievers et al, 2011).

Data Availability

The mass spectrometry data have been deposited to the ProteomeXchange Consortium (Deutsch et al, 2020) via the PRIDE (Perez-Riverol et al, 2022) partner repository and are accessible using the dataset identifiers PXD039631 (SILAC IP data) and PXD039634 (RNAi data).

Supplementary Information

Supplementary Information is available at https://doi.org/10.26508/lsa.202302004.

Acknowledgements

We thank Bettina Knapp for technical assistance. We thank Noemis Zbären and Gabriel Klesse for help at the initial stage of the project. Work in the laboratory of B Warscheid was supported by the Deutsche Forschungsgemeinschaft (DFG, German Research Foundation) project ID 403222702/SFB 1381 and Germany's Excellence Strategy (CIBSS—EXC-2189—Project ID 390939984). Work in the laboratory of A Schneider was supported in part by NCCR RNA and Disease, a National Centre of Competence in Research (grant number 205601), and by project grant SNF 205200, both funded by the Swiss National Science Foundation.

Author Contributions

M Gerber: conceptualization, investigation, methodology, and writing—original draft, review, and editing.
I Suppanz: formal analysis and investigation.
S Oeljeklaus: formal analysis and investigation.
M Niemann: investigation and writing—review and editing.
S Käser: investigation.
B Warscheid: conceptualization, supervision, funding acquisition, and writing—review and editing.
A Schneider: conceptualization, supervision, funding acquisition, and writing—original draft, review, and editing.
CE Dewar: conceptualization, supervision, investigation, methodology, and writing—original draft, review, and editing.

Conflict of Interest Statement

The authors declare that they have no conflict of interest.

References

Alexander K, Parsons M (1993) Characterization of a divergent glycosomal microbody phosphoglycerate kinase from Trypanosoma brucei. *Mol Biochem Parasitol* 60: 265–272. doi:10.1016/0166-6851(93)90137-m

Becker T, Wenz LS, Krüger V, Lehmann W, Müller JM, Goroncy L, Zufall N, Lithgow T, Guiard B, Chacinska A, et al (2011) The mitochondrial import protein Mim1 promotes biogenesis of multispanning outer membrane proteins. *J Cell Biol* 194: 387–395. doi:10.1083/jcb.201102044

Bentley SJ, Jamabo M, Boshoff A (2019) The Hsp70/J-protein machinery of the African trypanosome, Trypanosoma brucei. *Cell Stress Chaperones* 24: 125–148. doi:10.1007/s12192-018-0950-x

Bochud-Allemann N, Schneider A (2002) Mitochondrial substrate level phosphorylation is essential for growth of procyclic Trypanosoma brucei. *J Biol Chem* 277: 32849–32854. doi:10.1074/jbc.M205776200

Bruggisser J, Käser S, Mani J, Schneider A (2017) Biogenesis of a mitochondrial outer membrane protein in Trypanosoma brucei: Targeting signal and dependence on a unique biogenesis factor. *J Biol Chem* 292: 3400–3410. doi:10.1074/jbc.M116.755983

Brun R, Schonenberger M (1979) Cultivation and in vitro cloning of procyclic culture forms of Trypanosoma brucei in a semi-defined medium. Short communication. *Acta Trop* 36: 289–292.

Buchberger A, Schindelin H, Hänzelmann P (2015) Control of p97 function by cofactor binding. *FEBS Lett* 589: 2578–2589. doi:10.1016/j.febslet.2015.08.028

Chen Y-C, Umanah GKE, Dephoure N, Andrabi SA, Gygi SP, Dawson TM, Dawson VL, Rutter J (2014) Msp1/ATAD1 maintains mitochondrial function by facilitating the degradation of mislocalized tail-anchored proteins. *EMBO J* 33: 1548–1564. doi:10.15252/embj.201487943

Chomczynski P, Sacchi N (1987) Single-step method of RNA isolation by acid guanidinium thiocyanate-phenol-chloroform extraction. *Anal Biochem* 162: 156–159. doi:10.1006/abio.1987.9999

Cinti DL, Cook L, Nagi MN, Suneja SK (1992) The fatty acid chain elongation system of mammalian endoplasmic reticulum. *Prog Lipid Res* 31: 1–51. doi:10.1016/0163-7827(92)90014-a

Colasante C, Ellis M, Ruppert T, Voncken F (2006) Comparative proteomics of glycosomes from bloodstream form and procyclic culture form Trypanosoma brucei brucei. *Proteomics* 6: 3275–3293. doi:10.1002/pmic.200500668

Collins GA, Goldberg AL (2020) Proteins containing ubiquitin-like (Ubl) domains not only bind to 26S proteasomes but also induce their activation. *Proc Natl Acad Sci U S A* 117: 4664–4674. doi:10.1073/pnas.1915534117

Costello JL, Castro IG, Camões F, Schrader TA, McNeall D, Yang J, Giannopoulou EA, Gomes S, Pogenberg V, Bonekamp NA, et al (2017) Predicting the targeting of tail-anchored proteins to subcellular compartments in mammalian cells. *J Cell Sci* 130: 1675–1687. doi:10.1242/jcs.200204

Coustou V, Biran M, Besteiro S, Rivière L, Baltz T, Franconi JM, Bringaud F (2006) Fumarate is an essential intermediary metabolite produced by the procyclic trypanosoma brucei. *J Biol Chem* 281: 26832–26846. doi:10.1074/jbc.M601377200

Cox J, Mann M (2008) MaxQuant enables high peptide identification rates, individualized p.p.b.-range mass accuracies and proteome-wide protein quantification. *Nat Biotechnol* 26: 1367–1372. doi:10.1038/nbt.1511

Cox J, Neuhauser N, Michalski A, Scheltema RA, Olsen JV, Mann M (2011) Andromeda: A peptide search engine integrated into the MaxQuant environment. *J Proteome Res* 10: 1794–1805. doi:10.1021/pr101065j

Esseiva AC, Chanez AL, Bochud-Allemann N, Martinou JC, Hemphill A, Schneider A (2004) Temporal dissection of Bax-induced events leading to fission of the single mitochondrion in Trypanosoma brucei. *EMBO Rep* 5: 268–273. doi:10.1038/sj.embor.7400095

Dederer V, Khmelinskii A, Huhn AG, Okreglak V, Knop M, Lemberg MK (2019) Cooperation of mitochondrial and er factors in quality control of tail-anchored proteins. *Elife* 8: e45506. doi:10.7554/eLife.45506

den Brave F, Gupta A, Becker T (2021) Protein quality control at the mitochondrial surface. *Front Cell Dev Biol* 9: 795685. doi:10.3389/fcell.2021.795685

Deutsch EW, Bandeira N, Sharma V, Perez-Riverol Y, Carver JJ, Kundu DJ, García-Seisdedos D, Jarnuczak AF, Hewapathirana S, Pullman BS, et al (2020) The ProteomeXchange consortium in 2020: Enabling 'big data' approaches in proteomics. *Nucleic Acids Res* 48: D1145–D1152. doi:10.1093/nar/gkz984

Dewar CE, Oeljeklaus S, Mani J, Mühlhäuser WWD, von Känel C, Zimmermann J, Ochsenreiter T, Warscheid B, Schneider A (2022a) Mistargeting of aggregation prone mitochondrial proteins activates a nucleus-mediated posttranscriptional quality control pathway in trypanosomes. *Nat Commun* 13: 3084. doi:10.1038/s41467-022-30748-z

Dewar CE, Oeljeklaus S, Wenger C, Warscheid B, Schneider A (2022b) Characterization of a highly diverged mitochondrial ATP synthase Fo subunit in Trypanosoma brucei. *J Biol Chem* 298: 101829. doi:10.1016/j.jbc.2022.101829

Dimmer KS, Papić D, Schumann B, Sperl D, Krumpe K, Walther DM, Rapaport D (2012) A crucial role for Mim2 in the biogenesis of mitochondrial outer membrane proteins. *J Cell Sci* 125: 3464–3473. doi:10.1242/jcs.103804

Doan KN, Grevel A, Mårtensson CU, Ellenrieder L, Thornton N, Wenz LS, Opaliński Ł, Guiard B, Pfanner N, Becker T (2020) The mitochondrial import complex MIM functions as main translocase for α-helical outer membrane proteins. *Cell Rep* 31: 107567. doi:10.1016/j.celrep.2020.107567

Dolezal P, Likic V, Tachezy J, Lithgow T (2006) Evolution of the molecular machines for protein import into mitochondria. *Science* 313: 314–318. doi:10.1126/science.1127895

Escobar-Henriques M, Anton V (2020) Mitochondrial surveillance by Cdc48/p97: MAD vs. Membrane fusion. *Int J Mol Sci* 21: 6841. doi:10.3390/ijms21186841

Fresenius HL, Wohlever ML (2019) Sorting out how Msp1 maintains mitochondrial membrane proteostasis. *Mitochondrion* 49: 128–134. doi:10.1016/j.mito.2019.07.011

Guna A, Stevens TA, Inglis AJ, Replogle JM, Esantsi TK, Muthukumar G, Shaffer KCL, Wang ML, Pogson AN, Jones JJ, et al (2022) MTCH2 is a mitochondrial outer membrane protein insertase. *Science* 378: 317–322. doi:10.1126/science.add1856

Güther MLS, Urbaniak MD, Tavendale A, Prescott A, Ferguson MAJ (2014) High-confidence glycosome proteome for procyclic form Trypanosoma brucei by epitope-tag organelle enrichment and SILAC proteomics. *J Proteome Res* 13: 2796–2806. doi:10.1021/pr401209w

Harsman A, Schneider A (2017) Mitochondrial protein import in trypanosomes: Expect the unexpected. *Traffic* 18: 96–109. doi:10.1111/tra.12463

Hegde RS (2014) Msp1: Patrolling mitochondria for lost proteins. *EMBO J* 33: 1509–1510. doi:10.15252/embj.201488930

Heo JM, Livnat-Levanon N, Taylor EB, Jones KT, Dephoure N, Ring J, Xie J, Brodsky JL, Madeo F, Gygi SP, et al (2010) A stress-responsive system for mitochondrial protein degradation. *Mol Cell* 40: 465–480. doi:10.1016/j.molcel.2010.10.021

Igoillo-Esteve M, Mazet M, Deumer G, Wallemacq P, Michels PAM (2011) Glycosomal ABC transporters of Trypanosoma brucei: Characterisation of their expression, topology and substrate specificity. *Int J Parasitol* 41: 429–438. doi:10.1016/j.ijpara.2010.11.002

Jonikas MC, Collins SR, Denic V, Oh E, Quan EM, Schmid V, Weibezahn J, Schwappach B, Walter P, Weissman JS, et al (2009) Comprehensive characterization of genes required for protein folding in the endoplasmic reticulum. *Science* 323: 1693–1697. doi:10.1126/science.1167983

Kalbfleisch T, Cambon A, Wattenberg BW (2007) A bioinformatics approach to identifying tail-anchored proteins in the human genome. *Traffic* 8: 1687–1694. doi:10.1111/j.1600-0854.2007.00661.x

Käser S, Oeljeklaus S, Týč J, Vaughan S, Warscheid B, Schneider A (2016) Outer membrane protein functions as integrator of protein import and DNA inheritance in mitochondria. *Proc Natl Acad Sci U S A* 113: E4467–E4475. doi:10.1073/pnas.1605497113

Kemper C, Habib SJ, Engl G, Heckmeyer P, Dimmer KS, Rapaport D (2008) Integration of tail-anchored proteins into the mitochondrial outer membrane does not require any known import components. *J Cell Sci* 121: 1990–1998. doi:10.1242/jcs.024034

Kohlwein SD, Eder S, Oh C-S, Martin CE, Gable K, Bacikova D, Dunn T (2001) Tsc13p is required for fatty acid elongation and localizes to a novel structure at the nuclear-vacuolar interface in Saccharomyces cerevisiae. *Mol Cell Biol* 21: 109–125. doi:10.1128/MCB.21.1.109-125.2001

Krämer L, Groh C, Herrmann JM (2021) The proteasome: Friend and foe of mitochondrial biogenesis. *FEBS Lett* 595: 1223–1238. doi:10.1002/1873-3468.14010

Lamb JR, Fu V, Wirtz E, Bangs JD (2001) Functional analysis of the trypanosomal AAA protein TbVCP with trans-dominant ATP hydrolysis mutants. *J Biol Chem* 276: 21512–21520. doi:10.1074/jbc.M100235200

Li L, Zheng J, Wu X, Jiang H (2019) Mitochondrial AAA-ATPase Msp1 detects mislocalized tail-anchored proteins through a dual-recognition mechanism. *EMBO Rep* 20: e46989. doi:10.15252/embr.201846989

Lorenz P, Maier AG, Baumgart E, Erdmann R, Clayton C (1998) Elongation and clustering of glycosomes in Trypanosoma brucei overexpressing the glycosomal Pex11p. *EMBO J* 17: 3542–3555. doi:10.1093/emboj/17.13.3542

Madeira F, Pearce M, Tivey ARN, Basutkar P, Lee J, Edbali O, Madhusoodanan N, Kolesnikov A, Lopez R (2022) Search and sequence analysis tools services from EMBL-EBI in 2022. *Nucleic Acids Res* 50: W276–W279. doi:10.1093/nar/gkac240

Mani J, Desy S, Niemann M, Chanfon A, Oeljeklaus S, Pusnik M, Schmidt O, Gerbeth C, Meisinger C, Warscheid B, et al (2015) Mitochondrial protein import receptors in Kinetoplastids reveal convergent evolution over large phylogenetic distances. *Nat Commun* 6: 6646. doi:10.1038/ncomms7646

Mani J, Meisinger C, Schneider A (2016) Peeping at TOMs - diverse entry gates to mitochondria provide insights into the evolution of eukaryotes. *Mol Biol Evol* 33: 337–351. doi:10.1093/molbev/msv219

Martin A, Baker TA, Sauer RT (2008) Pore loops of the AAA+ ClpX machine grip substrates to drive translocation and unfolding. *Nat Struct Mol Biol* 15: 1147–1151. doi:10.1038/nsmb.1503

Matsumoto S, Nakatsukasa K, Kakuta C, Tamura Y, Esaki M, Endo T (2019) Msp1 clears mistargeted proteins by facilitating their transfer from mitochondria to the ER. *Mol Cell* 76: 191–205.e10. doi:10.1016/j.molcel.2019.07.006

Miinalainen IJ, Chen Z-J, Torkko JM, Pirilä PL, Sormunen RT, Bergmann U, Qin Y-M, Hiltunen JK (2003) Characterization of 2-enoyl thioester reductase from mammals. An ortholog of YBR026p/MRF1'p of the yeast mitochondrial fatty acid synthesis type II. *J Biol Chem* 278: 20154–20161. doi:10.1074/jbc.M302851200

Mohanraj K, Nowicka U, Chacinska A (2020) Mitochondrial control of cellular protein homeostasis. *Biochem J* 477: 3033–3054. doi:10.1042/BCJ20190654

Morgenstern M, Peikert CD, Lübbert P, Suppanz I, Klemm C, Alka O, Steiert C, Naumenko N, Schendzielorz A, Melchionda L, et al (2021) Quantitative high-confidence human mitochondrial proteome and its dynamics in cellular context. *Cell Metab* 33: 2464–2483.e18. doi:10.1016/j.cmet.2021.11.001

Muñoz-Gómez SA, Slamovits CH, Dacks JB, Wideman JG (2015) The evolution of MICOS: Ancestral and derived functions and interactions. *Commun Integr Biol* 8: e1094593. doi:10.1080/19420889.2015.1094593

Mutterer J, Zinck E (2013) Quick-and-clean article figures with FigureJ. *J Microsc* 252: 89–91. doi:10.1111/jmi.12069

Nakai M, Endo T, Hase T, Matsubara H (1993) Intramitochondrial protein sorting. Isolation and characterization of the yeast MSP1 gene which

belongs to a novel family of putative ATPases. *J Biol Chem* 268: 24262–24269. doi:10.1016/s0021-9258(20)80519-5

Niemann M, Wiese S, Mani J, Chanfon A, Jackson C, Meisinger C, Warscheid B, Schneider A (2013) Mitochondrial outer membrane proteome of Trypanosoma brucei reveals novel factors required to maintain mitochondrial morphology. *Mol Cell Proteomics* 12: 515–528. doi:10.1074/mcp.M112.023093

Oberholzer M, Morand S, Kunz S, Seebeck T (2006) A vector series for rapid PCR-mediated C-terminal in situ tagging of Trypanosoma brucei genes. *Mol Biochem Parasitol* 145: 117–120. doi:10.1016/j.molbiopara.2005.09.002

Ogura T, Whiteheart SW, Wilkinson AJ (2004) Conserved arginine residues implicated in ATP hydrolysis, nucleotide-sensing, and inter-subunit interactions in AAA and AAA+ ATPases. *J Struct Biol* 146: 106–112. doi:10.1016/j.jsb.2003.11.008

Okreglak V, Walter P (2014) The conserved AAA-ATPase Msp1 confers organelle specificity to tail-anchored proteins. *Proc Natl Acad Sci U S A* 111: 8019–8024. doi:10.1073/pnas.1405755111

Papić D, Krumpe K, Dukanovic J, Dimmer KS, Rapaport D (2011) Multispan mitochondrial outer membrane protein Ugo1 follows a unique Mim1-dependent import pathway. *J Cell Biol* 194: 397–405. doi:10.1083/jcb.201102041

Parl A, Mitchell SL, Clay HB, Reiss S, Li Z, Murdock DG (2013) The mitochondrial fatty acid synthesis (mtFASII) pathway is capable of mediating nuclear-mitochondrial cross talk through the PPAR system of transcriptional activation. *Biochem Biophys Res Commun* 441: 418–424. doi:10.1016/j.bbrc.2013.10.072

Peikert CD, Mani J, Morgenstern M, Käser S, Knapp B, Wenger C, Harsman A, Oeljeklaus S, Schneider A, Warscheid B (2017) Charting organellar importomes by quantitative mass spectrometry. *Nat Commun* 8: 15272. doi:10.1038/ncomms15272

Perez-Riverol Y, Bai J, Bandla C, García-Seisdedos D, Hewapathirana S, Kamatchinathan S, Kundu DJ, Prakash A, Frericks-Zipper A, Eisenacher M, et al (2022) The PRIDE database resources in 2022: A hub for mass spectrometry-based proteomics evidences. *Nucleic Acids Res* 50: D543–D552. doi:10.1093/nar/gkab1038

Perry AJ, Hulett JM, Likić VA, Lithgow T, Gooley PR (2006) Convergent evolution of receptors for protein import into mitochondria. *Curr Biol* 16: 221–229. doi:10.1016/j.cub.2005.12.034

Peterson GC, Sommer JM, Klosterman S, Wang CC, Parsons M (1997) Trypanosoma brucei: Identification of an internal region of phosphoglycerate kinase required for targeting to glycosomal microbodies. *Exp Parasitol* 85: 16–23. doi:10.1006/expr.1996.4114

Potter SC, Luciani A, Eddy SR, Park Y, Lopez R, Finn RD (2018) HMMER web server: 2018 update. *Nucleic Acids Res* 46: W200–W204. doi:10.1093/nar/gky448

Pusnik M, Mani J, Schmidt O, Niemann M, Oeljeklaus S, Schnarwiler F, Warscheid B, Lithgow T, Meisinger C, Schneider A (2012) An essential novel component of the noncanonical mitochondrial outer membrane protein import system of trypanosomatids. *Mol Biol Cell* 23: 3420–3428. doi:10.1091/mbc.E12-02-0107

Rao M, Okreglak V, Chio US, Cho H, Walter P, Shan SO (2016) Multiple selection filters ensure accurate tail-anchored membrane protein targeting. *Elife* 5: e21301. doi:10.7554/eLife.21301

Reinders J, Zahedi RP, Pfanner N, Meisinger C, Sickmann A (2006) Toward the complete yeast mitochondrial proteome: Multidimensional separation techniques for mitochondrial proteomics. *J Proteome Res* 5: 1543–1554. doi:10.1021/pr050477f

Roggy JL, Bangs JD (1999) Molecular cloning and biochemical characterization of a VCP homolog in African trypanosomes. *Mol Biochem Parasitol* 98: 1–15. doi:10.1016/s0166-6851(98)00114-5

Rout S, Oeljeklaus S, Makki A, Tachezy J, Warscheid B, Schneider A (2021) Determinism and contingencies shaped the evolution of mitochondrial protein import. *Proc Natl Acad Sci U S A* 118: e2017774118. doi:10.1073/pnas.2017774118

Schindelin J, Arganda-Carreras I, Frise E, Kaynig V, Longair M, Pietzsch T, Preibisch S, Rueden C, Saalfeld S, Schmid B, et al (2012) Fiji: An open-source platform for biological-image analysis. *Nat Methods* 9: 676–682. doi:10.1038/nmeth.2019

Schneider A (2020) Evolution of mitochondrial protein import - lessons from trypanosomes. *Biol Chem* 401: 663–676. doi:10.1515/hsz-2019-0444

Schuldiner M, Metz J, Schmid V, Denic V, Rakwalska M, Schmitt HD, Schwappach B, Weissman JS (2008) The GET complex mediates insertion of tail-anchored proteins into the ER membrane. *Cell* 134: 634–645. doi:10.1016/j.cell.2008.06.025

Sickmann A, Reinders J, Wagner Y, Joppich C, Zahedi R, Meyer HE, Schönfisch B, Perschil I, Chacinska A, Guiard B, et al (2003) The proteome of Saccharomyces cerevisiae mitochondria. *Proc Natl Acad Sci U S A* 100: 13207–13212. doi:10.1073/pnas.2135385100

Sievers F, Wilm A, Dineen D, Gibson TJ, Karplus K, Li W, Lopez R, McWilliam H, Remmert M, Söding J, et al (2011) Fast, scalable generation of high-quality protein multiple sequence alignments using Clustal Omega. *Mol Syst Biol* 7: 539. doi:10.1038/msb.2011.75

Tusnády GE, Simon I (1998) Principles governing amino acid composition of integral membrane proteins: Application to topology prediction. *J Mol Biol* 283: 489–506. doi:10.1006/jmbi.1998.2107

Uchida Y, Yamamoto Y, Sakisaka T (2021) Trans-2-enoyl-CoA reductase limits Ca2+ accumulation in the endoplasmic reticulum by inhibiting the Ca2+ pump SERCA2b. *J Biol Chem* 296: 100310. doi:10.1016/j.jbc.2021.100310

Verner Z, Basu S, Benz C, Dixit S, Dobáková E, Faktorová D, Hashimi H, Horáková E, Huang Z, Paris Z, et al (2015) Malleable mitochondrion of trypanosoma brucei. *Int Rev Cell Mol Biol* 315: 73–151. doi:10.1016/bs.ircmb.2014.11.001

Violitzi F, Perivolidi VI, Thireou T, Grivas I, Haralambous S, Samiotaki M, Panayotou G, Douni E (2019) Mapping interactome networks of DNAJC11, a novel mitochondrial protein causing neuromuscular pathology in mice. *J Proteome Res* 18: 3896–3912. doi:10.1021/acs.jproteome.9b00338

Vitali DG, Käser S, Kolb A, Dimmer KS, Schneider A, Rapaport D (2018) Independent evolution of functionally exchangeable mitochondrial outer membrane import complexes. *Elife* 7: e34488. doi:10.7554/eLife.34488

Vögtle FN, Keller M, Taskin AA, Horvath SE, Guan XL, Prinz C, Opalińska M, Zorzin C, van der Laan M, Wenk MR, et al (2015) The fusogenic lipid phosphatidic acid promotes the biogenesis of mitochondrial outer membrane protein Ugo1. *J Cell Biol* 210: 951–960. doi:10.1083/jcb.201506085

von Känel C, Muñoz-Gómez SA, Oeljeklaus S, Wenger C, Warscheid B, Wideman JG, Harsman A, Schneider A (2020) Homologue replacement in the import motor of the mitochondrial inner membrane of trypanosomes. *Elife* 9: e52560. doi:10.7554/eLife.52560

Wang L, Myasnikov A, Pan X, Walter P (2020) Structure of the AAA protein Msp1 reveals mechanism of mislocalized membrane protein extraction. *Elife* 9: e54031. doi:10.7554/eLife.54031

Weidberg H, Amon A (2018) MitoCPR—a surveillance pathway that protects mitochondria in response to protein import stress. *Science* 360: eaan4146. doi:10.1126/science.aan4146

Weir NR, Kamber RA, Martenson JS, Denic V (2017) The AAA protein Msp1 mediates clearance of excess tail-anchored proteins from the peroxisomal membrane. *Elife* 6: e28507. doi:10.7554/eLife.28507

Wessel D, Flügge UI (1984) A method for the quantitative recovery of protein in dilute solution in the presence of detergents and lipids. *Anal Biochem* 138: 141–143. doi:10.1016/0003-2697(84)90782-6

Wirtz E, Leal S, Ochatt C, Cross GAM (1999) A tightly regulated inducible expression system for conditional gene knock-outs and dominant-negative genetics in Trypanosoma brucei. *Mol Biochem Parasitol* 99: 89–101. doi:10.1016/s0166-6851(99)00002-x

Wohlever ML, Mateja A, McGilvray PT, Day KJ, Keenan RJ (2017) Msp1 is a membrane protein dislocase for tail-anchored proteins. *Mol Cell* 67: 194–202.e6. doi:10.1016/j.molcel.2017.06.019

Xie J, Marusich MF, Souda P, Whitelegge J, Capaldi RA (2007) The mitochondrial inner membrane protein Mitofilin exists as a complex with SAM50, metaxins 1 and 2, coiled-coil-helix coiled-coil-helix domain-containing protein 3 and 6 and DnaJC11. *FEBS Lett* 581: 3545–3549. doi:10.1016/j.febslet.2007.06.052

Yernaux C, Fransen M, Brees C, Lorenzen S, Michels PAM (2006) Trypanosoma brucei glycosomal ABC transporters: Identification and membrane targeting. *Mol Membr Biol* 23: 157–172. doi:10.1080/09687860500460124

Zheng J, Li L, Jiang H (2019) Molecular pathways of mitochondrial outer membrane protein degradation. *Biochem Soc Trans* 47: 1437–1447. doi:10.1042/BST20190275

Zimmermann L, Stephens A, Nam SZ, Rau D, Kübler J, Lozajic M, Gabler F, Söding J, Lupas AN, Alva V (2018) A completely reimplemented MPI bioinformatics toolkit with a new HHpred server at its Core. *J Mol Biol* 430: 2237–2243. doi:10.1016/j.jmb.2017.12.007

Supplementary Figures:

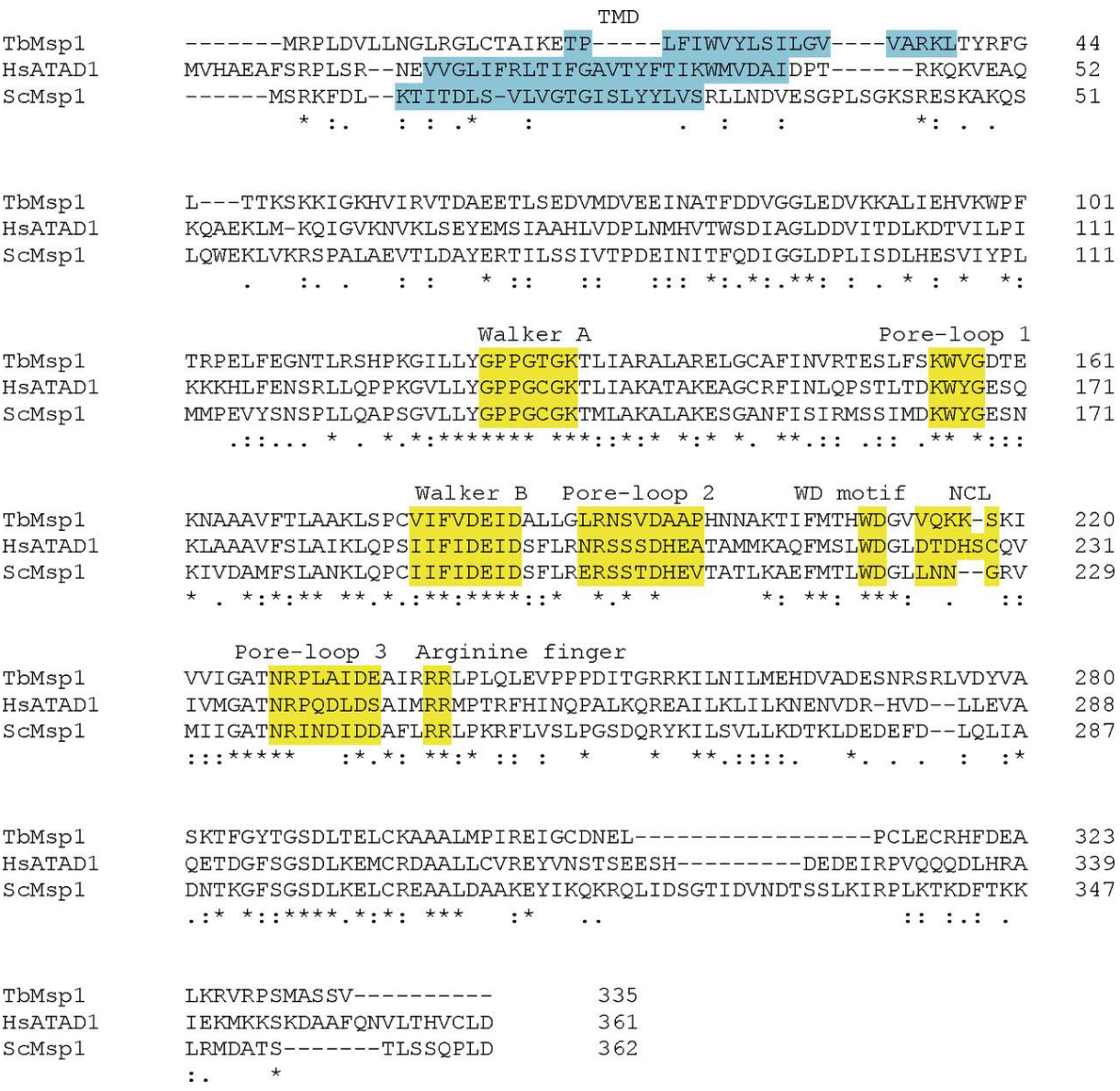

Figure S1.

TbMsp1 contains motifs conserved across species.

Clustal Omega multiple sequence alignment of amino acid sequences of TbMsp1, ATAD1 from H. sapiens (HsATAD1), and Msp1 from S. cerevisiae (ScMsp1). Predicted transmembrane domains are coloured in blue. The conserved structural elements coloured in yellow are: (i) the Walker A and B motif for nucleotide binding and ATP hydrolysis, (ii) three pore-loop motifs, which are involved in gripping and unfolding substrates and driving translocation through the pore, (iii) a WD motif, which likely contributes to the coupling of ATP hydrolysis to conformational changes required for successful substrate translocation, (iv) a nucleotide communication loop, and (v) an arginine finger motif.

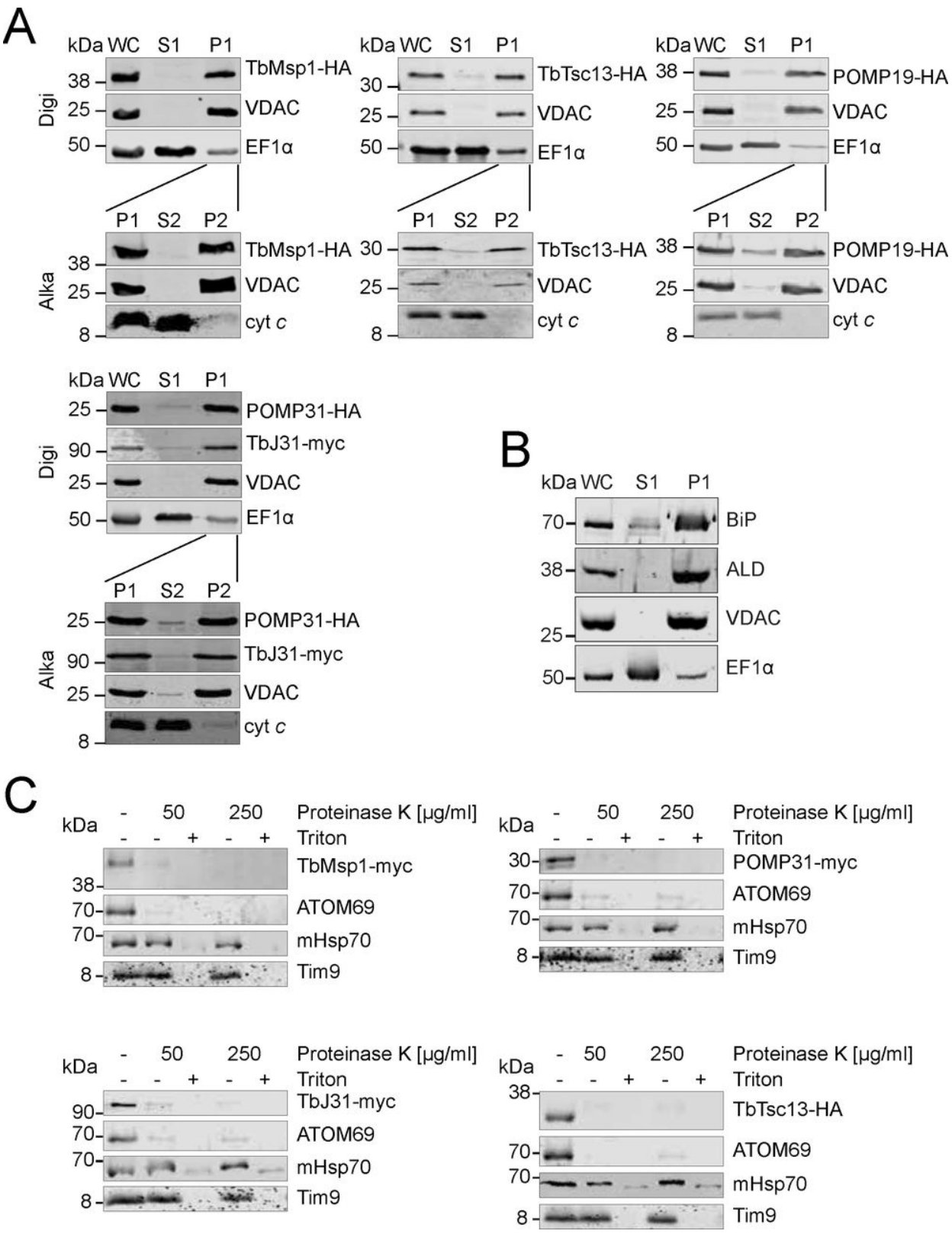

Figure S2.

TbMsp1, POMP31, TbJ31, POMP19, and TbTsc13 are integral OM proteins.

(A) Immunoblot analysis of whole cells (WC), soluble cytosolic (S1) fractions, and digitonin-extracted mitochondria-enriched (P1) from cells overexpressing the indicated C-terminally myc- or HA-tagged proteins. Immunoblots were probed with anti-tag antibodies and antisera against voltage-dependent

anion channel and EF1α, which serve as markers for mitochondria and cytosol, respectively. P1 fractions were subjected to alkaline carbonate extraction at pH 11.5 resulting in soluble supernatant (S2) and membrane-enriched pellet (P2) fractions. Immunoblots were probed with anti-tag antibodies and antisera against voltage-dependent anion channel and cytochrome c (cyt c), which serve as markers for integral and peripheral membrane proteins, respectively. (B) Immunoblot analysis of whole cells (WC), soluble cytosolic (S1) fractions, and digitonin-extracted mitochondria-enriched (P1) from cells expressing TbMsp1-myc probed with antisera against the ER marker binding protein and the glycosomal marker aldolase. (C) Immunoblot analysis of proteinase K protection assays on digitonin-extracted mitochondria-enriched fractions from cells overexpressing the indicated HA or myc-tagged proteins. An untreated sample serves as the control (left lane). Proteinase K and Triton X-100 were added as indicated.

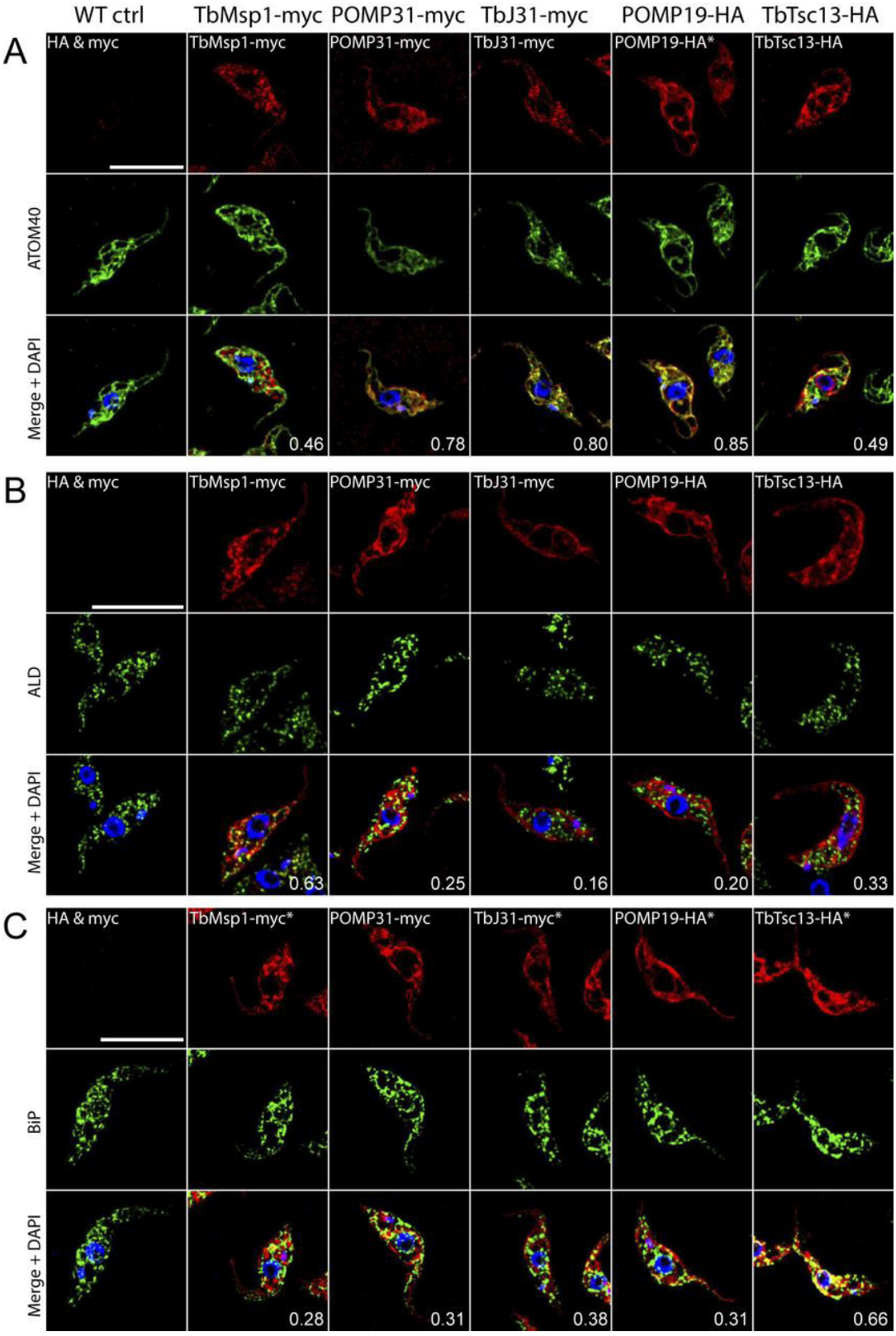

Figure S3.

TbMsp1, POMP31, TbJ31, POMP19, and TbTsc13 localise to mitochondria in an immunofluorescence analysis.

Immunofluorescence analysis of either WT cells or cells overexpressing the C-terminally myc or HA-tagged proteins (as indicated at the top of each column). (A, B, C) Cells were stained using anti-tag

antibodies (top row) and co-stained either with the mitochondrial marker ATOM40 (A), the glycosomal marker aldolase (B), or the ER marker binding protein (C) (middle row). All slides were also stained with DAPI, which marks both nuclear and mitochondrial DNA in merged images (bottom row). All images have been deconvoluted, and the Pearson R-values for colocalization of the indicated antigens are depicted. Scale bars: 10 µm. All images were acquired using the same microscope settings. Panels in which the brightness and contrast have been reduced to avoid saturation are indicated by asterisks.

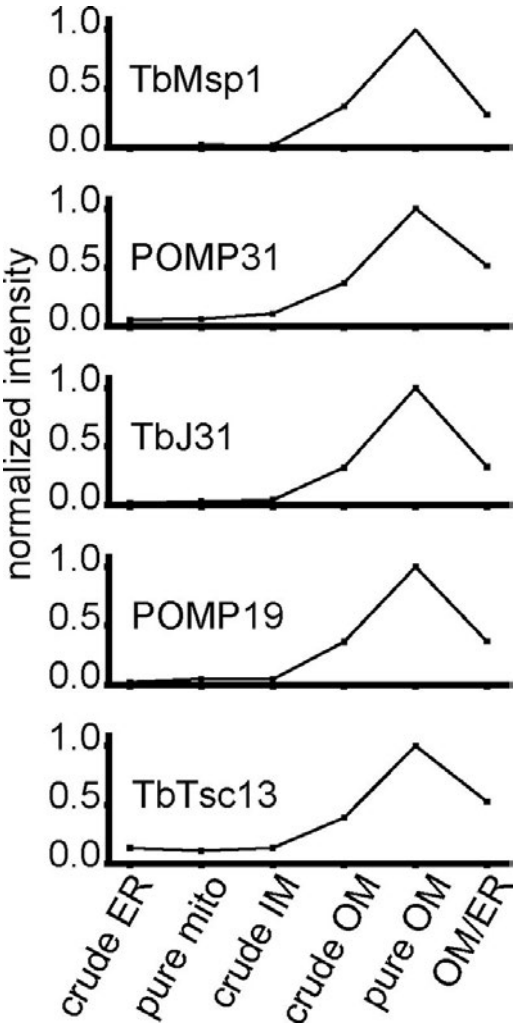

Figure S4.

Normalised abundance profiles confirm OM localisation.

Normalised abundance profiles of TbMsp1, POMP19, POMP31, TbJ31, and TbTsc13 over six subcellular fractions, from a previously published proteomic analysis, showing maximal intensity in the OM fraction (Niemann et al, 2013).

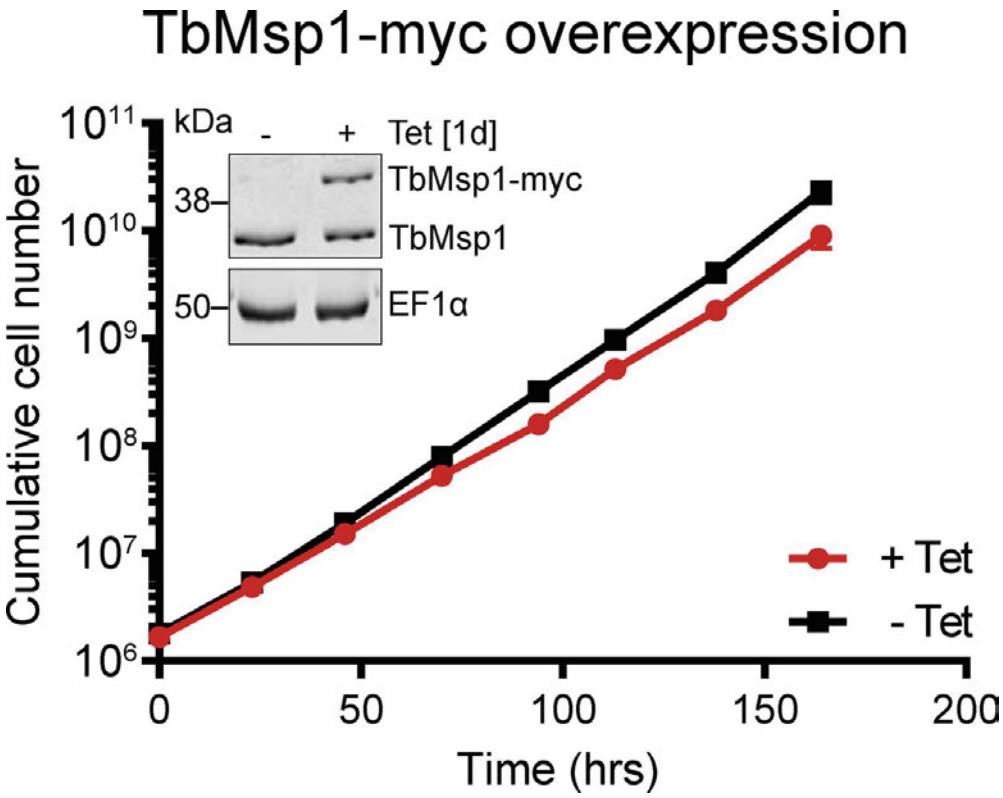

Figure S5.

Growth curve of T. brucei cells ectopically expressing TbMsp1-myc.

Growth curve of induced (+Tet) and uninduced (−Tet) cells ectopically expressing TbMsp1-myc. Error bars corresponding to the SD (n = 3) are too small to be displayed. The inset panel shows the overexpression of TbMsp1-myc 1 d after induction as analysed by immunoblot decorated with antisera against TbMsp1 and EF1α.

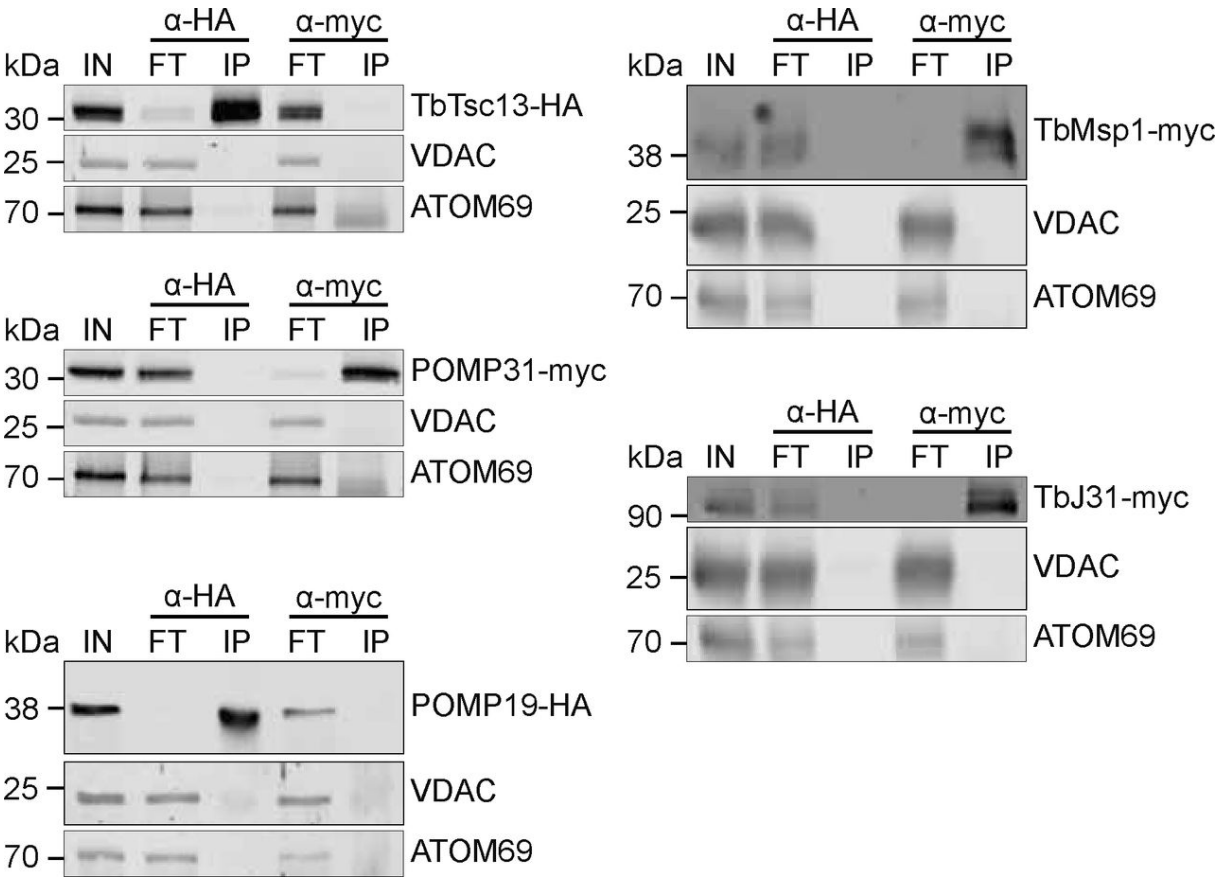

Figure S6.

Control experiments for the immunoprecipitations shown in Fig 2.

Crude mitochondrial fractions from cells overexpressing the indicated C-terminally myc- or HA-tagged proteins were analysed by immunoprecipitation using HA or myc beads, respectively. Crude mitochondrial fractions (IN), unbound proteins (FT), and final eluates (IP) were separated by SDS–PAGE. Resulting immunoblots were probed with anti-tag antibodies and antisera against voltage-dependent anion channel and ATOM69.

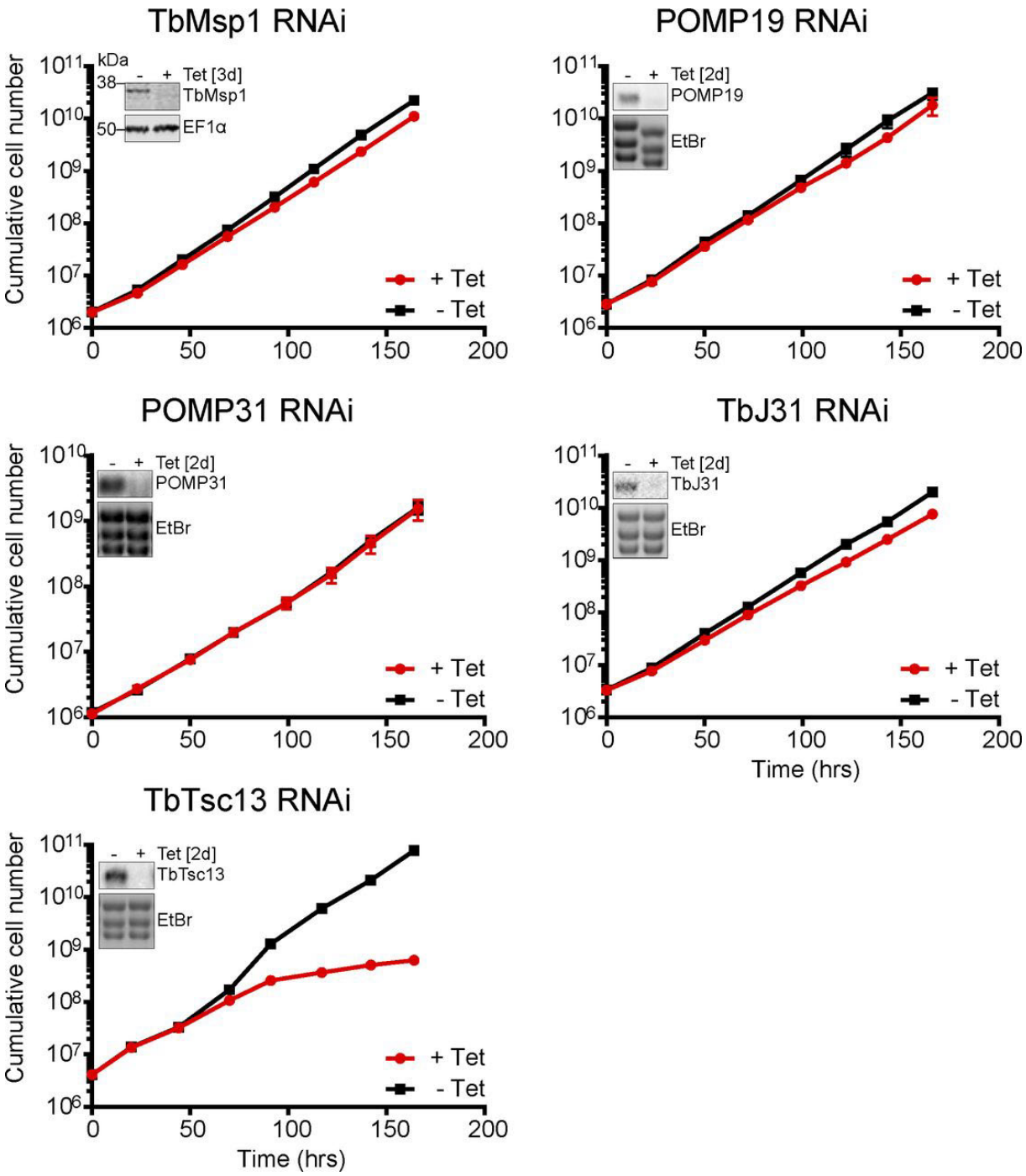

Figure S7.

Verification and growth analysis of TbMsp1, POMP19, POMP31, TbJ31, and TbTsc13 RNAi cell lines.

Growth curve of the indicated induced (+Tet) and uninduced (−Tet) RNAi cell lines. The growth curves were performed in triplicate, but the SD are too small to be displayed. The inset panels show the efficiency of RNAi for the indicated cell lines, either 3 d after induction when analysed by Western blot or 2 d after induction when analysed by Northern blot. EF1α or ethidium bromide-stained rRNAs serve as loading controls, respectively.

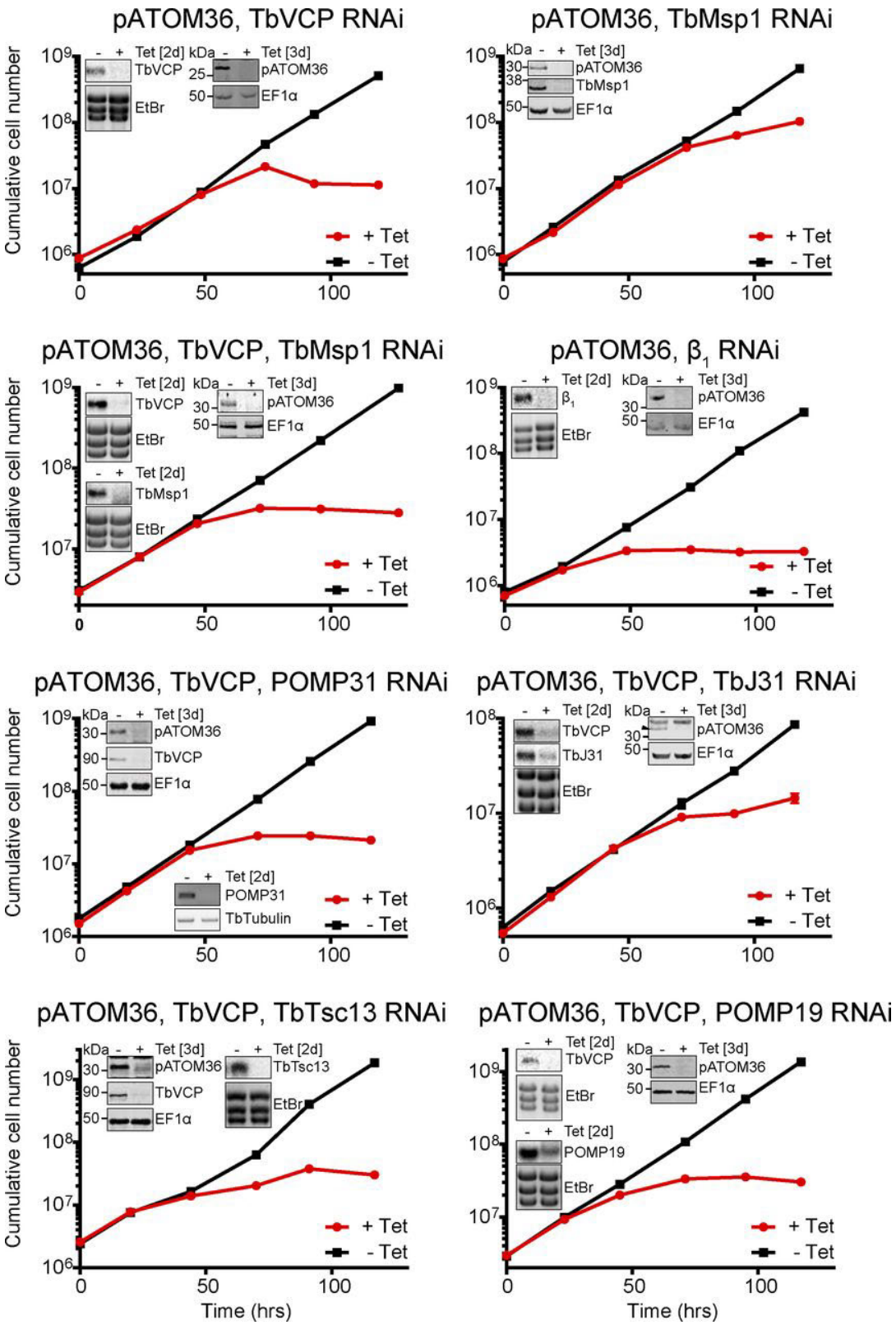

Figure S8.

Verification and growth analysis of double and triple RNAi cell lines.

Growth curve of induced (+Tet) and uninduced (−Tet) double and triple RNAi cell lines. The growth curves were performed in triplicate, but most SDs are too small to be displayed. The inset panels show the efficiency of RNAi for the indicated targets, either 2 d after induction when analysed by Northern blot

or RT–PCR, or 3 d after induction when analysed by immunoblot. Ethidium bromide-stained rRNAs, tubulin cDNA, or EF1α serve as loading controls, respectively.

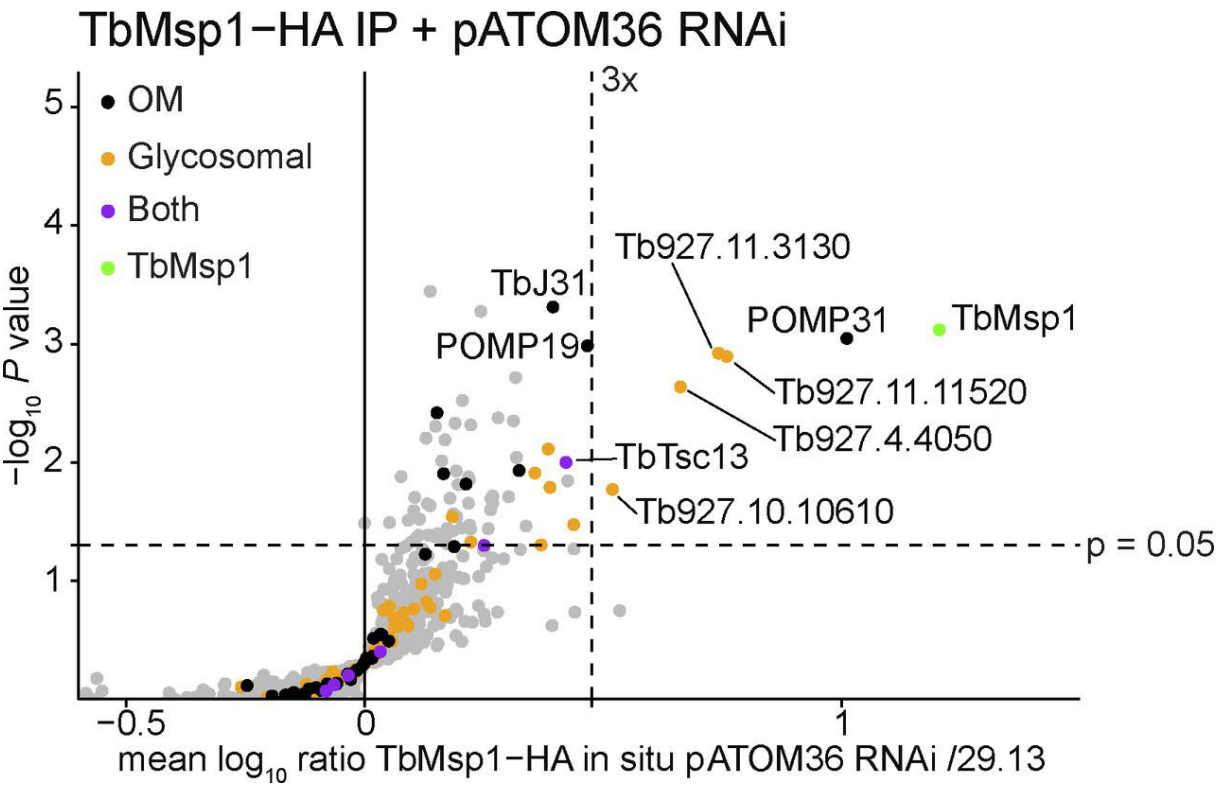

Figure S9.

Stable isotope labelling by amino acids in cell pulldown of TbMsp1-HA in pATOM36-depleted cells.

TbMsp1 complexes were immunoprecipitated from crude mitochondrial fractions of differentially stable isotope labelling by amino acids in cell-labelled 29.13 parent cells and cells expressing in situ tagged TbMsp1-HA depleted for pATOM36 RNAi and analysed by quantitative mass spectrometry (n = 3).

3.2 Examining the involvement of ubiquitination in TbMsp1- and TbVCP-assisted mitochondria-associated degradation in *Trypanosoma brucei*

Markus Gerber[1, 2], Caroline E. Dewar[1], André Schneider[1]

[1] Department of Chemistry, Biochemistry and Pharmaceutical Sciences, University of Bern, Bern, Switzerland

[2] Graduate School for Cellular and Biomedical Sciences, University of Bern, Switzerland

Contribution

All data presented in this chapter are unpublished and not part of a submitted manuscript. Dr. Caroline E. Dewar supervised this project.

My contributions:

- Cloning and generation of cell lines used
- Performing all experiments presented here
- Creating all the figures
- The text presented here

Abstract

Mitochondria are organelles shared between essentially all eukaryotes. To maintain their vital functions, cells have several pathways that monitor and maintain mitochondrial proteostasis. We recently published a paper describing a mitochondria-associated degradation (MAD) pathway in Trypanosoma brucei, which is triggered upon ablation of the mitochondrial import complex (MIM) analogue pATOM36. The ablation of pATOM36 leads to complex subunits of the atypical protein translocase of the outer membrane (ATOM) being removed from the mitochondrial outer membrane (OM) by one of the two ATPases TbMsp1 or TbVCP followed by degradation by the cytosolic proteasome. While it is known that VCP function is dependent on ubiquitination of its substrates, it is unclear whether substrates need to be ubiquitinated for removal by TbMsp1. To test this, we in situ expressed the ATOM component and MAD substrate ATOM19 with all of its lysines replaced by arginine. We hypothesized that these mutations would prevent the ubiquitination of this substrate and therefore TbVCP would not be able to remove it from the OMM. We could show by blue native PAGE analysis that ATOM19 without lysines is integrated in a large molecular weight complex, which presumably is the ATOM complex. Upon induction of pATOM36 RNAi, ATOM19 and the ATOM19 variant without lysines both are depleted from the cells. Interestingly, both versions of the protein are also equally depleted in a cell line simultaneously ablated for pATOM36 and TbMsp1. This suggests that even though if ATOM19 does not have any lysines, ubiquitination of the protein might still be possible. Further experiments are needed to reveal the role of ubiquitination in TbMsp1- or TbVCP-assisted degradation of destabilized OM proteins in T. brucei.

Introduction

Mitochondria are essential organelles that perform a number of vital functions in eukaryotes. The mitochondrial outer membrane (OM) that surrounds the mitochondrion, harbours a complex and dynamic proteome (Niemann et al., 2013; Schmitt et al., 2006). While OM proteins can have various topologies, proteins that are anchored in the membrane by a single alpha-helical transmembrane domain make up a considerable proportion of the OM proteome. Several studies conducted in yeast have suggested that the mitochondrial import complex (MIM), consisting of Mim1 and Mim2, is mediating the biogenesis of α-helically anchored OM proteins (Becker et al., 2011; Dimmer et al., 2012; Doan et al., 2020; Papić et al., 2011). Interestingly, MIM is fungi-specific and appears to have the same function as the mitochondrial animal-specific carrier homolog 2 (MTCH2) in animals and the peripheral atypical protein translocase of the outer mitochondrial membrane of 36 kDa (pATOM36) in kinetoplastids (Bruggisser et al., 2017; Guna et al., 2022; Käser et al., 2016). These three proteins are non-homologous, providing an example of convergent evolution in mitochondrial protein import. In

fact it could be shown that MIM of yeast and pATOM36 in trypanosomes reciprocally complement each other in the two organisms (Vitali et al., 2018).

It has been shown by our group that ablation of pATOM36 leads to the removal and degradation of several α-helically anchored proteins by the cytosolic proteasome (Gerber et al., 2023; Käser et al., 2016). In order to be accessible to the cytosolic protein degradation machinery these proteins need to be removed from the lipid bilayer of the OM. The two ATPases TbVCP and TbMsp1 both contribute to this function in a synergistic manner (Gerber et al., 2023). It has been shown that yeast Msp1 functions in a reconstituted liposome assay without any substrate modifications or associated proteins (Wohlever et al., 2017). However, in trypanosomes, the processing of certain substrates has been demonstrated to depend on the presence of both, TbMsp1 and TbMsp1-interacting proteins (Gerber et al., 2023). Since Msp1 is well conserved, it is reasonable to assume that this difference is mainly due to the different substrates analysed and that yeast Msp1 and TbMsp1 are not functioning fundamentally different (Gerber et al., 2023). There might be different substrate recognition mechanisms or substrate modifications for some of which TbMsp1 is dependent on its interacting proteins for correct recognition.

Proteins targeted for proteasomal degradation are often marked with a ubiquitin polymer a various lengths (Chau et al., 1989; Hershko and Ciechanover, 1998). Ubiquitin consists of 76 amino acids and can be covalently attached via its C-terminus to a substrate lysine or to other ubiquitins. However, alternative ubiquitination sites have been reported, for example the N-terminus of the protein MyoD (Breitschopf et al., 1998). The TbVCP yeast homologue Cdc48 has been shown to rely on ubiquitination of its substrates to remove them from membranes (Bodnar et al., 2018; Olszewski et al., 2019; Twomey et al., 2019). VCP and Cdc48 are highly conserved and involved in common eukaryotic processes such as endoplasmic reticulum-associated degradation (ERAD). Therefore, it is very likely that these findings also apply to TbVCP.

In this study we wanted to investigate whether ubiquitination plays a role in the TbMsp1 assisted mitochondria-associated degradation (MAD) pathway that is triggered by pATOM36 ablation. We expressed a version of the MAD substrate ATOM19 where all the lysines were replaced by arginines. Using blue native PAGE, we could show that ATOM19 without lysines is still integrated into a large molecular weight complex. Upon ablation of pATOM36, ATOM19 and the ATOM19 variant without lysines are both depleted from the cells. Moreover, both versions of ATOM19 are equally depleted in cells induced for pATOM36 and TbMsp1 RNAi. Hence, these results show that, should ubiquitination be required for the TbVCP linked MAD pathway, it is not attached to internal lysines in ATOM19.

Results

ATOM19 is 168 amino acids long and contains four lysines (Figure 1). The short length and the low number of lysines make this protein a good candidate to investigate the role of ubiquitination in the previously described MAD pathway. Lysines are the primary target for ubiquitination and mutating lysines to arginine in a protein of interest has been demonstrated to prevent its ubiquitination (G. Chen et al., 2014). We hypothesized that a variant of ATOM19 where all lysines are replaced by arginines might be resistant to ubiquitination. Thus, ATOM19 without lysines (Figure 1) was expressed in situ with a C-terminal HA-tag in cells that can either be induced for pATOM36 RNAi or for pATOM36, TbMsp1 double RNAi (Figure 2).

```
ATOM19              1 MDSLAHSVSSMVHCAENFHIPLVRSRTVVTAVAVGIPIAVLLHDTAEHWM     50
                      ||||||||||||||||||||||||||||||||||||||||||||||||||
ATOM19_no_K         1 MDSLAHSVSSMVHCAENFHIPLVRSRTVVTAVAVGIPIAVLLHDTAEHWM     50

ATOM19             51 PTSFQLPIISWFRRKWRQNPEVKSSHLTLARNAIIFFYLAMVLSEGTFYE    100
                      ||||||||||||||:|||||||:||||||||||||||||||||||||||||
ATOM19_no_K        51 PTSFQLPIISWFRRRWRQNPEVRSSHLTLARNAIIFFYLAMVLSEGTFYE    100

ATOM19            101 TPIDYVADRVSGAPARKAFNERIQKGRHSAFSAAEEVASEEGLNEASSRQ    150
                      ||||||||||||||||:|||||||:||||||||||||||||||||||||||
ATOM19_no_K       101 TPIDYVADRVSGAPARRAFNERIQRGRHSAFSAAEEVASEEGLNEASSRQ    150

ATOM19            151 QRDTALRRRFLHESRTSN    168
                      ||||||||||||||||||
ATOM19_no_K       151 QRDTALRRRFLHESRTSN    168
```

Figure 1: Emboss needle alignment of amino acid sequences of ATOM19 and ATOM19 without lysines (ATOM19_no_K). Replaced lysines are highlighted in red.

As shown in Figure 2A ATOM19 without lysines as well as wild type ATOM19 are expressed in uninduced cells and are essentially completely degraded upon pATOM36 RNAi induction. If our hypothesis holds true and ATOM19 without lysines cannot be ubiquitinated we expect the protein to be extracted from the membrane by TbMsp1 and not TbVCP, as based on results in other organisms, TbVCP most likely depends on ubiquitination (Bodnar et al., 2018; Olszewski et al., 2019; Twomey et al., 2019). Figure 2B illustrates that in the presence of pATOM36, ATOM19 without lysines is integrated in a high molecular weight complex, that likely corresponds to the ATOM complex. We expect only orphaned proteins to be substrates of the pATOM36-associated MAD pathway. Therefore, ATOM19 without lysines was expected to integrate in a complex because it is only targeted for degradation upon pATOM36 ablation.

However, surprisingly, Figure 2C shows that ATOM19 without lysines in the absence of pATOM36 and TbMsp1 is degraded to the same extent as wildtype ATOM19. These results suggest that even though lysines are the primary target for ubiquitination, ATOM19 without lysines can be extracted from the OM by TbVCP. This can be explained either by TbVCP

functioning in a fundamentally different manner than its yeast homologue Cdc48 or, more likely, by ATOM19 still being ubiquitinated despite having no lysines.

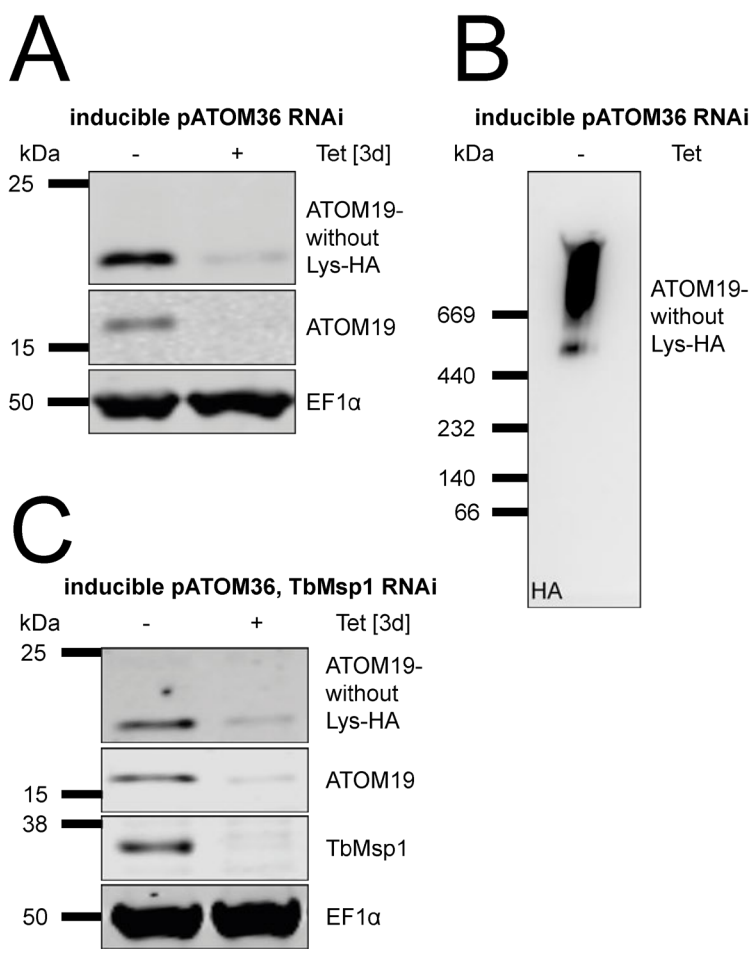

Figure 2: No difference between ATOM19 without lysin and wild type ATOM19 A) Western blot analysis of total cellular extract (3 × 10^6 cells each) of uninduced and induced pATOM36 RNAi cells in situ expressing ATOM19 without lysines. Immunoblots were probed with HA and ATOM19 antisera. EF1α serves as a loading control. B) BN-PAGE immunoblot analysis of mitochondria enriched fractions of cells in situ expressing ATOM19 without lysines. Immunoblot was decorated with HA antiserum. C) Western blot analysis of total cellular extract (3 × 10^6 cells each) of uninduced and induced pATOM36, TbMsp1 RNAi cells in situ expressing ATOM19 without lysines. Immunoblots were probed with HA, ATOM19 and TbMsp1 antisera. EF1α serves as a loading control.

Discussion

This study could not determine if ubiquitination plays a role in TbMsp1-assisted MAD upon pATOM36 ablation. We have discovered that in situ expressed C-terminally HA tagged ATOM19 without lysines is degraded if pATOM36 is ablated. We have recently published a model where MAD substrates can be removed from the OM by either TbVCP or TbMsp1 (Gerber et al., 2023). Our experiments demonstrate that ATOM19 without lysines is integrated into a large molecular weight complex which is most likely the ATOM complex. The high molecular weight complex we detect by BN-PAGE analysis is very similar to previously published BN immunoblots stained for ATOM components (Mani et al., 2015).To gain further evidence, a coimmunoprecipitation (CoIP) experiment with ATOM19 lacking lysines could be performed. If lysine-less ATOM19 and other ATOM components are detected in the CoIP eluate, it would prove that integration of ATOM19 without lysines into the ATOM complex is possible.

ATOM19 lacking lysines was further investigated in cells knocked down for either pATOM36 or pATOM36 in combination with TbMsp1. The efficiency of the TbMsp1 RNAi was demonstrated directly by the decrease of the protein by western blot. The efficiency of the pATOM36 RNAi was shown indirectly by the decrease of wild type ATOM19 signal on western blot, which is a direct consequence of the lack of pATOM36 (Gerber et al., 2023; Käser et al., 2016). Surprisingly, in situ expressed ATOM19 without lysines in cells induced for pATOM36 and TbMsp1 RNAi was still subjected to MAD. Since TbMsp1 is absent in these cells, the protein is most likely extracted from the OM by TbVCP. This could be explained by TbVCP functioning in a fundamentally different manner than its yeast homologue Cdc48. However, due to the high conservation of this protein in all eukaryotes this seems unlikely. It is more probable that ATOM19 without lysines can still be ubiquitinated, possibly at the N-terminus.

It would be interesting to experimentally determine whether ATOM19 without lysines can be ubiquitinated at its N-terminus. To prevent the N-terminal ubiquitination one could add a large tag e.g., a 6x myc tag, to the N-terminus of the protein. This has been demonstrated to effectively prevent ubiquitination in mammalian cells (Breitschopf et al., 1998). Another method successfully applied was expressing the protein of interest fused to a deubiquitination enzyme (DUb) (Henning et al., 2022; Stringer and Piper, 2011). The presented set of experiments could be repeated with the addition of either a bulky tag or a DUb to the N-terminus of ATOM19 without lysines.

In summary, further experiments are needed to determine more definitively whether ubiquitination of pATOM36 substrates is required for them to be processed by TbMsp1 or TbVCP assisted MAD.

Material and Methods

Transgenic cell lines

Transgenic *T. brucei* cell lines were generated using cell lines descending from the procyclic strain 29.13 (Wirtz et al., 1999). ATOM19 without lysines was introduced into published pATOM36 RNAi, and pATOM36, TbMsp1 RNAi cell lines (Gerber et al., 2023; Pusnik et al., 2012). Cells were cultivated at 27°C in SDM-79 (Brun and Schönenberger, 1979) supplemented with 10% (vol/vol) FCS, containing G418 (15 µg/ml; Gibco), hygromycin (25 µg/ml; InvivoGen), puromycin (2 µg/ml; InvivoGen), blasticidin (10 µg/ml; InvivoGen), and phleomycin (2.5 µg/ml; LifeSpan BioSciences) as required. RNAi was induced by adding 1 µg/ml tetracycline to the medium.

ATOM19 without lysines was ordered as a synthetic gene from biomatik as the following sequence:

ATGGATAGCCTTGCACACAGTGTGAGTTCTATGGTGCACTGCGCCGAAAACTTTCACAT
CCCGCTTGTGCGCAGCCGGACTGTAGTGACCGCTGTGGCTGTGGGCATTCCCATTGCC
GTTTTGCTTCACGACACAGCCGAACACTGGATGCCTACCTCATTTCAACTCCCCATTATT
TCATGGTTTCGCCGACGGTGGCGGCAGAACCCGGAAGTGCGTTCATCACACCTGACAC
TTGCGCGCAATGCCATTATATTCTTTTACTTAGCCATGGTGCTGAGTGAAGGCACATTTT
ACGAAACGCCTATAGATTATGTGGCGGATCGGGTATCTGGAGCTCCCGCACGACGCGC
ATTTAACGAGCGCATTCAACGAGGTCGCCATAGTGCCTTTTCAGCTGCTGAAGAGGTTG
CTAGTGAAGAAGGTTTGAATGAAGCGAGTTCCAGGCAGCAGCGAGACACCGCACTCCG
TCGCCGTTTCTTACATGAAAGCCGTACTTCCAACTAA

All four lysin codons that were changed to arginine are highlighted in green. A *SacI* (GAGCTC) restriction site was also mutated without changing the amino acid sequence to facilitate cloning, highlighted in yellow. The protein was cloned into a plasmid based on pMO-3HA, pBluescriptII KS+ plasmid (Oberholzer et al., 2006).

DNA construct for transfection was obtained using PCR with the following oligonucleotides:
Forward primer:
ttgaaggtttttttttgaaaaaagaagagaagaaaaataaggggtaaataaaattaatatacaaaagaaataaggcaatATG
GATAGCCTTGCACACAGTGTGAGTTCTATGGTG

Reverse primer:
ccccctctctctctcctattcgccttcttcaagttctttccccaaactttccccctttctatttttttttttcacaactcTGGCGGCCGCT
CTAGAACTAGTGGAT

SDS-PAGE and western blot

Cells were treated with tetracycline for three days to induce RNAi and ectopic protein expression as indicated. After the cells were washed with PBS, they were lysed in SDS buffer (2% SDS, 0.0025% bromophenol blue (w/v), 100mM β-mercaptoethanol in 60 mM Tris-HCl pH 6.8). $3x10^6$ cell equivalents per lane were separated on a 14% acrylamide gel in an electrophoresis cell (Bio-rad, Mini-PROTEAN Tetra Vertical Electrophoresis Cell). After transfer on a nitrocellulose membrane (Amersham) and blocking in 5% milk in PBS antisera against indicated proteins were added in 2.5% milk, PBST (HA 1:5'000 (BioLegend, 901503 (MMS-101R)), ATOM19 1:500 (Gerber et al., 2023), TbMsp1 1:1'000 (Gerber et al., 2023), EF1α 1:10'000 (Merk Millipore, 05-235)). After three PBST washes the membranes were incubated with secondary antibodies (Anti-mouse IRDye 680LT conjugated (goat) and Anti-rabbit IRDye 800CW conjugated (goat), 1:20'000, LI-COR Biosciences). The membranes were imaged using a LI-COR ODYSSEY scanner and analysed using the corresponding software (Image Studio Lite v. 5.2.5., LI-COR Biosciences).

Digitonin extraction followed by BN-PAGE

Crude mitochondria-enriched fractions were obtained by incubating 1 × 10^8 uninduced cells, in situ expressing ATOM19 without lysines, in 0.6 M sorbitol, 20 mM Tris–HCl (pH 7.5), and 2 mM EDTA (pH 8) containing 0.015% (w/v) digitonin (Biosynth) on ice. Centrifugation (5 min, 6,800 g, 4°C) yielded a cytosolic supernatant and a mitochondria-enriched pellet. This pellet was solubilized in solubilization buffer (20 mM Tris–HCl pH 7.4, 50 mM NaCl, 10% glycerol, 0.1 mM EDTA) containing 1% (w/v) digitonin and incubated on ice for 15 min. After centrifugation (20,000 g, 4°C, 15 min), the supernatant was separated on 4–13% gradient acrylamide gels. 5 x 10^7 cell equivalent was loaded per well. Before western blotting, the gel was incubated in SDS-PAGE running buffer (25 mM Tris, 1 mM EDTA, 190 mM glycine, 0.05% (w/v) SDS) to facilitate transfer of the proteins to a PVDF membrane (Immobilon-FL). The immunoblot was decorated with HA antiserum (BioLegend, 1:5000 in PBST, 2.5% milk). Anti-mouse (goat, HRP-coupled, Sigma Aldrich) antibodies were used as secondary antibodies.

References

Becker, T., Wenz, L.-S., Krüger, V., Lehmann, W., Müller, J.M., Goroncy, L., Zufall, N., Lithgow, T., Guiard, B., Chacinska, A., Wagner, R., Meisinger, C., Pfanner, N., 2011. The mitochondrial import protein Mim1 promotes biogenesis of multispanning outer membrane proteins. Journal of Cell Biology 194, 387–395. https://doi.org/10.1083/jcb.201102044

Bodnar, N.O., Kim, K.H., Ji, Z., Wales, T.E., Svetlov, V., Nudler, E., Engen, J.R., Walz, T., Rapoport, T.A., 2018. Structure of the Cdc48 ATPase with its ubiquitin-binding cofactor Ufd1–Npl4. Nat Struct Mol Biol 25, 616–622. https://doi.org/10.1038/s41594-018-0085-x

Breitschopf, K., Bengal, E., Ziv, T., Admon, A., Ciechanover, A., 1998. A novel site for ubiquitination: the N-terminal residue, and not internal lysines of MyoD, is essential for conjugation and degradation of the protein. The EMBO Journal 17, 5964–5973. https://doi.org/10.1093/emboj/17.20.5964

Bruggisser, J., Käser, S., Mani, J., Schneider, A., 2017. Biogenesis of a Mitochondrial Outer Membrane Protein in *Trypanosoma brucei*. J Biol Chem 292, 3400–3410. https://doi.org/10.1074/jbc.M116.755983

Brun, R., Schönenberger, 1979. Cultivation and in vitro cloning or procyclic culture forms of *Trypanosoma brucei* in a semi-defined medium. Short communication. Acta Trop 36, 289–292.

Chau, V., Tobias, J.W., Bachmair, A., Marriott, D., Ecker, D.J., Gonda, D.K., Varshavsky, A., 1989. A multiubiquitin chain is confined to specific lysine in a targeted short-lived protein. Science 243, 1576–1583. https://doi.org/10.1126/science.2538923

Chen, G., Xu, X., Tong, J., Han, K., Zhang, Z., Tang, J., Li, S., Yang, C., Li, J., Cao, B., Zhou, H., Wu, D., Moran, M.F., Mao, X., 2014. Ubiquitination of the transcription factor c-MAF is mediated by multiple lysine residues. The International Journal of Biochemistry & Cell Biology 57, 157–166. https://doi.org/10.1016/j.biocel.2014.10.024

Dimmer, K.S., Papić, D., Schumann, B., Sperl, D., Krumpe, K., Walther, D.M., Rapaport, D., 2012. A crucial role for Mim2 in the biogenesis of mitochondrial outer membrane proteins. Journal of Cell Science 125, 3464–3473. https://doi.org/10.1242/jcs.103804

Doan, K.N., Grevel, A., Mårtensson, C.U., Ellenrieder, L., Thornton, N., Wenz, L.-S., Opaliński, Ł., Guiard, B., Pfanner, N., Becker, T., 2020. The Mitochondrial Import Complex MIM Functions as Main Translocase for α-Helical Outer Membrane Proteins. Cell Reports 31, 107567. https://doi.org/10.1016/j.celrep.2020.107567

Gerber, M., Suppanz, I., Oeljeklaus, S., Niemann, M., Käser, S., Warscheid, B., Schneider, A., Dewar, C.E., 2023. A Msp1-containing complex removes orphaned proteins in the mitochondrial outer membrane of T. brucei. Life Science Alliance 6. https://doi.org/10.26508/lsa.202302004

Guna, A., Stevens, T.A., Inglis, A.J., Replogle, J.M., Esantsi, T.K., Muthukumar, G., Shaffer, K.C.L., Wang, M.L., Pogson, A.N., Jones, J.J., Lomenick, B., Chou, T.-F., Weissman, J.S., Voorhees, R.M., 2022. MTCH2 is a mitochondrial outer membrane protein insertase. Science 378, 317–322. https://doi.org/10.1126/science.add1856

Henning, N.J., Boike, L., Spradlin, J.N., Ward, C.C., Liu, G., Zhang, E., Belcher, B.P., Brittain, S.M., Hesse, M.J., Dovala, D., McGregor, L.M., Valdez Misiolek, R., Plasschaert, L.W., Rowlands, D.J., Wang, F., Frank, A.O., Fuller, D., Estes, A.R., Randal, K.L., Panidapu, A., McKenna, J.M., Tallarico, J.A., Schirle, M., Nomura, D.K., 2022. Deubiquitinase-targeting chimeras for targeted protein stabilization. Nat Chem Biol 18, 412–421. https://doi.org/10.1038/s41589-022-00971-2

Hershko, A., Ciechanover, A., 1998. THE UBIQUITIN SYSTEM.

Käser, S., Oeljeklaus, S., Týč, J., Vaughan, S., Warscheid, B., Schneider, A., 2016. Outer membrane protein functions as integrator of protein import and DNA inheritance in mitochondria. Proc Natl Acad Sci USA 113, E4467–E4475. https://doi.org/10.1073/pnas.1605497113

Mani, J., Desy, S., Niemann, M., Chanfon, A., Oeljeklaus, S., Pusnik, M., Schmidt, O., Gerbeth, C., Meisinger, C., Warscheid, B., Schneider, A., 2015. Mitochondrial protein import receptors in Kinetoplastids reveal convergent evolution over large phylogenetic distances. Nat Commun 6, 6646. https://doi.org/10.1038/ncomms7646

Niemann, M., Wiese, S., Mani, J., Chanfon, A., Jackson, C., Meisinger, C., Warscheid, B., Schneider, A., 2013. Mitochondrial Outer Membrane Proteome of *Trypanosoma brucei* Reveals Novel Factors Required to Maintain Mitochondrial Morphology. Mol Cell Proteomics 12, 515–528. https://doi.org/10.1074/mcp.M112.023093

Oberholzer, M., Morand, S., Kunz, S., Seebeck, T., 2006. A vector series for rapid PCR-mediated C-terminal in situ tagging of *Trypanosoma brucei* genes. Molecular and Biochemical Parasitology 145, 117–120. https://doi.org/10.1016/j.molbiopara.2005.09.002

Olszewski, M.M., Williams, C., Dong, K.C., Martin, A., 2019. The Cdc48 unfoldase prepares well-folded protein substrates for degradation by the 26S proteasome. Commun Biol 2, 1–8. https://doi.org/10.1038/s42003-019-0283-z

Papić, D., Krumpe, K., Dukanovic, J., Dimmer, K.S., Rapaport, D., 2011. Multispan mitochondrial outer membrane protein Ugo1 follows a unique Mim1-dependent import pathway. Journal of Cell Biology 194, 397–405. https://doi.org/10.1083/jcb.201102041

Pusnik, M., Mani, J., Schmidt, O., Niemann, M., Oeljeklaus, S., Schnarwiler, F., Warscheid, B., Lithgow, T., Meisinger, C., Schneider, A., 2012. An essential novel component of the noncanonical mitochondrial outer membrane protein import system of trypanosomatids. MBoC 23, 3420–3428. https://doi.org/10.1091/mbc.e12-02-0107

Schmitt, S., Prokisch, H., Schlunck, T., Camp II, D.G., Ahting, U., Waizenegger, T., Scharfe, C., Meitinger, T., Imhof, A., Neupert, W., Oefner, P.J., Rapaport, D., 2006. Proteome analysis of mitochondrial outer membrane from Neurospora crassa. PROTEOMICS 6, 72–80. https://doi.org/10.1002/pmic.200402084

Stringer, D.K., Piper, R.C., 2011. Terminating protein ubiquitination. Cell Cycle 10, 3067–3071. https://doi.org/10.4161/cc.10.18.17191

Twomey, E.C., Ji, Z., Wales, T.E., Bodnar, N.O., Ficarro, S.B., Marto, J.A., Engen, J.R., Rapoport, T.A., 2019. Substrate processing by the Cdc48 ATPase complex is initiated by ubiquitin unfolding. Science 365, eaax1033. https://doi.org/10.1126/science.aax1033

Vitali, D.G., Käser, S., Kolb, A., Dimmer, K.S., Schneider, A., Rapaport, D., 2018. Independent evolution of functionally exchangeable mitochondrial outer membrane import complexes. eLife 7, e34488. https://doi.org/10.7554/eLife.34488

Wirtz, E., Leal, S., Ochatt, C., Cross, GeorgeA.M., 1999. A tightly regulated inducible expression system for conditional gene knock-outs and dominant-negative genetics in *Trypanosoma brucei*. Molecular and Biochemical Parasitology 99, 89–101. https://doi.org/10.1016/S0166-6851(99)00002-X

Wohlever, M.L., Mateja, A., McGilvray, P.T., Day, K.J., Keenan, R.J., 2017. Msp1 Is a Membrane Protein Dislocase for Tail-Anchored Proteins. Molecular Cell 67, 194-202.e6. https://doi.org/10.1016/j.molcel.2017.06.019

3.3 Indication for the interaction between Msp1 and endoplasmic reticulum proteins in *T. brucei*

Markus Gerber[1, 2], Caroline E. Dewar[1], Silke Oeljeklaus[3], Bettina Warscheid[3], André Schneider[1]

[1] Department of Chemistry, Biochemistry and Pharmaceutical Sciences, University of Bern, Bern, Switzerland

[2] Graduate School for Cellular and Biomedical Sciences, University of Bern, Switzerland

[3] Faculty of Chemistry and Pharmacy, Biochemistry II, Theodor Boveri-Institute, University of Würzburg, Würzburg, Germany

Contribution

All data presented in this chapter are unpublished and not part of a submitted manuscript. Dr. Caroline E. Dewar supervised this project.

My contributions:

- Cloning and generation of cell lines used

- Performing all experiments presented here, with the exception of the mass spectrometry analysis which was performed by the Warscheid group in Würzburg.

- Creating all the figures

- The text presented here

Abstract

Mitochondria are essential organelles, most prominently known for their role in ATP generation. Eukaryotes have developed a variety of pathways to restore defective mitochondria upon mitochondrial stress. Some of these pathways involve mitochondrial sorting of proteins 1 (Msp1), an ATPase associated with diverse cellular activities. Msp1 removes mislocalized as well as destabilized alpha-helically anchored membrane proteins from the mitochondrial outer membrane (OM), and subjects them for degradation by the cytosolic proteasome. Additionally, Msp1 can clear stuck substrates from the translocase of the outer membrane (TOM). It is known, for a subset of Msp1 substrates that they are reinserted into the endoplasmic reticulum (ER) membrane before they are degraded using components of the ER-associated degradation machinery (ERAD). Other Msp1 substrates may follow different degradation routes. However, the molecular components and the mechanisms connecting Msp1 to the ER, or potentially directly to the proteasome have yet to be elucidated. Here we investigate Msp1-mediated OM protein degradation in the unicellular parasite Trypanosoma brucei. We further characterize T. brucei Msp1 (TbMsp1) by exclusively expressing a substrate trap (ST) mutant TbMsp1 which is able to bind the substrate as well as ATP but is unable to hydrolyse ATP and therefore cannot release its substrates. We ablated pATOM36 to trigger a previously described mitochondrial quality control pathway in the presence of wildtype (WT)- and ST-TbMsp1-myc and performed stable isotope labelling by amino acids in cell culture (SILAC) followed by coimmunoprecipitation (CoIP) and mass spectrometry (MS) of ST-TbMsp1-myc, using WT-TbMsp1-myc as a control. Surprisingly, there were no known pATOM36 substrates specifically enriched with ST-TbMsp1-myc. These results indicate that these substrates might be preferentially removed from the OM by TbVCP. However, in the list of proteins which were pulled down, we not only uncovered potential new TbMsp1 substrates, but also potential downstream components of the TbMsp1 pathway. Among the enriched proteins we found three members of the endoplasmic reticulum membrane protein complex (EMC). Among other functions, the EMC complex mediates the insertion of tail-anchored proteins into the ER membrane. These results suggest that TbMsp1 and the EMC potentially interact with each other at mitochondria-ER contact sites.

Introduction

Eukaryotic cells harbour a variety of organelles, each of which contains a subset of nuclear encoded proteins. These proteins are translated by cytosolic ribosomes and subsequently targeted to their respective organelle. Tail-anchored (TA) membrane proteins of the endoplasmic reticulum (ER) for example are shuttled to the ER via the Guided Entry of Tail-Anchored (Get) protein import pathway (Schuldiner et al., 2008; Stefanovic and Hegde, 2007).

Upon interference with the Get pathway, some these TA proteins, which normally localize to the ER membrane, are inserted into the mitochondrial OM instead (Okreglak and Walter, 2014). The conserved, membrane-anchored ATPase Associated with various cellular Activities (AAA), mitochondrial sorting of proteins 1 (Msp1) is a crucial component of a mitochondria-associated degradation (MAD) pathway which clears the OM from such mislocalized TA ER proteins (Okreglak and Walter, 2014). Pex15 is such a TA protein; it normally inserts into the ER membrane, but is cleared upon mislocalisation to the OM via Msp1 followed by degradation by the cytosolic proteasome (Okreglak and Walter, 2014). Interestingly, Pex15Δ30 that is removed from the OM by Msp1 is not directly shuttled to the proteasome, but reinserted into the ER membrane, before it is further processed and degraded via part of the ER-associated degradation (ERAD) pathway (Dederer et al., 2019; Matsumoto et al., 2019). It seems counterintuitive for the cell to reinsert a protein into another membrane and use even more ATP to extract it before it can be degraded. However, this localisation to the ER offers the option for the cell to divert the protein to the correct localisation pathway. This re-localisation pathway was also observed for the Golgi protein Gos1 (Y.-C. Chen et al., 2014; Matsumoto, 2023). It has been suggested that Msp1 substrates contain exposed hydrophobic patches which are recognized by Msp1 if the substrates fail to assemble into their correct complexes in the OM. This suggests that these recognition signals are hidden if the Msp1-substrate is present in complexes (Li et al., 2019). AAA proteins, such as Msp1 have been intensively studied, and the molecular mechanisms of how substrate proteins are extracted are known in great detail (L. Wang et al., 2020). However, how proteins extracted by Msp1 travel to the ER, and whether all Msp1 substrates follow this route remains elusive.

Most studies on Msp1 have been conducted in yeast and mammals, which belong to the same eukaryotic supergroup of the Opisthokonts. We have recently discovered a novel Msp1 dependent mitochondrial quality control (MQC) pathway in the protozoan parasite *Trypanosoma brucei* (Gerber et al., 2023). Upon the knockdown of the pATOM36 which is a yeast OM protein insertase MIM analogue, several ATOM complex components are removed from the OM either by *T. brucei* valosin-containing protein (TbVCP) or *T. brucei* Msp1 (TbMsp1) and degraded (Gerber et al., 2023; Käser et al., 2016; Vitali et al., 2018). We determined that TbMsp1 forms a stable complex with four integral OM proteins. Additionally, three of these TbMsp1 interacting proteins, TbJ31, POMP31 and TbTsc13, are needed for TbMsp1-dependent removal of pATOM36 substrates from the OM (Gerber et al., 2023).

In this study we aimed to identify additional TbMsp1 substrates in trypanosomes. For this purpose we used a synthetic RNAi resistant version of TbMsp1 containing a point mutation changing the amino acid from glutamic acid (E) to glutamine (Q) in the highly conserved Walker B motif of the AAA domain of TbMsp1(Gerber et al., 2023). The resulting mutant TbMsp1 loses the ability to hydrolyse ATP (Li et al., 2019). The same approach was used before with yeast

Msp1 (Basch et al., 2020; Castanzo et al., 2020; Li et al., 2019; Matsumoto et al., 2019; Okreglak and Walter, 2014). We expressed this C-terminally myc-tagged RNAi-resistant substrate trap (ST) mutant ST-TbMsp1 in the background of a TbMsp1, pATOM36 double RNAi cell line. As a control, the same cell lines were created expressing a C terminally myc tagged RNAi resistant version of wildtype (WT) WT-TbMsp1 was used. We could show that the ST-TbMsp1 localizes similar to WT-TbMsp1 in immunofluorescence assays (IFA). Furthermore, using blue native (BN) PAGE of mitochondrial enriched fractions we could observe ST-TbMsp1 but not WT-TbMsp1 in a complex. Finally, we attempted to assess tagged ST-TbMsp1s ability to pull down substrates. We subjected tagged WT- or ST-TbMsp1 expressed in the pATOM36, TbMsp1 double RNAi cell line to stable isotope labelling with amino acids in cell culture (SILAC) coimmunoprecipitation (CoIP) followed by mass spectrometry (MS). The resulting analysis provided us with a dozen proteins that show significantly stronger interaction with ST-TbMsp1 than WT-TbMsp1. Surprisingly, none of the expected pATOM36 substrates appeared among these 12 proteins. Interestingly, we did pull down three components of the ER membrane protein complex (EMC). These findings suggest that TbMsp1 may interact with the EMC at the mitochondrial – ER interface.

Results

Ectopic expression of ST-TbMsp1 has no effect on growth of procyclic trypanosomes. We ectopically expressed ST- and WT-TbMsp1 in transgenic cell lines which allow inducible RNAi for either TbMsp1 or for TbMsp1 and pATOM36 together. As can be seen in the top left panel of Figure 1, the exclusive ectopic expression of a RNAi resistant WT-TbMsp1 marginally affects the growth of procyclic trypanosomes induced for TbMsp1 RNAi. For unknown reasons endogenous TbMsp1 is not detected in non-induced cells (Figure 1, top left). Possibly the RNAi in those cells is leaky. Importantly, the expression of ST-TbMsp1 does not affect growth (Figure 1, top right). In the two cell lines that exclusively express either ST- or WT-TbMsp1 in the background of pATOM36 RNAi the TbMsp1 RNAi is probably leaky as well (Figure 1, bottom left & right). However, pATOM36 is present in non-induced, and absent in induced cells (Figure 1, bottom left & right). Both of these double RNAi cell lines also show growth inhibition starting at around three days after induction, which aligns with previous experiments were pATOM36 was depleted (Gerber et al., 2023; Käser et al., 2016).

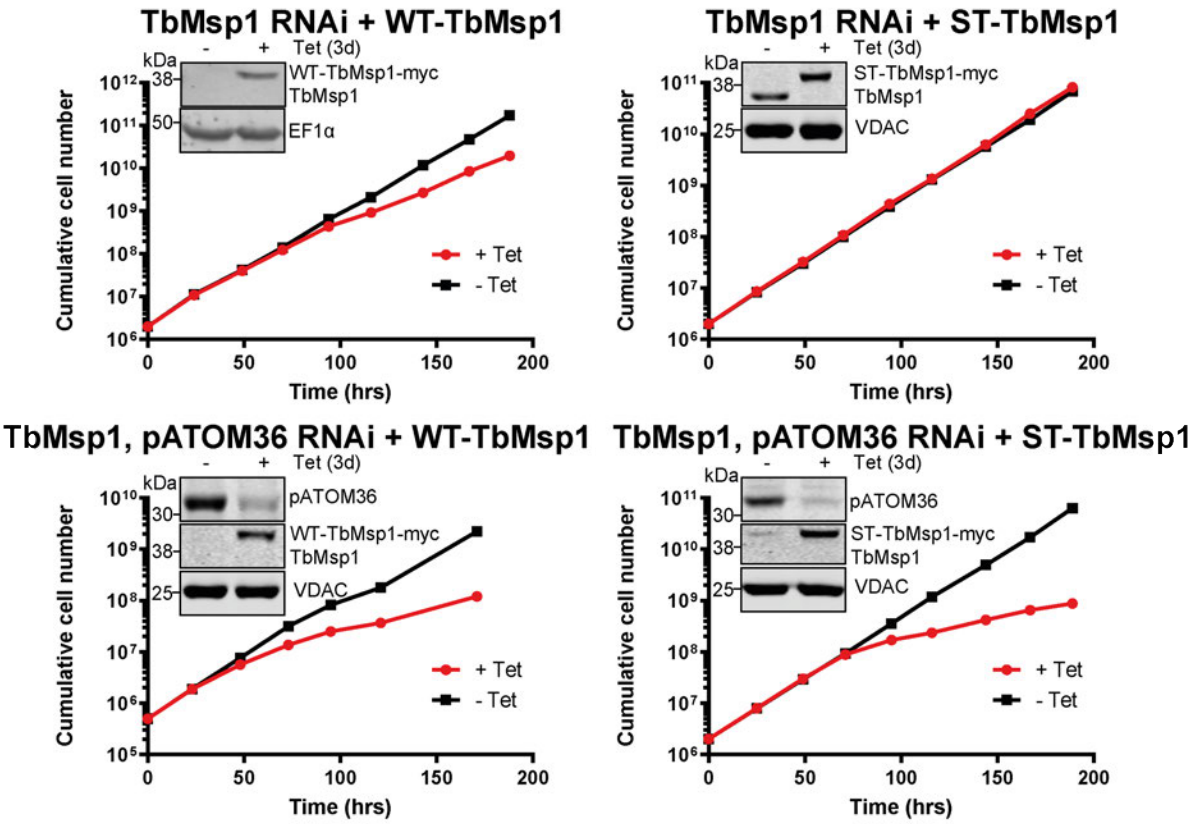

Figure 1: Verification and growth analysis of ectopic expression of WT- and ST-TbMsp1-myc and indicated RNAis.

Growth curve of the indicated induced (+Tet) and uninduced (−Tet) RNAi cell lines. The growth curves were performed in triplicate, but the SD are too small to be displayed. The inset panels show the efficiency of RNAi for the indicated cell lines, 3 d after induction when analysed by Western blot using anti TbMsp1 antiserum. Voltage dependent anion channel (VDAC) or eukaryotic elongation factor 1 α (EF1α) serve as loading control.

Ectopically expressed ST and WT-TbMsp1 localise alike in an immunofluorescence analysis. All four cell lines exclusively expressing WT- or ST-TbMsp1 either in the presence or the absence of pATOM36 RNAi were subjected to immunofluorescence analysis (IFA) (Figure 2). It was previously shown that TbMsp1 localizes to glycosomes and the OM, it therefore does not colocalize perfectly with any of the tested organellar markers (Gerber et al., 2023). Nonetheless, both WT- and ST-TbMsp1 overlap with the mitochondrial marker protein ATOM40 to a similar extent as has been observed for unclogged TbMsp1 (Gerber et al., 2023). This indicates that the ST mutation does not lead to mislocalisation of TbMsp1.

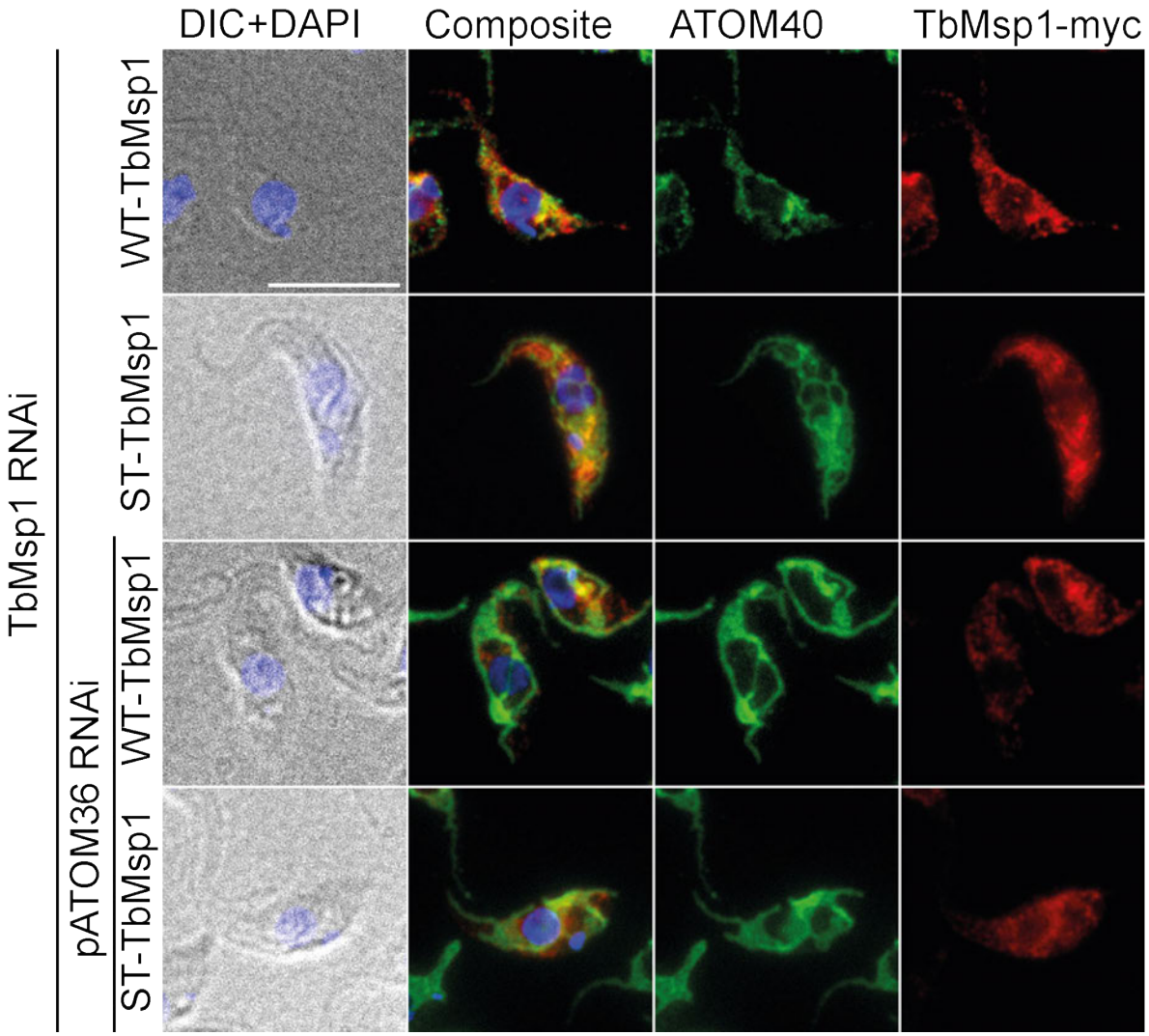

Figure 2: WT- and ST-TbMsp1 localise alike in an immunofluorescence analysis. Immunofluorescence analysis of cells exclusively expressing the C-terminally myc tagged WT- or ST-TbMsp1 (as indicated at the left of each row) in the presence and absence of pATOM36 RNAi (as indicated at the left). Cells were stained using anti-myc antibodies (right column) and co-stained with the mitochondrial marker ATOM40 (third column). All slides were also stained with DAPI, which marks both nuclear and mitochondrial DNA in merged images (first and second column). Scale bar = 10 µm.

The ST mutation renders the TbMsp1 complex stable for blue native polyacrylamide gel electrophoresis. The WT-TbMsp1 forms a complex that is not stable during blue native polyacrylamide gel electrophoresis (BN-PAGE) analysis (Figure 3, lanes 1, 3, 5, 7). However, the ST mutation stabilizes a TbMsp1-myc-containing complex that can be detected by BN-PAGE of around 666 kDa. TbMsp1 has a molecular weight of ~37 kDa, meaning that the expected hexameric TbMsp1 complex would have an expected molecular weight of approximately 223 kDa. This indicates that the 666 kDa complex likely contains additional proteins such as possible substrates but maybe also stably interacting proteins. Furthermore,

the addition of ATP to all the buffers after lysis seems to stabilize the TbMsp1-myc-containing high molecular weight complex resulting in a more intense band (Figure 3, lanes 6 and 8).

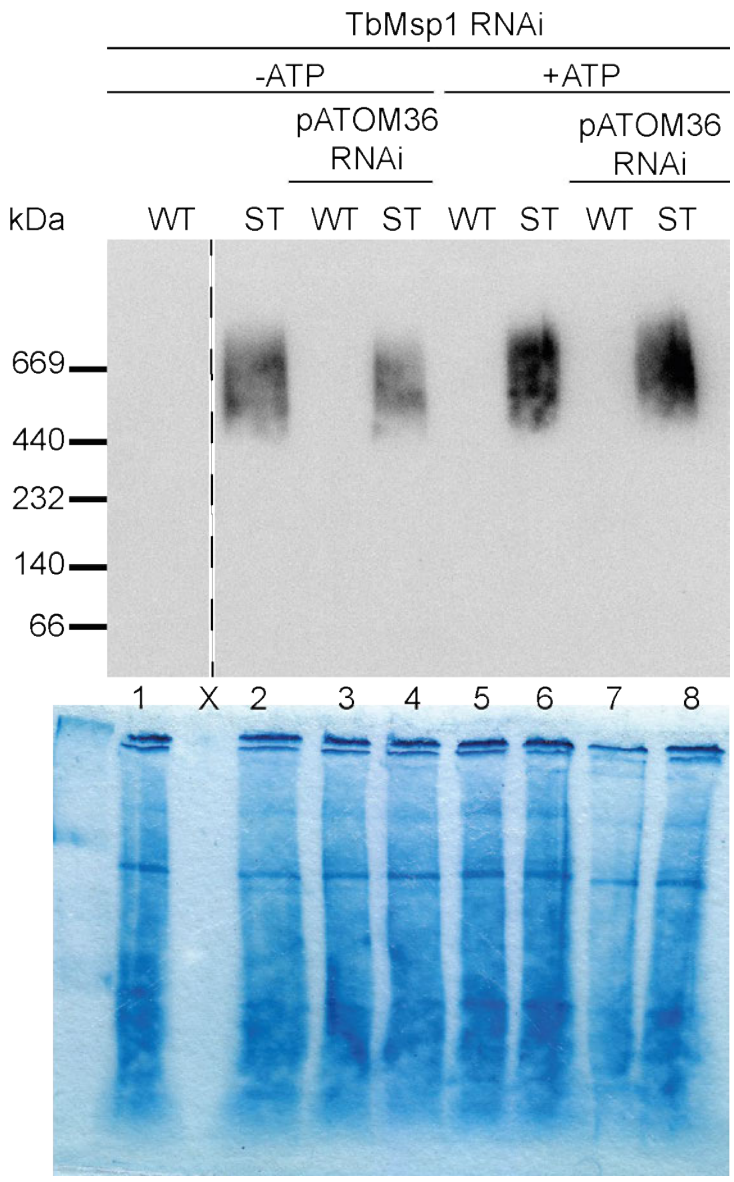

Figure 3: TbMsp1 complex is stabilized by the ST mutation. BN-PAGE immunoblot analysis of solubilized mitochondrial fractions of the cell lines exclusively expressing the indicated WT or ST-TbMsp1-myc variants in the presence and absence of pATOM36 RNAi as well as the presence and absence of ATP. The immunoblot was probed for myc. The Coomassie gel serves as a loading control.

ST-TbMsp1 does not bind to pATOM36 substrates upon pATOM36 RNAi. A CoIP was performed in cells exclusively expressing myc-tagged ST- or WT-TbMsp1 that were induced for pATOM36 RNAi. The resulting Immunoblot was analysed with myc and ATOM19 antibodies, revealing that in both cases the pulldown of TbMsp1-myc was very efficient (Figure 4). However, the ATOM subunit ATOM19, a known substrate of pATOM36, was recovered in neither of the IP eluates (Figure 4).

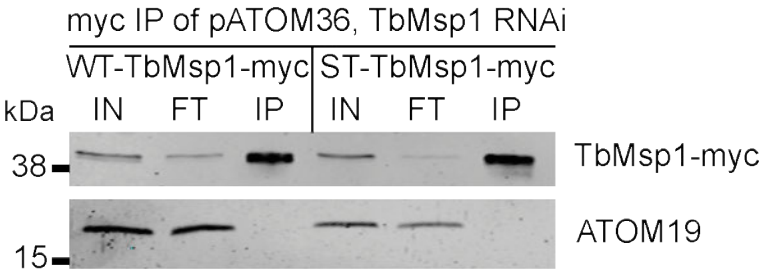

Figure 4: ATOM19 cannot be pulled down using ST-TbMsp1 as bait in pATOM36 RNAi cells. Crude mitochondrial fractions from three days induced cells ablating pATOM36 and overexpressing the indicated C-terminally myc- tagged TbMsp1 variants were analysed by immunoprecipitation. Crude mitochondrial fractions (IN), unbound proteins (FT), and final eluates (IP) were separated by SDS–PAGE. Resulting immunoblots were probed with anti-myc antibodies and antisera ATOM19.

Proteomic analysis of ST-TbMsp1 interacting proteins. Nonetheless, we wanted to test whether a group of proteins specifically binds to ST-TbMsp1. Therefore, cells exclusively expressing ST- and WT-TbMsp1 in the background of pATOM36 RNAi were subjected to SILAC, CoIP and analysed by mass spectrometry (Figure 5). In the volcano blots of Figure 5 all proteins that are specifically enriched with the ST-TbMsp1 bait are in the top right quadrant. In the top volcano plot in Figure 5, known pATOM36 substrates are highlighted in red. Only ATOM69, VDAC and TbJ31 have been detected and none of them bound to the ST-TbMsp1 more than to the WT-TbMsp1 (Figure 5). TbMsp1 localizes to glycosomes and the OM (Gerber et al., 2023; Güther et al., 2014; Niemann et al., 2013). However, surprisingly, the proteins that were specifically enriched with ST-TbMsp1 were neither glycosomal nor in the OM (Figure 5) (Güther et al., 2014; Niemann et al., 2013). Moreover, only two of the 12 proteins could also be found in the mitochondrial importome of *T. brucei* (Peikert et al., 2017).

The first such protein is FtsH16, a mitochondrial protease with a single transmembrane domain (TMD) in the inner membrane (IM) with the AAA domain facing in the intermembrane space (IMS) (Billington et al., 2023; Kovalinka et al., 2020). Interestingly, FtsH16 is kinetoplastid-specific and does not have homologs outside of this clade (Kovalinka et al., 2020).

The second mitochondrial protein specifically enriched in the ST-TbMsp1 pulldown is Tb927.8.5560 (5560). 5560 was identified as a protein that associates with the NADH dehydrogenase (ubiquinone) 1 β subcomplex (Acestor et al., 2011). It contains a S-adenosyl-l-methionine-dependent methyltransferase domain. However, ablation of 5560 via RNAi does not affect growth of procyclic trypanosomes (Mbang-Benet et al., 2015).

The remaining 10 enriched proteins were Tb927.11.14910, the vesicle-associated membrane protein (VAMP)-associated protein (VAP) (Tb927.11.13230), Tb927.8.610, Tb927.8.7560, Tb927.7.1470, Tb11.02.5420, ER membrane protein complex subunit 1 (EMC1)

(Tb927.4.590), EMC2 (Tb927.7.6260), Tb927.8.650 and EMC4 (Tb927.6.2600). Tb927.11.14910 was bioinformatically classified as protein phosphatase 2C and based on IFA it was determined to mainly localize to the ER (Billington et al., 2023; Brenchley et al., 2007). Tb927.11.13230 is a putative vesicle-associated membrane protein (VAMP)-associated protein (VAP). IFA indicates association of this protein with the flagellum (Billington et al., 2023). Interestingly, this VAP plays a pivotal role in flagellum attachment zone (FAZ) ER structures (Lacomble et al., 2012). Tb927.8.610, also known as TZP96.2, is associated with the transition zone (TZ) (Dean et al., 2016). Tb927.8.7560 is a putative CorA-like Mg2+ transporter protein and in IFA localized to reticulated cytoplasm (Billington et al., 2023; Lunin et al., 2006). However, it's putative function would require Tb927.8.7560 to be anchored in a membrane. Interestingly, Tb927.8.7560 is included in the African trypanosome cell surface phylome and is a member of Fam55, a group of metal ion transporters (Jackson et al., 2013). Tb927.7.1470 corresponds to the mitochondrial ATP synthase subunit c-3 (ATPc3)(Gulde et al., 2013) but IFA could not confirm its mitochondrial localisation (Billington et al., 2023; Gulde et al., 2013). Tb11.02.5420 corresponds to a putative NADPH-cytochrome p450 reductase and is suggested to localize to the mitochondrion (Acestor et al., 2009). Tb927.4.590 is EMC1 and part of the EMC complex (Iyer et al., 2022). The EMC is a multifaceted complex crucial for ER membrane protein insertion and folding (Guna et al., 2018; Jonikas et al., 2009). Interestingly, the EMC localizes to the mitochondria - ER interface in trypanosomes (Iyer et al., 2022). Furthermore, with Tb927.7.6260 (EMC2) and Tb927.6.2600 (EMC4), two other EMC components were significantly enriched in the ST-TbMsp1 CoIPs (Figure 5). EMC10 was also detected to be more than two-fold enriched. However, the *P* value was slightly below the cutoff of 0.05. Finally, Tb927.8.650 corresponds to a putative cation-transporting ATPase which likely localizes to the ER (Billington et al., 2023).

Surprisingly, one protein was more enriched in the WT- than the ST-TbMsp1 CoIP. This was Tb927.5.3640 which corresponds to a putative mitochondrial small subunit (SSU) ribosomal protein mS65 (Zíková et al., 2008).

Taken together, our results show that ectopically expressed WT and ST-TbMsp1-myc localize similarly in the cell and the ST mutation stabilizes a TbMsp1-containing complex detectable by BN-PAGE. Interestingly, ST-TbMsp1 does not preferentially bind to known pATOM36 substrates when expressed in a pATOM36 RNAi background. Instead, we identified a list of potential alternate substrates or interaction partners that specifically interact with the ST-TbMsp1 complex.

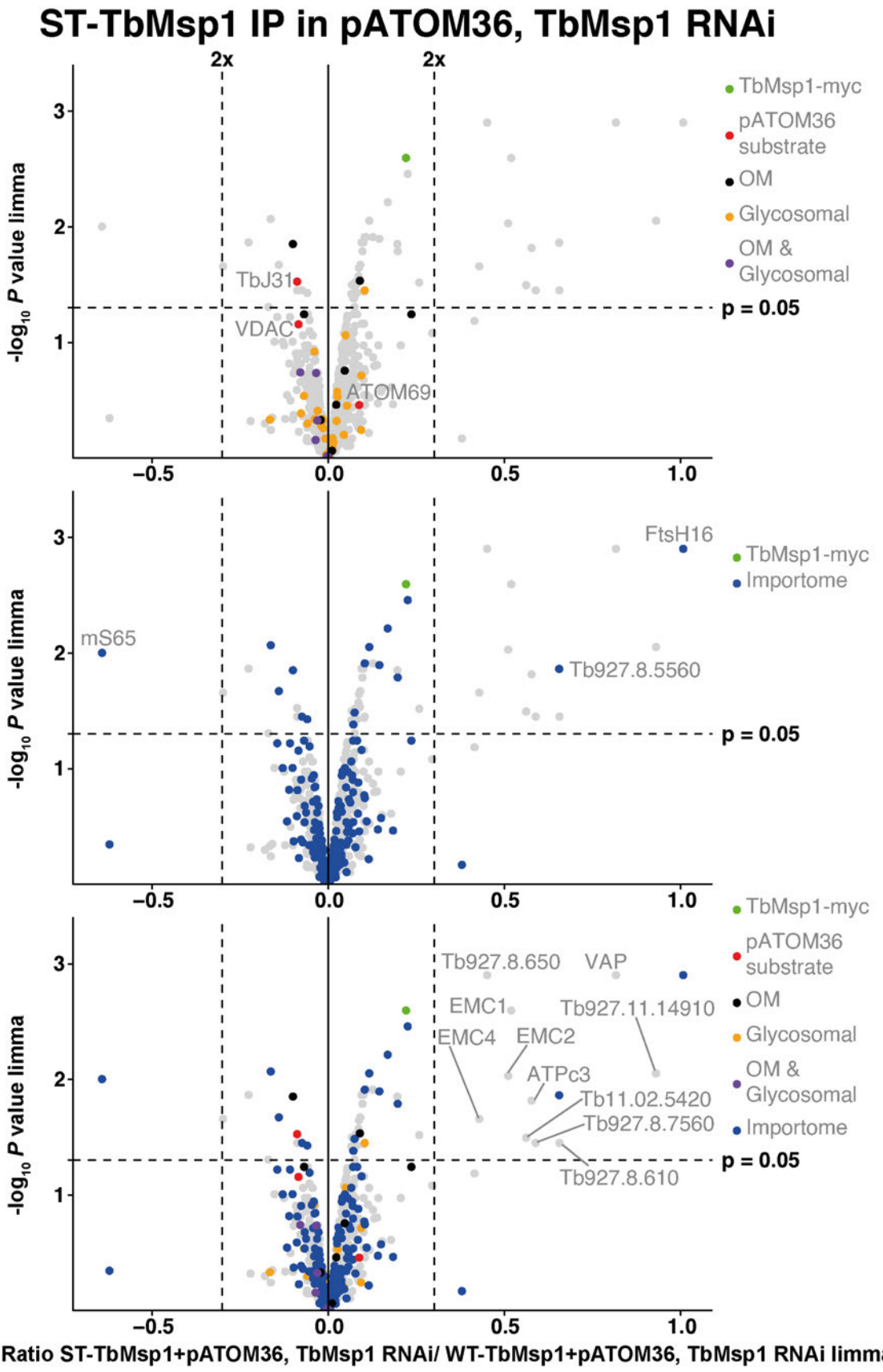

Figure 5: Proteomic analysis shows ST-TbMsp1 complexes do not contain pATOM36 substrates when ectopically expressed in pATOM36 RNAi cells. TbMsp1 complexes were immunoprecipitated from crude mitochondrial fractions of differentially stable isotope labelling by

amino acids in cell culture (SILAC) labelled cells expressing pATOM36 RNAi and either WT- or ST-TbMsp1-myc. Precipitates were analysed by quantitative mass spectrometry (n=3). Proteins found to be significantly enriched more than twofold in ST-TbMsp1 compared to WT-TbMsp1, or the other way around, are labelled with either their name or their accession number in one of the volcano plots.

Discussion

We could not detect a direct interaction of ST-TbMsp1 with pATOM36 substrates. Note however that if pATOM36 substrates bind to the same extent to both WT- and ST-TbMsp1, we would not detect their binding. Nonetheless, our experiments demonstrate that ST- and WT-TbMsp1-myc are similarly localized in the cell when investigated by IFA. Notably, the RNAi against TbMsp1 appears in most experiments to be leaky. This results in TbMsp1 also being ablated in non-induced cells, which may result in cells that are adapted to the loss of TbMsp1 if kept in cell culture over a long time. TbMsp1 was ablated in induced and uninduced cells in cell lines expressing ST or WT-TbMsp1 and pATOM36 RNAi additionally. The same is true for the cell line expressing WT-TbMsp1. However, the cell line expressing ST-TbMsp1 only lost the endogenous RNAi sensitive TbMsp1 upon induction. Which means that comparing the cell lines exclusively expressing WT or ST-TbMsp1 could potentially be problematic. These results also suggest that the parental cell lines used for the generation of these cell lines are likely not clonal, as the parental cell lines only lost TbMsp1 upon induction of the RNAi (Gerber et al., 2023). However, since in both pATOM36 RNAi-containing cell lines the TbMsp1 RNAi was equally leaky and therefore their only difference is the ST mutation, we considered them suitable for this study.

Furthermore, we established that the ST mutation stabilizes a TbMsp1-containing complex detectable by BN-PAGE. Interestingly, the size of the detected complex is much bigger, than expected for a single TbMsp1 hexamer containing a substrate. This further points to the stable interaction of the TbMsp1 complex with other proteins (Gerber et al., 2023).

Our attempts to detect pATOM36 substrates that are specifically bound to the ST-TbMsp1 via CoIPs followed by western blots, as well as mass spectrometry, have not succeeded. None of the proteins we found significantly enriched in the ST- compared to the WT-TbMsp1 CoIP mass spectrometry analysis were pATOM36 substrates. It is tempting to speculate, that this is due to them being equally enriched in the WT-TbMsp1 CoIP. However, it was demonstrated in our recent publication that upon pATOM36 RNAi, in situ tagged unmutated TbMsp1-HA does not specifically pull down any pATOM36 substrates (Gerber et al., 2023). Even though there were differences in the expression of the bait, one being in situ tagged TbMsp1-HA and the other being exclusive ectopic expressed WT- and ST-TbMsp1-myc, we would not expect the pATOM36 substrates to be specifically enriched in the WT-TbMsp1-myc CoIP. The western

blot result of the WT-TbMsp1 CoIP in pATOM36 RNAi showing no pulldown of ATOM19 further supports this hypothesis. To further substantiate this, one could perform a SILAC CoIP followed by MS using the WT-TbMsp1-myc, pATOM36 RNAi cell line and compare it with the pATOM36 RNAi cell line without a myc tagged bait.

Notably, in pATOM36 RNAi background in the CoIPs a dozen proteins were significantly and specifically enriched in ST-TbMsp1 compared to WT-TbMsp1; FtsH16, Tb927.8.5560, Tb927.11.14910, VAP, Tb927.8.610, Tb927.8.7560, Tb927.7.1470, Tb11.02.5420, EMC1, EMC2, Tb927.8.650 and EMC4. None of them were significantly changed in the previously published pATOM36 RNAi dataset (Gerber et al., 2023). Therefore, there is no evidence that the interaction between the TbMsp1 complex and these proteins is only occurring when pATOM36 is ablated. Thus, they might also interact with ST-TbMsp1 in the presence of pATOM36. This could be tested by performing the ST- and WT-TbMsp1 pulldown experiments without pATOM36 RNAi. Irrespective of whether their interaction with ST-TbMsp1 is dependent on the absence pATOM36 or not, it is not clear what their relationship to TbMsp1 is. Since none of the proteins are present in the OM or glycosomes, it could be that they are TbMsp1 substrates that happen to mislocalize to the OM or glycosomes more frequently than other proteins. Interestingly, about half of the protein enriched in the ST-TbMsp1 CoIP are putative ER proteins. Especially intriguing is the fact that three EMC components were found to interact with ST-TbMsp1. This leads to a second hypothesis delineating the relationship between ST-TbMsp1 and the EMC. Msp1 extracts mislocalized C terminally anchored proteins from the OM (Weir et al., 2017). After extraction Msp1-substrates are inserted into the ER (Matsumoto et al., 2019). However, the molecular mechanisms underlaying the transfer to the ER after extraction has yet to be elucidated. Interestingly, the EMC is specialized in inserting C terminally anchored proteins into the ER membrane. Furthermore, the EMC has been localized at ER-mitochondria contact sites in trypanosomes (Iyer et al., 2022). Additionally, IFA experiments in yeast have shown overlap of the EMC with an EMC-substrate at ER-mitochondria contact sites (Matsumoto et al., 2019). Our results indicate that there is a direct interaction between ST-TbMsp1 and the EMC complex. Therefore, one could speculate that these ER proteins are part of TbMsp1 mediated mitochondrial quality control mediating downstream processes such as transfer and insertion to the ER membrane. However, presently these are speculations and require substantial further experimental investigation. One possible follow up experiment could be to investigate the impact of the downregulation of EMC on TbMsp1 mediated mitochondrial quality control. In summary, further experiments are needed to determine more definitively whether the EMC plays an active role in TbMsp1-mediated mitochondrial or possibly also glycosomal quality control.

Material and Methods

Transgenic cell lines

Transgenic *T. brucei* cell lines were generated using cell lines descending from the procyclic strain 29.13 (Wirtz et al., 1999). RNAi resistant wildtype (WT) TbMsp1 was ordered at Biomatik. With the following sequence:

ATG CGA CCT CTG GAC GTG TTG CTG AAT GGG TTG CGC GGG CTG TGT ACC GCC ATT AAG GAA ACA CCC CTC TTC ATA TGG GTG TAC CTT TCT ATA CTG GGC GTG GTG GCT CGG AAG CTG ACG TAC CGT TTT GGT CTT ACG ACT AAA AGC AAA AAG ATA GGA AAA CAC GTC ATC CGC GTT ACG GAT GCG GAA GAA ACC CTT TCA GAG GAT GTA ATG GAC GTG GAA GAA ATT AAT GCG ACA TTT GAC GAC GTG GGG GGT CTG GAA GAT GTG AAA AAG GCA CTA ATT GAA CAC GTG AAG TGG CCG TTT ACC CGC CCG GAA CTA TTT GAG GGA AAC ACG CTG AGG TCG CAT CCT AAG GGT ATC TTA CTC TAT GGT CCT CCA GGT ACG GGT AAG ACA CTC ATA GCT AGA GCT CTT GCC CGT GAA TTA GGT TGC GCA TTC ATT AAT GTG CGT ACT GAG TCT TTA TTC AGC AAG TGG GTA GGA GAT ACG GAG AAA AAC GCT GCT GCC GTT TTC ACA CTT GCT GCC AAA CTG AGC CCT TGT GTG ATA TTC GTT GAC GAA ATA GAC GCC TTA CTT GGC TTA CGT AAT AGC GTG GAC GCC GCT CCG CAC AAC AAT GCG AAA ACA ATA TTT ATG ACT CAT TGG GAT GGT GTT GTC CAA AAA AAA TCA AAA ATT GTA GTC ATT GGG GCT ACG AAT CGG CCA TTG GCA ATT GAC GAA GCT ATA AGA AGG AGG CTG CCT CTC CAA CTG GAA GTA CCT CCA CCT GAT ATA ACT GGT CGG CGT AAG ATA TTA AAC ATT TTA ATG GAG CAT GAC GTG GCT GAC GAA TCG AAT CGT TCA CGA TTA GTG GAT TAT GTT GCG AGT AAG ACT TTT GGT TAC ACA GGG AGC GAT CTT ACT GAG CTG TGT AAA GCT GCC GCT CTT ATG CCA ATC AGA GAA ATT GGC TGT GAC AAT GAA TTG CCC TGC TTG GAA TGT CGC CAC TTT GAC GAG GCC CTC AAG CGG GTC CGG CCT TCG ATG GCA TCA AGC GTT TGA

In yellow indicated is the region targeted by RNAi in TbMsp1 RNAi cell lines (Gerber et al., 2023). In red indicated are nucleotides that have been changed, to make the mRNA immune to the RNAi.

Using the “QuickChange II Site-Directed Mutagenesis Kit” (Agilent, Catalog #200523) a point mutation was introduced in the sequence to generate a plasmid encoding the substrate trap (ST) mutant with the following sequence:

ATG CGA CCT CTG GAC GTG TTG CTG AAT GGG TTG CGC GGG CTG TGT ACC GCC ATT AAG GAA ACA CCC CTC TTC ATA TGG GTG TAC CTT TCT ATA CTG GGC GTG GTG GCT CGG AAG CTG ACG TAC CGT TTT GGT CTT ACG ACT AAA AGC AAA AAG ATA GGA AAA CAC GTC ATC CGC GTT ACG GAT GCG GAA GAA ACC CTT TCA GAG GAT GTA ATG GAC GTG GAA GAA ATT AAT GCG ACA TTT GAC GAC GTG GGG GGT CTG

GAA GAT GTG AAA AAG GCA CTA ATT GAA CAC GTG AAG TGG CCG TTT ACC CGC CCG GAA CTA TTT GAG GGA AAC ACG CTG AGG TCG CAT CCT AAG GGT ATC TTA CTC TAT GGT CCT CCA GGT ACG GGT AAG ACA CTC ATA GCT AGA GCT CTT GCC CGT GAA TTA GGT TGC GCA TTC ATT AAT GTG CGT ACT GAG TCT TTA TTC AGC AAG TGG GTA GGA GAT ACG GAG AAA AAC GCT GCT GCC GTT TTC ACA CTT GCT GCC AAA CTG AGC CCT TGT GTG ATA TTC GTT GAC CAA ATA GAC GCC TTA CTT GGC TTA CGT AAT AGC GTG GAC GCC GCT CCG CAC AAC AAT GCG AAA ACA ATA TTT ATG ACT CAT TGG GAT GGT GTT GTC CAA AAA AAA TCA AAA ATT GTA GTC ATT GGG GCT ACG AAT CGG CCA TTG GCA ATT GAC GAA GCT ATA AGA AGG AGG CTG CCT CTC CAA CTG GAA GTA CCT CCA CCT GAT ATA ACT GGT CGG CGT AAG ATA TTA AAC ATT TTA ATG GAG CAT GAC GTG GCT GAC GAA TCG AAT CGT TCA CGA TTA GTG GAT TAT GTT GCG AGT AAG ACT TTT GGT TAC ACA GGG AGC GAT CTT ACT GAG CTG TGT AAA GCT GCC GCT CTT ATG CCA ATC AGA GAA ATT GGC TGT GAC AAT GAA TTG CCC TGC TTG GAA TGT CGC CAC TTT GAC GAG GCC CTC AAG CGG GTC CGG CCT TCG ATG GCA TCA AGC GTT TGA

The changed nucleotide is indicated in turquoise. This point mutation changes the encoded amino acid from glutamic acid to glutamine.

Primers used:

5’-CCAAGTAAGGCGTCTATTTGGTCAACGAATATCACACAA-3’

5’-TTGTGTGATATTCGTTGACCAAATAGACGCCTTACTTGG-3’

The WT- and ST-TbMsp1 were cloned in a modified pLew100 vector containing a C-terminal triple c-myc-tag (Bochud-Allemann and Schneider, 2002; Oberholzer et al., 2006; Wirtz et al., 1999). The resulting WT and ST-TbMsp1-containing plasmids were introduced into published TbMsp1 and TbMsp1, pATOM36 RNAi cell lines (Gerber et al., 2023). Cells were cultivated at 27°C in SDM-79 (Brun and Schönenberger, 1979) supplemented with 10% (vol/vol) FCS, containing G418 (15 µg/ml; Gibco), hygromycin (25 µg/ml; InvivoGen), puromycin (2 µg/ml; InvivoGen), blasticidin (10 µg/ml; InvivoGen), and phleomycin (2.5 µg/ml; LifeSpan BioSciences) as required. RNAi and ectopic protein expression was induced by adding 1 µg/ml tetracycline to the medium.

SDS-PAGE and western blot

Cells were treated with tetracycline for three days to induce RNAi and ectopic protein expression as indicated. After the cells were washed with PBS, they were lysed in SDS buffer (2% SDS, 0.0025% bromophenol blue (w/v), 100mM β-mercaptoethanol in 60 mM Tris-HCl pH

6.8). 2x10^6 cell equivalents per lane were separated on a 12% or 14% acrylamide gel in an electrophoresis cell (Bio-rad, Mini-PROTEAN Tetra Vertical Electrophoresis Cell). After transfer on a nitrocellulose membrane (Amersham) and blocking in 5% milk in PBS, antisera against indicated proteins were added in 2.5% milk, PBST (ATOM19 1:500 (Gerber et al., 2023), TbMsp1 1:1'000 (Gerber et al., 2023), EF1α 1:10'000 (Merk Millipore, 05-235), pATOM36 1 :250 (Vitali et al., 2018), VDAC 1 :1'000 (Niemann et al., 2013), myc 1:200 (Invitrogen, 132500)). After three PBST washes the membranes were incubated with secondary antibodies (Anti-mouse IRDye 680LT conjugated (goat) and Anti-rabbit IRDye 800CW conjugated (goat), 1:20'000, LI-COR Biosciences). The membranes were imaged using a LI-COR ODYSSEY scanner and analysed using the corresponding software (Image Studio Lite v. 5.2.5., LI-COR Biosciences).

Digitonin extraction followed by BN-PAGE

Crude mitochondria-enriched fractions were obtained by incubating 1 × 10^8 induced cells expressing ST- or WT-TbMsp1 in TbMsp1 RNAi or TbMsp1, pATOM36 double RNAi cells, in 0.6 M sorbitol, 20 mM Tris–HCl (pH 7.5), 1 mM DTT, 5mM $MgCl_2$ and 2 mM EDTA (pH 8) containing 0.015% (w/v) digitonin (Biosynth) and 2mM ATP as indicated on ice. Centrifugation (5 min, 6'800 g, 4°C) yielded a cytosolic supernatant and a mitochondria-enriched pellet. This pellet was solubilized in solubilization buffer (20 mM Tris–HCl pH 7.4, 50 mM NaCl, 10% glycerol, 0.1 mM EDTA, 1 mM DTT, 5mM $MgCl_2$ and if indicated 2mM ATP) containing 1% (w/v) digitonin and incubated on ice for 15 min. After centrifugation (20,000 g, 4°C, 15 min), the supernatant was separated on 4–13% gels. 5 x 10^7 cell equivalent was loaded per well. Before western blotting, the gel was incubated in SDS-PAGE running buffer (25 mM Tris, 1 mM EDTA, 190 mM glycine, 0.05% (w/v) SDS) to facilitate transfer of the proteins to a PVDF membrane (Immobilon-FL). The immunoblot was decorated with HA antiserum (BioLegend, 1:5000 in PBST, 2.5% milk). Anti-mouse (goat, HRP-coupled, Sigma Aldrich) antibodies were used as secondary antibodies.

Immunofluorescence microscopy

Induced 1 x 10^6 cells overexpressing the WT- or ST-TbMsp1-myc in TbMsp1 RNAi or TbMsp1, pATOM36 double RNAi, were harvested by centrifugation (5 min, 1'800 g) and washed with 1x PBS. After resuspension in 1x PBS, the cells were left adhering on a glass slide in a wet chamber. The cells were fixed with 4% PFA, permeabilised with 0.2% Triton X-100, and blocked with 2% BSA in 1x PBS. Antibodies were incubated on the slides in 1% BSA and 1x PBS (myc 1:50 (Invitrogen, 132500), ATOM40 1:1'000 (Niemann et al., 2013)). The dried slides

were mounted with Vectashield containing DAPI (Vector Laboratories, P/N H-1200). Images were acquired with a DFC360 FX monochrome camera (Leica Microsystems) mounted on a DMI6000B microscope (Leica Microsystems). Image analysis was performed using LASX software (version 3.6.20104.0; Leica Microsystems). The acquired images were processed using Fiji (ImageJ version 2.10./1.53; Java 1.8.0_172 [64 bit]). Microscopy figures were composed using FigureJ (Mutterer and Zinck, 2013).

Immunoprecipitation

Digitonin-extracted mitochondria-enriched fractions of 1 × 10^8 induced cells were solubilized on ice in 20 mM Tris–HCl (pH 7.4), 0.1 mM EDTA, 100 mM NaCl, 25 mM KCl, 1x protease inhibitor mix (EDTA-free; Roche), 1 mM DTT, 5mM $MgCl_2$, 2mM ATP and 1% (wt/vol) digitonin. After centrifugation (15 min, 20'817 g, 4°C), the lysate (IN, input) was transferred to 50 µl c-myc bead slurry (EZview red anti-c-myc affinity gel; Sigma-Aldrich), which had been equilibrated in wash buffer (20 mM Tris–HCl [pH 7.4], 0.1 mM EDTA, 100 mM NaCl, 10% glycerol, 0.2% [wt/vol] digitonin, 1 mM DTT, 5mM $MgCl_2$, 2mM ATP). After incubating at 4°C for 2 h on a rotating wheel, the supernatant containing the unbound proteins (FT, flow through) was removed. The bead slurry was washed three times with wash buffer. Bound proteins were eluted by boiling the resin in 60 mM Tris–HCl (pH 6.8) containing 2% SDS (IP). 2.5% of crude mitochondrial fractions (Input, IN), unbound proteins in the flow through (FT), and 50% of the final eluates (IP) were separated by SDS–PAGE and analysed by Western blot.

SILAC immunoprecipitations

Cells were grown for 5 days in SILAC medium (SDM80 containing 5.55 mM glucose, supplemented with 10% dialyzed, heat-inactivated FCS, 7.5 mg/l hemin) containing isotopically distinct variants of arginine ($^{12}C_6{}^{14}N_4$/Arg0, $^{13}C_6{}^{14}N_4$/Arg6, or $^{13}C_6{}^{15}N_4$/Arg10; 226 mg/l each) and lysine ($^{12}C_6{}^{14}N_2$/Lys0, $^{12}C_6{}^{14}N_2{}^{2}H_4$/Lys4, or $^{13}C_6{}^{15}N_4$/Lys8; 73 mg/l each) (Eurisotope). 2 × 10^8 cells expressing WT-TbMsp1-myc in TbMsp1, pATOM36 RNAi TbMsp1 and 2 × 10^8 cells expressing ST-TbMsp1-myc in TbMsp1, pATOM36 RNAi were mixed and washed with 1x PBS. Crude mitochondria-enriched fractions were obtained by digitonin extraction as described above. The pellet of the digitonin extraction was subjected to immunoprecipitation as described above. Proteins were precipitated after the methanol-chloroform protocol (Wessel and Flügge, 1984) and further processed for liquid chromatography-mass spectrometry (LC-MS) analysis including reduction in cysteine residues, alkylation of thiol groups, and tryptic digestion as described before (Dewar et al., 2022b). The experiment was performed in three biological replicates with different labelling schemes. Further processing and quantitative LC-

MS analysis was conducted by the Warscheid group in Würzburg. The resulting data was analysed and visualized using R studio (Posit PBC).

References

Acestor, N., Panigrahi, A.K., Ogata, Y., Anupama, A., Stuart, K.D., 2009. Protein composition of *Trypanosoma brucei* mitochondrial membranes. Proteomics 9, 5497–5508. https://doi.org/10.1002/pmic.200900354

Acestor, N., Zíková, A., Dalley, R.A., Anupama, A., Panigrahi, A.K., Stuart, K.D., 2011. *Trypanosoma brucei* Mitochondrial Respiratome: Composition and Organization in Procyclic Form. Mol Cell Proteomics 10, M110.006908. https://doi.org/10.1074/mcp.M110.006908

Basch, M., Wagner, M., Rolland, S., Carbonell, A., Zeng, R., Khosravi, S., Schmidt, A., Aftab, W., Imhof, A., Wagener, J., Conradt, B., Wagener, N., 2020. Msp1 cooperates with the proteasome for extraction of arrested mitochondrial import intermediates. Mol Biol Cell 31, 753–767. https://doi.org/10.1091/mbc.E19-06-0329

Billington, K., Halliday, C., Madden, R., Dyer, P., Barker, A.R., Moreira-Leite, F.F., Carrington, M., Vaughan, S., Hertz-Fowler, C., Dean, S., Sunter, J.D., Wheeler, R.J., Gull, K., 2023. Genome-wide subcellular protein map for the flagellate parasite *Trypanosoma brucei*. Nat Microbiol 8, 533–547. https://doi.org/10.1038/s41564-022-01295-6

Bochud-Allemann, N., Schneider, A., 2002. Mitochondrial Substrate Level Phosphorylation Is Essential for Growth of Procyclic *Trypanosoma brucei*. Journal of Biological Chemistry 277, 32849–32854. https://doi.org/10.1074/jbc.M205776200

Brenchley, R., Tariq, H., McElhinney, H., Szöor, B., Huxley-Jones, J., Stevens, R., Matthews, K., Tabernero, L., 2007. The TriTryp phosphatome: analysis of the protein phosphatase catalytic domains. BMC Genomics 8, 434. https://doi.org/10.1186/1471-2164-8-434

Brun, R., Schönenberger, M., 1979. Cultivation and in vitro cloning or procyclic culture forms of *Trypanosoma brucei* in a semi-defined medium. Short communication. Acta Trop 36, 289–292.

Castanzo, D.T., LaFrance, B., Martin, A., 2020. The AAA+ ATPase Msp1 is a processive protein translocase with robust unfoldase activity. Proceedings of the National Academy of Sciences 117, 14970–14977. https://doi.org/10.1073/pnas.1920109117

Chen, Y.-C., Umanah, G.K.E., Dephoure, N., Andrabi, S.A., Gygi, S.P., Dawson, T.M., Dawson, V.L., Rutter, J., 2014. Msp1/ATAD1 maintains mitochondrial function by facilitating the degradation of mislocalized tail-anchored proteins. The EMBO Journal 33, 1548–1564. https://doi.org/10.15252/embj.201487943

Dean, S., Moreira-Leite, F., Varga, V., Gull, K., 2016. Cilium transition zone proteome reveals compartmentalization and differential dynamics of ciliopathy complexes. Proc Natl Acad Sci USA 113, E5135-5143. https://doi.org/10.1073/pnas.1604258113

Dederer, V., Khmelinskii, A., Huhn, A.G., Okreglak, V., Knop, M., Lemberg, M.K., 2019. Cooperation of mitochondrial and ER factors in quality control of tail-anchored proteins. eLife 8, e45506. https://doi.org/10.7554/eLife.45506

Dewar, C.E., Oeljeklaus, S., Wenger, C., Warscheid, B., Schneider, A., 2022. Characterization of a highly diverged mitochondrial ATP synthase Fo subunit in *Trypanosoma brucei*. Journal of Biological Chemistry 298. https://doi.org/10.1016/j.jbc.2022.101829

Gerber, M., Suppanz, I., Oeljeklaus, S., Niemann, M., Käser, S., Warscheid, B., Schneider, A., Dewar, C.E., 2023. A Msp1-containing complex removes orphaned proteins in the mitochondrial outer membrane of T. brucei. Life Science Alliance 6. https://doi.org/10.26508/lsa.202302004

Gulde, P.E., Christen, L., Brown, S.V., Williams, N., 2013. Three Distinct Isoforms of ATP Synthase Subunit c Are Expressed in T. brucei and Assembled into the Mitochondrial ATP Synthase Complex. PLOS ONE 8, e54039. https://doi.org/10.1371/journal.pone.0054039

Guna, A., Volkmar, N., Christianson, J.C., Hegde, R.S., 2018. The ER membrane protein complex is a transmembrane domain insertase. Science 359, 470–473. https://doi.org/10.1126/science.aao3099

Güther, M.L.S., Urbaniak, M.D., Tavendale, A., Prescott, A., Ferguson, M.A.J., 2014. High-Confidence Glycosome Proteome for Procyclic Form *Trypanosoma brucei* by Epitope-Tag Organelle Enrichment and SILAC Proteomics. J. Proteome Res. 13, 2796–2806. https://doi.org/10.1021/pr401209w

Iyer, A., Niemann, M., Serricchio, M., Dewar, C.E., Oeljeklaus, S., Farine, L., Warscheid, B., Schneider, A., Bütikofer, P., 2022. The endoplasmic reticulum membrane protein complex localizes to the mitochondrial - endoplasmic reticulum interface and its subunits modulate phospholipid biosynthesis in *Trypanosoma brucei*. PLoS Pathog 18, e1009717. https://doi.org/10.1371/journal.ppat.1009717

Jackson, A.P., Allison, H.C., Barry, J.D., Field, M.C., Hertz-Fowler, C., Berriman, M., 2013. A Cell-surface Phylome for African Trypanosomes. PLOS Neglected Tropical Diseases 7, e2121. https://doi.org/10.1371/journal.pntd.0002121

Jonikas, M.C., Collins, S.R., Denic, V., Oh, E., Quan, E.M., Schmid, V., Weibezahn, J., Schwappach, B., Walter, P., Weissman, J.S., Schuldiner, M., 2009. Comprehensive characterization of genes required for protein folding in the endoplasmic reticulum. Science 323, 1693–1697. https://doi.org/10.1126/science.1167983

Käser, S., Oeljeklaus, S., Týč, J., Vaughan, S., Warscheid, B., Schneider, A., 2016. Outer membrane protein functions as integrator of protein import and DNA inheritance in mitochondria. Proc Natl Acad Sci USA 113, E4467–E4475. https://doi.org/10.1073/pnas.1605497113

Kovalinka, T., Pánek, T., Kováčová, B., Horváth, A., 2020. Orientation of FtsH protease homologs in *Trypanosoma brucei* inner mitochondrial membrane and its evolutionary implications. Molecular and Biochemical Parasitology 238, 111282. https://doi.org/10.1016/j.molbiopara.2020.111282

Lacomble, S., Vaughan, S., Deghelt, M., Moreira-Leite, F.F., Gull, K., 2012. A *Trypanosoma brucei* protein required for maintenance of the flagellum attachment zone and flagellar pocket ER domains. Protist 163, 602–615. https://doi.org/10.1016/j.protis.2011.10.010

Li, L., Zheng, J., Wu, X., Jiang, H., 2019. Mitochondrial AAA-ATPase Msp1 detects mislocalized tail-anchored proteins through a dual-recognition mechanism. EMBO Rep 20, e46989. https://doi.org/10.15252/embr.201846989

Lunin, V.V., Dobrovetsky, E., Khutoreskaya, G., Zhang, R., Joachimiak, A., Doyle, D.A., Bochkarev, A., Maguire, M.E., Edwards, A.M., Koth, C.M., 2006. Crystal structure of the CorA Mg2+ transporter. Nature 440, 10.1038/nature04642. https://doi.org/10.1038/nature04642

Matsumoto, S., 2023. Msp1-mediated proofreading mechanism for localization of tail-anchored membrane proteins. The Journal of Biochemistry 174, 13–20. https://doi.org/10.1093/jb/mvad025

Matsumoto, S., Nakatsukasa, K., Kakuta, C., Tamura, Y., Esaki, M., Endo, T., 2019. Msp1 Clears Mistargeted Proteins by Facilitating Their Transfer from Mitochondria to the ER. Molecular Cell 76, 191-205.e10. https://doi.org/10.1016/j.molcel.2019.07.006

Mbang-Benet, D.-E., Sterkers, Y., Crobu, L., Sarrazin, A., Bastien, P., Pagès, M., 2015. RNA interference screen reveals a high proportion of mitochondrial proteins essential for correct cell cycle progress in *Trypanosoma brucei*. BMC Genomics 16, 297. https://doi.org/10.1186/s12864-015-1505-5

Mutterer, J., Zinck, E., 2013. Quick-and-clean article figures with FigureJ. Journal of Microscopy 252, 89–91. https://doi.org/10.1111/jmi.12069

Niemann, M., Wiese, S., Mani, J., Chanfon, A., Jackson, C., Meisinger, C., Warscheid, B., Schneider, A., 2013. Mitochondrial Outer Membrane Proteome of *Trypanosoma brucei* Reveals Novel Factors Required to Maintain Mitochondrial Morphology. Mol Cell Proteomics 12, 515–528. https://doi.org/10.1074/mcp.M112.023093

Oberholzer, M., Morand, S., Kunz, S., Seebeck, T., 2006. A vector series for rapid PCR-mediated C-terminal in situ tagging of *Trypanosoma brucei* genes. Molecular and

Biochemical Parasitology 145, 117–120. https://doi.org/10.1016/j.molbiopara.2005.09.002
Okreglak, V., Walter, P., 2014. The conserved AAA-ATPase Msp1 confers organelle specificity to tail-anchored proteins. Proc Natl Acad Sci USA 111, 8019–8024. https://doi.org/10.1073/pnas.1405755111
Peikert, C.D., Mani, J., Morgenstern, M., Käser, S., Knapp, B., Wenger, C., Harsman, A., Oeljeklaus, S., Schneider, A., Warscheid, B., 2017. Charting organellar importomes by quantitative mass spectrometry. Nat Commun 8, 15272. https://doi.org/10.1038/ncomms15272
Schuldiner, M., Metz, J., Schmid, V., Denic, V., Rakwalska, M., Schmitt, H.D., Schwappach, B., Weissman, J.S., 2008. The GET complex mediates insertion of tail-anchored proteins into the ER membrane. Cell 134, 634–645. https://doi.org/10.1016/j.cell.2008.06.025
Stefanovic, S., Hegde, R.S., 2007. Identification of a targeting factor for posttranslational membrane protein insertion into the ER. Cell 128, 1147–1159. https://doi.org/10.1016/j.cell.2007.01.036
Vitali, D.G., Käser, S., Kolb, A., Dimmer, K.S., Schneider, A., Rapaport, D., 2018. Independent evolution of functionally exchangeable mitochondrial outer membrane import complexes. eLife 7, e34488. https://doi.org/10.7554/eLife.34488
Wang, L., Myasnikov, A., Pan, X., Walter, P., 2020. Structure of the AAA protein Msp1 reveals mechanism of mislocalized membrane protein extraction. eLife 9, e54031. https://doi.org/10.7554/eLife.54031
Wessel, D., Flügge, U.I., 1984. A method for the quantitative recovery of protein in dilute solution in the presence of detergents and lipids. Anal Biochem 138, 141–143. https://doi.org/10.1016/0003-2697(84)90782-6
Wirtz, E., Leal, S., Ochatt, C., Cross, G. A., 1999. A tightly regulated inducible expression system for conditional gene knock-outs and dominant-negative genetics in *Trypanosoma brucei*. Molecular and Biochemical Parasitology 99, 89–101. https://doi.org/10.1016/S0166-6851(99)00002-X
Zíková, A., Panigrahi, A.K., Dalley, R.A., Acestor, N., Anupama, A., Ogata, Y., Myler, P.J., Stuart, K., 2008. *Trypanosoma brucei* mitochondrial ribosomes: affinity purification and component identification by mass spectrometry. Mol Cell Proteomics 7, 1286–1296. https://doi.org/10.1074/mcp.M700490-MCP200

4. Discussion

Mitochondria are involved in several vital pathways and are therefore essential for almost all eukaryotes (Henze and Martin, 2003; Karnkowska et al., 2016; Simpson et al., 2002; Tovar et al., 2003; Yahalomi et al., 2020). Interestingly, mitochondria derive from a bacterial ancestor and contain their own genome (Nass and Nass, 1963). However, all but a few genes have been transferred to the nucleus (Brandvain and Wade, 2009). Hence, most mitochondrial proteins are synthesized by cytosolic ribosomes and subsequently imported into mitochondria. A variety of problems can occur during mitochondrial biogenesis and disturb mitochondrial function (Boos et al., 2020). Over the last decade several mitochondrial quality control (MQC) pathways were discovered which aim to not only minimize the damage caused by impaired mitochondria but also to maintain mitochondrial function (den Brave et al., 2021; Ng et al., 2021). Some of these pathways involve the ATPase associated with diverse cellular activities (AAA) mitochondrial sorting of proteins 1 (Msp1) (Castanzo et al., 2020; Matsumoto et al., 2019; Weidberg and Amon, 2018). In one such pathway Msp1 mediates the extraction of mislocalized tail-anchored proteins from the outer mitochondrial membrane (OM) which are subsequently degraded by the cytosolic proteasome (Weir et al., 2017). Mislocalisation can be induced experimentally by preventing the correct localisation of such proteins via the ablation of components of their respective biogenesis pathways (Castanzo et al., 2020; Weir et al., 2017; Wohlever et al., 2017). In this mitochondria-associated degradation (MAD) pathway Msp1 can function independently of cofactors or substrate modifications (Wohlever et al., 2017). However, in yeast Msp1 is dependent on cofactor Cis1 in a pathway which clears clogged translocase of the outer mitochondrial membrane (TOM) complexes (Weidberg and Amon, 2018). Up to date essentially all experiments investigating Msp1 were conducted in yeast or in mammalian cell culture.

We aimed to characterize Msp1 in the protozoan parasite *Trypanosoma brucei*. *T. brucei* is essentially unrelated to Opisthokonts to which most popular eukaryotic model organisms such as yeast, flies, mice, and humans belong to. The characterisation of MQC pathways in distantly related model organisms provides interesting insights in eukaryotic evolution. Our group discovered a novel MAD pathway in which destabilised α-helically anchored proteins from the OM are degraded by the cytosolic proteasome (Käser et al., 2016). This pathway is triggered by the destabilisation of the atypical protein translocase of the outer mitochondrial membrane (ATOM) complex via ablation of the MIM complex analogue pATOM36. pATOM36 is involved in the insertion of α-helically anchored OM proteins such as present in the outer membrane proteome 10 (POMP10), but importantly also in the assembly of ATOM complex subunits (Bruggisser et al., 2017; Käser et al., 2016). It has been found that ATOM complex subunits are removed from the OM and degraded by the cytosolic proteasome upon ablation of pATOM36 (Käser et al., 2016). In my PhD I further investigated this MQC pathway and found

that *T. brucei* valosin-containing protein (TbVCP) and TbMsp1 play synergistic roles in removing these proteins from the OM.

Surprisingly, we found four OM proteins which stably interact with TbMsp1 in a coimmunoprecipitation (CoIP) experiment with in situ tagged TbMsp1: POMP31, the putative DnaJ-like protein TbJ31, the putative trans-2-enoyl-CoA reductase TbTsc13, and POMP19. However, while this complex was detectable via reciprocal CoIPs using dually tagged cell lines, a complex containing wildtype TbMsp1 could not be detected by blue native polyacrylamide gel electrophoresis (BN-PAGE).

Even more surprisingly, by using double and triple RNAi cell lines we found that the TbMsp1 mediated extraction of unassembled ATOM subunits depended on the TbMsp1 interacting proteins POMP31, TbJ31 and TbTsc13 (Gerber et al., 2023). This contrasts with experiments in yeast that demonstrated the independence of Msp1 from any associated proteins (Wohlever et al., 2017). The precise roles of the three TbMsp1 interacting proteins have yet to be determined. However, it is likely that they function in recognizing or recruiting substrates to the hexameric TbMsp1 complex. Not all the substrates we identified to be part of the pathway that is triggered by ablation of pATOM36 are canonical Msp1 substrates with a single C-terminal transmembrane domain (TMD). ATOM19 for example is predicted to contain two TMDs. Therefore, it could also be hypothesized that these TbMsp1 interacting proteins assist in the extraction of noncanonical TbMsp1 substrates. Interestingly, none of these proteins nor their homologs in yeast have been linked to MQC previously.

However, TbTsc13 has some properties of a potential MQC factor. Interestingly, upon DNA replication stress the yeast homolog of TbTsc13 increases in abundance and more of the protein is found in endoplasmic reticulon (ER) foci, indicating that Tsc13 is responsive to cellular stress (Breker et al., 2013; Tkach et al., 2012). Furthermore, TbTsc13 harbours an N-terminal ubiquitin-like domain, that probably faces the cytosol. This domain could possibly be involved in interactions with the cytosolic proteasome. It has been shown for some Msp1 substrates of yeast that they are reinserted into the ER membrane where they are ubiquitinated and extracted by VCP before they are degraded by the proteasome. However, not all Msp1 substrates need to follow this route (Matsumoto et al., 2019). It is not known how Msp1-extracted proteins are shuttled from the OM to the ER. It is possible that TbTsc13 recruits the proteasome towards the TbMsp1-containing complex so that the extracted proteins can be degraded directly, without the detour to the ER. Interestingly, yeast Msp1 has been shown to cooperate with the proteasome in the mitochondrial compromised protein import response (mitoCPR) (Basch et al., 2020). An interesting follow-up experiment would be to investigate the impact of the expression of an N-terminally truncated RNAi-resistant TbTsc13 version lacking the ubiquitin-like domain in a pATOM36, TbVCP and TbTsc13 triple RNAi cell line. This

could show us whether the ubiquitin-like domain contributes to the function of this MQC pathway.

POMP31 (Tb927.6.3680) is a kinetoplast-specific protein. It has four predicted TMDs, and localizes to the OM. The dependency of TbMsp1-mediated extraction on a kinetoplast-specific protein indicates that this pathway likely functions different to the ones in yeast and humans as they do not have a POMP31 homolog. However, it is possible that a protein unrelated to POMP31 functions in a similar way. We do not know the specific function of POMP31 in this pathway. It might be involved in substrate recognition or the recruitment of substrates to the TbMsp1-containing complex. Interestingly, the ATOM components that are extracted upon pATOM36 ablation are not homologues of the corresponding TOM components in yeast. Therefore, it might not be surprising if the pathways surveying the integrity of the ATOM complex may have evolved independently of their counterparts in yeast and mammals. Whether POMP31 is directly required for TbMsp1 function or whether it is only involved in the clearing of destabilized ATOM components has yet to be elucidated.

TbJ31 is an orthologue of the mammalian OM J-protein, DNAJ11 (Muñoz-Gómez et al., 2015). TbJ31 and DNAJ11 both contain the C-terminal domain of unknown function 3395 (DUF3395), which is hypothesized to mediate interactions between proteins (Violitzi et al., 2019). Therefore, TbJ31 could be involved in substrate recruitment, or it could mediate the assembly or stability of the TbMsp1-containing complex. Interestingly, the structure predicted by AlphaFold suggests that TbJ31 not only contains an alpha-helical TMD, but also might contain a beta barrel structure that is embedded in the OM (Wheeler, 2021). TbJ31 is significantly depleted from the cell upon ablation of pATOM36. If TbJ31 contains indeed a beta-barrel membrane embedded domain, insertion into the OM membrane should be mediated by the sorting and assembly machinery (SAM). However, TbJ31 was not found to be significantly downregulated upon ablation of SAM in trypanosomes (Bruggisser et al., 2017). Thus, it would be interesting to determine whether TbJ31 indeed contains a beta-barrel protein domain, for example by expressing it in an inducible Sam50 RNAi cell line to see whether Sam50 plays a role in its biogenesis.

Our studies indicated that POMP19 is not required for the TbMsp1 pathway degrading pATOM36 substrates. Yet, this protein is stably integrated into the TbMsp1-containing complex. It would be possible that POMP19 is involved in the recruitment of another yet unknown subset of TbMsp1 client proteins that are different from the known pATOM36 substrates. Alternatively, it is possible that the ablation of POMP19 in the triple RNAi cell line was not efficient enough to cause a detectable biochemical phenotype. Like POMP31, POMP19 is kinetoplastid specific, indicating its role in the Msp1-complex, if it has any, is not conserved across eukaryotic groups.

To gain a more complete picture of the TbMsp1 complex and its role in the removal of destabilized OM proteins it would be interesting to investigate TbMsp1-assissted extraction without the lethal pATOM36 RNAi, under more physiological conditions. A mutated ATOM19, which is inserted into the OM but is unable to assemble into the ATOM complex, could potentially be targeted for TbMsp1-assisted degradation in the presence of pATOM36. However, TbVCP is likely simultaneously targeting destabilized OM proteins, possibly even more efficiently than TbMsp1. TbVCP RNAi is lethal to the cells, two to three days post induction (Gerber et al., 2023). Therefore, it would also be interesting to design an experiment in which the substrate is specifically removed from the OM by TbMsp1, without ablating TbVCP. Presently, we did not achieve this.

VCP requires ubiquitination of its quality control substrates for efficient removal, while Msp1 is believed to function independently of ubiquitin (Ub) (Twomey et al., 2019; Wohlever et al., 2017). Therefore, we hypothesized that a ubiquitination-resistant substrate protein might also be resistant to TbVCP mediated extraction. Ub is attached to lysine residues of substrate proteins. We used a synthetic ATOM19 gene in which all lysine codons were replaced by arginine codons. We hypothesized that lysine-free ATOM19 might be degraded exclusively via TbMsp1 upon pATOM36 depletion because TbMsp1 likely functions independently from Ub. Upon TbMsp1 and pATOM36 double RNAi we expected only the wildtype ATOM19 to be degraded via TbVCP, but not the lysine-free ATOM19. However, in all experiments lysine-free ATOM19 phenocopied wildtype ATOM19. Both were depleted upon pATOM36 single RNAi as well as upon pATOM36, TbMsp1 double RNAi. There are two possible explanations for this outcome. Firstly, it could indicate that TbVCP functions independently from Ub, which is highly unlikely due to the high conservation of VCP across all eukaryotes. More likely the ablation of lysines is not sufficient to prevent ATOM19 from being ubiquitinated. Proteins can also be ubiquitinated at their N-terminus (Breitschopf et al., 1998). With the results obtained from these experiments the involvement of Ub in TbMsp1-mediated degradation remains unclear. The addition of a large N-terminal tag prevents the N-terminal ubiquitination of proteins (Breitschopf et al., 1998). Another method used to prevent the Ub-dependent degradation of a substrate protein is fusing it to a deubiquitination enzyme (DUb) (Stringer and Piper, 2011). Therefore, the set of experiments conducted could be expanded with lysine-free ATOM19 fused to either a tag or a DUb at the N-terminus.

Moreover, we aimed to investigate a substrate trap (ST)-TbMsp1, containing a point mutation changing a glutamic acid to a glutamine within the highly conserved Walker B motif of the ATPase domain. This mutation impedes the hydrolysation of bound ATP (Stratford et al., 2007; Wohlever et al., 2017). ST-TbMsp1 therefore remains in a stable complex bound to ATP and the substrate protein. In contrast to the wildtype (WT) hexameric TbMsp1 complex, ST-TbMsp1 is stable enough to be visualized by BN-PAGE followed by western blot. The complex

appears to be stabilized further by adding excess ATP to the buffers when preparing the sample.

Interestingly, ATOM19 did not copurify with the ST-TbMsp1 in pATOM36 RNAi CoIP experiments analysed via western blot. Neither did it or any other pATOM36 substrate when we performed the same CoIP in a SILAC experiment analysed by mass spectrometry. A potential explanation could be that pATOM36 substrates are primarily removed from the OM by TbVCP, and TbMsp1 is only used in this pathway upon TbVCP ablation.

However, some other proteins did enrich significantly to the ST-TbMsp1 compared to the WT-TbMsp1 in the presence of pATOM36 RNAi. A dozen proteins were significantly enriched in ST-TbMsp1 pulldowns compared to WT-TbMsp1 pulldowns. These proteins may interact with ST-TbMsp1 regardless of presence or absence of pATOM36. Their connection to the TbMsp1-mediated pathway described in this thesis is therefore unclear, but since they are neither in the OM nor glycosomal proteins, they could be TbMsp1 substrates which are mislocalizing to either one of these locations. Half of the proteins enriched in ST-TbMsp1 CoIP are likely ER proteins, 3 of them belong to the endoplasmic reticulum membrane protein complex (EMC), suggesting a potential interaction between ST-TbMsp1 and the EMC. Interestingly a fourth EMC component copurified with ST-TbMsp1 just below the significance threshold to a similar extent as the other three. This raises the question whether ER proteins, and the EMC in particular, could be involved in TbMsp1-mediated MQC, possibly facilitating transfer and insertion into the ER membrane. The EMC could thereby be the missing link between the OM and the ER in Msp1 mediated MAD. Further experiments, such as investigating the impact of EMC downregulation on TbMsp1-mediated MAD, are needed to confirm these speculations, and determine the EMC's role in TbMsp1-mediated MQC definitively.

5. References

Abuaita, B.H., Schultz, T.L., O'Riordan, M.X., 2018. Mitochondria-Derived Vesicles Deliver Antimicrobial Reactive Oxygen Species to Control Phagosome-Localized Staphylococcus aureus. Cell Host Microbe 24, 625-636.e5. https://doi.org/10.1016/j.chom.2018.10.005

Acestor, N., Panigrahi, A.K., Ogata, Y., Anupama, A., Stuart, K.D., 2009. Protein composition of *Trypanosoma brucei* mitochondrial membranes. Proteomics 9, 5497–5508. https://doi.org/10.1002/pmic.200900354

Acestor, N., Zíková, A., Dalley, R.A., Anupama, A., Panigrahi, A.K., Stuart, K.D., 2011. *Trypanosoma brucei* Mitochondrial Respiratome: Composition and Organization in Procyclic Form. Mol. Cell. Proteomics MCP 10, M110.006908. https://doi.org/10.1074/mcp.M110.006908

Acharya, U., Jacobs, R., Peters, J.-M., Watson, N., Farquhar, M.G., Malhotra, V., 1995. The formation of golgi stacks from vesiculated golgi membranes requires two distinct fusion events. Cell 82, 895–904. https://doi.org/10.1016/0092-8674(95)90269-4

Aeschlimann, S., Stettler, P., Schneider, A., 2023. DNA segregation in mitochondria and beyond: insights from the trypanosomal tripartite attachment complex. Trends Biochem. Sci. 48, 1058–1070. https://doi.org/10.1016/j.tibs.2023.08.012

Ahmad, T., Aggarwal, K., Pattnaik, B., Mukherjee, S., Sethi, T., Tiwari, B.K., Kumar, M., Micheal, A., Mabalirajan, U., Ghosh, B., Sinha Roy, S., Agrawal, A., 2013. Computational classification of mitochondrial shapes reflects stress and redox state. Cell Death Dis. 4, e461. https://doi.org/10.1038/cddis.2012.213

Ahting, U., Thieffry, M., Engelhardt, H., Hegerl, R., Neupert, W., Nussberger, S., 2001. Tom40, the Pore-Forming Component of the Protein-Conducting Tom Channel in the Outer Membrane of Mitochondria. J. Cell Biol. 153, 1151–1160. https://doi.org/10.1083/jcb.153.6.1151

Al-Furoukh, N., Ianni, A., Nolte, H., Hölper, S., Krüger, M., Wanrooij, S., Braun, T., 2015. ClpX stimulates the mitochondrial unfolded protein response (UPRmt) in mammalian cells. Biochim. Biophys. Acta 1853, 2580–2591. https://doi.org/10.1016/j.bbamcr.2015.06.016

Al-Furoukh, N., Kardon, J.R., Krüger, M., Szibor, M., Baker, T.A., Braun, T., 2014. NOA1, a novel ClpXP substrate, takes an unexpected nuclear detour prior to mitochondrial import. PloS One 9, e103141. https://doi.org/10.1371/journal.pone.0103141

Amor, A.J., Schmitz, K.R., Baker, T.A., Sauer, R.T., 2019. Roles of the ClpX IGF loops in ClpP association, dissociation, and protein degradation. Protein Sci. Publ. Protein Soc. 28, 756–765. https://doi.org/10.1002/pro.3590

Ashrafi, G., Schwarz, T.L., 2013. The pathways of mitophagy for quality control and clearance of mitochondria. Cell Death Differ. 20, 31–42. https://doi.org/10.1038/cdd.2012.81

Audano, M., Pedretti, S., Ligorio, S., Crestani, M., Caruso, D., De Fabiani, E., Mitro, N., 2020. "The Loss of Golden Touch": Mitochondria-Organelle Interactions, Metabolism, and Cancer. Cells 9, 2519. https://doi.org/10.3390/cells9112519

Augustin, S., Gerdes, F., Lee, S., Tsai, F.T.F., Langer, T., Tatsuta, T., 2009. An Intersubunit Signaling Network Coordinates ATP Hydrolysis by m-AAA Proteases. Mol. Cell 35, 574–585. https://doi.org/10.1016/j.molcel.2009.07.018

Baker, B.M., Haynes, C.M., 2011. Mitochondrial protein quality control during biogenesis and aging. Trends Biochem. Sci. 36, 254–261. https://doi.org/10.1016/j.tibs.2011.01.004

Baker, B.M., Nargund, A.M., Sun, T., Haynes, C.M., 2012. Protective coupling of mitochondrial function and protein synthesis via the eIF2α kinase GCN-2. PLoS Genet. 8, e1002760. https://doi.org/10.1371/journal.pgen.1002760

Balfour, A., 1912. NOTES ON SLEEPING SICKNESS. Br. Med. J. 2, 10–11.

Barbosa, C., Peixeiro, I., Romão, L., 2013. Gene expression regulation by upstream open reading frames and human disease. PLoS Genet. 9, e1003529. https://doi.org/10.1371/journal.pgen.1003529

Barrett, M.P., Burchmore, R.J.S., Stich, A., Lazzari, J.O., Frasch, A.C., Cazzulo, J.J., Krishna, S., 2003. The trypanosomiases. Lancet Lond. Engl. 362, 1469–1480. https://doi.org/10.1016/S0140-6736(03)14694-6

Basch, M., Wagner, M., Rolland, S., Carbonell, A., Zeng, R., Khosravi, S., Schmidt, A., Aftab, W., Imhof, A., Wagener, J., Conradt, B., Wagener, N., 2020. Msp1 cooperates with the proteasome for extraction of arrested mitochondrial import intermediates. Mol. Biol. Cell 31, 753–767. https://doi.org/10.1091/mbc.E19-06-0329

Batista, J.S., Rodrigues, C.M.F., García, H.A., Bezerra, F.S.B., Olinda, R.G., Teixeira, M.M.G., Soto-Blanco, B., 2011. Association of *Trypanosoma vivax* in extracellular sites with central nervous system lesions and changes in cerebrospinal fluid in experimentally infected goats. Vet. Res. 42, 63. https://doi.org/10.1186/1297-9716-42-63

Baugh, J.M., Viktorova, E.G., Pilipenko, E.V., 2009. Proteasomes Can Degrade a Significant Proportion of Cellular Proteins Independent of Ubiquitination. J. Mol. Biol. 386, 814–827. https://doi.org/10.1016/j.jmb.2008.12.081

Becker, S.H., Darwin, K.H., 2016. Bacterial Proteasomes: Mechanistic and Functional Insights. Microbiol. Mol. Biol. Rev. MMBR 81, e00036-16. https://doi.org/10.1128/MMBR.00036-16

Becker, T., Wenz, L.-S., Krüger, V., Lehmann, W., Müller, J.M., Goroncy, L., Zufall, N., Lithgow, T., Guiard, B., Chacinska, A., Wagner, R., Meisinger, C., Pfanner, N., 2011. The mitochondrial import protein Mim1 promotes biogenesis of multispanning outer membrane proteins. J. Cell Biol. 194, 387–395. https://doi.org/10.1083/jcb.201102044

Benedetti, C., Haynes, C.M., Yang, Y., Harding, H.P., Ron, D., 2006. Ubiquitin-like protein 5 positively regulates chaperone gene expression in the mitochondrial unfolded protein response. Genetics 174, 229–239. https://doi.org/10.1534/genetics.106.061580

Berendzen, K.M., Durieux, J., Shao, L.-W., Tian, Y., Kim, H.-E., Wolff, S., Liu, Y., Dillin, A., 2016. Neuroendocrine Coordination of Mitochondrial Stress Signaling and Proteostasis. Cell 166, 1553-1563.e10. https://doi.org/10.1016/j.cell.2016.08.042

Besse, A., Brezavar, D., Hanson, J., Larson, A., Bonnen, P.E., 2020. LONP1 de novo dominant mutation causes mitochondrial encephalopathy with loss of LONP1 chaperone activity and excessive LONP1 proteolytic activity. Mitochondrion 51, 68–78. https://doi.org/10.1016/j.mito.2020.01.004

Bezawork-Geleta, A., Saiyed, T., Dougan, D.A., Truscott, K.N., 2014. Mitochondrial matrix proteostasis is linked to hereditary paraganglioma: LON-mediated turnover of the human flavinylation factor SDH5 is regulated by its interaction with SDHA. FASEB J. 28, 1794–1804. https://doi.org/10.1096/fj.13-242420

Billington, K., Halliday, C., Madden, R., Dyer, P., Barker, A.R., Moreira-Leite, F.F., Carrington, M., Vaughan, S., Hertz-Fowler, C., Dean, S., Sunter, J.D., Wheeler, R.J., Gull, K., 2023. Genome-wide subcellular protein map for the flagellate parasite *Trypanosoma brucei*. Nat. Microbiol. 8, 533–547. https://doi.org/10.1038/s41564-022-01295-6

Bochtler, M., Ditzel, L., Groll, M., Hartmann, C., Huber, R., 1999. The Proteasome. Annu. Rev. Biophys. Biomol. Struct. 28, 295–317. https://doi.org/10.1146/annurev.biophys.28.1.295

Bochud-Allemann, N., Schneider, A., 2002. Mitochondrial Substrate Level Phosphorylation Is Essential for Growth of Procyclic *Trypanosoma brucei*. J. Biol. Chem. 277, 32849–32854. https://doi.org/10.1074/jbc.M205776200

Bodnar, N.O., Kim, K.H., Ji, Z., Wales, T.E., Svetlov, V., Nudler, E., Engen, J.R., Walz, T., Rapoport, T.A., 2018. Structure of the Cdc48 ATPase with its ubiquitin-binding cofactor Ufd1–Npl4. Nat. Struct. Mol. Biol. 25, 616–622. https://doi.org/10.1038/s41594-018-0085-x

Bogenhagen, D.F., 2012. Mitochondrial DNA nucleoid structure. Biochim. Biophys. Acta BBA - Gene Regul. Mech., Mitochondrial Gene Expression 1819, 914–920. https://doi.org/10.1016/j.bbagrm.2011.11.005

Bohovych, I., Chan, S.S.L., Khalimonchuk, O., 2015. Mitochondrial Protein Quality Control: The Mechanisms Guarding Mitochondrial Health. Antioxid. Redox Signal. 22, 977–994. https://doi.org/10.1089/ars.2014.6199

Boos, F., Krämer, L., Groh, C., Jung, F., Haberkant, P., Stein, F., Wollweber, F., Gackstatter, A., Zöller, E., van der Laan, M., Savitski, M.M., Benes, V., Herrmann, J.M., 2019. Mitochondrial protein-induced stress triggers a global adaptive transcriptional programme. Nat. Cell Biol. 21, 442–451. https://doi.org/10.1038/s41556-019-0294-5

Boos, F., Labbadia, J., Herrmann, J.M., 2020. How the Mitoprotein-Induced Stress Response Safeguards the Cytosol: A Unified View. Trends Cell Biol. 30, 241–254. https://doi.org/10.1016/j.tcb.2019.12.003

Bragoszewski, P., Wasilewski, M., Sakowska, P., Gornicka, A., Böttinger, L., Qiu, J., Wiedemann, N., Chacinska, A., 2015. Retro-translocation of mitochondrial intermembrane space proteins. Proc. Natl. Acad. Sci. 112, 7713–7718. https://doi.org/10.1073/pnas.1504615112

Brandvain, Y., Wade, M.J., 2009. The Functional Transfer of Genes From the Mitochondria to the Nucleus: The Effects of Selection, Mutation, Population Size and Rate of Self-Fertilization. Genetics 182, 1129–1139. https://doi.org/10.1534/genetics.108.100024

Breitschopf, K., Bengal, E., Ziv, T., Admon, A., Ciechanover, A., 1998. A novel site for ubiquitination: the N-terminal residue, and not internal lysines of MyoD, is essential for conjugation and degradation of the protein. EMBO J. 17, 5964–5973. https://doi.org/10.1093/emboj/17.20.5964

Breker, M., Gymrek, M., Schuldiner, M., 2013. A novel single-cell screening platform reveals proteome plasticity during yeast stress responses. J. Cell Biol. 200, 839–850. https://doi.org/10.1083/jcb.201301120

Brenchley, R., Tariq, H., McElhinney, H., Szöor, B., Huxley-Jones, J., Stevens, R., Matthews, K., Tabernero, L., 2007. The TriTryp phosphatome: analysis of the protein phosphatase catalytic domains. BMC Genomics 8, 434. https://doi.org/10.1186/1471-2164-8-434

Bruggisser, J., Käser, S., Mani, J., Schneider, A., 2017. Biogenesis of a Mitochondrial Outer Membrane Protein in *Trypanosoma brucei*. J. Biol. Chem. 292, 3400–3410. https://doi.org/10.1074/jbc.M116.755983

Brun, R., Blum, J., Chappuis, F., Burri, C., 2010. Human African trypanosomiasis. Lancet Lond. Engl. 375, 148–159. https://doi.org/10.1016/S0140-6736(09)60829-1

Brun, R., Schönenberger, M., 1979. Cultivation and in vitro cloning or procyclic culture forms of *Trypanosoma brucei* in a semi-defined medium. Short communication. Acta Trop. 36, 289–292.

Burd, C., Cullen, P.J., 2014. Retromer: a master conductor of endosome sorting. Cold Spring Harb. Perspect. Biol. 6, a016774. https://doi.org/10.1101/cshperspect.a016774

Burki, F., Roger, A.J., Brown, M.W., Simpson, A.G.B., 2020. The New Tree of Eukaryotes. Trends Ecol. Evol. 35, 43–55. https://doi.org/10.1016/j.tree.2019.08.008

Büscher, P., Cecchi, G., Jamonneau, V., Priotto, G., 2017. Human African trypanosomiasis. Lancet Lond. Engl. 390, 2397–2409. https://doi.org/10.1016/S0140-6736(17)31510-6

Callegari, S., Dennerlein, S., 2018. Sensing the Stress: A Role for the UPRmt and UPRam in the Quality Control of Mitochondria. Front. Cell Dev. Biol. 6.

Callis, J., 2014. The ubiquitination machinery of the ubiquitin system. Arab. Book 12, e0174. https://doi.org/10.1199/tab.0174

Calvo, S.E., Clauser, K.R., Mootha, V.K., 2016. MitoCarta2.0: an updated inventory of mammalian mitochondrial proteins. Nucleic Acids Res. 44, D1251–D1257. https://doi.org/10.1093/nar/gkv1003

Calvo, S.E., Mootha, V.K., 2010. The Mitochondrial Proteome and Human Disease. Annu. Rev. Genomics Hum. Genet. 11, 25–44. https://doi.org/10.1146/annurev-genom-082509-141720

Castanzo, D.T., LaFrance, B., Martin, A., 2020. The AAA+ ATPase Msp1 is a processive protein translocase with robust unfoldase activity. Proc. Natl. Acad. Sci. 117, 14970–14977. https://doi.org/10.1073/pnas.1920109117

Chang, Y.-C., Peng, Y.-X., Yu, B.-H., Chang, H.C., Liang, P.-S., Huang, T.-Y., Shih, C.-J., Chu, L.-A., Sang, T.-K., 2021. VCP maintains nuclear size by regulating the DNA damage-associated MDC1–p53–autophagy axis in Drosophila. Nat. Commun. 12, 4258. https://doi.org/10.1038/s41467-021-24556-0

Chau, V., Tobias, J.W., Bachmair, A., Marriott, D., Ecker, D.J., Gonda, D.K., Varshavsky, A., 1989. A multiubiquitin chain is confined to specific lysine in a targeted short-lived protein. Science 243, 1576–1583. https://doi.org/10.1126/science.2538923

Chen, G., Xu, X., Tong, J., Han, K., Zhang, Z., Tang, J., Li, S., Yang, C., Li, J., Cao, B., Zhou, H., Wu, D., Moran, M.F., Mao, X., 2014. Ubiquitination of the transcription factor c-MAF is mediated by multiple lysine residues. Int. J. Biochem. Cell Biol. 57, 157–166. https://doi.org/10.1016/j.biocel.2014.10.024

Chen, Y.-C., Umanah, G.K.E., Dephoure, N., Andrabi, S.A., Gygi, S.P., Dawson, T.M., Dawson, V.L., Rutter, J., 2014. Msp1/ATAD1 maintains mitochondrial function by facilitating the degradation of mislocalized tail-anchored proteins. EMBO J. 33, 1548–1564. https://doi.org/10.15252/embj.201487943

Chen, Z., Liu, L., Cheng, Q., Li, Y., Wu, H., Zhang, W., Wang, Y., Sehgal, S.A., Siraj, S., Wang, X., Wang, J., Zhu, Y., Chen, Q., 2017. Mitochondrial E3 ligase MARCH5 regulates FUNDC1 to fine-tune hypoxic mitophagy. EMBO Rep. 18, 495–509. https://doi.org/10.15252/embr.201643309

Christianson, J.C., Ye, Y., 2014. Cleaning up in the endoplasmic reticulum: ubiquitin in charge. Nat. Struct. Mol. Biol. 21, 325–335. https://doi.org/10.1038/nsmb.2793

Ciechanover, A., Schwartz, A.L., 1998. The ubiquitin-proteasome pathway: The complexity and myriad functions of proteins death. Proc. Natl. Acad. Sci. U. S. A. 95, 2727. https://doi.org/10.1073/pnas.95.6.2727

Clayton, C., 2019. Regulation of gene expression in trypanosomatids: living with polycistronic transcription. Open Biol. 9, 190072. https://doi.org/10.1098/rsob.190072

Collier, J.J., Oláhová, M., McWilliams, T.G., Taylor, R.W., 2023. Mitochondrial signalling and homeostasis: from cell biology to neurological disease. Trends Neurosci. 46, 137–152. https://doi.org/10.1016/j.tins.2022.12.001

Coonrod, E.M., Karren, M.A., Shaw, J.M., 2007. Ugo1p Is a Multipass Transmembrane Protein with a Single Carrier Domain Required for Mitochondrial Fusion. Traffic 8, 500–511. https://doi.org/10.1111/j.1600-0854.2007.00550.x

Cormio, A., Musicco, C., Gasparre, G., Cormio, G., Pesce, V., Sardanelli, A.M., Gadaleta, M.N., 2017. Increase in proteins involved in mitochondrial fission, mitophagy, proteolysis and antioxidant response in type I endometrial cancer as an adaptive response to respiratory complex I deficiency. Biochem. Biophys. Res. Commun. 491, 85–90. https://doi.org/10.1016/j.bbrc.2017.07.047

Cotter, D., Guda, P., Fahy, E., Subramaniam, S., 2004. MitoProteome: mitochondrial protein sequence database and annotation system. Nucleic Acids Res. 32, D463–D467. https://doi.org/10.1093/nar/gkh048

Da Cruz, S., Martinou, J.-C., 2008. Purification and Proteomic Analysis of the Mouse Liver Mitochondrial Inner Membrane, in: Pflieger, D., Rossier, J. (Eds.), Organelle Proteomics, Methods in Molecular Biology™. Humana Press, Totowa, NJ, pp. 101–116. https://doi.org/10.1007/978-1-59745-028-7_7

Dean, S., Moreira-Leite, F., Varga, V., Gull, K., 2016. Cilium transition zone proteome reveals compartmentalization and differential dynamics of ciliopathy complexes. Proc. Natl. Acad. Sci. U. S. A. 113, E5135-5143. https://doi.org/10.1073/pnas.1604258113

Deas, E., Plun-Favreau, H., Gandhi, S., Desmond, H., Kjaer, S., Loh, S.H.Y., Renton, A.E.M., Harvey, R.J., Whitworth, A.J., Martins, L.M., Abramov, A.Y., Wood, N.W., 2011. PINK1 cleavage at position A103 by the mitochondrial protease PARL. Hum. Mol. Genet. 20, 867–879. https://doi.org/10.1093/hmg/ddq526

Dederer, V., Khmelinskii, A., Huhn, A.G., Okreglak, V., Knop, M., Lemberg, M.K., 2019. Cooperation of mitochondrial and ER factors in quality control of tail-anchored proteins. eLife 8, e45506. https://doi.org/10.7554/eLife.45506

Deepa, S.S., Bhaskaran, S., Ranjit, R., Qaisar, R., Nair, B.C., Liu, Y., Walsh, M.E., Fok, W.C., Van Remmen, H., 2016. Down-regulation of the mitochondrial matrix peptidase ClpP in muscle cells causes mitochondrial dysfunction and decreases cell proliferation. Free Radic. Biol. Med. 91, 281–292. https://doi.org/10.1016/j.freeradbiomed.2015.12.021

den Brave, F., Gupta, A., Becker, T., 2021. Protein Quality Control at the Mitochondrial Surface. Front. Cell Dev. Biol. 9, 795685. https://doi.org/10.3389/fcell.2021.795685

Deshwal, S., Fiedler, K.U., Langer, T., 2020. Mitochondrial Proteases: Multifaceted Regulators of Mitochondrial Plasticity. Annu. Rev. Biochem. 89, 501–528. https://doi.org/10.1146/annurev-biochem-062917-012739

Desjardins, P., Frost, E., Morais, R., 1985. Ethidium bromide-induced loss of mitochondrial DNA from primary chicken embryo fibroblasts. Mol. Cell. Biol. 5, 1163–1169. https://doi.org/10.1128/mcb.5.5.1163-1169.1985

Dewar, C.E., Oeljeklaus, S., Mani, J., Mühlhäuser, W.W.D., von Känel, C., Zimmermann, J., Ochsenreiter, T., Warscheid, B., Schneider, A., 2022a. Mistargeting of aggregation prone mitochondrial proteins activates a nucleus-mediated posttranscriptional quality control pathway in trypanosomes. Nat. Commun. 13, 3084. https://doi.org/10.1038/s41467-022-30748-z

Dewar, C.E., Oeljeklaus, S., Wenger, C., Warscheid, B., Schneider, A., 2022b. Characterization of a highly diverged mitochondrial ATP synthase Fo subunit in *Trypanosoma brucei*. J. Biol. Chem. 298. https://doi.org/10.1016/j.jbc.2022.101829

Diederichs, K.A., Ni, X., Rollauer, S.E., Botos, I., Tan, X., King, M.S., Kunji, E.R.S., Jiang, J., Buchanan, S.K., 2020. Structural insight into mitochondrial β-barrel outer membrane protein biogenesis. Nat. Commun. 11, 3290. https://doi.org/10.1038/s41467-020-17144-1

Dimmer, K.S., Papić, D., Schumann, B., Sperl, D., Krumpe, K., Walther, D.M., Rapaport, D., 2012. A crucial role for Mim2 in the biogenesis of mitochondrial outer membrane proteins. J. Cell Sci. 125, 3464–3473. https://doi.org/10.1242/jcs.103804

Dinur-Mills, M., Tal, M., Pines, O., 2008. Dual targeted mitochondrial proteins are characterized by lower MTS parameters and total net charge. PloS One 3, e2161. https://doi.org/10.1371/journal.pone.0002161

Doan, K.N., Grevel, A., Mårtensson, C.U., Ellenrieder, L., Thornton, N., Wenz, L.-S., Opaliński, Ł., Guiard, B., Pfanner, N., Becker, T., 2020. The Mitochondrial Import Complex MIM Functions as Main Translocase for α-Helical Outer Membrane Proteins. Cell Rep. 31, 107567. https://doi.org/10.1016/j.celrep.2020.107567

Dobrynin, G., Popp, O., Romer, T., Bremer, S., Schmitz, M.H.A., Gerlich, D.W., Meyer, H., 2011. Cdc48/p97-Ufd1-Npl4 antagonizes Aurora B during chromosome segregation in HeLa cells. J. Cell Sci. 124, 1571–1580. https://doi.org/10.1242/jcs.069500

Dolezal, P., Likic, V., Tachezy, J., Lithgow, T., 2006. Evolution of the Molecular Machines for Protein Import into Mitochondria. Science 313, 314–318. https://doi.org/10.1126/science.1127895

Durieux, J., Wolff, S., Dillin, A., 2011. The cell-non-autonomous nature of electron transport chain-mediated longevity. Cell 144, 79–91. https://doi.org/10.1016/j.cell.2010.12.016

Edwards, R., Eaglesfield, R., Tokatlidis, K., 2021. The mitochondrial intermembrane space: the most constricted mitochondrial sub-compartment with the largest variety of protein import pathways. Open Biol. 11, 210002. https://doi.org/10.1098/rsob.210002

Fang, L., Hemion, C., Pinho Ferreira Bento, A.C., Bippes, C.C., Flammer, J., Neutzner, A., 2015. Mitochondrial function in neuronal cells depends on p97/VCP/Cdc48-mediated quality control. Front. Cell. Neurosci. 9. doi.org/10.3389/fncel.2015.00016

Fiorese, C.J., Schulz, A.M., Lin, Y.-F., Rosin, N., Pellegrino, M.W., Haynes, C.M., 2016. The Transcription Factor ATF5 Mediates a Mammalian Mitochondrial UPR. Curr. Biol. CB 26, 2037–2043. https://doi.org/10.1016/j.cub.2016.06.002

Fischer, F., Hamann, A., Osiewacz, H.D., 2012. Mitochondrial quality control: an integrated network of pathways. Trends Biochem. Sci. 37, 284–292. https://doi.org/10.1016/j.tibs.2012.02.004

Fischer, F., Langer, J.D., Osiewacz, H.D., 2015. Identification of potential mitochondrial CLPXP protease interactors and substrates suggests its central role in energy metabolism. Sci. Rep. 5, 18375. https://doi.org/10.1038/srep18375

Fischer, F., Weil, A., Hamann, A., Osiewacz, H.D., 2013. Human CLPP reverts the longevity phenotype of a fungal ClpP deletion strain. Nat. Commun. 4, 1397. https://doi.org/10.1038/ncomms2397

Franco, J.R., Simarro, P.P., Diarra, A., Jannin, J.G., 2014. Epidemiology of human African trypanosomiasis. Clin. Epidemiol. 6, 257–275. https://doi.org/10.2147/CLEP.S39728

Friedman, J.R., Nunnari, J., 2014. Mitochondrial form and function. Nature 505, 335–343. https://doi.org/10.1038/nature12985
Fritz, S., Rapaport, D., Klanner, E., Neupert, W., Westermann, B., 2001. Connection of the Mitochondrial Outer and Inner Membranes by Fzo1 Is Critical for Organellar Fusion. J. Cell Biol. 152, 683–692. https://doi.org/10.1083/jcb.152.4.683
Fritz, S., Weinbach, N., Westermann, B., 2003. Mdm30 Is an F-Box Protein Required for Maintenance of Fusion-competent Mitochondria in Yeast. Mol. Biol. Cell 14, 2303–2313. https://doi.org/10.1091/mbc.e02-12-0831
Fu, M., St-Pierre, P., Shankar, J., Wang, P.T.C., Joshi, B., Nabi, I.R., 2013. Regulation of mitophagy by the Gp78 E3 ubiquitin ligase. Mol. Biol. Cell 24, 1153–1162. https://doi.org/10.1091/mbc.E12-08-0607
Fukasawa, Y., Oda, T., Tomii, K., Imai, K., 2017. Origin and Evolutionary Alteration of the Mitochondrial Import System in Eukaryotic Lineages. Mol. Biol. Evol. 34, 1574–1586. https://doi.org/10.1093/molbev/msx096
Fukasawa, Y., Tsuji, J., Fu, S.-C., Tomii, K., Horton, P., Imai, K., 2015. MitoFates: improved prediction of mitochondrial targeting sequences and their cleavage sites. Mol. Cell. Proteomics MCP 14, 1113–1126. https://doi.org/10.1074/mcp.M114.043083
Gabaldón, T., 2021. Origin and Early Evolution of the Eukaryotic Cell. Annu. Rev. Microbiol. 75, 631–647. https://doi.org/10.1146/annurev-micro-090817-062213
Gargaud, M., López-Garcìa, P., Martin, H., 2011. Origins and Evolution of Life: An Astrobiological Perspective. Cambridge University Press.
Gerber, M., Suppanz, I., Oeljeklaus, S., Niemann, M., Käser, S., Warscheid, B., Schneider, A., Dewar, C.E., 2023. A Msp1-containing complex removes orphaned proteins in the mitochondrial outer membrane of T. brucei. Life Sci. Alliance 6. https://doi.org/10.26508/lsa.202302004
Ghifari, A.S., Gill-Hille, M., Murcha, M.W., 2018. Plant mitochondrial protein import: the ins and outs. Biochem. J. 475, 2191–2208. https://doi.org/10.1042/BCJ20170521
Gispert, S., Parganlija, D., Klinkenberg, M., Dröse, S., Wittig, I., Mittelbronn, M., Grzmil, P., Koob, S., Hamann, A., Walter, M., Büchel, F., Adler, T., Hrabé de Angelis, M., Busch, D.H., Zell, A., Reichert, A.S., Brandt, U., Osiewacz, H.D., Jendrach, M., Auburger, G., 2013. Loss of mitochondrial peptidase Clpp leads to infertility, hearing loss plus growth retardation via accumulation of CLPX, mtDNA and inflammatory factors. Hum. Mol. Genet. 22, 4871–4887. https://doi.org/10.1093/hmg/ddt338
Goodrum, J.M., Lever, A.R., Coody, T.K., Gottschling, D.E., Hughes, A.L., 2019. Rsp5 and Mdm30 reshape the mitochondrial network in response to age-induced vacuole stress. Mol. Biol. Cell 30, 2141–2154. https://doi.org/10.1091/mbc.E19-02-0094
Gulde, P.E., Christen, L., Brown, S.V., Williams, N., 2013. Three Distinct Isoforms of ATP Synthase Subunit c Are Expressed in T. brucei and Assembled into the Mitochondrial ATP Synthase Complex. PLOS ONE 8, e54039. https://doi.org/10.1371/journal.pone.0054039
Guna, A., Stevens, T.A., Inglis, A.J., Replogle, J.M., Esantsi, T.K., Muthukumar, G., Shaffer, K.C.L., Wang, M.L., Pogson, A.N., Jones, J.J., Lomenick, B., Chou, T.-F., Weissman, J.S., Voorhees, R.M., 2022. MTCH2 is a mitochondrial outer membrane protein insertase. Science 378, 317–322. https://doi.org/10.1126/science.add1856
Guna, A., Volkmar, N., Christianson, J.C., Hegde, R.S., 2018. The ER membrane protein complex is a transmembrane domain insertase. Science 359, 470–473. https://doi.org/10.1126/science.aao3099
Guo, H.J., Rahimi, N., Tadi, P., 2023. Biochemistry, Ubiquitination, in: StatPearls. StatPearls Publishing, Treasure Island (FL).
Güther, M.L.S., Urbaniak, M.D., Tavendale, A., Prescott, A., Ferguson, M.A.J., 2014. High-Confidence Glycosome Proteome for Procyclic Form *Trypanosoma brucei* by Epitope-Tag Organelle Enrichment and SILAC Proteomics. J. Proteome Res. 13, 2796–2806. https://doi.org/10.1021/pr401209w
Haaften-Visser, D.Y. van, Harakalova, M., Mocholi, E., Montfrans, J.M. van, Elkadri, A., Rieter, E., Fiedler, K., Hasselt, P.M. van, Triffaux, E.M.M., Haelst, M.M. van, Nijman, I.J., Kloosterman, W.P., Nieuwenhuis, E.E.S., Muise, A.M., Cuppen, E., Houwen, R.H.J.,

Coffer, P.J., 2017. Ankyrin repeat and zinc-finger domain-containing 1 mutations are associated with infantile-onset inflammatory bowel disease. J. Biol. Chem. 292, 7904–7920. https://doi.org/10.1074/jbc.M116.772038
Hanson, P.I., Whiteheart, S.W., 2005. AAA+ proteins: have engine, will work. Nat. Rev. Mol. Cell Biol. 6, 519–529. https://doi.org/10.1038/nrm1684
Hartkamp, J., Carpenter, B., Roberts, S.G.E., 2010. The Wilms' Tumor Suppressor Protein WT1 Is Processed by the Serine Protease HtrA2/Omi. Mol. Cell 37, 159–171. https://doi.org/10.1016/j.molcel.2009.12.023
Haynes, C.M., Petrova, K., Benedetti, C., Yang, Y., Ron, D., 2007. ClpP mediates activation of a mitochondrial unfolded protein response in C. elegans. Dev. Cell 13, 467–480. https://doi.org/10.1016/j.devcel.2007.07.016
Haynes, C.M., Yang, Y., Blais, S.P., Neubert, T.A., Ron, D., 2010. The matrix peptide exporter HAF-1 signals a mitochondrial UPR by activating the transcription factor ZC376.7 in C. elegans. Mol. Cell 37, 529–540. https://doi.org/10.1016/j.molcel.2010.01.015
He, J.Y., Xi, W.H., Zhu, L.B., Long, X.H., Chen, X.Y., Liu, J.M., Luo, Q.F., Zhu, X.P., Liu, Z.L., 2015. Knockdown of Aurora-B alters osteosarcoma cell malignant phenotype via decreasing phosphorylation of VCP and NF-κB signaling. Tumour Biol. J. Int. Soc. Oncodevelopmental Biol. Med. 36, 3895–3902. https://doi.org/10.1007/s13277-014-3032-4
Hedges, S.B., Blair, J.E., Venturi, M.L., Shoe, J.L., 2004. A molecular timescale of eukaryote evolution and the rise of complex multicellular life. BMC Evol. Biol. 4, 2. https://doi.org/10.1186/1471-2148-4-2
Henning, N.J., Boike, L., Spradlin, J.N., Ward, C.C., Liu, G., Zhang, E., Belcher, B.P., Brittain, S.M., Hesse, M.J., Dovala, D., McGregor, L.M., Valdez Misiolek, R., Plasschaert, L.W., Rowlands, D.J., Wang, F., Frank, A.O., Fuller, D., Estes, A.R., Randal, K.L., Panidapu, A., McKenna, J.M., Tallarico, J.A., Schirle, M., Nomura, D.K., 2022. Deubiquitinase-targeting chimeras for targeted protein stabilization. Nat. Chem. Biol. 18, 412–421. https://doi.org/10.1038/s41589-022-00971-2
Henze, K., Martin, W., 2003. Essence of mitochondria. Nature 426, 127–128. https://doi.org/10.1038/426127a
Heo, J.-M., Ordureau, A., Swarup, S., Paulo, J.A., Shen, K., Sabatini, D.M., Harper, J.W., 2018. RAB7A phosphorylation by TBK1 promotes mitophagy via the PINK-PARKIN pathway. Sci. Adv. 4, eaav0443. https://doi.org/10.1126/sciadv.aav0443
Hershko, A., Ciechanover, A., 1998. THE UBIQUITIN SYSTEM.
Hill, K., Model, K., Ryan, M.T., Dietmeier, K., Martin, F., Wagner, R., Pfanner, N., 1998. Tom40 forms the hydrophilic channel of the mitochondrial import pore for preproteins. Nature 395, 516–521. https://doi.org/10.1038/26780
Hoogenboom, B.W., Suda, K., Engel, A., Fotiadis, D., 2007. The Supramolecular Assemblies of Voltage-dependent Anion Channels in the Native Membrane. J. Mol. Biol. 370, 246–255. https://doi.org/10.1016/j.jmb.2007.04.073
Hoogenraad, N.J., Ward, L.A., Ryan, M.T., 2002. Import and assembly of proteins into mitochondria of mammalian cells. Biochim. Biophys. Acta BBA - Mol. Cell Res. 1592, 97–105. https://doi.org/10.1016/S0167-4889(02)00268-9
Hua, S., To, W.Y., Nguyen, T.T., Wong, M.L., Wang, C.C., 1996. Purification and characterization of proteasomes from *Trypanosoma brucei*. Mol. Biochem. Parasitol. 78, 33–46. https://doi.org/10.1016/s0166-6851(96)02599-6
Huang, L., Shen, M., Chernushevich, I., Burlingame, A.L., Wang, C.C., Robertson, C.D., 1999. Identification and isolation of three proteasome subunits and their encoding genes from *Trypanosoma brucei*. Mol. Biochem. Parasitol. 102, 211–223. https://doi.org/10.1016/s0166-6851(99)00096-1
Hung, V., Lam, S.S., Udeshi, N.D., Svinkina, T., Guzman, G., Mootha, V.K., Carr, S.A., Ting, A.Y., 2017. Proteomic mapping of cytosol-facing outer mitochondrial and ER membranes in living human cells by proximity biotinylation. eLife 6, e24463. https://doi.org/10.7554/eLife.24463
Hung, V., Zou, P., Rhee, H.-W., Udeshi, N.D., Cracan, V., Svinkina, T., Carr, S.A., Mootha, V.K., Ting, A.Y., 2014. Proteomic Mapping of the Human Mitochondrial Intermembrane

Space in Live Cells via Ratiometric APEX Tagging. Mol. Cell 55, 332–341. https://doi.org/10.1016/j.molcel.2014.06.003
Igarashi, R., Yamashita, S., Yamashita, T., Inoue, K., Fukuda, T., Fukuchi, T., Kanki, T., 2020. Gemcitabine induces Parkin-independent mitophagy through mitochondrial-resident E3 ligase MUL1-mediated stabilization of PINK1. Sci. Rep. 10, 1465. https://doi.org/10.1038/s41598-020-58315-w
Iyer, A., Niemann, M., Serricchio, M., Dewar, C.E., Oeljeklaus, S., Farine, L., Warscheid, B., Schneider, A., Bütikofer, P., 2022. The endoplasmic reticulum membrane protein complex localizes to the mitochondrial - endoplasmic reticulum interface and its subunits modulate phospholipid biosynthesis in *Trypanosoma brucei*. PLoS Pathog. 18, e1009717. https://doi.org/10.1371/journal.ppat.1009717
Izawa, T., Park, S.-H., Zhao, L., Hartl, F.U., Neupert, W., 2017. Cytosolic Protein Vms1 Links Ribosome Quality Control to Mitochondrial and Cellular Homeostasis. Cell 171, 890-903.e18. https://doi.org/10.1016/j.cell.2017.10.002
Jackson, A.P., Allison, H.C., Barry, J.D., Field, M.C., Hertz-Fowler, C., Berriman, M., 2013. A Cell-surface Phylome for African Trypanosomes. PLoS Negl. Trop. Dis. 7, e2121. https://doi.org/10.1371/journal.pntd.0002121
Jakob, M., Hoffmann, A., Amodeo, S., Peitsch, C., Zuber, B., Ochsenreiter, T., 2016. Mitochondrial growth during the cell cycle of *Trypanosoma brucei* bloodstream forms. Sci. Rep. 6, 36565. https://doi.org/10.1038/srep36565
Jonikas, M.C., Collins, S.R., Denic, V., Oh, E., Quan, E.M., Schmid, V., Weibezahn, J., Schwappach, B., Walter, P., Weissman, J.S., Schuldiner, M., 2009. Comprehensive characterization of genes required for protein folding in the endoplasmic reticulum. Science 323, 1693–1697. https://doi.org/10.1126/science.1167983
Jores, T., Klinger, A., Groß, L.E., Kawano, S., Flinner, N., Duchardt-Ferner, E., Wöhnert, J., Kalbacher, H., Endo, T., Schleiff, E., Rapaport, D., 2016. Characterization of the targeting signal in mitochondrial β-barrel proteins. Nat. Commun. 7, 12036. https://doi.org/10.1038/ncomms12036
Joubert, J.J., Schutte, C.H., Irons, D.J., Fripp, P.J., 1993. Ubombo and the site of David Bruce's discovery of *Trypanosoma brucei*. Trans. R. Soc. Trop. Med. Hyg. 87, 494–495. https://doi.org/10.1016/0035-9203(93)90056-v
Kang, S.G., Dimitrova, M.N., Ortega, J., Ginsburg, A., Maurizi, M.R., 2005. Human Mitochondrial ClpP Is a Stable Heptamer That Assembles into a Tetradecamer in the Presence of ClpX. J. Biol. Chem. 280, 35424–35432. https://doi.org/10.1074/jbc.M507240200
Kao, T.-Y., Chiu, Y.-C., Fang, W.-C., Cheng, C.-W., Kuo, C.-Y., Juan, H.-F., Wu, S.-H., Lee, A.Y.-L., 2015. Mitochondrial Lon regulates apoptosis through the association with Hsp60–mtHsp70 complex. Cell Death Dis. 6, e1642–e1642. https://doi.org/10.1038/cddis.2015.9
Karnkowska, A., Vacek, V., Zubáčová, Z., Treitli, S.C., Petrželková, R., Eme, L., Novák, L., Žárský, V., Barlow, L.D., Herman, E.K., Soukal, P., Hroudová, M., Doležal, P., Stairs, C.W., Roger, A.J., Eliáš, M., Dacks, J.B., Vlček, Č., Hampl, V., 2016. A Eukaryote without a Mitochondrial Organelle. Curr. Biol. 26, 1274–1284. https://doi.org/10.1016/j.cub.2016.03.053
Kasashima, K., Sumitani, M., Endo, H., 2012. Maintenance of mitochondrial genome distribution by mitochondrial AAA+ protein ClpX. Exp. Cell Res. 318, 2335–2343. https://doi.org/10.1016/j.yexcr.2012.07.012
Käser, S., Oeljeklaus, S., Týč, J., Vaughan, S., Warscheid, B., Schneider, A., 2016. Outer membrane protein functions as integrator of protein import and DNA inheritance in mitochondria. Proc. Natl. Acad. Sci. U. S. A. 113, E4467–E4475. https://doi.org/10.1073/pnas.1605497113
Kazlauskaite, A., Martínez-Torres, R.J., Wilkie, S., Kumar, A., Peltier, J., Gonzalez, A., Johnson, C., Zhang, J., Hope, A.G., Peggie, M., Trost, M., van Aalten, D.M.F., Alessi, D.R., Prescott, A.R., Knebel, A., Walden, H., Muqit, M.M.K., 2015. Binding to serine 65-phosphorylated ubiquitin primes Parkin for optimal PINK1-dependent

phosphorylation and activation. EMBO Rep. 16, 939–954. https://doi.org/10.15252/embr.201540352
Kennedy, P.G., 2013. Clinical features, diagnosis, and treatment of human African trypanosomiasis (sleeping sickness). Lancet Neurol. 12, 186–194. https://doi.org/10.1016/S1474-4422(12)70296-X
Khan, N.A., Nikkanen, J., Yatsuga, S., Jackson, C., Wang, L., Pradhan, S., Kivelä, R., Pessia, A., Velagapudi, V., Suomalainen, A., 2017. mTORC1 Regulates Mitochondrial Integrated Stress Response and Mitochondrial Myopathy Progression. Cell Metab. 26, 419-428.e5. https://doi.org/10.1016/j.cmet.2017.07.007
Kim, H.-E., Grant, A.R., Simic, M.S., Kohnz, R.A., Nomura, D.K., Durieux, J., Riera, C.E., Sanchez, M., Kapernick, E., Wolff, S., Dillin, A., 2016. Lipid Biosynthesis Coordinates a Mitochondrial-to-Cytosolic Stress Response. Cell 166, 1539-1552.e16. https://doi.org/10.1016/j.cell.2016.08.027
Koller, K.J., Brownstein, M.J., 1987. Use of a cDNA clone to identify a supposed precursor protein containing valosin. Nature 325, 542–545. https://doi.org/10.1038/325542a0
König, T., Nolte, H., Aaltonen, M.J., Tatsuta, T., Krols, M., Stroh, T., Langer, T., McBride, H.M., 2021. MIROs and DRP1 drive mitochondrial-derived vesicle biogenesis and promote quality control. Nat. Cell Biol. 23, 1271–1286. https://doi.org/10.1038/s41556-021-00798-4
Koppen, M., Metodiev, M.D., Casari, G., Rugarli, E.I., Langer, T., 2007. Variable and Tissue-Specific Subunit Composition of Mitochondrial m-AAA Protease Complexes Linked to Hereditary Spastic Paraplegia. Mol. Cell. Biol. 27, 758–767. https://doi.org/10.1128/MCB.01470-06
Kovalinka, T., Pánek, T., Kováčová, B., Horváth, A., 2020. Orientation of FtsH protease homologs in *Trypanosoma brucei* inner mitochondrial membrane and its evolutionary implications. Mol. Biochem. Parasitol. 238, 111282. https://doi.org/10.1016/j.molbiopara.2020.111282
Kowalski, L., Bragoszewski, P., Khmelinskii, A., Glow, E., Knop, M., Chacinska, A., 2018. Determinants of the cytosolic turnover of mitochondrial intermembrane space proteins. BMC Biol. 16, 66. https://doi.org/10.1186/s12915-018-0536-1
Kozjak-Pavlovic, V., Ross, K., Benlasfer, N., Kimmig, S., Karlas, A., Rudel, T., 2007. Conserved roles of Sam50 and metaxins in VDAC biogenesis. EMBO Rep. 8, 576–582. https://doi.org/10.1038/sj.embor.7400982
Krämer, L., Groh, C., Herrmann, J.M., 2021. The proteasome: friend and foe of mitochondrial biogenesis. FEBS Lett. 595, 1223–1238. https://doi.org/10.1002/1873-3468.14010
Küey, C., Sittewelle, M., Larocque, G., Hernández-González, M., Royle, S.J., 2022. Recruitment of clathrin to intracellular membranes is sufficient for vesicle formation. eLife 11. https://doi.org/10.7554/ELIFE.78929
Kuroha, K., Zinoviev, A., Hellen, C.U.T., Pestova, T.V., 2018. Release of Ubiquitinated and Non-ubiquitinated Nascent Chains from Stalled Mammalian Ribosomal Complexes by ANKZF1 and Ptrh1. Mol. Cell 72, 286-302.e8. https://doi.org/10.1016/j.molcel.2018.08.022
Lacomble, S., Vaughan, S., Deghelt, M., Moreira-Leite, F.F., Gull, K., 2012. A *Trypanosoma brucei* protein required for maintenance of the flagellum attachment zone and flagellar pocket ER domains. Protist 163, 602–615. https://doi.org/10.1016/j.protis.2011.10.010
Lakemeyer, M., Bertosin, E., Möller, F., Balogh, D., Strasser, R., Dietz, H., Sieber, S.A., 2019. Tailored Peptide Phenyl Esters Block ClpXP Proteolysis by an Unusual Breakdown into a Heptamer–Hexamer Assembly. Angew. Chem. Int. Ed. 58, 7127–7132. https://doi.org/10.1002/anie.201901056
Lamb, C.A., Yoshimori, T., Tooze, S.A., 2013. The autophagosome: origins unknown, biogenesis complex. Nat. Rev. Mol. Cell Biol. 14, 759–774. https://doi.org/10.1038/nrm3696
Latterich, M., Fröhlich, K.-U., Schekman, R., 1995. Membrane fusion and the cell cycle: Cdc48p participates in the fusion of ER membranes. Cell 82, 885–893. https://doi.org/10.1016/0092-8674(95)90268-6

Lazarou, M., Sliter, D.A., Kane, L.A., Sarraf, S.A., Wang, C., Burman, J.L., Sideris, D.P., Fogel, A.I., Youle, R.J., 2015. The ubiquitin kinase PINK1 recruits autophagy receptors to induce mitophagy. Nature 524, 309–314. https://doi.org/10.1038/nature14893

Leonhard, K., Guiard, B., Pellecchia, G., Tzagoloff, A., Neupert, W., Langer, T., 2000. Membrane Protein Degradation by AAA Proteases in Mitochondria: Extraction of Substrates from Either Membrane Surface. Mol. Cell 5, 629–638. https://doi.org/10.1016/S1097-2765(00)80242-7

Levytskyy, R.M., Bohovych, I., Khalimonchuk, O., 2017. Metalloproteases of the Inner Mitochondrial Membrane. Biochemistry 56, 4737–4746. https://doi.org/10.1021/acs.biochem.7b00663

Li, B., Zhao, H., Wu, Y., Zhu, Y., Zhang, J., Yang, G., Yan, Q., Li, J., Li, T., Liu, L., 2020. Mitochondrial-Derived Vesicles Protect Cardiomyocytes Against Hypoxic Damage. Front. Cell Dev. Biol. 8, 214. https://doi.org/10.3389/fcell.2020.00214

Li, L., Zheng, J., Wu, X., Jiang, H., 2019. Mitochondrial AAA-ATPase Msp1 detects mislocalized tail-anchored proteins through a dual-recognition mechanism. EMBO Rep. 20, e46989. https://doi.org/10.15252/embr.201846989

Liao, P.-C., Wolken, D.M.A., Serrano, E., Srivastava, P., Pon, L.A., 2020. Mitochondria-Associated Degradation Pathway (MAD) Function beyond the Outer Membrane. Cell Rep. 32, 107902. https://doi.org/10.1016/j.celrep.2020.107902

Liao, Y., Dong, Y., Cheng, J., 2020. The Molecular Determinants of Mitochondrial Membrane Contact With ER, Lysosomes and Peroxisomes in Neuronal Physiology and Pathology. Front. Cell. Neurosci. 14.

Lin, Q., Li, S., Jiang, N., Jin, H., Shao, X., Zhu, X., Wu, J., Zhang, M., Zhang, Z., Shen, J., Zhou, W., Gu, L., Lu, R., Ni, Z., 2021. Inhibiting NLRP3 inflammasome attenuates apoptosis in contrast-induced acute kidney injury through the upregulation of HIF1A and BNIP3-mediated mitophagy. Autophagy 17, 2975–2990. https://doi.org/10.1080/15548627.2020.1848971

Liu, L., Feng, D., Chen, G., Chen, M., Zheng, Q., Song, P., Ma, Q., Zhu, C., Wang, R., Qi, W., Huang, L., Xue, P., Li, B., Wang, X., Jin, H., Wang, J., Yang, F., Liu, P., Zhu, Y., Sui, S., Chen, Q., 2012. Mitochondrial outer-membrane protein FUNDC1 mediates hypoxia-induced mitophagy in mammalian cells. Nat. Cell Biol. 14, 177–185. https://doi.org/10.1038/ncb2422

Lorch, Y., Kornberg, R.D., 2015. Chromatin-remodeling and the initiation of transcription. Q. Rev. Biophys. 48, 465–470. https://doi.org/10.1017/S0033583515000116

Lowrie, D.J., Giffin, B.F., Ventullo, R.M., 1993. The ubiquitin-ligase system in *Trypanosoma brucei brucei*. Am. J. Trop. Med. Hyg. 49, 545–551. https://doi.org/10.4269/ajtmh.1993.49.545

Lu, Y., Li, Z., Zhang, S., Zhang, T., Liu, Y., Zhang, L., 2023. Cellular mitophagy: Mechanism, roles in diseases and small molecule pharmacological regulation. Theranostics 13, 736–766. https://doi.org/10.7150/thno.79876

Lunin, V.V., Dobrovetsky, E., Khutoreskaya, G., Zhang, R., Joachimiak, A., Doyle, D.A., Bochkarev, A., Maguire, M.E., Edwards, A.M., Koth, C.M., 2006. Crystal structure of the CorA Mg2+ transporter. Nature 440, 10.1038/nature04642. https://doi.org/10.1038/nature04642

Madeo, F., Schlauer, J., Zischka, H., Mecke, D., Fröhlich, K.-U., 1998. Tyrosine Phosphorylation Regulates Cell Cycle-dependent Nuclear Localization of Cdc48p. Mol. Biol. Cell 9, 131–141. https://doi.org/10.1091/mbc.9.1.131

Magnuson, B., Ekim, B., Fingar, D.C., 2012. Regulation and function of ribosomal protein S6 kinase (S6K) within mTOR signalling networks. Biochem. J. 441, 1–21. https://doi.org/10.1042/BJ20110892

Mani, J., Desy, S., Niemann, M., Chanfon, A., Oeljeklaus, S., Pusnik, M., Schmidt, O., Gerbeth, C., Meisinger, C., Warscheid, B., Schneider, A., 2015. Mitochondrial protein import receptors in Kinetoplastids reveal convergent evolution over large phylogenetic distances. Nat. Commun. 6, 6646. https://doi.org/10.1038/ncomms7646

Mannella, C.A., 2006. Structure and dynamics of the mitochondrial inner membrane cristae. Biochim. Biophys. Acta BBA - Mol. Cell Res., Mitochondrial Dynamics in Cell Life and Death 1763, 542–548. https://doi.org/10.1016/j.bbamcr.2006.04.006

Mannella, C.A., Neuwald, A.F., Lawrence, C.E., 1996. Detection of likely transmembrane β-strand regions in sequences of mitochondrial pore proteins using the Gibbs sampler. J. Bioenerg. Biomembr. 28, 163–169. https://doi.org/10.1007/BF02110647

Mårtensson, C.U., Priesnitz, C., Song, J., Ellenrieder, L., Doan, K.N., Boos, F., Floerchinger, A., Zufall, N., Oeljeklaus, S., Warscheid, B., Becker, T., 2019. Mitochondrial protein translocation-associated degradation. Nature 569, 679–683. https://doi.org/10.1038/s41586-019-1227-y

Martínez-Reyes, I., Sánchez-Aragó, M., Cuezva, J.M., 2012. AMPK and GCN2-ATF4 signal the repression of mitochondria in colon cancer cells. Biochem. J. 444, 249–259. https://doi.org/10.1042/BJ20111829

Martinus, R.D., Garth, G.P., Webster, T.L., Cartwright, P., Naylor, D.J., Høj, P.B., Hoogenraad, N.J., 1996. Selective induction of mitochondrial chaperones in response to loss of the mitochondrial genome. Eur. J. Biochem. 240, 98–103. https://doi.org/10.1111/j.1432-1033.1996.0098h.x

Matheoud, D., Cannon, T., Voisin, A., Penttinen, A.-M., Ramet, L., Fahmy, A.M., Ducrot, C., Laplante, A., Bourque, M.-J., Zhu, L., Cayrol, R., Le Campion, A., McBride, H.M., Gruenheid, S., Trudeau, L.-E., Desjardins, M., 2019. Intestinal infection triggers Parkinson's disease-like symptoms in Pink1−/− mice. Nature 571, 565–569. https://doi.org/10.1038/s41586-019-1405-y

Matheoud, D., Sugiura, A., Bellemare-Pelletier, A., Laplante, A., Rondeau, C., Chemali, M., Fazel, A., Bergeron, J.J., Trudeau, L.-E., Burelle, Y., Gagnon, E., McBride, H.M., Desjardins, M., 2016. Parkinson's Disease-Related Proteins PINK1 and Parkin Repress Mitochondrial Antigen Presentation. Cell 166, 314–327. https://doi.org/10.1016/j.cell.2016.05.039

Matsuda, N., Sato, S., Shiba, K., Okatsu, K., Saisho, K., Gautier, C.A., Sou, Y.-S., Saiki, S., Kawajiri, S., Sato, F., Kimura, M., Komatsu, M., Hattori, N., Tanaka, K., 2010. PINK1 stabilized by mitochondrial depolarization recruits Parkin to damaged mitochondria and activates latent Parkin for mitophagy. J. Cell Biol. 189, 211–221. https://doi.org/10.1083/jcb.200910140

Matsumoto, S., 2023. Msp1-mediated proofreading mechanism for localization of tail-anchored membrane proteins. J. Biochem. (Tokyo) 174, 13–20. https://doi.org/10.1093/jb/mvad025

Matsumoto, S., Nakatsukasa, K., Kakuta, C., Tamura, Y., Esaki, M., Endo, T., 2019. Msp1 Clears Mistargeted Proteins by Facilitating Their Transfer from Mitochondria to the ER. Mol. Cell 76, 191-205.e10. https://doi.org/10.1016/j.molcel.2019.07.006

Maupin-Furlow, J.A., Humbard, M.A., Kirkland, P.A., Li, W., Reuter, C.J., Wright, A.J., Zhou, G., 2006. Proteasomes from structure to function: perspectives from Archaea. Curr. Top. Dev. Biol. 75, 125–169. https://doi.org/10.1016/S0070-2153(06)75005-0

Mazunin, I.O., Levitskii, S.A., Patrushev, M.V., Kamenski, P.A., 2015. Mitochondrial Matrix Processes. Biochem. Biokhimiia 80, 1418–1428. https://doi.org/10.1134/S0006297915110036

Mbang-Benet, D.-E., Sterkers, Y., Crobu, L., Sarrazin, A., Bastien, P., Pagès, M., 2015. RNA interference screen reveals a high proportion of mitochondrial proteins essential for correct cell cycle progress in *Trypanosoma brucei*. BMC Genomics 16, 297. https://doi.org/10.1186/s12864-015-1505-5

Melber, A., Haynes, C.M., 2018. UPRmt regulation and output: a stress response mediated by mitochondrial-nuclear communication. Cell Res. 28, 281–295. https://doi.org/10.1038/cr.2018.16

Merkwirth, C., Jovaisaite, V., Durieux, J., Matilainen, O., Jordan, S.D., Quiros, P.M., Steffen, K.K., Williams, E.G., Mouchiroud, L., Tronnes, S.U., Murillo, V., Wolff, S.C., Shaw, R.J., Auwerx, J., Dillin, A., 2016. Two Conserved Histone Demethylases Regulate Mitochondrial Stress-Induced Longevity. Cell 165, 1209–1223. https://doi.org/10.1016/j.cell.2016.04.012

Mesecke, N., Terziyska, N., Kozany, C., Baumann, F., Neupert, W., Hell, K., Herrmann, J.M., 2005. A Disulfide Relay System in the Intermembrane Space of Mitochondria that Mediates Protein Import. Cell 121, 1059–1069. https://doi.org/10.1016/j.cell.2005.04.011

Michel, S., Canonne, M., Arnould, T., Renard, P., 2015. Inhibition of mitochondrial genome expression triggers the activation of CHOP-10 by a cell signaling dependent on the integrated stress response but not the mitochondrial unfolded protein response. Mitochondrion 21, 58–68. https://doi.org/10.1016/j.mito.2015.01.005

Migdal, I., Skibior-Blaszczyk, R., Heidorn-Czarna, M., Kolodziejczak, M., Garbiec, A., Janska, H., 2017. AtOMA1 Affects the OXPHOS System and Plant Growth in Contrast to Other Newly Identified ATP-Independent Proteases in Arabidopsis Mitochondria. Front. Plant Sci. 8.

Mishra, A., 2017. Mitochondrial DNA, in: Vonk, J., Shackelford, T. (Eds.), Encyclopedia of Animal Cognition and Behavior. Springer International Publishing, Cham, pp. 1–4. https://doi.org/10.1007/978-3-319-47829-6_162-1

Model, K., Prinz, T., Ruiz, T., Radermacher, M., Krimmer, T., Kühlbrandt, W., Pfanner, N., Meisinger, C., 2002. Protein translocase of the outer mitochondrial membrane: role of import receptors in the structural organization of the TOM complex1 1Edited by M. Yaniv. J. Mol. Biol. 316, 657–666. https://doi.org/10.1006/jmbi.2001.5365

Molyneux, D.H., 1973. Animal reservoirs and Gambian trypanosomiasis. Ann. Soc. Belg. Med. Trop. 53, 605–618.

Morgenstern, M., Stiller, S.B., Lübbert, P., Peikert, C.D., Dannenmaier, S., Drepper, F., Weill, U., Höß, P., Feuerstein, R., Gebert, M., Bohnert, M., Laan, M. van der, Schuldiner, M., Schütze, C., Oeljeklaus, S., Pfanner, N., Wiedemann, N., Warscheid, B., 2017. Definition of a High-Confidence Mitochondrial Proteome at Quantitative Scale. Cell Rep. 19, 2836–2852. https://doi.org/10.1016/j.celrep.2017.06.014

Mossmann, D., Meisinger, C., Vögtle, F.-N., 2012. Processing of mitochondrial presequences. Biochim. Biophys. Acta BBA - Gene Regul. Mech., Mitochondrial Gene Expression 1819, 1098–1106. https://doi.org/10.1016/j.bbagrm.2011.11.007

Moullan, N., Mouchiroud, L., Wang, X., Ryu, D., Williams, E.G., Mottis, A., Jovaisaite, V., Frochaux, M.V., Quiros, P.M., Deplancke, B., Houtkooper, R.H., Auwerx, J., 2015. Tetracyclines Disturb Mitochondrial Function across Eukaryotic Models: A Call for Caution in Biomedical Research. Cell Rep. 10, 1681–1691. https://doi.org/10.1016/j.celrep.2015.02.034

Mukherjee, R., Chakrabarti, O., 2016. Ubiquitin-mediated regulation of the E3 ligase GP78 by MGRN1 in trans affects mitochondrial homeostasis. J. Cell Sci. 129, 757–773. https://doi.org/10.1242/jcs.176537

Muñoz-Gómez, S.A., Slamovits, C.H., Dacks, J.B., Wideman, J.G., 2015. The evolution of MICOS: Ancestral and derived functions and interactions. Commun. Integr. Biol. 8, e1094593. https://doi.org/10.1080/19420889.2015.1094593

Murakami, Y., Matsufuji, S., Kameji, T., Hayashi, S., Igarashi, K., Tamura, T., Tanaka, K., Ichihara, A., 1992. Ornithine decarboxylase is degraded by the 26S proteasome without ubiquitination. Nature 360, 597–599. https://doi.org/10.1038/360597a0

Mutterer, J., Zinck, E., 2013. Quick-and-clean article figures with FigureJ. J. Microsc. 252, 89–91. https://doi.org/10.1111/jmi.12069

Nahar, S., Chowdhury, A., Ogura, T., Esaki, M., 2020. A AAA ATPase Cdc48 with a cofactor Ubx2 facilitates ubiquitylation of a mitochondrial fusion-promoting factor Fzo1 for proteasomal degradation. J. Biochem. (Tokyo) 167, 279–286. https://doi.org/10.1093/jb/mvz104

Nare, Z., Moses, T., Burgess, K., Schnaufer, A., Walkinshaw, M.D., Michels, P.A.M., 2023. Metabolic insights into phosphofructokinase inhibition in bloodstream-form trypanosomes. Front. Cell. Infect. Microbiol. 13.

Narendra, D.P., Jin, S.M., Tanaka, A., Suen, D.-F., Gautier, C.A., Shen, J., Cookson, M.R., Youle, R.J., 2010. PINK1 is selectively stabilized on impaired mitochondria to activate Parkin. PLoS Biol. 8, e1000298. https://doi.org/10.1371/journal.pbio.1000298

Nargund, A.M., Fiorese, C.J., Pellegrino, M.W., Deng, P., Haynes, C.M., 2015. Mitochondrial and nuclear accumulation of the transcription factor ATFS-1 promotes OXPHOS recovery during the UPR(mt). Mol. Cell 58, 123–133. https://doi.org/10.1016/j.molcel.2015.02.008

Nargund, A.M., Pellegrino, M.W., Fiorese, C.J., Baker, B.M., Haynes, C.M., 2012. Mitochondrial import efficiency of ATFS-1 regulates mitochondrial UPR activation. Science 337, 587–590. https://doi.org/10.1126/science.1223560

Nass, S., Nass, M.M.K., 1963. INTRAMITOCHONDRIAL FIBERS WITH DNA CHARACTERISTICS. J. Cell Biol. 19, 613–629.

Ndoja, A., Cohen, R.E., Yao, T., 2014. Ubiquitin Signals Proteolysis-Independent Stripping of Transcription Factors. Mol. Cell 53, 893–903. https://doi.org/10.1016/j.molcel.2014.02.002

Neuspiel, M., Schauss, A.C., Braschi, E., Zunino, R., Rippstein, P., Rachubinski, R.A., Andrade-Navarro, M.A., McBride, H.M., 2008. Cargo-Selected Transport from the Mitochondria to Peroxisomes Is Mediated by Vesicular Carriers. Curr. Biol. 18, 102–108. https://doi.org/10.1016/j.cub.2007.12.038

Neutzner, A., Youle, R.J., 2005. Instability of the Mitofusin Fzo1 Regulates Mitochondrial Morphology during the Mating Response of the Yeast *Saccharomyces cerevisiae*. J. Biol. Chem. 280, 18598–18603. https://doi.org/10.1074/jbc.M500807200

Neves, R.P. das, Jones, N.S., Andreu, L., Gupta, R., Enver, T., Iborra, F.J., 2010. Connecting Variability in Global Transcription Rate to Mitochondrial Variability. PLOS Biol. 8, e1000560. https://doi.org/10.1371/journal.pbio.1000560

Ng, M.Y.W., Wai, T., Simonsen, A., 2021. Quality control of the mitochondrion. Dev. Cell 56, 881–905. https://doi.org/10.1016/j.devcel.2021.02.009

Niemann, M., Wiese, S., Mani, J., Chanfon, A., Jackson, C., Meisinger, C., Warscheid, B., Schneider, A., 2013. Mitochondrial Outer Membrane Proteome of *Trypanosoma brucei* Reveals Novel Factors Required to Maintain Mitochondrial Morphology. Mol. Cell. Proteomics MCP 12, 515–528. https://doi.org/10.1074/mcp.M112.023093

Niwa, H., Ewens, C.A., Tsang, C., Yeung, H.O., Zhang, X., Freemont, P.S., 2012. The Role of the N-Domain in the ATPase Activity of the Mammalian AAA ATPase p97/VCP. J. Biol. Chem. 287, 8561–8570. https://doi.org/10.1074/jbc.M111.302778

Nouri, K., Feng, Y., Schimmer, A.D., 2020. Mitochondrial ClpP serine protease-biological function and emerging target for cancer therapy. Cell Death Dis. 11, 841. https://doi.org/10.1038/s41419-020-03062-z

Novak, I., Kirkin, V., McEwan, D.G., Zhang, J., Wild, P., Rozenknop, A., Rogov, V., Löhr, F., Popovic, D., Occhipinti, A., Reichert, A.S., Terzic, J., Dötsch, V., Ney, P.A., Dikic, I., 2010. Nix is a selective autophagy receptor for mitochondrial clearance. EMBO Rep. 11, 45–51. https://doi.org/10.1038/embor.2009.256

Nowis, D., McConnell, E., Wójcik, C., 2006. Destabilization of the VCP-Ufd1-Npl4 complex is associated with decreased levels of ERAD substrates. Exp. Cell Res. 312, 2921–2932. https://doi.org/10.1016/j.yexcr.2006.05.013

Nunnari, J., Suomalainen, A., 2012. Mitochondria: In Sickness and in Health. Cell 148, 1145–1159. https://doi.org/10.1016/j.cell.2012.02.035

Oberholzer, M., Morand, S., Kunz, S., Seebeck, T., 2006. A vector series for rapid PCR-mediated C-terminal in situ tagging of *Trypanosoma brucei* genes. Mol. Biochem. Parasitol. 145, 117–120. https://doi.org/10.1016/j.molbiopara.2005.09.002

Okreglak, V., Walter, P., 2014. The conserved AAA-ATPase Msp1 confers organelle specificity to tail-anchored proteins. Proc. Natl. Acad. Sci. U. S. A. 111, 8019–8024. https://doi.org/10.1073/pnas.1405755111

Olszewski, M.M., Williams, C., Dong, K.C., Martin, A., 2019. The Cdc48 unfoldase prepares well-folded protein substrates for degradation by the 26S proteasome. Commun. Biol. 2, 1–8. https://doi.org/10.1038/s42003-019-0283-z

Onishi, M., Yamano, K., Sato, M., Matsuda, N., Okamoto, K., 2021. Molecular mechanisms and physiological functions of mitophagy. EMBO J. 40, e104705. https://doi.org/10.15252/embj.2020104705

Ordureau, A., Paulo, J.A., Zhang, J., An, H., Swatek, K.N., Cannon, J.R., Wan, Q., Komander, D., Harper, J.W., 2020. Global Landscape and Dynamics of Parkin and USP30-Dependent Ubiquitylomes in iNeurons during Mitophagic Signaling. Mol. Cell 77, 1124-1142.e10. https://doi.org/10.1016/j.molcel.2019.11.013

Orvedahl, A., Sumpter, R., Xiao, G., Ng, A., Zou, Z., Tang, Y., Narimatsu, M., Gilpin, C., Sun, Q., Roth, M., Forst, C.V., Wrana, J.L., Zhang, Y.E., Luby-Phelps, K., Xavier, R.J., Xie, Y., Levine, B., 2011. Image-based genome-wide siRNA screen identifies selective autophagy factors. Nature 480, 113–117. https://doi.org/10.1038/nature10546

Osman, C., Wilmes, C., Tatsuta, T., Langer, T., 2007. Prohibitins Interact Genetically with Atp23, a Novel Processing Peptidase and Chaperone for the F1FO-ATP Synthase. Mol. Biol. Cell 18, 627–635. https://doi.org/10.1091/mbc.e06-09-0839

Otera, H., Taira, Y., Horie, C., Suzuki, Y., Suzuki, H., Setoguchi, K., Kato, H., Oka, T., Mihara, K., 2007. A novel insertion pathway of mitochondrial outer membrane proteins with multiple transmembrane segments. J. Cell Biol. 179, 1355–1363. https://doi.org/10.1083/jcb.200702143

Padman, B.S., Nguyen, T.N., Uoselis, L., Skulsuppaisarn, M., Nguyen, L.K., Lazarou, M., 2019. LC3/GABARAPs drive ubiquitin-independent recruitment of Optineurin and NDP52 to amplify mitophagy. Nat. Commun. 10, 408. https://doi.org/10.1038/s41467-019-08335-6

Pagliarini, D.J., Calvo, S.E., Chang, B., Sheth, S.A., Vafai, S.B., Ong, S.-E., Walford, G.A., Sugiana, C., Boneh, A., Chen, W.K., Hill, D.E., Vidal, M., Evans, J.G., Thorburn, D.R., Carr, S.A., Mootha, V.K., 2008. A mitochondrial protein compendium elucidates complex I disease biology. Cell 134, 112–123. https://doi.org/10.1016/j.cell.2008.06.016

Pakos-Zebrucka, K., Koryga, I., Mnich, K., Ljujic, M., Samali, A., Gorman, A.M., 2016. The integrated stress response. EMBO Rep. 17, 1374–1395. https://doi.org/10.15252/embr.201642195

Pamnani, V., Tamura, T., Lupas, A., Peters, J., Cejka, Z., Ashraf, W., Baumeister, W., 1997. Cloning, sequencing and expression of VAT, a CDC48/p97 ATPase homologue from the archaeon Thermoplasma acidophilum. FEBS Lett. 404, 263–268. https://doi.org/10.1016/s0014-5793(97)00138-5

Papa, L., Germain, D., 2014. SirT3 Regulates the Mitochondrial Unfolded Protein Response. Mol. Cell. Biol. 34, 699–710. https://doi.org/10.1128/MCB.01337-13

Papić, D., Krumpe, K., Dukanovic, J., Dimmer, K.S., Rapaport, D., 2011. Multispan mitochondrial outer membrane protein Ugo1 follows a unique Mim1-dependent import pathway. J. Cell Biol. 194, 397–405. https://doi.org/10.1083/jcb.201102041

Pearse, B.M., 1976. Clathrin: a unique protein associated with intracellular transfer of membrane by coated vesicles. Proc. Natl. Acad. Sci. U. S. A. 73, 1255–1259. https://doi.org/10.1073/pnas.73.4.1255

Peikert, C.D., Mani, J., Morgenstern, M., Käser, S., Knapp, B., Wenger, C., Harsman, A., Oeljeklaus, S., Schneider, A., Warscheid, B., 2017. Charting organellar importomes by quantitative mass spectrometry. Nat. Commun. 8, 15272. https://doi.org/10.1038/ncomms15272

Peters, J.M., Franke, W.W., Kleinschmidt, J.A., 1994. Distinct 19 S and 20 S subcomplexes of the 26 S proteasome and their distribution in the nucleus and the cytoplasm. J. Biol. Chem. 269, 7709–7718. https://doi.org/10.1016/S0021-9258(17)37345-3

Phu, L., Rose, C.M., Tea, J.S., Wall, C.E., Verschueren, E., Cheung, T.K., Kirkpatrick, D.S., Bingol, B., 2020. Dynamic Regulation of Mitochondrial Import by the Ubiquitin System. Mol. Cell 77, 1107-1123.e10. https://doi.org/10.1016/j.molcel.2020.02.012

Picca, A., Guerra, F., Calvani, R., Bucci, C., Lo Monaco, M.R., Bentivoglio, A.R., Coelho-Júnior, H.J., Landi, F., Bernabei, R., Marzetti, E., 2019. Mitochondrial Dysfunction and Aging: Insights from the Analysis of Extracellular Vesicles. Int. J. Mol. Sci. 20, 805. https://doi.org/10.3390/ijms20040805

Poillet-Perez, L., White, E., 2021. MDVs to the rescue: How autophagy-deficient cancer cells adapt to defective mitophagy. Dev. Cell 56, 2010–2012. https://doi.org/10.1016/j.devcel.2021.06.022

Popov, L., 2022. Mitochondrial-derived vesicles: Recent insights. J. Cell. Mol. Med. 26, 3323–3328. https://doi.org/10.1111/jcmm.17391
Potting, C., Wilmes, C., Engmann, T., Osman, C., Langer, T., 2010. Regulation of mitochondrial phospholipids by Ups1/PRELI-like proteins depends on proteolysis and Mdm35. EMBO J. 29, 2888–2898. https://doi.org/10.1038/emboj.2010.169
Pryde, K.R., Taanman, J.W., Schapira, A.H., 2016. A LON-ClpP Proteolytic Axis Degrades Complex I to Extinguish ROS Production in Depolarized Mitochondria. Cell Rep. 17, 2522–2531. https://doi.org/10.1016/j.celrep.2016.11.027
Puchades, C., Rampello, A.J., Shin, M., Giuliano, C.J., Wiseman, R.L., Glynn, S.E., Lander, G.C., 2017. Structure of the mitochondrial inner membrane AAA+ protease YME1 gives insight into substrate processing. Science 358, eaao0464. https://doi.org/10.1126/science.aao0464
Puchades, C., Sandate, C.R., Lander, G.C., 2020. The molecular principles governing the activity and functional diversity of AAA+ proteins. Nat. Rev. Mol. Cell Biol. 21, 43–58. https://doi.org/10.1038/s41580-019-0183-6
Pusnik, M., Mani, J., Schmidt, O., Niemann, M., Oeljeklaus, S., Schnarwiler, F., Warscheid, B., Lithgow, T., Meisinger, C., Schneider, A., 2012. An essential novel component of the noncanonical mitochondrial outer membrane protein import system of trypanosomatids. Mol. Biol. Cell 23, 3420–3428. https://doi.org/10.1091/mbc.e12-02-0107
Qiu, Y., Wang, Jincheng, Li, H., Yang, B., Wang, Jiajia, He, Q., Weng, Q., 2022. Emerging views of OPTN (optineurin) function in the autophagic process associated with disease. Autophagy 18, 73–85. https://doi.org/10.1080/15548627.2021.1908722
Quiles, J.M., Gustafsson, Å.B., 2020. Mitochondrial Quality Control and Cellular Proteostasis: Two Sides of the Same Coin. Front. Physiol. 11, 515. https://doi.org/10.3389/fphys.2020.00515
Quirós, P.M., Langer, T., López-Otín, C., 2015. New roles for mitochondrial proteases in health, ageing and disease. Nat. Rev. Mol. Cell Biol. 16, 345–359. https://doi.org/10.1038/nrm3984
Quirós, P.M., Prado, M.A., Zamboni, N., D'Amico, D., Williams, R.W., Finley, D., Gygi, S.P., Auwerx, J., 2017. Multi-omics analysis identifies ATF4 as a key regulator of the mitochondrial stress response in mammals. J. Cell Biol. 216, 2027–2045. https://doi.org/10.1083/jcb.201702058
Rabouille, C., Levine, T.P., Peters, J.-M., Warren, G., 1995. An NSF-like ATPase, p97, and NSF mediate cisternal regrowth from mitotic golgi fragments. Cell 82, 905–914. https://doi.org/10.1016/0092-8674(95)90270-8
Ramadan, K., Bruderer, R., Spiga, F.M., Popp, O., Baur, T., Gotta, M., Meyer, H.H., 2007. Cdc48/p97 promotes reformation of the nucleus by extracting the kinase Aurora B from chromatin. Nature 450, 1258–1262. https://doi.org/10.1038/nature06388
Ramanathan, H.N., Ye, Y., 2012. The p97 ATPase associates with EEA1 to regulate the size of early endosomes. Cell Res. 22, 346–359. https://doi.org/10.1038/cr.2011.80
Ramirez, A., Old, W., Selwood, D.L., Liu, X., 2022. Cannabidiol activates PINK1-Parkin-dependent mitophagy and mitochondrial-derived vesicles. Eur. J. Cell Biol. 101, 151185. https://doi.org/10.1016/j.ejcb.2021.151185
Rapaport, D., 2003. Finding the right organelle. EMBO Rep. 4, 948–952. https://doi.org/10.1038/sj.embor.embor937
Rhee, H.-W., Zou, P., Udeshi, N.D., Martell, J.D., Mootha, V.K., Carr, S.A., Ting, A.Y., 2013. Proteomic Mapping of Mitochondria in Living Cells via Spatially-Restricted Enzymatic Tagging. Science 339, 1328–1331. https://doi.org/10.1126/science.1230593
Richter, B., Sliter, D.A., Herhaus, L., Stolz, A., Wang, C., Beli, P., Zaffagnini, G., Wild, P., Martens, S., Wagner, S.A., Youle, R.J., Dikic, I., 2016. Phosphorylation of OPTN by TBK1 enhances its binding to Ub chains and promotes selective autophagy of damaged mitochondria. Proc. Natl. Acad. Sci. U. S. A. 113, 4039–4044. https://doi.org/10.1073/pnas.1523926113

Rifkin, M.R., 1984. *Trypanosoma brucei*: biochemical and morphological studies of cytotoxicity caused by normal human serum. Exp. Parasitol. 58, 81–93. https://doi.org/10.1016/0014-4894(84)90023-7

Riley, B.E., Lougheed, J.C., Callaway, K., Velasquez, M., Brecht, E., Nguyen, L., Shaler, T., Walker, D., Yang, Y., Regnstrom, K., Diep, L., Zhang, Z., Chiou, S., Bova, M., Artis, D.R., Yao, N., Baker, J., Yednock, T., Johnston, J.A., 2013. Structure and function of Parkin E3 ubiquitin ligase reveals aspects of RING and HECT ligases. Nat. Commun. 4, 1982. https://doi.org/10.1038/ncomms2982

Rojo, M., Legros, F., Chateau, D., Lombès, A., 2002. Membrane topology and mitochondrial targeting of mitofusins, ubiquitous mammalian homologs of the transmembrane GTPase Fzo. J. Cell Sci. 115, 1663–1674. https://doi.org/10.1242/jcs.115.8.1663

Rondelli, C.M., Perfetto, M., Danoff, A., Bergonia, H., Gillis, S., O'Neill, L., Jackson, L., Nicolas, G., Puy, H., West, R., Phillips, J.D., Yien, Y.Y., 2021. The ubiquitous mitochondrial protein unfoldase CLPX regulates erythroid heme synthesis by control of iron utilization and heme synthesis enzyme activation and turnover. J. Biol. Chem. 297, 100972. https://doi.org/10.1016/j.jbc.2021.100972

Rout, S., Oeljeklaus, S., Makki, A., Tachezy, J., Warscheid, B., Schneider, A., 2021. Determinism and contingencies shaped the evolution of mitochondrial protein import. Proc. Natl. Acad. Sci. 118, e2017774118. https://doi.org/10.1073/pnas.2017774118

Royle, S.J., Bright, N.A., Lagnado, L., 2005. Clathrin is required for the function of the mitotic spindle. Nature 434, 1152–1157. https://doi.org/10.1038/nature03502

Ryan, T.A., Phillips, E.O., Collier, C.L., JB Robinson, A., Routledge, D., Wood, R.E., Assar, E.A., Tumbarello, D.A., 2020. Tollip coordinates Parkin-dependent trafficking of mitochondrial-derived vesicles. EMBO J. 39. https://doi.org/10.15252/embj.2019102539

Saini, R.K., Orindi, B.O., Mbahin, N., Andoke, J.A., Muasa, P.N., Mbuvi, D.M., Muya, C.M., Pickett, J.A., Borgemeister, C.W., 2017. Protecting cows in small holder farms in East Africa from tsetse flies by mimicking the odor profile of a non-host bovid. PLoS Negl. Trop. Dis. 11, e0005977. https://doi.org/10.1371/journal.pntd.0005977

Saladi, S., Boos, F., Poglitsch, M., Meyer, H., Sommer, F., Mühlhaus, T., Schroda, M., Schuldiner, M., Madeo, F., Herrmann, J.M., 2020. The NADH Dehydrogenase Nde1 Executes Cell Death after Integrating Signals from Metabolism and Proteostasis on the Mitochondrial Surface. Mol. Cell 77, 189-202.e6. https://doi.org/10.1016/j.molcel.2019.09.027

Sandoval, H., Thiagarajan, P., Dasgupta, S.K., Schumacher, A., Prchal, J.T., Chen, M., Wang, J., 2008. Essential role for Nix in autophagic maturation of erythroid cells. Nature 454, 232–235. https://doi.org/10.1038/nature07006

Schlame, M., 2021. Protein crowding in the inner mitochondrial membrane. Biochim. Biophys. Acta BBA - Bioenerg. 1862, 148305. https://doi.org/10.1016/j.bbabio.2020.148305

Schmidt, O., Pfanner, N., Meisinger, C., 2010. Mitochondrial protein import: from proteomics to functional mechanisms. Nat. Rev. Mol. Cell Biol. 11, 655–667. https://doi.org/10.1038/nrm2959

Schmitt, S., Prokisch, H., Schlunck, T., Camp II, D.G., Ahting, U., Waizenegger, T., Scharfe, C., Meitinger, T., Imhof, A., Neupert, W., Oefner, P.J., Rapaport, D., 2006. Proteome analysis of mitochondrial outer membrane from *Neurospora crassa*. PROTEOMICS 6, 72–80. https://doi.org/10.1002/pmic.200402084

Schneider, A., 2022. Evolution and diversification of mitochondrial protein import systems. Curr. Opin. Cell Biol. 75, 102077. https://doi.org/10.1016/j.ceb.2022.102077

Schuberth, C., Buchberger, A., 2005. Membrane-bound Ubx2 recruits Cdc48 to ubiquitin ligases and their substrates to ensure efficient ER-associated protein degradation. Nat. Cell Biol. 7, 999–1006. https://doi.org/10.1038/ncb1299

Schuldiner, M., Metz, J., Schmid, V., Denic, V., Rakwalska, M., Schmitt, H.D., Schwappach, B., Weissman, J.S., 2008. The GET complex mediates insertion of tail-anchored proteins into the ER membrane. Cell 134, 634–645. https://doi.org/10.1016/j.cell.2008.06.025

Schweers, R.L., Zhang, J., Randall, M.S., Loyd, M.R., Li, W., Dorsey, F.C., Kundu, M., Opferman, J.T., Cleveland, J.L., Miller, J.L., Ney, P.A., 2007. NIX is required for programmed mitochondrial clearance during reticulocyte maturation. Proc. Natl. Acad. Sci. U. S. A. 104, 19500–19505. https://doi.org/10.1073/pnas.0708818104

Seo, J.H., Rivadeneira, D.B., Caino, M.C., Chae, Y.C., Speicher, D.W., Tang, H.-Y., Vaira, V., Bosari, S., Palleschi, A., Rampini, P., Kossenkov, A.V., Languino, L.R., Altieri, D.C., 2016. The Mitochondrial Unfoldase-Peptidase Complex ClpXP Controls Bioenergetics Stress and Metastasis. PLoS Biol. 14, e1002507. https://doi.org/10.1371/journal.pbio.1002507

Serricchio, M., Bütikofer, P., 2021. A Conserved Mitochondrial Chaperone-Protease Complex Involved in Protein Homeostasis. Front. Mol. Biosci. 8, 767088. https://doi.org/10.3389/fmolb.2021.767088

Sha, Z., Fishovitz, J., Wang, S., Chilakala, S., Xu, Y., Lee, I., 2020. A Selective Fluorogenic Peptide Substrate for the Human Mitochondrial ATP-Dependent Protease Complex ClpXP. Chembiochem Eur. J. Chem. Biol. 21, 2037–2048. https://doi.org/10.1002/cbic.202000030

Shao, L.-W., Niu, R., Liu, Y., 2016. Neuropeptide signals cell non-autonomous mitochondrial unfolded protein response. Cell Res. 26, 1182–1196. https://doi.org/10.1038/cr.2016.118

Shapiro, T.A., Englund, P.T., 1995. The structure and replication of kinetoplast DNA. Annu. Rev. Microbiol. 49, 117–143. https://doi.org/10.1146/annurev.mi.49.100195.001001

Shaw, J.M., Nunnari, J., 2002. Mitochondrial dynamics and division in budding yeast. Trends Cell Biol. 12, 178–184.

Shen, P.S., Park, J., Qin, Y., Li, X., Parsawar, K., Larson, M.H., Cox, J., Cheng, Y., Lambowitz, A.M., Weissman, J.S., Brandman, O., Frost, A., 2015. Rqc2p and 60S ribosomal subunits mediate mRNA-independent elongation of nascent chains. Science 347, 75–78. https://doi.org/10.1126/science.1259724

Shi, R., Zhu, S., Li, V., Gibson, S.B., Xu, X., Kong, J., 2014. BNIP3 Interacting with LC3 Triggers Excessive Mitophagy in Delayed Neuronal Death in Stroke. CNS Neurosci. Ther. 20, 1045–1055. https://doi.org/10.1111/cns.12325

Shin, C.-S., Meng, S., Garbis, S.D., Moradian, A., Taylor, R.W., Sweredoski, M.J., Lomenick, B., Chan, D.C., 2021. LONP1 and mtHSP70 cooperate to promote mitochondrial protein folding. Nat. Commun. 12, 265. https://doi.org/10.1038/s41467-020-20597-z

Shin, M., Watson, E.R., Song, A.S., Mindrebo, J.T., Novick, S.J., Griffin, P.R., Wiseman, R.L., Lander, G.C., 2021. Structures of the human LONP1 protease reveal regulatory steps involved in protease activation. Nat. Commun. 12, 3239. https://doi.org/10.1038/s41467-021-23495-0

Shoshan-Barmatz, V., De Pinto, V., Zweckstetter, M., Raviv, Z., Keinan, N., Arbel, N., 2010. VDAC, a multi-functional mitochondrial protein regulating cell life and death. Mol. Aspects Med. 31, 227–285. https://doi.org/10.1016/j.mam.2010.03.002

Silva, J.M., Wong, A., Carelli, V., Cortopassi, G.A., 2009. Inhibition of mitochondrial function induces an integrated stress response in oligodendroglia. Neurobiol. Dis. 34, 357–365. https://doi.org/10.1016/j.nbd.2009.02.005

Sim, S.I., Chen, Y., Park, E., 2021. Structural basis of mitochondrial protein import by the TIM complex. https://doi.org/10.1101/2021.10.10.463828

Simpson, A.G.B., Radek, R., Dacks, J.B., O'kelly, C.J., 2002. How Oxymonads Lost Their Groove: An Ultrastructural Comparison of Monocercomonoides and Excavate Taxa. J. Eukaryot. Microbiol. 49, 239–248. https://doi.org/10.1111/j.1550-7408.2002.tb00529.x

Sirrenberg, C., Bauer, M.F., Guiard, B., Neupert, W., Brunner, M., 1996. Import of carrier proteins into the mitochondrial inner membrane mediated by Tim22. Nature 384, 582–585. https://doi.org/10.1038/384582a0

Sitron, C.S., Brandman, O., 2019. CAT tails drive degradation of stalled polypeptides on and off the ribosome. Nat. Struct. Mol. Biol. 26, 450–459. https://doi.org/10.1038/s41594-019-0230-1

Smith, T.K., Bringaud, F., Nolan, D.P., Figueiredo, L.M., 2017. Metabolic reprogramming during the *Trypanosoma* brucei life cycle. F1000Research 6, F1000 Faculty Rev-683. https://doi.org/10.12688/f1000research.10342.2

Song, C., Wang, Q., Li, C.-C.H., 2003. ATPase activity of p97-valosin-containing protein (VCP). D2 mediates the major enzyme activity, and D1 contributes to the heat-induced activity. J. Biol. Chem. 278, 3648–3655. https://doi.org/10.1074/jbc.M208422200

Soubannier, V., McLelland, G.-L., Zunino, R., Braschi, E., Rippstein, P., Fon, E.A., McBride, H.M., 2012a. A Vesicular Transport Pathway Shuttles Cargo from Mitochondria to Lysosomes. Curr. Biol. 22, 135–141. https://doi.org/10.1016/j.cub.2011.11.057

Soubannier, V., Rippstein, P., Kaufman, B.A., Shoubridge, E.A., McBride, H.M., 2012b. Reconstitution of Mitochondria Derived Vesicle Formation Demonstrates Selective Enrichment of Oxidized Cargo. PLOS ONE 7, e52830. https://doi.org/10.1371/journal.pone.0052830

Stahl, M., Korotkov, V.S., Balogh, D., Kick, L.M., Gersch, M., Pahl, A., Kielkowski, P., Richter, K., Schneider, S., Sieber, S.A., 2018. Selective Activation of Human Caseinolytic Protease P (ClpP). Angew. Chem. Int. Ed Engl. 57, 14602–14607. https://doi.org/10.1002/anie.201808189

Stahl, M., Sieber, S.A., 2017. An amino acid domino effect orchestrates ClpP's conformational states. Curr. Opin. Chem. Biol., Synthetic Biology * Synthetic Biomolecules 40, 102–110. https://doi.org/10.1016/j.cbpa.2017.08.007

Stefanovic, S., Hegde, R.S., 2007. Identification of a targeting factor for posttranslational membrane protein insertion into the ER. Cell 128, 1147–1159. https://doi.org/10.1016/j.cell.2007.01.036

Stephens, N.A., Kieft, R., Macleod, A., Hajduk, S.L., 2012. Trypanosome resistance to human innate immunity: targeting Achilles' heel. Trends Parasitol. 28, 539–545. https://doi.org/10.1016/j.pt.2012.09.002

Stiburek, L., Cesnekova, J., Kostkova, O., Fornuskova, D., Vinsova, K., Wenchich, L., Houstek, J., Zeman, J., 2012. YME1L controls the accumulation of respiratory chain subunits and is required for apoptotic resistance, cristae morphogenesis, and cell proliferation. Mol. Biol. Cell 23, 1010–1023. https://doi.org/10.1091/mbc.e11-08-0674

Stiller, S.B., Höpker, J., Oeljeklaus, S., Schütze, C., Schrempp, S.G., Vent-Schmidt, J., Horvath, S.E., Frazier, A.E., Gebert, N., van der Laan, M., Bohnert, M., Warscheid, B., Pfanner, N., Wiedemann, N., 2016. Mitochondrial OXA Translocase Plays a Major Role in Biogenesis of Inner-Membrane Proteins. Cell Metab. 23, 901–908. https://doi.org/10.1016/j.cmet.2016.04.005

Stitt, E.R., Strong, R.P., 1944. Stitt's Diagnosis, Prevention and Treatment of Tropical Diseases. Blakiston Company.

Stratford, F.L.L., Ramjeesingh, M., Cheung, J.C., Huan, L.-J., Bear, C.E., 2007. The Walker B motif of the second nucleotide-binding domain (NBD2) of CFTR plays a key role in ATPase activity by the NBD1–NBD2 heterodimer. Biochem. J. 401, 581–586. https://doi.org/10.1042/BJ20060968

Stringer, D.K., Piper, R.C., 2011. Terminating protein ubiquitination. Cell Cycle 10, 3067–3071. https://doi.org/10.4161/cc.10.18.17191

Stuart, R.A., 2002. Insertion of proteins into the inner membrane of mitochondria: the role of the Oxa1 complex. Biochim. Biophys. Acta BBA - Mol. Cell Res., Protein Transport into Mitochondria and Chloroplasts Part II 1592, 79–87. https://doi.org/10.1016/S0167-4889(02)00266-5

Sugiura, A., Mattie, S., Prudent, J., McBride, H.M., 2017. Newly born peroxisomes are a hybrid of mitochondrial and ER-derived pre-peroxisomes. Nature 542, 251–254. https://doi.org/10.1038/nature21375

Sugiura, A., McLelland, G.-L., Fon, E.A., McBride, H.M., 2014. A new pathway for mitochondrial quality control: mitochondrial-derived vesicles. EMBO J. 33, 2142–2156. https://doi.org/10.15252/embj.201488104

Sung, Y.-J., Kao, T.-Y., Kuo, C.-L., Fan, C.-C., Cheng, A.N., Fang, W.-C., Chou, H.-Y., Lo, Y.-K., Chen, C.-H., Jiang, S.S., Chang, I.-S., Hsu, C.-H., Lee, J.-C., Lee, A.Y.-L., 2018. Mitochondrial Lon sequesters and stabilizes p53 in the matrix to restrain apoptosis

under oxidative stress via its chaperone activity. Cell Death Dis. 9, 1–16. https://doi.org/10.1038/s41419-018-0730-7
Tanaka, A., Cleland, M.M., Xu, S., Narendra, D.P., Suen, D.-F., Karbowski, M., Youle, R.J., 2010. Proteasome and p97 mediate mitophagy and degradation of mitofusins induced by Parkin. J. Cell Biol. 191, 1367–1380. https://doi.org/10.1083/jcb.201007013
Tanaka, K., 2009. The proteasome: Overview of structure and functions. Proc. Jpn. Acad. Ser. B Phys. Biol. Sci. 85, 12–36. https://doi.org/10.2183/pjab.85.12
Taylor, S.W., Fahy, E., Zhang, B., Glenn, G.M., Warnock, D.E., Wiley, S., Murphy, A.N., Gaucher, S.P., Capaldi, R.A., Gibson, B.W., Ghosh, S.S., 2003. Characterization of the human heart mitochondrial proteome. Nat. Biotechnol. 21, 281–286. https://doi.org/10.1038/nbt793
Teske, B.F., Fusakio, M.E., Zhou, D., Shan, J., McClintick, J.N., Kilberg, M.S., Wek, R.C., 2013. CHOP induces activating transcription factor 5 (ATF5) to trigger apoptosis in response to perturbations in protein homeostasis. Mol. Biol. Cell 24, 2477–2490. https://doi.org/10.1091/mbc.E13-01-0067
Thoreen, C.C., Chantranupong, L., Keys, H.R., Wang, T., Gray, N.S., Sabatini, D.M., 2012. A unifying model for mTORC1-mediated regulation of mRNA translation. Nature 485, 109–113. https://doi.org/10.1038/nature11083
Tian, Y., Garcia, G., Bian, Q., Steffen, K.K., Joe, L., Wolff, S., Meyer, B.J., Dillin, A., 2016. Mitochondrial Stress Induces Chromatin Reorganization to Promote Longevity and UPR(mt). Cell 165, 1197–1208. https://doi.org/10.1016/j.cell.2016.04.011
Tkach, J.M., Yimit, A., Lee, A.Y., Riffle, M., Costanzo, M., Jaschob, D., Hendry, J.A., Ou, J., Moffat, J., Boone, C., Davis, T.N., Nislow, C., Brown, G.W., 2012. Dissecting DNA damage response pathways by analysing protein localization and abundance changes during DNA replication stress. Nat. Cell Biol. 14, 966–976. https://doi.org/10.1038/ncb2549
Todkar, K., Chikhi, L., Desjardins, V., El-Mortada, F., Pépin, G., Germain, M., 2021. Selective packaging of mitochondrial proteins into extracellular vesicles prevents the release of mitochondrial DAMPs. Nat. Commun. 12. https://doi.org/10.1038/s41467-021-21984-w
Topf, U., Wrobel, L., Chacinska, A., 2016. Chatty Mitochondria: Keeping Balance in Cellular Protein Homeostasis. Trends Cell Biol. 26, 577–586. https://doi.org/10.1016/j.tcb.2016.03.002
Tovar, J., León-Avila, G., Sánchez, L.B., Sutak, R., Tachezy, J., van der Giezen, M., Hernández, M., Müller, M., Lucocq, J.M., 2003. Mitochondrial remnant organelles of Giardia function in iron-sulphur protein maturation. Nature 426, 172–176. https://doi.org/10.1038/nature01945
Towers, C.G., Wodetzki, D.K., Thorburn, J., Smith, K.R., Caino, M.C., Thorburn, A., 2021. Mitochondrial-derived vesicles compensate for loss of LC3-mediated mitophagy. Dev. Cell 56, 2029-2042.e5. https://doi.org/10.1016/j.devcel.2021.06.003
Tremblay, C.Y., Vass, R.H., Vachet, R.W., Chien, P., 2020. The Cleavage Profile of Protein Substrates by ClpXP Reveals Deliberate Starts and Pauses. Biochemistry 59, 4294–4301. https://doi.org/10.1021/acs.biochem.0c00553
Twomey, E.C., Ji, Z., Wales, T.E., Bodnar, N.O., Ficarro, S.B., Marto, J.A., Engen, J.R., Rapoport, T.A., 2019. Substrate processing by the Cdc48 ATPase complex is initiated by ubiquitin unfolding. Science 365, eaax1033. https://doi.org/10.1126/science.aax1033
Tyynismaa, H., Carroll, C.J., Raimundo, N., Ahola-Erkkilä, S., Wenz, T., Ruhanen, H., Guse, K., Hemminki, A., Peltola-Mjøsund, K.E., Tulkki, V., Oresic, M., Moraes, C.T., Pietiläinen, K., Hovatta, I., Suomalainen, A., 2010. Mitochondrial myopathy induces a starvation-like response. Hum. Mol. Genet. 19, 3948–3958. https://doi.org/10.1093/hmg/ddq310
van den Boom, J., Meyer, H., 2018. VCP/p97-Mediated Unfolding as a Principle in Protein Homeostasis and Signaling. Mol. Cell 69, 182–194. https://doi.org/10.1016/j.molcel.2017.10.028

van Ginkel, J., Filius, M., Szczepaniak, M., Tulinski, P., Meyer, A.S., Joo, C., 2018. Single-molecule peptide fingerprinting. Proc. Natl. Acad. Sci. U. S. A. 115, 3338–3343. https://doi.org/10.1073/pnas.1707207115

Vande Walle, L., Lamkanfi, M., Vandenabeele, P., 2008. The mitochondrial serine protease HtrA2/Omi: an overview. Cell Death Differ. 15, 453–460. https://doi.org/10.1038/sj.cdd.4402291

Vargas, J.N.S., Wang, C., Bunker, E., Hao, L., Maric, D., Schiavo, G., Randow, F., Youle, R.J., 2019. Spatiotemporal Control of ULK1 Activation by NDP52 and TBK1 during Selective Autophagy. Mol. Cell 74, 347-362.e6. https://doi.org/10.1016/j.molcel.2019.02.010

Verma, R., Reichermeier, K.M., Burroughs, A.M., Oania, R.S., Reitsma, J.M., Aravind, L., Deshaies, R.J., 2018. Vms1 and ANKZF1 peptidyl-tRNA hydrolases release nascent chains from stalled ribosomes. Nature 557, 446–451. https://doi.org/10.1038/s41586-018-0022-5

Vieux, E.F., Wohlever, M.L., Chen, J.Z., Sauer, R.T., Baker, T.A., 2013. Distinct quaternary structures of the AAA+ Lon protease control substrate degradation. Proc. Natl. Acad. Sci. 110, E2002–E2008. https://doi.org/10.1073/pnas.1307066110

Violitzi, F., Perivolidi, V.-I., Thireou, T., Grivas, I., Haralambous, S., Samiotaki, M., Panayotou, G., Douni, E., 2019. Mapping Interactome Networks of DNAJC11, a Novel Mitochondrial Protein Causing Neuromuscular Pathology in Mice. J. Proteome Res. 18, 3896–3912. https://doi.org/10.1021/acs.jproteome.9b00338

Vitali, D.G., Käser, S., Kolb, A., Dimmer, K.S., Schneider, A., Rapaport, D., 2018. Independent evolution of functionally exchangeable mitochondrial outer membrane import complexes. eLife 7, e34488. https://doi.org/10.7554/eLife.34488

Vögtle, F.-N., Burkhart, J.M., Gonczarowska-Jorge, H., Kücükköse, C., Taskin, A.A., Kopczynski, D., Ahrends, R., Mossmann, D., Sickmann, A., Zahedi, R.P., Meisinger, C., 2017. Landscape of submitochondrial protein distribution. Nat. Commun. 8, 290. https://doi.org/10.1038/s41467-017-00359-0

Vögtle, F.-N., Burkhart, J.M., Rao, S., Gerbeth, C., Hinrichs, J., Martinou, J.-C., Chacinska, A., Sickmann, A., Zahedi, R.P., Meisinger, C., 2012. Intermembrane Space Proteome of Yeast Mitochondria. Mol. Cell. Proteomics MCP 11, 1840–1852. https://doi.org/10.1074/mcp.M112.021105

Walther, D.M., Rapaport, D., 2009. Biogenesis of mitochondrial outer membrane proteins. Biochim. Biophys. Acta BBA - Mol. Cell Res., Assembly of the Mitochondrial Respiratory Chain 1793, 42–51. https://doi.org/10.1016/j.bbamcr.2008.04.013

Wang, L., Myasnikov, A., Pan, X., Walter, P., 2020. Structure of the AAA protein Msp1 reveals mechanism of mislocalized membrane protein extraction. eLife 9, e54031. https://doi.org/10.7554/eLife.54031

Wang, L., Walter, P., 2020. Msp1/ATAD1 in Protein Quality Control and Regulation of Synaptic Activities. Annu. Rev. Cell Dev. Biol. 36, 141–164. https://doi.org/10.1146/annurev-cellbio-031220-015840

Wang, N., Zhu, P., Huang, R., Wang, C., Sun, L., Lan, B., He, Y., Zhao, H., Gao, Y., 2020. PINK1: The guard of mitochondria. Life Sci. 259, 118247. https://doi.org/10.1016/j.lfs.2020.118247

Wang, Q., Song, C., Li, C.-C.H., 2003. Hexamerization of p97-VCP is promoted by ATP binding to the D1 domain and required for ATPase and biological activities. Biochem. Biophys. Res. Commun. 300, 253–260. https://doi.org/10.1016/S0006-291X(02)02840-1

Wang, S., Luo, H., 2021. Dating Alphaproteobacteria evolution with eukaryotic fossils. Nat. Commun. 12, 3324. https://doi.org/10.1038/s41467-021-23645-4

Wang, T., Xu, W., Qin, M., Yang, Y., Bao, P., Shen, F., Zhang, Z., Xu, J., 2016. Pathogenic Mutations in the Valosin-containing Protein/p97(VCP) N-domain Inhibit the SUMOylation of VCP and Lead to Impaired Stress Response. J. Biol. Chem. 291, 14373–14384. https://doi.org/10.1074/jbc.M116.729343

Wang, X., Chen, X.J., 2015. A cytosolic network suppressing mitochondria-mediated proteostatic stress and cell death. Nature 524, 481–484. https://doi.org/10.1038/nature14859

Wasilewski, M., Chojnacka, K., Chacinska, A., 2017. Protein trafficking at the crossroads to mitochondria. Biochim. Biophys. Acta BBA - Mol. Cell Res. 1864, 125–137. https://doi.org/10.1016/j.bbamcr.2016.10.019

Weidberg, H., Amon, A., 2018. MitoCPR—A surveillance pathway that protects mitochondria in response to protein import stress. Science 360, eaan4146. https://doi.org/10.1126/science.aan4146

Weir, N.R., Kamber, R.A., Martenson, J.S., Denic, V., 2017. The AAA protein Msp1 mediates clearance of excess tail-anchored proteins from the peroxisomal membrane. eLife 6, e28507. https://doi.org/10.7554/eLife.28507

Wessel, D., Flügge, U.I., 1984. A method for the quantitative recovery of protein in dilute solution in the presence of detergents and lipids. Anal. Biochem. 138, 141–143. https://doi.org/10.1016/0003-2697(84)90782-6

Wheeler, R.J., 2021. A resource for improved predictions of *Trypanosoma* and *Leishmania* protein three-dimensional structure. PLOS ONE 16, e0259871. https://doi.org/10.1371/journal.pone.0259871

Wheeler, R.J., Gull, K., Sunter, J.D., 2019. Coordination of the Cell Cycle in Trypanosomes. Annu. Rev. Microbiol. 73, 133–154. https://doi.org/10.1146/annurev-micro-020518-115617

Wilcox, A.J., Laney, J.D., 2009. A ubiquitin-selective AAA-ATPase mediates transcriptional switching by remodelling a repressor–promoter DNA complex. Nat. Cell Biol. 11, 1481–1486. https://doi.org/10.1038/ncb1997

Wirtz, E., Leal, S., Ochatt, C., Cross, GeorgeA.M., 1999. A tightly regulated inducible expression system for conditional gene knock-outs and dominant-negative genetics in *Trypanosoma brucei*. Mol. Biochem. Parasitol. 99, 89–101. https://doi.org/10.1016/S0166-6851(99)00002-X

Wohlever, M.L., Mateja, A., McGilvray, P.T., Day, K.J., Keenan, R.J., 2017. Msp1 Is a Membrane Protein Dislocase for Tail-Anchored Proteins. Mol. Cell 67, 194-202.e6. https://doi.org/10.1016/j.molcel.2017.06.019

Wong, K.S., Houry, W.A., 2019. Chemical Modulation of Human Mitochondrial ClpP: Potential Application in Cancer Therapeutics. ACS Chem. Biol. 14, 2349–2360. https://doi.org/10.1021/acschembio.9b00347

Wong, S., Elgort, M.G., Gottesdiener, K., Campbell, D.A., 1992. Allelic polymorphism of the *Trypanosoma brucei* polyubiquitin gene. Mol. Biochem. Parasitol. 55, 187–195. https://doi.org/10.1016/0166-6851(92)90139-b

Wright, G., Terada, K., Yano, M., Sergeev, I., Mori, M., 2001. Oxidative stress inhibits the mitochondrial import of preproteins and leads to their degradation. Exp. Cell Res. 263, 107–117. https://doi.org/10.1006/excr.2000.5096

Wrobel, L., Topf, U., Bragoszewski, P., Wiese, S., Sztolsztener, M.E., Oeljeklaus, S., Varabyova, A., Lirski, M., Chroscicki, P., Mroczek, S., Januszewicz, E., Dziembowski, A., Koblowska, M., Warscheid, B., Chacinska, A., 2015. Mistargeted mitochondrial proteins activate a proteostatic response in the cytosol. Nature 524, 485–488. https://doi.org/10.1038/nature14951

Wu, X., Li, L., Jiang, H., 2016. Doa1 targets ubiquitinated substrates for mitochondria-associated degradation. J. Cell Biol. 213, 49–63. https://doi.org/10.1083/jcb.201510098

Xu, S., Peng, G., Wang, Y., Fang, S., Karbowski, M., 2011. The AAA-ATPase p97 is essential for outer mitochondrial membrane protein turnover. Mol. Biol. Cell 22, 291–300. https://doi.org/10.1091/mbc.e10-09-0748

Yahalomi, D., Atkinson, S.D., Neuhof, M., Chang, E.S., Philippe, H., Cartwright, P., Bartholomew, J.L., Huchon, D., 2020. A cnidarian parasite of salmon (Myxozoa: Henneguya) lacks a mitochondrial genome. Proc. Natl. Acad. Sci. U. S. A. 117, 5358–5363. https://doi.org/10.1073/pnas.1909907117

Ye, Y., 2006. Diverse functions with a common regulator: Ubiquitin takes command of an AAA ATPase. J. Struct. Biol., 156, 29–40. https://doi.org/10.1016/j.jsb.2006.01.005

Ye, Y., Tang, W.K., Zhang, T., Xia, D., 2017. A Mighty “Protein Extractor” of the Cell: Structure and Function of the p97/CDC48 ATPase. Front. Mol. Biosci. 4. https://doi/10.3389/fmolb.2017.00039

Yedidi, R.S., Wendler, P., Enenkel, C., 2017. AAA-ATPases in Protein Degradation. Front. Mol. Biosci. 4.

Yip, M.C.J., Keszei, A.F.A., Feng, Q., Chu, V., McKenna, M.J., Shao, S., 2019. Mechanism for recycling tRNAs on stalled ribosomes. Nat. Struct. Mol. Biol. 26, 343–349. https://doi.org/10.1038/s41594-019-0211-4

Yoneda, T., Benedetti, C., Urano, F., Clark, S.G., Harding, H.P., Ron, D., 2004. Compartment-specific perturbation of protein handling activates genes encoding mitochondrial chaperones. J. Cell Sci. 117, 4055–4066. https://doi.org/10.1242/jcs.01275

Zahedi, R.P., Sickmann, A., Boehm, A.M., Winkler, C., Zufall, N., Schönfisch, B., Guiard, B., Pfanner, N., Meisinger, C., 2006. Proteomic Analysis of the Yeast Mitochondrial Outer Membrane Reveals Accumulation of a Subclass of Preproteins. Mol. Biol. Cell 17, 1436–1450. https://doi.org/10.1091/mbc.e05-08-0740

Zehr, E., Szyk, A., Piszczek, G., Szczesna, E., Zuo, X., Roll-Mecak, A., 2017. Katanin spiral and ring structures shed light on power stroke for microtubule severing. Nat. Struct. Mol. Biol. 24, 717–725. https://doi.org/10.1038/nsmb.3448

Zeng, X., Neupert, W., Tzagoloff, A., 2007. The Metalloprotease Encoded by ATP23 Has a Dual Function in Processing and Assembly of Subunit 6 of Mitochondrial ATPase. Mol. Biol. Cell 18, 617–626. https://doi.org/10.1091/mbc.e06-09-0801

Zhao, J., Zhai, B., Gygi, S.P., Goldberg, A.L., 2015. mTOR inhibition activates overall protein degradation by the ubiquitin proteasome system as well as by autophagy. Proc. Natl. Acad. Sci. U. S. A. 112, 15790–15797. https://doi.org/10.1073/pnas.1521919112

Zhao, Q., Wang, J., Levichkin, I.V., Stasinopoulos, S., Ryan, M.T., Hoogenraad, N.J., 2002. A mitochondrial specific stress response in mammalian cells. EMBO J. 21, 4411–4419. https://doi.org/10.1093/emboj/cdf445

Zhao, Z., Lindsay, M.E., Roy Chowdhury, A., Robinson, D.R., Englund, P.T., 2008. p166, a link between the trypanosome mitochondrial DNA and flagellum, mediates genome segregation. EMBO J. 27, 143–154. https://doi.org/10.1038/sj.emboj.7601956

Zheng, J., Li, L., Jiang, H., 2019. Molecular pathways of mitochondrial outer membrane protein degradation. Biochem. Soc. Trans. 47, 1437–1447. https://doi.org/10.1042/BST20190275

Zhou, D., Palam, L.R., Jiang, L., Narasimhan, J., Staschke, K.A., Wek, R.C., 2008. Phosphorylation of eIF2 directs ATF5 translational control in response to diverse stress conditions. J. Biol. Chem. 283, 7064–7073. https://doi.org/10.1074/jbc.M708530200

Zhou, H., Zhu, P., Guo, J., Hu, N., Wang, S., Li, D., Hu, S., Ren, J., Cao, F., Chen, Y., 2017. Ripk3 induces mitochondrial apoptosis via inhibition of FUNDC1 mitophagy in cardiac IR injury. Redox Biol. 13, 498–507. https://doi.org/10.1016/j.redox.2017.07.007

Zhou, J., Jung, M., Dimmer, K.S., Rapaport, D., 2022. The multi-factor modulated biogenesis of the mitochondrial multi-span protein Om14. J. Cell Biol. 221, e202112030. https://doi.org/10.1083/jcb.202112030

Zíková, A., Panigrahi, A.K., Dalley, R.A., Acestor, N., Anupama, A., Ogata, Y., Myler, P.J., Stuart, K., 2008. *Trypanosoma brucei* mitochondrial ribosomes: affinity purification and component identification by mass spectrometry. Mol. Cell. Proteomics MCP 7, 1286–1296. https://doi.org/10.1074/mcp.M700490-MCP200

Zurita Rendón, O., Shoubridge, E.A., 2018. LONP1 Is Required for Maturation of a Subset of Mitochondrial Proteins, and Its Loss Elicits an Integrated Stress Response. Mol. Cell. Biol. 38, e00412-17. https://doi.org/10.1128/MCB.00412-17

6. Acknowledgements

The time I spent in the Schneider lab during the last years was very enjoyable thanks to all the amazing people who accompanied me along the way. This journey wouldn't have been the same without each of you.

First of all, I would like to thank my supervisor, André Schneider. Your leadership and guidance have been invaluable, shaping my approach to work and fostering a very positive environment within our group.

I would like to thank Torsten Ochsenreiter who was my co-advisor during my PhD. You always followed my project with great interest, and I always left our meetings with valuable feedback. I am looking forward to soon join your group as your new lab manager.

I also thank my mentor, Benoît Zuber for overlooking my progress in the yearly GCB progress reports and Pascal Mäser who agreed to be my external co-referee. Your expertise will surely be of great value to the discussions at my defence.

I would like to thank all present and past members of the Schneider group for all the nice lab meetings, conferences, stimulating scientific discussions, coffee breaks, office chatter and everything else. Your collaboration, and camaraderie made our workplace truly special. Caroline Dewar, thank you for supervising a large part of my PhD and setting up a smooth start for my lab work in this group. I am very grateful for your continuous support and mentorship. Elke Horn, your helping hands, and your expertise have greatly contributed to the success of our projects. My office neighbour, Salome Äschlimann, thank you for your highly contagious cheerfulness and positive vibes. Corinne von Känel, I greatly appreciated you happily sharing your food as well as your wisdom. Thanks, Philip Stettler, our R expert, you were a great roommate at the meetings we went together. Stephan Berger, thank you for keeping us safe as our KOPAS and for being a great driver. Advaitha Iyer, you were an awesome office mate, our chats would have been podcast-worthy. Simona Amodeo, thank you for your kindness and all the shared laughter. Thanks, Christoph Wenger, for introducing me methods like BN-PAGE and miniature-painting. Thank you, Bernd Schimanski, Moritz Niemann, Tatiana Küster and Samuel Rout, very much for taking time to share your knowledge about experiments and methods. Big thanks also to Shikha, Mauro Fischli, Salvatore Calderaro and Carmela Esposito for all the good times we shared together inside and outside the lab. Working alongside you all has been a pleasure.

I would also like to extend my thanks to Volker Thiel and Philip V'kovski who supervised me as an undergrad student. This time has left a lasting impact and your fantastic introduction to science as well as your encouraging words greatly motivated me to enter this PhD journey.

I would also like to thank Monica Schaller and the GCB for providing a frame for the PhD program which highly benefits us students.

Furthermore, I am very grateful for the friends outside of the workplace that accompanied me through everything over the last couple of years. Going out to concerts, movies or just chilling, playing games and spending time together has been an inexhaustible source of joy and strength. I am very fortunate to have you as friends.

I would also like to thank my “Thy Gnosis”-bandmates for the good times on and off stage.

To my family: Your unwavering support has been my pillar of strength. Thank you for your love and encouragement and for always being home to me.

Lastly but most importantly, I thank my fiancé, Claudia Rüegsegger. Thank you for all the adventures and for always being there. I am beyond excited to tie the knot with you in just a couple of weeks. I love you!

Curriculum vitae

Markus Daniel Gerber [redacted]

Personal information

Address: [redacted]

Phone Nr.: [redacted]

Email: markus.gerber@unibe.ch

Education

Oct 2019 – now	**PhD in Biochemistry and Molecular Biology at the Department of Chemistry, Biochemistry and Pharmaceutical Sciences, Graduate School for Cellular and Biomedical Sciences, University of Bern** Supervised by Prof. Dr. André Schneider Working title: Msp1 in *Trypanosoma brucei* mitochondrial quality control
Aug 2017 - May 2019	**Master of Science in Molecular Life Science at the Institute of Veterinary Virology of the Vetsuisse Faculty, University of Bern** Supervised by Prof. Dr. Volker Thiel MSc thesis: Insights into dynamics of virus-host interactions at the coronavirus replication and transcription complex
Sep 2013 - Jul 2017	**Bachelor of Science in Biology at the Institute of Veterinary Virology of the Vetsuisse Faculty, University of Bern** Supervised by Prof. Dr. Volker Thiel BSc thesis: Visualization of stress granules during coronavirus infection
Aug 2009 – Jul 2013	**Matura at Gymnasium Neufeld, Bern** Matura thesis: Kommunikation von Nonprofit- Organisationen

Professional experience	
Jun 2019	**Substitute teaching**, Kindergarten, Ortschwaben
Oct 2018 – Dec 2018	**Private lessons**, Interlink, Bern
2014 – 2019	Occasional **substitute teaching**, Schule Stegmatt, Lyss
Jan 2014 – Dec 2018	**J+S scout leader**, Cevi Region Bern, evangelisch-reformierte Kirchgemeinde Lyss

Publications

M. Gerber, I. Suppanz, S. Oeljeklaus, M. Niemann, S. Käser, B. Warscheid, A. Schneider, C. E. Dewar: “A Msp1-containing complex removes orphaned proteins in the mitochondrial outer membrane of T. brucei” DOI: 10.26508/lsa.202302004

P. V'kovski, **M. Gerber**, J. Kelly, S. Pfaender, N. Ebert, S. B. Lagache, C. Simillion, J. Portmann, H. Stalder, V. Gaschen, R. Bruggmann, M. H. Stoffel, M. Heller, R. Dijkman, V. Thiel: “Determination of host proteins composing the microenvironment of coronavirus replicase complexes by proximity-labeling”, DOI: 10.7554/eLife.42037

Declaration of Originality

Last name, first name: **Gerber, Markus**

Matriculation number: **13-119-227**

I hereby declare that this thesis represents my original work and that I have used no other sources except as noted by citations.

All data, tables, figures and text citations which have been reproduced from any other source, including the internet, have been explicitly acknowledged as such.

I am aware that in case of non-compliance, the Senate is entitled to withdraw the doctorate degree awarded to me on the basis of the present thesis, in accordance with the “Statut der Universität Bern (Universitätsstatut; UniSt)”, Art. 69, of 7 June 2011.

Place, date

Bern, 02.05.2024

Signature